Tese de Doutorado
(PhD Dissertation)

Mecanismos envolvidos na resposta cerebral ao exercício e no papel do hipotálamo na regulação do balanço energético

(Mechanisms implicated in brain response to exercise and in the role of the hypothalamus in the regulation of energy balance)

Marcelo de Oliveira Dietrich

Volume I

Programa de Pós-graduação em Ciências Biológicas: Bioquímica
Departamento de Bioquímica
Instituto de Ciências Básicas da Saúde
Universidade Federal do Rio Grande do Sul

TESE DE DOUTORADO
(PhD Dissertation)

Mecanismos envolvidos na resposta cerebral ao exercício e no papel do hipotálamo na regulação do balanço energético

(Mechanisms implicated in brain response to exercise and in the role of the hypothalamus in the regulation of energy balance)

Marcelo de Oliveira Dietrich

Orientador
(Advisor)
Prof. Dr. Diogo Onofre Gomes de Souza
(Universidade Federal do Rio Grande do Sul, Porto Alegre, Brasil)

Tese apresentada ao Programa de Pós-graduação em Ciências Biológicas: Bioquímica como requisito parcial para a obtenção do título de Doutor em Ciências Biológicas: Bioquímica.

Dissertation submitted to the Graduate Program in Biological Sciences: Biochemistry, in partial fulfillment of the requirements for the degree of Doctor of Philosophy in Biological Sciences: Biochemistry.

Janeiro de 2012
(January 2012)

“I believe in the great discovery
I believe in the wasted years of work
My faith is strong, blind, and without foundation.”

Wisława Szymborska

Ao meus avós, Rovani e Diná, que me ensinaram desde cedo a sonhar e a sorrir.

PREÂMBULO

Apresentação

Esta tese está organizada em três partes, cada uma sendo constituída dos seguintes itens:

Parte I: Resumo, Introdução e Objetivos;

Parte II: Resultados que estão apresentados na forma de artigos científicos. Cada artigo científico representa um capítulo;

Parte III: Discussão, Conclusão e Referências bibliográficas citadas na Introdução da Parte I e Discussão da Parte III;

Em anexos estão conteúdos importantes que não fazem parte do corpo principal desta tese. Em Anexos A, podem-se encontrar diversos artigos e outras produções bibliográficas cujos trabalhos foram realizados durante o período de doutoramento e possuem conteúdo relacionado ao corpo principal da tese.

Os trabalhos elaborados durante esta tese foram desenvolvidos no Departamento de Bioquímica da UFRGS, laboratório 28, sob a orientação do Prof. Dr. Diogo O. Souza, como também no Seção de Medicina Comparativa da Universidade de Yale (New Haven, CT, EUA), sob a orientação do Prof. Dr. Tamas L. Horvath.

Presentation

This dissertation is organized in three parts, in accordance with local rules of the *Graduate Program in Biological Sciences: Biochemistry (UFRGS)*:

Part I: Abstract, Introduction and Aims. It is written in Portuguese, with the exception of the Abstract that has Portuguese and English versions.

Part II: Results presented as scientific articles. Each article corresponds to one chapter.

Part III: Discussion, conclusion, and references. References correspond to citations in Parts III and I. References in Part II are located in the end of each chapter.

Supplementary content that is not part of the main body of this dissertation can be found in “Anexos” (Attachments). In “Anexo A”, there are several articles and other types of publications that were developed during this PhD thesis which are somehow related to the main body of thesis, but were left as supportive information.

The experiments described in this dissertation were performed in the Department of Biochemistry – UFRGS (Porto Alegre, RS, Brazil) under the supervision of Dr. Diogo O. Souza and in the Section of Comparative Medicine - Yale School of Medicine (New Haven, CT, USA) under the supervision of Dr. Tamas L. Horvath.

SUMÁRIO (Table of Contents)

PARTE I

Onde uma introdução será apresentada e os objetivos serão traçados.

Resumo

O exercício físico regular é uma importante maneira de tratar e proteger contra o desenvolvimento de diversas doenças crônicas e seus efeitos no sistema nervoso central (SNC) podem revelar mecanismos importantes no processo saúde-doença. Aqui, mostramos que o exercício promove plasticidade sináptica em um processo que é dependente da adaptação funcional e morfológica das mitocôndrias neuronais. A ausência de UCP2, uma proteína desacopladora do fluxo de prótons, leva a anulação destes efeitos benéficos do exercício. Além dos efeitos do exercício no cérebro, também estudamos como o hipotálamo, uma região importante em diversas funções homeostáticas, regula o balanço energético e outros comportamentos em camundongos. Focamos principalmente na função de uma população de neurônios localizada no núcleo arqueado do hipotálamo, chamada de neurônios NPY/AgRP. Esses neurônios são orexigênicos, isto é, são responsáveis por promover aumento da ingesta de alimentos. Primeiramente, estudamos o papel da proteína Sirt1 nestes neurônios. Sirt1 é uma proteína com atividade deacetilase que está relacionada com adaptações metabólicas em períodos de balanço energético negativo, como restrição calórica e jejum. Portanto, tanto Sirt1 como os neurônios NPY/AgRP estão ativados em situações metabólicas semelhantes. Mostramos que o bloqueio da atividade de Sirt1 nesse grupo de neurônios, utilizando fármacos ou modelos de camundongos transgênicos, leva a uma diminuição da atividade neuronal e também a diminuição do apetite e do peso corporal. Esses efeitos foram dependentes da sinalização através dos receptores de melanocortinas e também da presença de UCP2. Essa função crucial de Sirt1 nos neurônios NPY/AgRP nos levou a estudar os animais deficientes em Sirt1 em modelos de restrição calórica. Animais nocaute para Sirt1 nos neurônios NPY/AgRP não tiveram nenhuma anormalidade metabólica em resposta a tal dieta. Entretanto, estes animais apresentaram resposta comportamental alterada em protocolos que testam atividade exploratória, principalmente em resposta à novidade. Subsequentemente, mostramos que esses neurônios são importantes para a plasticidade sináptica de neurônios dopaminérgicos na zona tegmental ventral. Corroborando o papel desta área na regulação de comportamentos motivacionais, nossos resultados mostram que os neurônios NPY/AgRP são críticos para o desenvolvimento desses neurônios dopaminérgicos e consequentemente para a regulação de uma série de comportamentos motivacionais, como resposta à cocaína e à novidade. Portanto, nossos resultados sugerem que o hipotálamo é importante para o desenvolvimento cerebral, com possível impacto em diversas funções cerebrais não classicamente relacionadas a este. Tais descobertas podem ser relevantes na pesquisa translacional.

Abstract

Exercise is a behavioral intervention that promotes beneficial effects in many chronic diseases. The effects of exercise in the central nervous system (CNS) can shed light on mechanisms relevant to pathophysiology of diseases. Here, we demonstrate that exercise promotes synaptogenesis in the hippocampus in a process that is dependent on mitochondrial adaptations. In the absence of the mitochondrial uncoupling protein UCP2, the beneficial effects of exercise are abrogated. In addition to study the effects of exercise on the brain, we also investigate the role of the hypothalamus, a brain area important in several homeostatic functions, in the regulation of energy balance and other behaviors. We focused on the role of the NPY/AgRP neurons located in the arcuate nucleus of the hypothalamus, which exert an orexigenic tone in the brain, promoting food intake. We first investigated potential cellular pathways that could be important in the maintenance of neuronal activity. Sirt1 is a deacetylase that senses the metabolic state of the cell and is activated during negative energy balance (for example, fasting and calorie restriction). The similarities between the metabolic states that activate Sirt1 and the AgRP neurons led us to evaluate the role of this protein in NPY/AgRP neuronal function. We found that Sirt1 is important to NPY/AgRP activation and consequent feeding behavior. Animals with decreased Sirt1 activity are leaner and eat less. These results were dependent of melanocortin signaling and the presence of UCP2. The critical role of Sirt1 in the AgRP neurons led us to evaluate the adaptive response of mice knockout for Sirt1 specifically in the AgRP neurons during calorie restriction. We show here that calorie restriction promotes the activity of NPY/AgRP neurons in the brain, and that disrupting Sirt1 in these cells lead to impaired behavioral but not metabolic responses to calorie restriction. These findings highlight the pivotal role of the NPY/AgRP neurons during calorie restriction in regulation of complex behaviors. Subsequently, we show that impairment of AgRP neuronal function in mice increases exploratory behavior unrelated to feeding. Behavioral responses to cocaine, were also altered in these animals. As a neurobiological substrate of these altered behaviors, in Agrp-Sirt1 KO mice, ventral tegmental (VTA) dopamine (DA) neurons, which targeted by AgRP efferents, exhibited enhanced spike- timing-dependent long-term potentiation (STD-LTP), decreased amplitude of mIPSCs, and increased DA levels in basal forebrain. Early postnatal ablation of AgRP neurons led to a phenotype resembling that of Agrp-Sirt1 KO mice, with enhanced LTP in VTA-DA cells and altered response to novelty. These observations reveal a fundamental regulatory role of AgRP neurons in determining the set point of the DA reward circuitry and associated behaviors during development. Our results are likely important in translational research.

Lista de Abreviaturas

SNC	Sistema nervoso central
DA	Doença de Alzheimer (ou Mal de Alzheimer ou Demência de Alzheimer)
DP	Doença de Parkinson (ou Mal de Parkinson)
GDNF	Fator neurotrófico derivado da glia
IGF-1	Fator de crescimento semelhante a insulina
GD	Giro denteado (região do hipocampo)
LTP	Potenciação de longo prazo (long-term potentiation)
NMDA	N-metil D-Aspartato
VEGF	Fator de crescimento endotelial vascular
VMH	Hipotálamo ventromedial
ARC	Núcleo arqueado do hipotálamo
CSF	Líquido cefalorraquidiano
BBB	Barreira hemato-encefálica
PVN	Núcleo paraventricular
PBN	Núcleo parabraquial
POMC	Pró-ópio-melanocortina
CART	Transcrição regulada de anfetamina e cocaína
MC3R	Receptor de melanocortina tipo 3
MC4R	Receptor de melanocortina tipo 4
ME	Eminência mediana
ROS	Espécies reativas de oxigênio
ATP	Trifosfato de adenosina
UCP	Proteínas desacopladoras

Introdução

Em geral, a qualidade de vida, o bem-estar social e a expectativa de vida da população vem aumentando consideravelmente. O avanço científico na área da saúde e o desenvolvimento de novas ferramentas de diagnóstico e tratamento alavancaram a medicina moderna. Este avanço proporciona ao paciente melhores cuidados e maiores oportunidades para promover diagnosticos e tratar enfermidades antes fatais. Paralelamente a esses avanços, o estilo de vida da população também vem mudando nas últimas décadas, principalmente nos grandes centros urbanos. Este estilo de vida, chamado de "estilo de vida Ocidental", caracteriza-se pelo sedentarismo, consumo de comidas ricas em gorduras e açúcares simples, além de elevados níveis de estresse e privação de sono. Esses diversos fatores comportamentais e ambientais, aliados certamente a predisposição genética e epigenética[1], vem ocasionando um crescimento de uma série de doenças crônicas que trazem profundas repercussões na saúde coletiva. Ainda que tenha havido avanço nas pesquisas e nos investimentos na área da saúde, a grande maioria das doenças crônicas não possuem mecanismos fisiopatológicos elucidados.

O sistema nervoso central (SNC) atua como orquestrador das diferentes funções homeostáticas e, portanto, é seguramente um dos principais tecidos que sofrem alterações marcantes nas doenças crônicas. A colocação do SNC como regulador principal das diversas funções teciduais tem múltiplas implicações para saúde, inclusive em nível de políticas de saúde pública. Governos vem priorizando e investindo em pesquisadas relacionadas ao cérebro, com o objetivo de melhor entender o processo de saúde-doença e, também, de melhor manejar o processo de

[1] Epigenética: Epigenética é definida como modificações do genoma, herdável durante a divisão celular, que não envolvem uma mudança na sequência de bases nucleotídicas da molécula de DNA.

diagnóstico e tratamento de enfermidades complexas. Ao mesmo tempo que o cérebro surge como principal regulador dos diversos tecidos, existe também um aumento na incidência de doenças crônicas neuropsiquiátricas. A importância destas doenças para às políticas públicas é enfatizada, por exemplo, pela Portaria do governo brasileiro no. 1.161, de 7 de julho de 2005, que ressalta a importância de ações de promoção e prevenção em todos os níveis de atenção à saúde em relação às doenças cerebrais, sugerindo fortemente ações educativas e preventivas visando à possibilidade de êxito da intervenção precoce e, por tanto, a diminuição de suas sequelas.

Mais de 450 milhões de pessoas sofrem de alguma doença cerebral no mundo, incluindo doenças mentais, neurológicas e problemas psicossociais decorrentes de abuso de drogas. Na população mundial, as doenças neurodegenerativas de Alzheimer (DA) e de Parkinson (DP) têm uma prevalência de 400 casos por 100 mil habitantes. As demências atingem cerca de 5% dos indivíduos acima dos 65 anos e 20% acima dos 80 anos; a doença de Alzheimer corresponde a 50% ou mais dos casos. No Brasil, o número de idosos é de aproximadamente 8 milhões, estimando-se que existam 1,2 milhões de idosos em todo país com algum grau de demência. Estima-se que no ano de 2020 a população idosa será em torno de 15 milhões de brasileiros. Portanto, o custo social e econômico destas doenças será muito maior do que o atual e tende a crescer proporcionalmente. Desta maneira, o conhecimento das alterações bioquímicas, fisiológicas e morfológicas nelas envolvidas pode direcionar à concepção de terapias para combater ou reduzir sua progressão e oferecer esperança de prevenção.

A forma mais eficaz de diminuir o impacto social das doenças crônicas, inclusive doenças neuropsiquiátricas, é através da prevenção e promoção precoce de saúde em pacientes afetados. Não é de hoje que se estudam a promoção de saúde e

prevenção de doenças. O primeiro pesquisador e filósofo a enumerar regras para promoção da saúde do indivíduo foi Galeno[2]. Este autor estudou medicina por mais de 50 anos e enumerou diversas leis para uma vida saudável (Tabela 1), que guiaram sua vida, seus ensinamentos e sua prática médica.

Tabela 1. Leis para uma vida saudável de acordo com Galeno (cerca de 140 d.C.)

1. Respirar ar puro
2. Comer alimentos apropriados
3. Beber as bebidas certas
4. Exercício
5. Dormir adequadamente
6. Evacuação diária
7. Controle das emoções

O estudo das alterações cerebrais decorrentes de um estilo de vida saudável sempre foram foco da minha atenção durante minha formação científica (Dietrich *et al.*, 2003; Dietrich *et al.*, 2004; Dietrich *et al.*, 2005; Dietrich *et al.*, 2007; Müller *et al.*, 2008). Nesta tese, avalia-se os efeitos do exercício e da alimentação nas funções cerebrais e no processo saúde-doença.

Exercício e função cerebral

O exercício físico regular promove vários benefícios à saúde, sendo indicado como uma importante intervenção para promover melhorias na qualidade de vida e no bem-estar, além de tratamento para algumas doenças crônicas (por exemplo, diabetes tipo 2) e fator de prevenção de inúmeras outras (por exemplo, obesidade). Diversos

[2] Claudius Galenus (Pérgamo, 129 – Roma, 200) célebre médico cirurgião grego, fez importantes descobertas sobre anatomia humana baseadas na dissecação de primatas. Galeno foi, provavelmente, o primeiro pesquisador a usar sistematicamente cobaias para estudar medicina comparada.

estudos, tanto com modelos animais quanto com humanos, mostram que a atividade física regular exerce efeitos positivos também sobre o cérebro e a saúde mental (Cotman & Berchtold, 2002; Cotman & Engesser-Cesar, 2002): mantém a função cognitiva, melhora o humor, protege contra toxicidade cerebral, etecetera (Carro *et al.*, 2000; Carro *et al.*, 2001; Lawlor & Hopker, 2001; Teri *et al.*, 2003). O exercício parece modular a plasticidade cerebral, através de uma complexa rede de fatores de crescimento, citocinas e neuro-hormônios (Vaynman *et al.*, 2003; Lopez-Lopez *et al.*, 2004; Vaynman *et al.*, 2004a; b). Exercício regular em animais promove plasticidade sináptica no hipocampo cerebral, aumentando neurogênese, LTP e angiogênese (Neeper *et al.*, 1995; van Praag *et al.*, 1999; Cotman & Berchtold, 2002; Cotman & Engesser-Cesar, 2002; Lopez-Lopez *et al.*, 2004; Vaynman *et al.*, 2004b; Dietrich *et al.*, 2008). Esses efeitos estão relacionados a um aumento do gasto energético cerebral, levando a um aumento da captação de glicose no cérebro (Lopez-Lopez *et al.*, 2004). O aumento do gasto energético no cérebro precisa, obrigatoriamente, estar acoplado a um aumento da capacidade oxidativa neste tecido. Como as atividades oxidativas ligadas à produção energética ocorrem nas mitocôndrias, é de se esperar que o exercício promova adaptações ao nível de metabolismo mitocondrial e que tal seja importante para as modificações no cérebro induzidas pelo exercício.

As UCPs são proteínas que desacoplam o fluxo de prótons da cadeia oxidativa nas mitocôndrias (Echtay *et al.*, 2002; Brand *et al.*, 2004; Andrews *et al.*, 2005), sendo classicamente conhecidas por modularem a produção de calor no tecido adiposo marrom (Cannon *et al.*, 1982; Lean *et al.*, 1983). No SNC, a UCP2 é uma das UCPs com maior nível de expressão em diversas regiões cerebrais (Richard *et al.*, 1998; Sanchis *et al.*, 1998; Strobel *et al.*, 1998; Richard *et al.*, 1999). Sua atividade no cérebro tem sido relacionada com vários mecanismos neuronais (Horvath *et al.*,

1999), estando envolvida em DA, epilepsia e isquemia cerebral (Nègre-Salvayre *et al.*, 1997; Horvath *et al.*, 1999; Andrews *et al.*, 2005; Brand & Esteves, 2005; Dietrich *et al.*, 2008; Andrews & Horvath, 2009). Além de ter papel determinante em doenças do SNC, a proteína UCP2 também é importante para o funcionamento normal de algumas regiões cerebrais (Coppola *et al.*, 2007; Andrews *et al.*, 2008; Dietrich *et al.*, 2008; Andrews *et al.*, 2009; Andrews & Horvath, 2009). O aumento na expressão tecidual de UCP2 está relacionada a um aumento na produção de ATP e diminuição da produção de ROS (Echtay *et al.*, 2002; Brand & Esteves, 2005; Mailloux & Harper, 2011).

Apesar do importante papel que a atividade mitocondrial exerce na função neuronal, existe uma carência de trabalhos mostrando uma importante função fisiológica da plasticidade mitocondrial na função cerebral em adultos. Uma das nossas hipóteses nesta tese é que exercício promove aumento da atividade metabólica do cérebro com consequente aumento da atividade mitocondrial e tal adaptação é essencial para os efeitos plásticos do exercício no cérebro. Aqui, mostramos que o exercício aumenta função mitocondrial no hipocampo de camundongos e tal efeito é dependente da expressão de UCP2 (Dietrich *et al.*, 2008). A ausência de UCP2 evita que o exercício tenha um efeito positivo da sinaptogênese hipocampal (ver "Exercise-Induced Synaptogenesis in the Hippocampus Is Dependent on UCP2-Regulated Mitochondrial Adaptation") (Dietrich *et al.*, 2008). No capítulo II, parte II (ver "The role of mitochondrial uncoupling proteins in lifespan"), abordamos de uma maneira mais extensa a função das proteínas desacopladoras (UCPs) (Dietrich & Horvath, 2010).

Em outros dois artigos incluídos nos Anexos desta tese, mostramos outros efeitos do exercício físico no SNC. Primeiro, mostramos que o exercício pode

influenciar a nocicepção e ser uma alternativa para o descobrimento de novas rotas terapêuticas (ver “Physiological modulation of the purinergic system induced by exercise influences nociception in mice: investigation of the mechanism of action”). Segundo, comparamos os efeitos do exercício e de uma dieta rica em gorduras na sinalização cerebral em uma área importante para funções cognitivas e mostramos que tais intervenções atuam em rotas independentes (ver “Different Effect of High Fat Diet and Physical Exercise in the Hippocampal Signaling”).

Regulação neuroendócrina do controle do apetite

Em mamíferos, o balanço energético possui somente dois constituintes, sendo eles a ingesta calórica e o gasto calórico. A ingesta calórica é, principalmente, vinculada ao consumo de alimentos e bebidas. A regulação do gasto energético é bastante mais complexo: existe um gasto calórico basal do organismo que está relacionado com as funções autonômicas deste individuo; existe ainda um gasto relacionado com a atividade metabólica deste individuo que, em estados não patológicos, está vinculada com atividade física.

O organismo como um todo está envolvido na regulação do balanço energético, com órgãos periféricos enviando sinais metabólicos para o cérebro, e vice-versa, para regular o balanço energético a curto e também a longo prazo. Mínimas alterações na homeostase do balanço energético acarretam consequências severas para o metabolismo. Por exemplo, em um indivíduo que ingere aproximadamente 3000 kcal/dia, um gasto calórico de 2970 kcal/dia levaria a um balanço energético positivo de 30 kcal/dia. Isso resulta em um balanço positivo de aproximadamente 12000 kcal ao longo de um ano. Como o depósito biológico de calorias é o tecido adiposo, então essas 12000 kcal se depositariam na forma de gordura no corpo. Como 1g de gordura

contém 9 kcal, essas 12000 kcal formariam mais de 1 kg de tecido adiposo por ano. Se tal desregulação do balanço energético se mantiver por 10 anos, por exemplo, então este indivíduo acumulará mais de 10 kg de tecido adiposo, levando inexoravelmente a um quadro de obesidade severa. A natureza desta desregulação do balanço energético ainda é desconhecida. O estilo de vida da sociedade moderna que associa sedentarismo (baixo gasto calórico) ao alto consumo de alimentos ricos em gorduras e açucares simples (alta ingesta calórica) é certamente o maior contribuinte para tal cenário. Além destes, outros fatores também contribuem para uma desregulação do balanço energético, como altos níveis de estresse e privação do sono. Os mecanismos moleculares e também os circuitos cerebrais envolvidos em orquestrar tal regulação são de singular importância para o entendimento da fisiologia da regulação do apetite e, consequentemente, para a elaboração de melhores estratégias de prevenção e tratamento de doenças crônicas dela decorrentes.

O cérebro como regulador central da ingesta de alimentos

O cérebro é uma parte essencial na regulação da ingestão e do gasto calórico, entretanto é importante também lembrar que diversos outros tecidos produzem substancias (hormônios, citocinas) que afetam por sua vez a função cerebral. Portanto, uma sinalização apropriada entre os órgãos periféricos e o cérebro é fator essencial para manutenção e regulação do balanço energético.

O cérebro tem uma estrutura complexa com uma rede de circuitos neurais envolvidos na regulação do apetite. Os primeiros estudos que inicialmente identificaram estruturas cerebrais importantes na regulação do balanço energético datam do inicio do século XX. Essas primeiras evidencias sugeriram que a parte mais basal do cérebro, hoje conhecida como hipotálamo, estava envolvida no controle das

funções homeostáticas. Nos anos 1940, estudos mais detalhados identificaram mais precisamente os núcleos que regulam o balanço energético em mamíferos. Nestes estudos, lesões de estruturas mediais do hipotálamo basal causaram hiperfagia e obesidade (Ranson *et al.*, 1938; Hetherington & Ranson, 1942; Hetherington, 1944; Brobeck, 1946; Anand & Brobeck, 1951a; Hetherington & Ranson, 1983). Essa região no hipotálamo médio-basal foi identificada como sendo o núcleo ventromedial do hipotálamo (VMH), sendo então considerado o 'centro da saciedade' no cérebro. Por outro lado, lesões bilaterais em regiões mais laterais do hipotálamo levaram a completa cessação da ingesta de alimento, e tal região foi identificada como 'centro da fome' (Anand & Brobeck, 1951b). Esta visão clássica de 'dois-centros' na regulação do apetite ainda é usada hoje em dia e vários trabalhos científicos tem confirmado esses dados com técnicas mais modernas.

Na parte mais medial e basal do hipotálamo encontra-se um núcleo com forma arqueada, assim chamado de núcleo arqueado do hipotálamo (ARC). Estudos com lesões neste núcleo não identificaram nenhum papel na regulação do balanço energético. Entretanto, estudos posteriores que utilizaram lesões químicas com glutamato monosódico que seletivamente causavam a morte de uma subpopulação de neurônios no ARC levaram a identificação deste centro como um local crítico na regulação do balanço energético (Brecher & Waxler, 1949; Marshall *et al.*, 1955; Olney, 1969; 1971). Roedores tratados com glutamato monosódico tornaram-se obesos, enfatizando a importância de células sensíveis a este químico na resposta anorexígena. Estes últimos resultados junto com os estudos anteriores que utilizaram lesões mecânicas completas do ARC - sem nenhum efeito no balanço energético - levaram a hipótese de que um grupo de células com função antagônica aquelas sensíveis ao glutamato monosódico deveriam existir. Essas células deveriam,

portanto, possuir uma função orexigênica. Essas primeiras observações foram muito importantes na descoberta do sistema das melanocortinas, que é critico na regulação energética pelo ARC.

O sistema de melanocortinas do ARC como crítico sensor do balanço energético

O ARC está localizado na região mais basal e medial do cérebro, ao lado do terceiro ventrículo, tendo importância singular na regulação de diversas respostas neuroendócrinas e homeostáticas. No ARC parece haver uma especialização da barreira hemato-encefálica (BBB), permitindo o acesso de elementos sanguíneos no interstício celular com grande permeabilidade (Broadwell & Brightman, 1976; Broadwell *et al.*, 1983; Norsted *et al.*, 2008). No ARC, estão localizados duas populações de neurônios que são críticos na regulação do apetite e na resposta neuroendócrina(Cone, 2005). Por um lado estão os neurônios produtores de NPY (Tatemoto *et al.*, 1982; Clark *et al.*, 1984; Stanley & Leibowitz, 1984) e AgRP (conhecidos como neurônios NPY/AgRP) (Hahn *et al.*, 1998), que estimulam o apetite quando ativados (resposta orexigênica) (Aponte *et al.*, 2011; Krashes *et al.*, 2011). Esses neurônios também produzem o neurotransmissor inibitório GABA (Horvath *et al.*, 1997), o qual é essencial para a resposta orexigênica exercida por esses neurônios (Dietrich & Horvath, 2009b; Wu *et al.*, 2009). Os neurônios NPY/AgRP enviam projeções para diversos outros núcleos do cérebro (Broberger *et al.*, 1998; Cone, 2005), sendo de vital importância para regulação do apetite as projeções para o núcleo paraventricular (PVN) e para o núcleo parabraquial (PBN) (Wu *et al.*, 2008b; Wu *et al.*, 2009). A importância crucial destes neurônios pode ser evidenciada nos diversos estudos em que os neurônios NPY/AgRP foram seletivamente eliminados levando a diminuição do apetite e, finalmente, morte por

inanição (Bewick *et al.*, 2005b; Gropp *et al.*, 2005; Luquet *et al.*, 2005; Wu *et al.*, 2008a; Wu *et al.*, 2008b; Wu *et al.*, 2009).

A outra população de neurônios no ARC com função na regulação do apetite e no balanço energético produz neuropeptídios derivados da POMC (Cone, 2005). Esses neurônios se caracterizam por expressar o gene da *pomc* e *cart*. Alfa-MSH é um dos produtos da degradação enzimática da POMC, sendo liberado no interstício se ligando aos receptores de melanocortina (MC3R e MC4R). A ativação dos neurônios POMC leva a cessação da ingesta calórica e saciedade (Zigman & Elmquist, 2003). A natureza oposta destas duas populações de neurônios no ARC explica porque lesões mecânicas desta região possuem pouco ou nenhum efeito na regulação do apetite. É também de extrema relevância enfatizar a peculiar rede intercelular que ocorre no ARC entre os neurônios NPY/AgRP e os neurônios POMC. Os neurônios NPY/AgRP enviam projeções inibitórias, GABAérgicas, para os neurônios POMC (Horvath *et al.*, 1992; Cowley *et al.*, 2001; Pinto *et al.*, 2004), inibindo a atividade destas células. Portanto, uma resposta que provoque o estímulo do apetite pode induzir a ingesta calórica através de um mecanismo redundante: (i) ativando os neurônios NPY/AgRP e (ii) concomitantemente inibindo os neurônios POMC. Esse mecanismo redundante no controle da ingesta calórica possui um aspecto positivo sob a ótica evolutiva, apresentando um mecanismo constitutivo em que a resposta orexigênica é preferida à resposta anorexigênica.

Plasticidade sináptica modula a resposta neuroendócrina do ARC

Estudos realizados pelo famoso fisiologista inglês, Sir Charles Sherrington, propuseram há mais de dois séculos que o controle da ingesta calórica deveria estar sob controle similar àquele da respiração, em que órgãos periféricos produzem

substâncias que viajam pela corrente sanguínea e sinalizam o cérebro. Essa hipótese começou a ser desvendada nos anos 1950 com estudos realizados nos laboratórios Jax, estudando os camundongos obesos e diabéticos que ocorriam naturalmente nas colônias de animais deste instituto. Os camundongos obesos foram primeiramente descritos no ano 1950, como animais que espontaneamente se tornavam morbidamente obesos devido a uma mutação recessiva (chamada ob/ob) (INGALLS *et al.*, 1950). O gene da obesidade (ob) foi posteriormente descoberto no cromossoma 6 dos camundongos (Zhang *et al.*, 1994).

Nos anos 1950-70, parabiose foi uma das poucas técnicas disponíveis para identificar se fatores sanguíneos poderiam influenciar funções fisiológicas. Com esta técnica, foi possível ligar cirurgicamente a circulação sanguínea de dois animais e estudar se fatores humorais de um animal poderiam influenciar o outro. Pesquisas lideradas por Coleman utilizaram parabiose para estudar o 'fator perdido' nos camundongos ob/ob (Coleman & Hummel, 1969; Coleman, 1973). Quando um camundongo ob/ob foi unido cirurgicamente com um camundongo normal, o peso corporal do camundongo obeso começou a diminuir gradativamente até atingir níveis de normalidade, indicando que um fator humoral do camundongo normal estava sinalizando o camundongo obeso a perder peso. Experimento similar foi realizado com o camundongo diabético (db/db) (Hummel *et al.*, 1966; Coleman, 1973; 1982). Quando o camundongo db/db foi unido por parabiose com o camundongo normal, não foi observada nenhuma variação no peso corporal do camundongo db/db (que além de diabético também desenvolve obesidade mórbida). Entretanto, neste último caso, o camundongo normal perdeu peso até entrar em inanição completa. Portanto, um fator produzido pelo camundongo db/db levava a cessação da ingesta calórica e perda de peso no camundongo normal (Coleman & Hummel, 1969; Coleman, 1973;

1982). Anos depois, uma pesquisa liderada por Jeffrey Friedman da Universidade de Rockefeller, identificou o gene envolvido no fenótipo de obesidade dos camundongos ob/ob (Coleman, 1978; Zhang *et al.*, 1994). A proteína sintetizada a partir do produto deste gene foi chamada de leptina, do grego *leptos*, magro. Após esta descoberta, o gene envolvido no fenótipo dos camundongos db/db também foi revelado, o qual codifica o receptor de leptina (Chen *et al.*, 1996). Essas descobertas tornaram claro porque o camundongo db/db era resistente ao fator humoral do camundongo normal (leptina) nos estudos de parabiose. A Leptina foi identificada principalmente no tecido adiposo. Os animais db/db, que eram obesos, tinham elevada produção de leptina que atuava nos camundongos normais ligados por parabiose, levando estes à inanição.

Após a descoberta da leptina, diversos grupos começaram a estudar como este hormônio produzido pelo tecido adiposo entrava no cérebro e sinalizava a regulação do apetite. Em 2004, uma pesquisa liderada por Tamas Horvath na Universidade de Yale (no laboratório do qual eu realizei parte dos estudos contidos nesta tese) revelou um importante mecanismo envolvido na adaptação do ARC a estímulos periféricos (Pinto *et al.*, 2004). Utilizando animais transgênicos que permitiam a identificação dos neurônios NPY/AgRP e POMC com proteínas fluorescentes, os autores desta descoberta viram que leptina promove um rápido rearranjo dos circuitos neuronais que são responsáveis por governar o balanço energético. Quando camundongos ob/ob deficientes em leptina foram comparados com camundongos controles, eles apresentaram um aumento no número de sinapses excitatórias nos neurônios NPY/AgRP, com concomitante diminuição no número de sinapses inibitórias nestas mesmas células. O oposto foi observado nos neurônios POMC. Quando os animais ob/ob foram tratados com leptina, essas alterações sinápticas se modificaram em

direção àquelas dos animais controles, indicando que tais mecanismos de plasticidade sináptica são sensíveis a estímulos periféricos que regulam o balanço energético.

Informação mais detalhada sobre os mecanismos implicados nesta regulação sináptica e na regulação neuroendócrina do apetite podem ser encontradas em um estudo de revisão realizado como parte desta dissertação (Ver "Feeding signals and brain circuitry") (Dietrich & Horvath, 2009a). Outros dois estudos contidos nesta dissertação analisam o possível impacto de tais mecanismos no controle do apetite através da revisão e comentário critico de dois artigos publicados na revista *Cell* (Ver "GABA keeps up an appetite for life" e "Synaptic plasticity of feeding circuits: hormones and hysteresis") (Dietrich & Horvath, 2009b; 2011).

Em anexo nesta dissertação podem ainda ser encontrados diversos capítulos que discutem vários aspectos da regulação neuroendócrina do balanço energético:

(i) em "Megalin mediates the transport of leptin across the blood-CSF barrier" é exposta a descoberta de um dos transportadores de leptina no SNC;

(ii) nos capítulos "Nesfatin-1-regulated oxytocinergic signaling in the paraventricular nucleus causes anorexia through a leptin-independent melanocortin pathway", Peroxisome proliferation-associated control of reactive oxygen species sets melanocortin tone and feeding in diet-induced obesity" e "Loss of autophagy in proopiomelanocortin neurons perturbs axon growth and causes metabolic dysregulation", são apresentados resultados adicionais que dissecam o sistema de melanocortinas em nível de biologia molecular, celular e comportamental;

(iii) no capítulo "Evidence that obesity is associated with hypothalamic injury in rodent models and humans", são apresentadas evidencias que indicam que obesidade se associa com lesão tecidual no hipotálamo de animais e humanos;

(iv) nos capítulos “Wired for hunger: the brain and obesity and Anorexia nervosa: a mortal clash between reward and hunger” e “Neural regulation of food intake and energy balance (Pôster)”, são apresentados produções bibliográficas destinadas ao ensino e a divulgação da ciência. Esse material é destinado ao público geral e não somente ao público especializado em pesquisa médica básica.

A função da proteína Sirt1 e seu envolvimento com os neurônios reguladores do apetite

O estudo dos mecanismos celulares que regulam a função dos neurônios NPY/AgRP e POMC é importante para a compreensão de como sinais extracelulares e modificações intracelulares levam a mudanças na atividade celular e, consequentemente, no comportamento animal.

Nos últimos 4 anos, diversos estudos feitos por nosso grupo buscaram averiguar tais mecanismos intracelulares. Uma das vias de sinalização que inicialmente estudamos foi a sinalização por sirtuinas. Essa fazem parte de uma família de deacetilases que utilizam NAD+ para sua atividade enzimática (Imai *et al.*, 2000), altamente conservadas na escala evolutiva (Brachmann *et al.*, 1995). Devido ao fato de que sirtuinas possuem atividade ligada às concentrações de NAD+, essas enzimas são consideradas sensores metabólicos celulares. Um extensa revisão sobre as principais sirtuinas está em fase de preparação e pode ser encontrada nos anexos desta dissertação (ver “Sirtuins and Metabolism”). Entre as sirtuinas, focamos nossos estudos na proteína Sirt1. Sirt1 é uma proteína cuja função tem sido relacionada aos benefícios da restrição calórica (Kaeberlein *et al.,* 1999; Lin *et al.*, 2000; Tissenbaum & Guarente, 2001; Cohen *et al.*, 2004; Rogina & Helfand, 2004; Chen *et al.*, 2005a). Restrição calórica é uma forma de balanço energético negativo crônico. A relação

entre Sirt1 e balanço energético negativo é corroborado por estudos que mostram que restrição de nutrientes promove aumento na expressão e/ou atividade de Sirt1 em diversos tecidos (Cohen *et al.*, 2004; Ramadori *et al.*, 2008). A ativação de Sirt1 em períodos de balanço energético negativo parece ser essencial para as adaptações metabólicas que ocorrem em tais momentos (Liu *et al.*, 2008). Essa semelhança entre a função de Sirt1 e os efeitos da restrição calórica indica que áreas do cérebro que promovem as adaptações ao balanço energético negativo, como os neurônios NPY/AgRP, poderiam necessitar a atividade de Sirt1 para promover tais adaptações. Neste dissertação, nós testamos esta hipótese e dois capítulos discutem diretamente esta questão (ver "AgRP neurons mediate Sirt1's action on the melanocortin system and energy balance: roles for sirt1 in neuronal firing and synaptic plasticity" e "Sirt1 in the AgRP neurons is necessary for exploratory behavior during calorie restriction") (Dietrich *et al.*, 2010). Adicionalmente, o papel da proteína Sirt1 no metabolismo periférico também foi estudado no contexto da sinalização de leptina através da proteína Stat3 no fígado (Ver anexo "Stat3 inhibition of gluconeogenesis is down-regulated by Sirt1") (Nie *et al.*, 2009).

A descoberta da função da proteína Sirt1 nos neurônios NPY/AgRP (Dietrich *et al.*, 2010) gerou diversas novas áreas de pesquisas no nosso grupo. Os neurônios NPY/AgRP que antes eram tidos como reguladores do balanço energético, são agora também relacionados com a regulação do desenvolvimento cerebral e da resposta a drogas de abuso e comportamento motivacional não relacionado com alimentação. Essa ideia é apresentada e discutida em um dois capítulos (Ver "AgRP neurons regulate the development of dopamine neuronal plasticity and non food-associated behaviors" e "Physiological roles of hunger-promoting neurons and implications for anti-obesity drugs"). As implicações de tais descobertas e uma avaliação crítica da

pesquisa na área da regulação hipotalâmica do apetite com consequências para a elaboração de tratamentos para combater obesidade são apresentadas no capítulo “Physiological roles of hunger-promoting neurons and implications for anti-obesity drugs”.

Objetivos

O objetivo principal desta tese é estudar os diversos aspectos envolvidos nos efeitos do exercício físico no cérebro e da função do hipotálamo na regulação do balanço energético e outras funções comportamentais. Buscamos estudar as adaptações que ocorrem desde o nível celular até o nível comportamental, focando no papel do sistema nervoso central (SNC) em roedores.

Os objetivos específicos de cada capítulo e também dos anexos desta tese estão contidos na introdução de cada capítulo/anexo, respectivamente.

PARTE II

Onde os resultados são apresentados na forma de artigos científicos.

Capítulo I. Exercise-induced synaptogenesis in the hippocampus is dependent on UCP2-regulated mitochondrial adaptation

Artigo publicado no periódico *Journal of Neuroscience*.

Brief Communications

Exercise-Induced Synaptogenesis in the Hippocampus Is Dependent on UCP2-Regulated Mitochondrial Adaptation

Marcelo O. Dietrich,[1,2,3,4] **Zane B. Andrews,**[1,2,3,5] **and Tamas L. Horvath**[1,2,3]

[1]Section of Comparative Medicine and Departments of [2]Obstetrics, Gynecology, and Reproductive Sciences and [3]Neurobiology, Yale University School of Medicine, New Haven, Connecticut 06520, [4]Programa de Pós-graduação em Bioquímica de Bioquímica, Universidade Federal do Rio Grande do Sul, 90035-003 Porto Alegre, RS, Brazil, and [5]Department of Physiology, Monash University, Clayton, Victoria 3183 Australia

Mitochondria are essential organelles in neurons providing appropriate energetic needs to maintain resting and action potentials as well as to modulate synaptic plasticity. Although neuronal events underlie various behavioral events, the behavior itself, such as voluntary exercise, feeds back to affect neuronal morphology and function as well as glial morphology and function. The hippocampal formation is a main site of synaptic plasticity induced by voluntary exercise. Here we show that voluntary exercise induces uncoupling protein 2 (UCP2) mRNA expression and mitochondrial oxygen consumption in coupled as well as uncoupled respiratory states in the hippocampus. These changes in mitochondrial metabolism coincided with an increase in mitochondrial number and dendritic spine synapses in granule cells of the dentate gyrus and the stratum radiatum of the CA1 region and were dependent on UCP2 expression, because in UCP2 knock-out mice such changes were not observed. Together, these observations reveal that a mitochondrial mechanism related to UCP2 function is essential for appropriate bioenergetic adaptation of neurons to increased neuronal activity and synaptic plasticity in response to exercise.

Key words: **physical activity; mitochondria respiration; uncoupling activity; synaptic plasticity; exercise; dendritic spine**

Introduction

Exercise is a behavioral intervention widely known to promote brain plasticity (Cotman and Berchtold, 2002). Regular exercise in rodents promotes hippocampal plasticity, increasing neurogenesis (van Praag et al., 1999a), long-term potentiation (van Praag et al., 1999b), and angiogenesis (Lopez-Lopez et al., 2004). These effects are coupled to mechanisms that increase energy demand in this brain area. Indeed, exercise enhances glucose uptake (Lopez-Lopez et al., 2004). These mechanisms must be coupled to oxidative energy transformation, dependent on mitochondrial respiration and the supply of energy substrates.

Uncoupling proteins (UCPs) are involved in mitochondrial processes and were first described as regulators of heat production in peripheral brown adipose tissue. One of these mitochondrial proteins, UCP2, is found in the CNS and has been implicated in various neuronal mechanisms (Andrews et al., 2005a). We and others have shown that UCP2 is involved in neuroprotection in mice models of Parkinson's disease (Andrews et al., 2005b; Conti et al., 2005), epilepsy (Diano et al., 2003), and stroke (Mattiasson et al., 2003) as well as in normal functioning of the nigrostriatal dopamine system (Andrews et al., 2006) and the arcuate nucleus melanocortin system (Coppola et al., 2007; Andrews et al., 2008). Induction of UCP2 expression in the brain by cellular stress increases the overall production of ATP, perhaps as a result of stimulation of mitochondrial proliferation, while decreasing superoxide production and associated damage (Bechmann et al., 2002; Diano et al., 2003, Andrews et al., 2005b, 2008).

Despite the important role that the mitochondria play in neuronal functions, there is a paucity of information regarding the potential direct role of this organelle in neuronal function and plasticity in the adult brain. An elegant study by Li et al. (2004) provided *in vitro* evidence that there is a dynamic mitochondrial response to neuronal activation and that this process is associated with synaptic plasticity, especially synaptogenesis and spine formation. The objective of our present study was to reveal whether there may be an *in vivo* correlate of such a mitochondrial process and, if so, whether this mechanism may be regulated by UCP2. We studied exercise-induced changes in the hippocampus in wild-type (UCP2wt) and UCP2 knock-out (UCP2ko) animals.

Materials and Methods

Animals. Adult (3–4 months old) male and female mice were used in this study. UCP2ko mice were generated as described previously (Zhang et al., 2001) and were kindly provided by Dr. Bradford Lowell (Beth Israel Deaconess Medical Center and Harvard Medical School, Boston, MA). Mice were maintained in a 12 h light/dark cycle with water and food provided *ad libitum*, housed in rat cages (to accommodate the running wheel; $n = 4$ per cage) equipped with a freely running wheel for 4 weeks. Sedentary (sed) controls were also maintained in rat cages but without the running wheel. Ten animals were analyzed for each readout. All procedures were approved by the Institutional Animal Care and Use

Received June 16, 2008; revised Aug. 24, 2008; accepted Sept. 11, 2008.

This work was supported by National Institutes of Health Grants DK 074386, DK 060711, DK 080000, and AG 022880 (T.L.H.). M.O.D. was supported by Conselho Nacional de Desenvolvimento Científico e Tecnológico, and Z.B.A. was the recipient of a New Zealand Foundation for Research Science and Technology Fellowship. We are indebted to Marya Shanabrough and Erzsebet Borok for their superb technical assistance and Dr. Brad Lowell for providing breeding pairs of UCP2 knock-out mice.

Correspondence should be addressed to Tamas L. Horvath, Section of Comparative Medicine, Yale University School of Medicine, 375 Congress Avenue, LSOG 117, New Haven, CT 06520. E-mail: tamas.horvath@yale.edu.

DOI:10.1523/JNEUROSCI.2744-08.2008

 0270-6474/08/2810766-06$15.00/0

Committee of Yale University. Wheel running activity was monitored at random times during the dark and light cycle.

Semiquantitative reverse transcription-PCR. Frozen hippocampus tissue was thawed into Trizol. RNA and cDNA were prepared as described previously (Diano et al., 2003). Reverse transcription-PCR was performed as described previously (Horvath et al., 2003) using primers for UCP2 (forward, 5′-CTACAAGACCATTGCACGAGAGG-3′; reverse, 5′-AGCTGCTCATAGGTGACAAACAT-3′), UCP4 (forward, 5′-GTGAAGGTCCAGATGCAAATG-3′; reverse, 5′-CATTCTCAGCCACGAGGG-3′), and UCP5 (forward, 5′-TGGGGTAGTGTCAGGAGTGATTTC-3′; reverse, 5′-AATGATGTTCCAGGGTCCAAGTC-3′). Specificity of amplification was confirmed by sequencing bands from test reactions. Amplification threshold values were measured, and endpoint reaction samples were run on 1% agarose gels in ethidium bromide to confirm the size and intensity of bands detected. UCP1 and UCP3 mRNAs were not assessed, because these transcripts have not been found in the brain (Andrews et al., 2005a).

Mitochondrial isolation and respiration measurements. The hippocampus was rapidly dissected and homogenized in the isolation buffer (215 mM mannitol, 75 mM sucrose, 0.1% fatty acid-free BSA, 20 mM HEPES, and 1 mM EGTA, pH adjusted to 7.2 with KOH). The homogenate was spun at 1300 × *g* for 3 min, the supernatant was removed, and the pellet was resuspended with isolation buffer and spun again at 1300 × *g* for 3 min. The two sets of supernatants from each sample were topped off with isolation buffer and spun at 13,000 × *g* for 10 min. The supernatant was discarded, and the step was repeated. After this second spin at 13,000 × *g*, the supernatant was discarded, and the pellets were resuspended with isolation buffer without EGTA and spun at 10,000 × *g* for 10 min. The final synaptosomal pellet was resuspended with 50 μl of isolation buffer without EGTA. Protein concentrations were determined with a BCA protein assay kit (Pierce). Mitochondrial respirations were assessed using a Clark-type oxygen electrode (Hansatech Instruments) at 37°C with pyruvate and malate (5 and 2.5 mM) as oxidative substrates in respiration buffer (215 mM mannitol, 75 mM sucrose, 0.1% fatty acid-free BSA, 20 mM HEPES, 2 mM MgCl, and 2.5 mM KH_2PO_4, pH adjusted to 7.2 with KOH). With the addition of oligomycin, uncoupled proton conductance was measured. Total respiration capacity was also measured after the addition of the photonophore carbonyl cyanide 4-(trifluoromethoxy) phenylhydrazone (FCCP). For analysis of ADP-dependent, coupled respiration, ADP was added after the addition of oxidative substrates.

Electron microscopy. Vibratome sections (50 μm thick) were cut from blocks of tissue containing the hippocampus and washed in 0.1 M phosphate buffer (PB). Sections were osmicated (15 min in 1% osmium tetroxide in PB) and dehydrated in increasing ethanol concentrations. During the dehydration, 1% uranyl acetate was added to the 70% ethanol to enhance ultrastructural membrane contrast. Dehydration was followed by flat embedding in Araldite. Ultrathin sections were cut on a Leica ultra microtome, collected on Formvar-coated single-slot grids, and analyzed with a Tecnai 12 Biotwin (FEI) electron microscope.

Quantitative synaptology and counting of mitochondria. The analysis of synapse number was performed in an unbiased manner (Pinto et al., 2004; Horvath and Gao, 2005; Diano et al., 2006) and is presented as number of synapses per cubic micrometer of tissue.

Mitochondrial number was determined using the optical dissector method on electron micrographs (Diano et al., 2003; Coppola et al., 2007). Sections to be sampled were randomly selected, and smaller grid areas (100 μm^2) were chosen from within each section in a similar systematic random manner. Within each area, an optical section was established between the surfaces of the tissue section, thus creating a three-dimensional sampling area of known dimensions. All mitochondrial planes within this area were counted, provided that they did not cross three of the borders of the sampling boxes considered as exclusionary borders. The counts obtained from these sampling boxes were determined and represent the number of mitochondria per unit volume of the structure of interest.

Statistical analysis. An *F* test analysis revealed a significant nonhomogeneity of variances between groups. The Kruskal–Wallis one-way nonparametric ANOVA was selected for multiple statistical comparisons. The Mann–Whitney *U* test was used to determine significance of differences between groups. $p < 0.05$ was considered statistically significant.

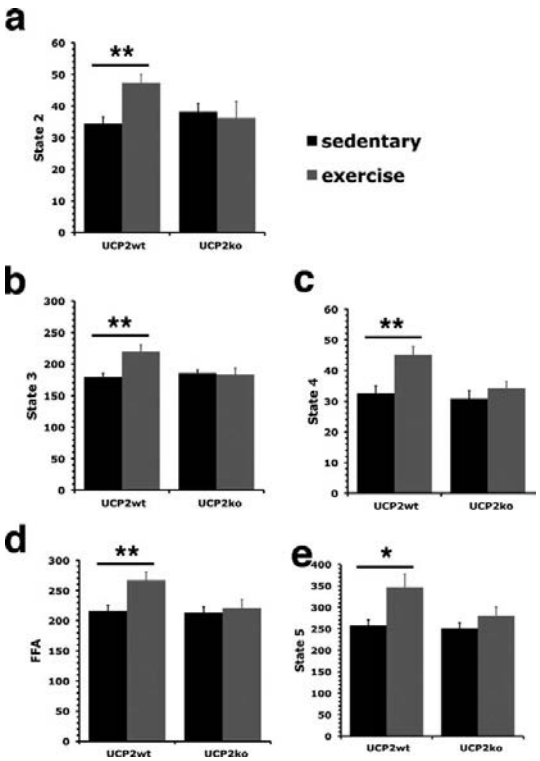

Figure 1. Mitochondrial respiration in sedentary ($n = 10$ of each genotype) and exercised ($n = 10$ of each genotype) UCP2wt and UCP2ko mice. ***a***, State 2 respiration after addition of palmitate/malate in the respiration buffer. ***b***, State 3 respiration induced by ADP. ***c***, State 4, representing respiration after addition of oligomycin, an H^+-transporting ATP synthase inhibitor. ***d***, FFA-induced mitochondrial respiration. ***e***, Total uncoupling activity after addition of FCCP. In the histograms, the *y*-axis units are nanomoles of O_2 per minute per milligram of protein. $^*p < 0.05$; $^{**}p < 0.01$. Error bars represent SEM.

Results

Exercise-induced hippocampal mitochondrial respiration is dependent on UCP2

We first explored whether voluntary exercise in mice, which induces hippocampal cell activation (Czurkó et al., 1999), could promote mitochondrial adaptation. First we determined that exercise induces increased UCP2 gene expression in wild-type mouse hippocampus (120 ± 10% compared with sedentary values; $p < 0.05$). No changes were observed in UCP4 (93 ± 5%) or UCP5 (91 ± 12%) mRNA expressions, and no effect was detected on either UCP4 or UCP5 gene expression in UCP2ko animals (data not shown). When UCP2 expression was analyzed in a gene trap knock-out line in which LacZ is inserted in the UCP2 gene (Horvath et al., 2002), we observed the most dense β-galactosidase-labeled nuclei in the granule layer of the dentate gyrus (DG), whereas few labeled cells could also be found in the pyramidal layer of the CA3 and CA1 regions (data not shown).

Next we studied the effects of exercise on mitochondrial respiration of wild-type and UCP2 knock-out mice. Voluntary

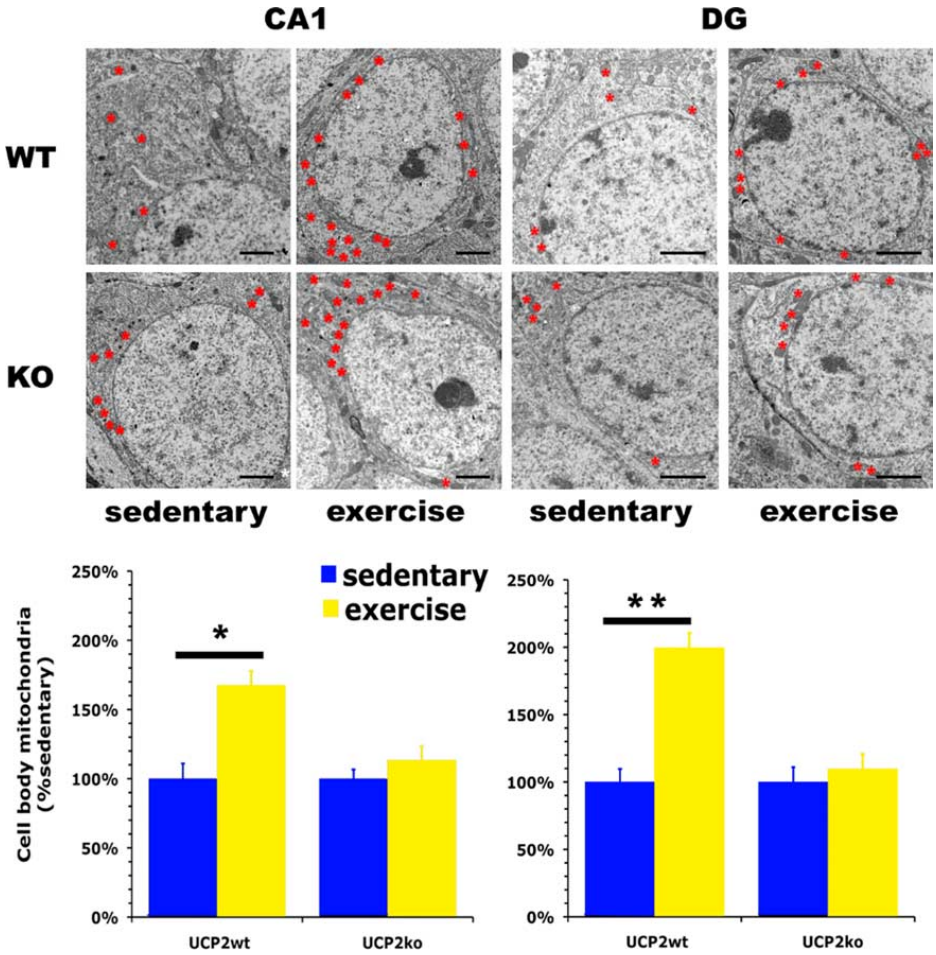

Figure 2. Mitochondrial number in the cell body of neurons from the dentate gyrus and CA1 of sedentary ($n = 10$ of each genotype) and exercised ($n = 10$ of each genotype) UCP2wt and UCP2ko mice. Top, Representative electron microscopic images of neuronal cell bodies with mitochondria marked in red. Bottom left, Histogram representing a quantitative analysis of mitochondrial number in cell bodies of CA1 pyramidal neurons. Bottom right, Histogram representing mitochondrial number in DG neurons. Scale bars, 1 μm. *$p < 0.05$; **$p < 0.01$. Error bars represent SEM.

exercise, which was not significantly different ($p > 0.05$) between wild-type (3487 ± 246 m/d; mean ± SEM) and UCP2 knock-out mice (3195 ± 176 m/d; mean ± SEM), induced elevations in oxygen consumption in all states of mitochondrial respiration in wild-type but not in knock-out mice (Fig. 1): state 2 [UCP2wt: sed, 34.46 ± 2.13; exercised (exe), 47.38 ± 2.64; UCP2ko: sed, 38.24 ± 2.55; exe, 36.25 ± 5.13 nmol $O_2 \cdot min^{-1} \cdot mg^{-1}$ protein], state 3 (mitochondrial respiration coupled to ATP production; UCP2wt: sed, 179.31 ± 5.52; exe, 219.32 ± 11.03; UCP2ko: sed, 185.18 ± 5.25; exe, 183.05 ± 10.77 nmol $O_2 \cdot min^{-1} \cdot mg^{-1}$ protein), state 4 (base uncoupled respiration; UCP2wt: sed, 32.59 ± 2.31; exe, 45.02 ± 2.77; UCP2ko: sed, 30.95 ± 2.40; exe, 34.11 ± 2.25 nmol $O_2 \cdot min^{-1} \cdot mg^{-1}$ protein), free-fat acid (FFA)-induced uncoupled respiration (UCP2wt: sed, 216.43 ± 8.80; exe, 264.14 ± 13.31; UCP2ko: sed, 213.15 ± 9.71; exe, 220.71 ± 14.05 nmol $O_2 \cdot min^{-1} \cdot mg^{-1}$ protein), and FCCP-induced oxygen consumption (UCP2wt: sed, 257.41 ± 13.46; exe, 346.78 ± 30.15; UCP2ko: sed, 250.91 ± 13.06; exe, 279.94 ± 20.86 nmol $O_2 \cdot min^{-1} \cdot mg^{-1}$ protein).

Exercise increases cell body mitochondrial number in hippocampal neurons dependent on UCP2

Because we determined that exercise increases mitochondrial respiration and was dependent on UCP2, we further explored whether exercise could alter mitochondria number. Compared with sedentary controls, 4 weeks of voluntary exercise increased the number of cell body mitochondria in neurons of the CA1 region by 67% (sedentary, 0.29 ± 0.03; exercise 0.49 ± 0.05 mitochondria/μm^2 cytoplasm area; $p < 0.001$) and of the DG by 99% (sedentary, 0.29 ± 0.03; exercise, 0.57 ± 0.06 mitochondrion/μm^2 cytoplasm area; $p < 0.001$) in UCP2wt mice (Fig. 2). As seen with mitochondrial respiration, exercise did not increase the number of mitochondria in the hippocampal cell bodies of UCP2ko mice either in the CA1 region (sedentary, 0.39 ± 0.03; exercise, 0.45 ± 0.04 mito-

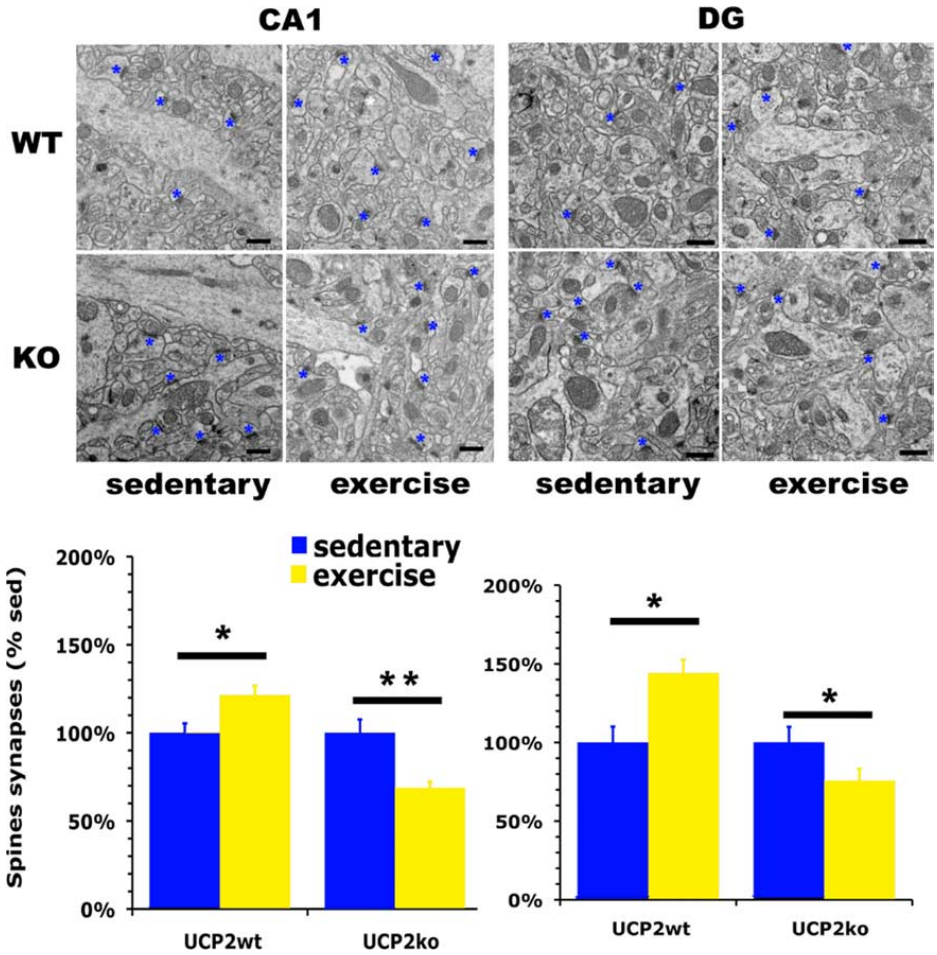

Figure 3. Spine synapse counts of neurons from the dentate gyrus and CA1 of sedentary ($n = 10$ of each genotype) and exercised ($n = 10$ of each genotype) UCP2wt and UCP2ko mice. Top, Representative electron microscopic images of spine synapses marked in blue. Bottom left, Histogram representing a quantitative analysis of spine synapse number in CA1 pyramidal neurons. Bottom right, Histogram representing spine synapse number in DG neurons. Scale bars, 1 μm. *$p < 0.05$; **$p < 0.01$. Error bars represent SEM.

chondria/μm^2 cytoplasm area; $p > 0.05$) or in the DG (sedentary, 0.40 ± 0.04; exercise, 0.44 ± 0.05 mitochondria/μm^2 cytoplasm area; $p > 0.05$) (Fig. 2). Interestingly, in sedentary animals, the number of mitochondria in these neuronal populations was higher in UCP2ko mice than in UCP2wt mice (CA1: 135.24 ± 6.64%, $p < 0.05$; DG: 139.43 ± 10.98, $p < 0.05$). Note that the respiration measurements were analyzed from synaptosomal preparations, which contain high level of mitochondria from axon terminals. We suggest that similar to our recent findings in specific hypothalamic neuronal populations (Andrews et al., 2008), UCP2-mediated increase in mitochondria number is present in both the perikarya and axon terminals.

Exercise-induced hippocampal synaptogenesis is coupled to UCP2 expression

Because exercise has been proposed to induce synaptic plasticity (Cotman and Berchtold, 2002), we also assessed the number of spine synapses on dendritic spines of granule cells in the DG and pyramidal cells of the stratum radiatum of the CA1 region in UCP2wt and UCP2ko mice (Fig. 3). Exercise increased the number of synapses in UCP2wt mice in both the CA1 [121.25 ± 5.44% (sed, 1.66 ± 0.09; exe, 2.10 ± 0.11 spine synapses/μm^3); $p < 0.05$] and DG [144.08 ± 8.53% (sed, 1.10 ± 0.11; exe, 1.59 ± 0.14 spine synapses/μm^3); $p < 0.01$]. UCP2ko mice, after exercise, presented a paradoxical response with a decreased number of synapses in the CA1 [68.70 ± 3.63% (sed, 2.04 ± 0.15; exe, 1.40 ± 0.05 spine synapses/μm^3); $p < 0.001$] and DG [75.63 ± 7.51% (sed, 1.73 ± 0.17; exe, 1.31 ± 0.10 spine synapses/μm^3); $p < 0.05$]. Similar to the results on mitochondria number, sedentary UCP2ko showed a higher number of synapses than sedentary UCP2wt mice (CA1: 122.87 ± 7.59%, $p < 0.05$; DG: 156.58 ± 9.99%, $p < 0.001$).

Discussion

This study revealed that voluntary exercise in mice increases mitochondrial respiration, mitochondria number, and spine synapse density in the dentate gyrus and the CA1 region of the

hippocampus, all of which are dependent on UCP2. In addition, UCP2ko mice manifested decrease in the number of synapses in both the CA1 and DG neurons in response to voluntary exercise, emphasizing the critical role for this mitochondrial protein in bioenergetic adaptation of neurons to increased cellular activity.

In certain species, the brain is responsible for ~10% of the total energy expenditure, whereas in humans this value rises to 20%. The brain is a tissue with high metabolic rate; it has been shown that ~90% of all of the brain's energy is used to maintain basal neuronal resting and action potentials (Attwell and Laughlin, 2001). Thus, slight increases in overall neuronal activity can generate a great increase in brain energy consumption. Physical exercise in rodents increases neuronal activity in the hippocampus (Czurkó et al., 1999). This occurs with a concomitant increase in the mechanisms of energy supply and energy usage by neurons and glial cells. Some authors have shown that exercise increases angiogenesis, an important mechanism by which tissue can be better supplied with nutrients and thus increase the metabolic capacity (Lopez-Lopez et al., 2004). Also, exercise-induced increases in mitochondrial activity and number have been described in muscle, an important adaptation to the high metabolic demand placed on this tissue during physical exercise (Irrcher et al., 2003). Our results showed similar mechanisms in hippocampal neurons with exercise inducing mitochondrial respiration and number, which in turn is likely to contribute to an overall increase in ATP production (Diano et al., 2003; Andrews et al., 2005a).

Our data reinforce the role of uncoupling proteins in promoting brain plasticity and their participation in physiological and pathological adaptations of the brain. Moreover, because exercise protects the brain against a myriad of injuries, and because of our finding that exercise-induced both mitochondrial and synaptic plasticity were dependent on UCP2 expression, these data can be taken together with previously published findings to strengthen the assertion that UCP2 is important in neuroprotection (Bechmann et al., 2002; Diano et al., 2003; Mattiasson et al., 2003; Andrews et al., 2005b). Indeed, these data highlight the role of UCPs as possible new targets of brain therapies with likely implications for many brain pathologies that are associated with energy deficits such as Parkinson's disease, schizophrenia, epilepsy, Alzheimer's disease, and many others.

Interestingly, we showed that in response to exercise, UCP2ko mice exhibited a decrease in the number of spine synapses on dendritic terminals of hippocampal neurons. This is consistent with the possibility that exercise-induced neuronal activation triggers increased free radical production, a process that is not counteracted by UCP2 in these transgenic animals (Andrews et al., 2005a,b, 2008). In absence of appropriate mitochondrial uncoupling, a physiological stimulus such as exercise that normally promotes positive brain plasticity can, in fact, result in a deleterious effect, perhaps because of increased production of free radicals. UCP2 has been shown to be a radical scavenger (Echtay et al., 2002; Produit-Zengaffinen et al., 2007; Giardina et al., 2008), which is one of the likely mechanisms via which UCP2 can exert a protective effect on cellular and synaptological adaptations to increased workload on hippocampal neuron triggered by increased voluntary exercise.

Together, our results reveal a new mechanism of exercise-induced brain plasticity through a mitochondria-dependent pathway related to the expression of UCP2.

References

Andrews ZB, Horvath B, Barnstable CJ, Elsworth J, Yang L, Beal MF, Roth RH, Matthews RT, Horvath TL (2005a) Uncoupling protein-2 is critical for nigral dopamine cell survival in a mouse model of Parkinson's disease. J Neurosci 25:184–191.

Andrews ZB, Diano S, Horvath TL (2005b) Mitochondrial uncoupling proteins in the CNS: in support of function and survival. Nat Rev Neurosci 6:829–840.

Andrews ZB, Rivera A, Elsworth JD, Roth RH, Agnati L, Gago B, Abizaid A, Schwartz M, Fuxe K, Horvath TL (2006) Uncoupling protein-2 promotes nigrostriatal dopamine neuronal function. Eur J Neurosci 24:32–36.

Andrews ZB, Liu Z-W, Walllingford N, Erion DM, Borok E, Friedman JM, Tschöp MH, Shanabrough M, Cline G, Shulman GI, Coppola A, Gao X-B, Horvath TL, Diano S (2008) UCP2 mediates ghrelin's action on NPY/AgRP neurons by lowering free radicals. Nature 454:846–851.

Attwell D, Laughlin SB (2001) An energy budget for signaling in the grey matter of the brain. J Cereb Blood Flow Metab 21:1133–1145.

Bechmann I, Diano S, Warden CH, Bartfai T, Nitsch R, Horvath TL (2002) Brain mitochondrial uncoupling protein 2 (UCP2): a protective stress signal in neuronal injury. Biochem Pharmacol 64:363–367.

Conti B, Sugama S, Lucero J, Winsky-Sommerer R, Wirz SA, Maher P, Andrews Z, Barr AM, Morale MC, Paneda C, Pemberton J, Gaidarova S, Behrens MM, Beal F, Sanna PP, Horvath T, Bartfai T (2005) UCP2 protects catecholaminergic neurons from acute MPTP toxicity. J Neurochem 93:493–501.

Coppola A, Liu ZW, Andrews ZB, Paradis E, Roy MC, Friedman JM, Ricquier D, Richard D, Horvath TL, Gao XB, Diano S (2007) A central thermogenic-like mechanism in feeding regulation: an interplay between arcuate nucleus T3 and UCP2. Cell Metab 5:21–33.

Cotman CW, Berchtold NC (2002) Exercise: a behavioral intervention to enhance brain health and plasticity. Trends Neurosci 25:295–301.

Czurkó A, Hirase H, Csicsvari J, Buzsáki G (1999) Sustained activation of hippocampal pyramidal cells by 'space clamping' in a running wheel. Eur J Neurosci 11:344–352.

Diano S, Matthews RT, Patrylo P, Yang L, Beal MF, Barnstable CJ, Horvath TL (2003) Uncoupling protein 2 prevents neuronal death including that occurring during seizures: a mechanism for preconditioning. Endocrinology 144:5014–5021.

Diano S, Farr SA, Benoit SC, McNay EC, da Silva I, Horvath B, Gaskin FS, Nonaka N, Jaeger LB, Banks WA, Morley JE, Pinto S, Sherwin RS, Xu L, Yamada KA, Sleeman MW, Tschöp MH, Horvath TL (2006) Ghrelin controls hippocampal spine synapse density and memory performance. Nat Neurosci 9:381–388.

Echtay KS, Roussel D, St-Pierre J, Jekabsons MB, Cadenas S, Stuart JA, Harper JA, Roebuck SJ, Morrison A, Pickering S, Clapham JC, Brand MD (2002) Superoxide activates mitochondrial uncoupling proteins. Nature 415:96–99.

Giardina TM, Steer JH, Lo SZ, Joyce DA (2008) Uncoupling protein-2 accumulates rapidly in the inner mitochondrial membrane during mitochondrial reactive oxygen stress in macrophages. Biochim Biophys Acta 1777:118–129.

Horvath B, Spies C, Horvath G, Kox WJ, Miyamoto S, Barry S, Warden CH, Bechmann I, Diano S, Heemskerk J, Horvath TL (2002) Uncoupling protein 2 (UCP2) lowers alcohol sensitivity and pain threshold. Biochem Pharm 64:369–374.

Horvath TL, Gao XB (2005) Input organization and plasticity of hypocretin neurons: possible clues to obesity's association with insomnia. Cell Metab 1:279–286.

Horvath TL, Diano S, Miyamoto S, Barry S, Gatti S, Alberati D, Livak F, Lombardi A, Moreno M, Goglia F, Mor G, Hamilton J, Kachinskas D, Horwitz B, Warden CH (2003) Uncoupling proteins-2 and 3 influence obesity and inflammation in transgenic mice. Int J Obes Relat Metab Disord 27:433–442.

Irrcher I, Adhihetty PJ, Joseph AM, Ljubicic V, Hood DA (2003) Regulation of mitochondrial biogenesis in muscle by endurance exercise. Sports Med 33:783–793.

Li Z, Okamoto K, Hayashi Y, Sheng M (2004) The importance of dendritic mitochondria in the morphogenesis and plasticity of spines and synapses. Cell 119:873–887.

Lopez-Lopez C, LeRoith D, Torres-Aleman I (2004) Insulin-like growth

factor I is required for vessel remodeling in the adult brain. Proc Natl Acad Sci U S A 101:9833–9838.

Mattiasson G, Shamloo M, Gido G, Mathi K, Tomasevic G, Yi S, Warden CH, Castilho RF, Melcher T, Gonzalez-Zulueta M, Nikolich K, Wieloch T (2003) Uncoupling protein-2 prevents neuronal death and diminishes brain dysfunction after stroke and brain trauma. Nat Med 9:1062–1068.

Pinto S, Roseberry AG, Liu H, Diano S, Shanabrough M, Cai X, Friedman JM, Horvath TL (2004) Rapid rewiring of arcuate nucleus feeding circuits by leptin. Science 304:110–115.

Produit-Zengaffinen N, Davis-Lameloise N, Perreten H, Bécard D, Gjinovci A, Keller PA, Wollheim CB, Herrera P, Muzzin P, Assimacopoulos-Jeannet F (2007) Increasing uncoupling protein-2 in pancreatic beta cells does not alter glucose-induced insulin secretion but decreases production of reactive oxygen species. Diabetologia 50:84–93.

van Praag H, Kempermann G, Gage FH (1999a) Running increases cell proliferation and neurogenesis in the adult mouse dentate gyrus. Nat Neurosci 2:266–270.

van Praag H, Christie BR, Sejnowski TJ, Gage FH (1999b) Running enhances neurogenesis, learning, and long-term potentiation in mice. Proc Natl Acad Sci U S A 96:13427–13431.

Zhang CY, Baffy G, Perret P, Krauss S, Peroni O, Grujic D, Hagen T, Vidal-Puig AJ, Boss O, Kim YB, Zheng XX, Wheeler MB, Shulman GI, Chan CB, Lowell BB (2001) Uncoupling protein-2 negatively regulates insulin secretion and is a major link between obesity, beta cell dysfunction, and type 2 diabetes. Cell 105:745–755.

Capítulo II. The role of mitochondrial uncoupling proteins in lifespan

Artigo publicado no periódico *Pflugers Archives - European Journal of Physiology*.

Pflugers Arch - Eur J Physiol (2010) 459:269–275
DOI 10.1007/s00424-009-0729-0

INTEGRATIVE PHYSIOLOGY

The role of mitochondrial uncoupling proteins in lifespan

Marcelo O. Dietrich · Tamas L. Horvath

Received: 12 August 2009 / Accepted: 26 August 2009 / Published online: 17 September 2009

Abstract The increased longevity in modern societies raised the attention to biological interventions that could promote a healthy aging. Mitochondria are main organelles involved in the production of adenosine triphosphate (ATP), the energetic substrate for cellular biochemical reactions. The production of ATP occurs through the oxidative phosphorylation of intermediate substrates derived from the breakdown of lipids, sugars, and proteins. This process is coupled to production of oxygen reactive species (ROS) that in excess will have a deleterious role in cellular function. The damage promoted by ROS has been emphasized as one of the main processes involved in senescence. In the last decades, the discovery of specialized proteins in the mitochondrial inner membrane that promote the uncoupling of proton flux (named uncoupling proteins–UCPs) from the ATP synthase shed light on possible mechanisms implicated in the buffering of ROS and consequently in the process of aging. UCPs are responsible for a physiological uncoupling that leads to decrease in ROS production inside the mitochondria. Thus, induction of uncoupling through UCPs could decrease the cellular damage that occurs during aging due to excess of ROS. This review will focus on the evidence supporting these mechanisms.

Keywords Aging · Mitochondria · Free radical · Oxidative phosphorylation · ATP

M. O. Dietrich · T. L. Horvath (✉)
Section of Comparative Medicine,
Yale University School of Medicine,
New Haven, CT 06520, USA
e-mail: tamas.horvath@yale.edu

M. O. Dietrich
Programa de Pós-graduação em Bioquímica,
Department of Biochemistry,
Universidade Federal do Rio Grande do Sul,
Porto Alegre, RS 90035, Brazil

T. L. Horvath
Departments of Obstetrics,
Gynecology and Reproductive Sciences,
Yale University School of Medicine,
New Haven, CT 06520, USA

T. L. Horvath
Neurobiology, Yale University School of Medicine,
New Haven, CT 06520, USA

The last two centuries have seen an increase in longevity in Western civilizations, mainly due to advances in medicine. This has been accompanied by an increase in the incidence of chronic diseases related to growing older. Thus, understanding the mechanisms implicated in the aging process has become a significant component in the treatment of these age-related diseases. Diverse hypotheses have been proposed to elucidate the biological properties of aging. One important theory that attempts to explain the harmful events that occur during aging concerns the role of reactive oxygen species (ROS) in promoting cellular damage, including damage to DNA, proteins, and cellular membranes. These deleterious effects could accumulate over the years leading to cellular dysfunction, and eventually, death. The predominant organelle involved in the production of ROS, and in its elimination, is the mitochondria. Mitochondria are located in the cytosol of eukaryotic cells, and are also involved in the production of energy. Indeed, the presence of mitochondria in eukaryotic cells is essential for survival, and only a few subtypes of cells exist with minimal cellular functions that can survive without mitochondria-derived ATP production. Curiously enough, this organelle is responsible for the production of the most important substrate for cellular function, ATP, but also for the most harmful molecules, ROS. Thus, an appropriate balance between ATP production and ROS buffering is essential to maintain cellular homeostasis. This review will focus on the role of mitochondria uncoupling proteins (UCP), specifically

UCP2, in the maintenance of this balance, emphasizing its role in the aging process.

Mitochondrial oxidative phosphorylation: the core of energy production

Metabolic intermediates derived from the breakdown of proteins, fatty acids, and sugars enter the mitochondria and are the substrates for the oxidative machinery to produce energy in the form of ATP. The oxidation of these substrates produces free energy, which is stored in special reduced carriers, such as flavin adenine dinucleotide ($FADH_2$) and nicotinamide adenine dinucleotide (NADH). These carriers will donate electrons to the mitochondrial respiratory complex located in the inner mitochondrial membrane. Complexes of enzymatic proteins, called complexes I, II, III, IV, and V compose the respiratory machinery. The donation of electrons from reduced carriers (NADH and $FADH_2$) to complexes I and II starts the process of pumping protons from the mitochondrial matrix into the mitochondrial intermembrane space, generating an electrochemical gradient, where the mitochondrial membrane potential ($\Delta\Psi_m$) is one of its components. Utilizing additional electron carriers, such as coenzyme Q and cytochrome C, complexes III and IV of the respiratory chain are activated and further increase the $\Delta\Psi_m$. The presence of protons in the intermembrane space together with the difference in membrane potential between this space and the mitochondrial matrix is the driving force for the conversion of adenosine diphosphate (ADP) to ATP by the ATP synthase (F_O–F_1 subunits, complex V). The phosphorylation of ADP to ATP is coupled to a flux of protons through the ATP synthase, which will pump the protons back to the mitochondrial matrix, reducing the difference in the mitochondrial membrane potential. The activity of the ATPase complex V is a rate-limiting step in the generation of ATP through mitochondrial respiration. Different metabolic conditions can variously modulate the coupling of mitochondrial respiration to the production of ATP. However, even in the best coupled condition, the machinery involved in the mitochondrial production of ATP is not perfectly efficient. Indeed, there are forms of dissipation of energy within the inner membrane of the mitochondria, for example, the "proton leak" which is not coupled to ATP production, and will decrease the efficiency of the respiratory complex.

Uncoupling the ATP synthase pump

The proton leak shuttles the protons from the intermembrane space back to the mitochondrial matrix reducing the number of protons flowing through the ATP synthase. Since the protons located in the intermembrane space are derived from oxidative metabolism, the proton leak dissipates the energy from the oxidative substrates. There are several forms of proton leak, as for example the passage of protons through pores in the lipids of the mitochondrial membrane. Another form of "proton leak" in the inner mitochondrial membrane is carried by specialized uncoupling proteins [30]. UCPs are members of the superfamily of mitochondrial anion transporters that contains about 40 proteins, including different carriers and transporters. The key strategy of UCPs is to regulate the flux of protons through the ATP synthase. Indeed, the phosphorylation of ADP by ATP synthase is regulated by the levels of ATP, which can in turn inhibit mitochondrial respiration. Thus, uncoupling the proton flux is an adaptative pathway to avoid inhibition of the mitochondrial respiration.

Mitochondrial uncoupling proteins

The first UCP described was UCP1, which has been shown to control the brown adipose tissue (BAT)-regulated thermogenesis [39]. In the BAT, the proton leak through UCP1 is a tightly regulated mechanism that utilizes energy from the oxidation of intermediate substrates to generate heat. The BAT-regulated thermogenesis by UCP1 is important in several physiological conditions, for example, during cold exposure, arousal from hibernation, in newborns and in overfed mammals [15]. More recently, it has been shown to be functional in adult humans, as well [17, 52].

Our knowledge to date concerning the role of UCPs is based mostly on studies utilizing UCP1 as the classic model. Structurally, UCPs have a tripartite configuration that contains three repeats of approximately 100 amino acids. Each repeat has two hydrophobic regions that extend across the inner mitochondrial membrane corresponding to alpha helices. These two alpha helices are connected by a long hydrophilic loop oriented towards the matrix side of the inner mitochondrial membrane, whereas the amino and carboxyl termini extend into the intermembrane space [36]. The functional UCP is a homodimer [28] that, therefore, contains 12 alpha helices. This complex is believed to form a hydrophilic channel, the access of which is regulated by gates formed by the hydrophilic loops [3]. The presence of 12 alpha helices in the functional structure of UCPs is a common feature to most of the anion carriers and channel proteins, and unifies the UCP family, even though the amino acid structure of some UCPs has very low identity.

UCPs are expressed in a myriad of species, including mammals and plants. In mammals, five different UCP homologues have been described, UCP1-5, that contain

different levels of identity. Compared to UCP1, the archetypal UCP, UCP2 [22] and UCP3 [12] have high levels of amino acid identity (59% and 57%, respectively). UCP4 [34] and UCP5 [45] (also known as BMCP1) have low levels of identity (30% and 33%, respectively).

Distribution of UCPs

UCP1, the classic UCP, is expressed exclusively in the BAT. UCP2 is more broadly expressed [40, 41, 44], occurring in many tissues, including the pancreatic ß-cells [54], cells of the immune system [4], and several neuronal populations in different brain nuclei [43]. In the brain, UCP2 is highly expressed in the hypothalamus in several nuclei important for the coordination of basic autonomic functions. Additionally, UCP2 is also expressed in high levels in the nucleus of the solitary tract (important for autonomic regulation), in neurons of the limbic system (important for higher cognitive tasks), and in dopaminergic neurons in the midbrain (which are impaired in Parkinson's disease) [18, 26, 41, 42, 53].

UCP3 is highly expressed in the skeletal muscle, and to a lesser extent in the heart and BAT [12, 24, 51]. Interestingly, in skeletal muscle, UCP3 is the only UCP that is expressed at the protein level [12]. Indeed, the expression of UCP homologues in different tissues is highly modulated at the posttranscriptional level, since in many cases the messenger RNA (mRNA) was identified, but the protein levels were not [41, 44, 46].

The role and distribution of the other two UCPs, UCP4, and UCP5, are more obscure. Their expression is more specific to the central nervous system, where both UCP4 [34] and UCP5 [27, 45] have a more widespread pattern of expression than UCP2. Further research to understand the basic aspects of these UCPs is warranted.

ROS production in the mitochondrial respiratory chain

The oxidative stress hypothesis to explain senescence proposes that reducing the production of reactive oxygen species within the mitochondria will concomitantly decrease their deleterious effects [8, 48]. Classically, complexes I and III have been described as the main producers of ROS (superoxide) in the mitochondria. Complex I seems to produce most of the superoxide, even though the relative contribution of other complexes to total superoxide production may vary greatly depending on the tissue analyzed [6, 7]. The high levels of superoxide produced by complex I utilizes reverse electron transport from the oxidation of succinate in complex II. Worthy of note is the observation that superoxide is produced mainly on the matrix side of the inner membrane, and is unable to cross it. Thus, due to its highly deleterious effects, it is essential that mechanisms exist to detoxify superoxide in the mitochondrial matrix. The most important of these mechanisms is the dismutation of superoxide $\left(O_2^- \rightarrow O_2 + H_2O_2\right)$, a process that occurs spontaneously. However, in biological tissues this process is not sufficiently fast enough to avoid its damaging effects to other molecules. In this scenario, the presence of superoxide dismutase (SOD) enzymes that accelerate this process is essential to maintain cellular homeostasis. In fact, the lack of either of the two major forms of SOD (SOD1 and SOD2) has a major impact on longevity in several organisms due to increased superoxide-induced cellular damage [31]. In addition to the production of superoxide in the respiratory chain, growing evidence indicates that other enzymes located within the mitochondria are capable of producing ROS and can play a role in the process of aging, as well [2, 50].

Thus, the development of strategies to decrease ROS production or damage is a key target for the study of senescence given the free radical theory. Copious amounts of research have been done in an attempt to elucidate the effect of various antioxidant agents against the damage promoted by ROS. This review will not analyze these sets of data, but will focus on the evidence that uncoupling the proton flux can minimize the production of superoxide, acting at the step before the damage occurs.

Interplay between superoxide and UCPs

The role of uncoupling in modulating the production of free radicals in the mitochondria was proposed a decade ago [13, 38, 47]. In the first report, Negre-Salvayre [38] and colleagues showed that the inhibitory effect of guanosine diphosphate (GDP) in mitochondrial uncoupling was accompanied by an increase in membrane potential and H_2O_2 production. The authors correlated their findings in tissues that showed low and high expressions of UCP1 or UCP2, demonstrating a lack of effect of GDP in tissues with low (or virtually absent) expression of both UCPs [38]. The authors concluded that inhibition of uncoupling by GDP was responsible for increasing the membrane potential due to the loss of proton leak, and it lead to increased ROS production. Subsequently, in plant mitochondria, Kowaltowski et al. [29] corroborated these observations showing that activity of mitochondrial uncoupling proteins decreases membrane potential and inhibit the formation of ROS at the level of the semiquinone forms of coenzyme Q.

Years later, the effect of ROS to activate UCPs in mammalian cells was shown by research headed by Martin

Brand and colleagues. They revealed strong evidence that superoxide (or one of its related metabolites) was capable of activating the proton conductance of UCPs on the matrix side of the inner mitochondrial membrane [20]. The superoxide-induced uncoupling required fatty acids and was inhibited by purine nucleotides [19]. The mechanism by which superoxide activates UCPs is still not completely understood, but accumulating evidence suggests that lipid peroxidation by ROS generates reactive alkenals which will, in turn, activate UCPs [20, 37]. These observations suggest that the interaction between ROS and UCPs functions as a mechanism to decrease levels of free radical concentrations inside the mitochondria and to reduce the consequent deleterious effects.

The role of UCPs in senescence

The studies highlighted above have immediate implications in several medical fields that postulate a role for mitochondrial free radical production as an underlying cause of many pathological processes and aging. Thus, a description of the putative cascade of events by which UCPs could regulate ROS production and damage inside the mitochondria can be drawn. This cascade of events could unfold as follows. An increase in cell metabolism due to high energy demand generates a concomitant increase in metabolic intermediates. These intermediates are used inside the mitochondria for oxidative phosphorylation of ADP to produce ATP. This process occurs through the mitochondrial respiratory chain in the inner membrane of the mitochondria and also generates superoxide, mainly by complexes I and III. The flux of electrons through the complexes in the electron transport chain is coupled to a flux of protons from the mitochondrial matrix to the intermembrane space, thereby increasing the difference in membrane potential. This difference in membrane potential is the driving force for ATPase to generate ATP from ADP + Pi. The superoxide radicals produced in complexes I and III cause local lipid peroxidation in the inner mitochondrial membrane. This peroxidation generates aldehydic lipid peroxidation intermediates that act directly upon UCPs (2 and 3) to stimulate proton leak. Additionally, other molecules such as fatty acids (and other endogenous activators) promote a mild uncoupling activity. This uncoupling of proton flux through the ATPase decreases the difference in membrane potential, thereby reducing the rate of ATP formation and decreasing the production of superoxide in complexes I and III. However, the presence of uncoupling activity promotes an ideal milieu for constant ATP production, since in the absence of uncoupling, high ATP production due to increased differences in membrane potential can cause inhibition of mitochondrial respiration. Additionally, high levels of oxidative phosphorylation can cause increases in superoxide formation, leading to undesired damage to the mitochondrial membrane, DNA and protein complexes. Also relevant to note, the mild uncoupling activity that is taken into account in this model differs from a high (almost complete) uncoupling activity that would halt the proton flux through the ATP synthase, and consequently the production of ATP.

Several lines of evidence suggest that the cascade of events outlined above are involved in aging, and that uncoupling the proton flux through UCPs (mainly UCP2) is a critical pathway in the regulation of senescence. This idea was first raised by Martin Brand [13] and was called the "uncoupling-to-survive" hypothesis of aging. In support of this idea, studies indicated that a stronger resistance to oxidative damage by ROS was positively correlated with enhanced longevity in several species [21, 32], including mammals [25]. In 2004, another correlative study published by Speakman et al. [49] found that mice in the upper quartile of metabolic intensity (measured by food assimilation divided by body weight) lived longer, had higher resting oxygen consumption, and higher mitochondrial uncoupling when compared to mice in the lowest quartile. Even though this study was based purely on correlations, it provided the first experimental evidence in support of the role of mitochondrial uncoupling in extending lifespan. Subsequent work has shown that calorie restriction, the only known intervention that reliably increases lifespan [11], induces an increase in the expression of both mRNA and protein levels of UCP2 and UCP3 in mice [9, 10, 35]. When Swiss albino mice were treated with low doses of the uncoupling agent 3,4-dinitrophenol, they exhibited a phenotype that resembled that of calorie restriction: decreased ROS production, reduced oxidative damage, improved metabolic parameters, and increased longevity [14].

The first attempt to study the direct effects of UCPs in senescence came in 2005 by Fridell and collaborators [23]. In this work, the authors overexpressed the human UCP2 (hUCP2) in adult fly neurons, and found an extension of lifespan in both male and female flies. In these transgenic flies, they found an increase in state 4 respiration (the respiration that occurs in the absence of ADP due to proton leak), and a decrease in ROS production and oxidative damage. Additionally, the long-lived hUCP2 flies showed no changes in physical activity or reproduction [23], thus, emphasizing the specificity of the transgenic fly in enhancing lifespan. In 2006, another elegant study by Conti et al. [16] showed the effect of selective overexpression of UCP2 in neurons and its role in longevity. The authors generated a transgenic mouse that overexpressed UCP2 selectively in the hypocretin neurons (Hcrt-UCP2) of the lateral hypothalamus (LH). They found that these mice have reduced body temperature and increased lifespan

compared to controls, an effect that is similar to that seen during calorie restriction. The authors provided evidence that this effect was due to elevated temperature in the central thermostat, which is located in a region adjacent to the LH [16].

Altogether, these data strongly implicate UCPs (mainly UCP2) in playing a role in the regulation of lifespan and confirms the "uncoupling-to-survive" hypothesis. However, in 2008 and 2009, three additional studies came out and provided more detailed data on the effects of UCP2 and UCP3 with regard to mammalian longevity. In an elegant study, Andrews and Horvath [1] showed that in rodents (rats and mice) mitochondrial uncoupling-induced (measured as the ratio between free fatty acids) respiration, and state 4 respiration increased during aging, an effect that was accompanied by increased levels of ROS and lipid peroxidation. When comparing both species (mice vs rats), the authors found that rats had significantly lower levels of mitochondrial uncoupling, ROS production, and lipid peroxidation. They correlated these results with the differences in longevity between rats and mice. In the same report, the authors studied the effect of UCP2 manipulations on the lifespan of mice utilizing different genetic approaches. First, wild-type mice were compared to UCP2 knockout mice (UCP2-/-). In this model, the UCP2-/- mice had a significantly shorter survival age. In another experiment, mice that overexpressed hUCP2 (hUCP2-Tg) were compared to their wild-type controls. In this set of data, the authors reported that hUCP2-Tg mice showed a delayed time of the first death, even though they had the same survival age as their controls. Subsequently, the authors backcrossed the UCP2 mutants with mice knocked out for superoxide dismutase 2 (SOD2). SOD2-/- mice have a severe phenotype, living no longer than 3 weeks [31]. The double knockout mice (SOD2-/-; UCP2-/-) had a significantly reduced lifespan when compared to SOD2-/-; UCP2 wild-type mice. The crossing of SOD2-/- with hUCP2-Tg mice increased the survival age compared to wild-type controls.

Two other studies lead by McDonald and collaborators [5, 35] elicited some contradictions on the topic of UCP2–3 and longevity. In these reports, the authors analyzed the phenotype of transgenic mice overexpressing UCP2/3, and also UCP2-/- and UCP3-/- mice. Overall, the authors reported that UCP3-/- mice presented minimal or no effects on their survival rate. When both UCP2/3 were overexpressed, the transgenic mice showed a slight increase in mean survival. However, the most conflicting result of these reports was the finding that UCP2-/- mice showed no difference in lifespan when compared to their wild-type littermates. This is in total opposition to what was found by Andrews and Horvath [1], and may be due to slight differences in their protocols [33].

Concluding remarks

In the last few years, growing evidence has been established to corroborate the theory of "uncoupling-to-survive," in which mitochondrial uncoupling is a key mechanism involved in the production and buffering of ROS and their associated damage. The major UCP involved in these processes seems to be UCP2, which is widely distributed throughout many tissues including the brain. In addition to the mechanisms highlighted in this review, there are other putative roles for the UCPs, such as the regulation of fatty acid metabolism, which will likely be implicated in the mechanisms of aging as well. Other functions of UCPs, including calcium transport, have been targets of intense debate, and much more investigation will be necessary to draw credible conclusions about the importance of UCPs in these processes.

Even though research in the field of mitochondrial uncoupling is progressing quickly and strong evidence exists to suggest a role of UCP manipulation in treating several pathological states, no good strategies have been put forward to date to be able to pharmacologically treat patients with specific and potent compounds. Thus, this remains a hot topic with more research needed that in all likelihood will provide significant advances in our understanding of several physiological and pathological states.

Acknowledgements MOD was partially supported by a fellowship from the Conselho Nacional de Pesquisa (CNPq), Brazil.

References

1. Andrews ZB, Horvath TL (2009) Uncoupling protein-2 regulates lifespan in mice. Am J Physiol Endocrinol Metab 296:E621–E627
2. Andreyev AY, Kushnareva YE, Starkov AA (2005) Mitochondrial metabolism of reactive oxygen species. Biochemistry (Mosc) 70:200–214
3. Arechaga I, Ledesma A, Rial E (2001) The mitochondrial uncoupling protein UCP1: a gated pore. IUBMB Life 52:165–173
4. Arsenijevic D, Onuma H, Pecqueur C et al (2000) Disruption of the uncoupling protein-2 gene in mice reveals a role in immunity and reactive oxygen species production. Nat Genet 26:435–439
5. Asami DK, McDonald RB, Hagopian K et al (2008) Effect of aging, caloric restriction, and uncoupling protein 3 (UCP3) on mitochondrial proton leak in mice. Exp Gerontol 43:1069–1076
6. Barja G (1998) Mitochondrial free radical production and aging in mammals and birds. Ann N Y Acad Sci 854:224–238
7. Barja G (1999) Mitochondrial oxygen radical generation and leak: sites of production in states 4 and 3, organ specificity, and relation to aging and longevity. J Bioenerg Biomembranes 31:347–366
8. Beckman KB, Ames BN (1998) The free radical theory of aging matures. Physiol Rev 78:547–581
9. Bevilacqua L, Ramsey JJ, Hagopian K et al (2004) Effects of short- and medium-term calorie restriction on muscle mitochondrial proton leak and reactive oxygen species production. Am J Physiol Endocrinol Metab 286:E852–E861

10. Bevilacqua L, Ramsey JJ, Hagopian K et al (2005) Long-term caloric restriction increases UCP3 content but decreases proton leak and reactive oxygen species production in rat skeletal muscle mitochondria. Am J Physiol Endocrinol Metab 289:E429–E438
11. Bishop NA, Guarente L (2007) Genetic links between diet and lifespan: shared mechanisms from yeast to humans. Nat Rev Genet 8:835–844
12. Boss O, Samec S, Paoloni-Giacobino A et al (1997) Uncoupling protein-3: a new member of the mitochondrial carrier family with tissue-specific expression. FEBS Lett 408:39–42
13. Brand MD (2000) Uncoupling to survive? The role of mitochondrial inefficiency in ageing. Exp Gerontol 35:811–820
14. Caldeira da Silva CC, Cerqueira FM, Barbosa LF et al (2008) Mild mitochondrial uncoupling in mice affects energy metabolism, redox balance and longevity. Aging Cell 7:552–560
15. Cannon B, Nedergaard J (2004) Brown adipose tissue: function and physiological significance. Physiol Rev 84:277–359
16. Conti B, Sanchez-Alavez M, Winsky-Sommerer R et al (2006) Transgenic mice with a reduced core body temperature have an increased life span. Science 314:825–828
17. Cypess AM, Lehman S, Williams G et al (2009) Identification and importance of brown adipose tissue in adult humans. N Engl J Med 360:1509–1517
18. Diano S, Urbanski HF, Horvath B et al (2000) Mitochondrial uncoupling protein 2 (UCP2) in the nonhuman primate brain and pituitary. Endocrinology 141:4226–4638
19. Echtay KS, Roussel D, St-Pierre J et al (2002) Superoxide activates mitochondrial uncoupling proteins. Nature 415:96–99
20. Echtay KS, Murphy MP, Smith RA et al (2002) Superoxide activates mitochondrial uncoupling protein 2 from the matrix side. Studies using targeted antioxidants. J Biol Chem 277:47129–47135
21. Feng J, Bussière F, Hekimi S (2001) Mitochondrial electron transport is a key determinant of life span in *Caenorhabditis elegans*. Dev Cell 1:633–644
22. Fleury C, Neverova M, Collins S et al (1997) Uncoupling protein-2: a novel gene linked to obesity and hyperinsulinemia. Nat Genet 15:269–272
23. Fridell YW, Sánchez-Blanco A, Silvia BA, Helfand SL (2005) Targeted expression of the human uncoupling protein 2 (hUCP2) to adult neurons extends life span in the fly. Cell Metab 1:145–152
24. Gong DW, He Y, Karas M, Reitman M (1997) Uncoupling protein-3 is a mediator of thermogenesis regulated by thyroid hormone, beta3-adrenergic agonists, and leptin. J Biol Chem 272:24129–24132
25. Holzenberger M, Dupont J, Ducos B et al (2003) IGF-1 receptor regulates lifespan and resistance to oxidative stress in mice. Nature 421:182–187
26. Horvath TL, Warden CH, Hajos M et al (1999) Brain uncoupling protein 2: uncoupled neuronal mitochondria predict thermal synapses in homeostatic centers. J Neurosci 19:10417–10427
27. Kim-Han JS, Reichert SA, Quick KL, Dugan LL (2001) BMCP1: a mitochondrial uncoupling protein in neurons which regulates mitochondrial function and oxidant production. J Neurochem 79:658–668
28. Klingenberg M, Appel M (1989) The uncoupling protein dimer can form a disulfide cross-link between the mobile C-terminal SH groups. Eur J Biochem 180:123–131
29. Kowaltowski AJ, Costa AD, Vercesi AE (1998) Activation of the potato plant uncoupling mitochondrial protein inhibits reactive oxygen species generation by the respiratory chain. FEBS Lett 425:213–216
30. Krauss S, Zhang CY, Lowell BB (2005) The mitochondrial uncoupling-protein homologues. Nature Rev Mol Cell Biol 6:248–261
31. Lebovitz RM, Zhang H, Vogel H et al (1996) Neurodegeneration, myocardial injury, and perinatal death in mitochondrial superoxide dismutase-deficient mice. Proc Natl Acad Sci USA 93:9782–9787
32. Lin SJ, Kaeberlein M, Andalis AA et al (2002) Calorie restriction extends *Saccharomyces cerevisiae* lifespan by increasing respiration. Nature 418:344–348
33. Lockie SH, Müller TD, Tschöp MH (2009) Coupled with uncouplers: the curious case of lifespan. Am J Physiol Endocrinol Metab 296:E619–E620
34. Mao W, Yu XX, Zhong A et al (1999) UCP4, a novel brain-specific mitochondrial protein that reduces membrane potential in mammalian cells. FEBS Lett 443:326–330
35. McDonald RB, Walker KM, Warman DB et al (2008) Characterization of survival and phenotype throughout the life span in UCP2/UCP3 genetically altered mice. Exp Gerontol 43:1061–1068
36. Miroux B, Frossard V, Raimbault S et al (1993) The topology of the brown adipose tissue mitochondrial uncoupling protein determined with antibodies against its antigenic sites revealed by a library of fusion proteins. EMBO J 12:3739–3745
37. Murphy MP, Echtay KS, Blaikie FH et al (2003) Superoxide activates uncoupling proteins by generating carbon-centered radicals and initiating lipid peroxidation: studies using a mitochondria-targeted spin trap derived from alpha-phenyl-N-tert-butylnitrone. J Biol Chem 278:48534–48545
38. Nègre-Salvayre A, Hirtz C, Carrera G et al (1997) A role for uncoupling protein-2 as a regulator of mitochondrial hydrogen peroxide generation. FASEB J 11:809–815
39. Nicholls DG, Locke RM (1984) Thermogenic mechanisms in brown fat. Physiol Rev 64:1–64
40. Pecqueur C, Alves-Guerra MC, Gelly C et al (1998) Distribution of the uncoupling protein 2 mRNA in the mouse brain. J Comp Neurol 397:549–560
41. Pecqueur C, Alves-Guerra MC, Gelly C et al (2001) Uncoupling protein 2, in vivo distribution, induction upon oxidative stress, and evidence for translational regulation. J Biol Chem 276:8705–8712
42. Richard D, Rivest R, Huang Q et al (1998) Distribution of the uncoupling protein 2 mRNA in the mouse brain. J Comp Neurol 397:549–560
43. Richard D, Clavel S, Huang Q et al (2001) Uncoupling protein 2 in the brain: distribution and function. Biochem Soc Trans 29:812–817
44. Ricquier D, Bouillaud F, Miroux B (2001) Uncoupling protein 2, in vivo distribution, induction upon oxidative stress, and evidence for translational regulation. J Biol Chem 276:8705–8712
45. Sanchis D, Fleury C, Chomiki N et al (1998) BMCP1, a novel mitochondrial carrier with high expression in the central nervous system of humans and rodents, and respiration uncoupling activity in recombinant yeast. J Biol Chem 273:34611–34615
46. Sivitz WI, Fink BD, Donohoue PA (1999) Fasting and leptin modulate adipose and muscle uncoupling protein: divergent effects between messenger ribonucleic acid and protein expression. Endocrinology 140:1511–1519
47. Skulachev VP (1998) Uncoupling: new approaches to an old problem of bioenergetics. Biochim Biophys Acta 1363:100–124
48. Sohal RS, Weindruch R (1996) Oxidative stress, caloric restriction, and aging. Science 273:59–63
49. Speakman JR, Talbot DA, Selman C et al (2004) Uncoupled and surviving: individual mice with high metabolism have greater mitochondrial uncoupling and live longer. Aging Cell 3:87–95
50. Tahara EB, Barros MH, Oliveira GA et al (2007) Dihydrolipoyl dehydrogenase as a source of reactive oxygen species inhibited by caloric restriction and involved in *Saccharomyces cerevisiae* aging. FASEB J 21:274–283

51. Vidal-Puig A, Solanes G, Grujic D et al (1997) UCP3: an uncoupling protein homologue expressed preferentially and abundantly in skeletal muscle and brown adipose tissue. Biochem Biophys Res Commun 235:79–82
52. van Marken Lichtenbelt WD, Vanhommerig JW, Smulders NM (2009) Cold-activated brown adipose tissue in healthy men. N Engl J Med 360:1500–1508
53. Yamada S, Isojima Y, Yamatodani A, Nagai K (2000) Uncoupling protein 2 influences dopamine secretion in PC12h cells. J Neurochem 87:461–469
54. Zhang CY, Baffy G, Perret P et al (2001) Uncoupling protein-2 negatively regulates insulin secretion and is a major link between obesity, beta cell dysfunction, and type 2 diabetes. Cell 105:745–755

Capítulo III. Feeding signals and brain circuitry

Artigo publicado no periódico *European Journal of Neuroscience*.

EJN fens EUROPEAN JOURNAL OF NEUROSCIENCE

European Journal of Neuroscience, Vol. 30, pp. 1688–1696, 2009 doi:10.1111/j.1460-9568.2009.06963.x

REVIEW ARTICLE
Feeding signals and brain circuitry

Marcelo O. Dietrich[1,2] and Tamas L. Horvath[1,3,4]
[1]Section of Comparative Medicine, Yale University School of Medicine, New Haven, CT 06520, USA
[2]Programa de Pós-graduação em Bioquímica, Department of Biochemistry, Universidade Federal do Rio Grande do Sul, Porto Alegre RS, Brazil
[3]Neurobiology, Yale University School of Medicine, New Haven CT 06520, USA
[4]Departments of Obstetrics, Gynecology and Reproductive Sciences, Yale University School of Medicine, New Haven, CT 06520, USA

Keywords: energy balance, obesity, reactive oxygen species, uncoupling proteins

Abstract

Food intake is a major physiological function in animals and must be entrained to the circadian oscillations in food availability. In the last two decades a growing number of reports have shed light on the hormonal, cellular and molecular mechanisms involved in the regulation of food intake. Brain areas located in the hypothalamus have been shown to play a pivotal role in the regulation of energy metabolism, controlling energy balance. In these areas, neuronal plasticity has been reported that is dependent upon key hormones, such as leptin and ghrelin, that are produced by peripheral organs. This review will provide an overview of recent discoveries relevant to understanding these issues.

Introduction

The 24-h cycle of biological, physiological and behavioral functions of living organisms, known as the circadian rhythm, was first observed in more modern history by J. S. Szymanski (Szymanski, 1918), who showed that animals were capable of maintaining 24-h activity patterns in the absence of external cues. The genetic basis for the mammalian circadian rhythm was discovered by J. Takahashi (Vitaterna *et al.*, 1994). However, looking back much further in time (a couple of billion years ago), perhaps the very first notion of circadian rhythms can be seen as a consequence of the production of light and UV radiation by the sun (Bonanno *et al.*, 2002). As a result, the energy derived from sunlight was a driving force in the evolution of the first living organisms (Roenneberg and Merrow, 2002). Subsequently, the early metazoans developed a migratory behavior to deep ocean waters during the daylight for protection from UV radiation (Gehring & Rosbash, 2003). The first terrestrial animals were probably nocturnal and only later did diurnal animals surge, once they evolved sufficient protection against UV radiation. Thus, the light–dark cycle as delimited by the Earth's rotation around the sun has had a major impact entraining the behavioral clock of animals.

In mammals, one of the most basic roles of the individual is to preserve the species through reproduction. In order to do so, the individual must seek and/or conserve energy at appropriate times to prevent compromising the organism's physiology. To this end, animal behaviors become entrained to the daily light cycle to synchronize feeding, rest, activity and putative reproductive cues. Even though sunlight is a major contributor to this daily (circadian) cycle, feeding *per se* also has an important role in entraining certain cell populations. Food intake provides the appropriate nutrient and energy substrates for the occurrence of biochemical reactions that generate oscillations in cellular metabolism. This is accompanied by hormonal fluctuations that will in turn regulate feeding and metabolism. This review focuses on the role of various nuclei of the hypothalamus, as well as the plasticity of these areas, in the regulation of feeding behavior governed by hormonal signals.

Correspondence: Dr Tamas L. Horvath, [1]Section of Comparative Medicine, as above.
E-mail: tamas.horvath@yale.edu

Received 28 May 2009, revised 19 July 2009, accepted 6 August 2009

The golden age of feeding research

Experiments conducted during the 1940s provided evidence that specific areas in the medial basal hypothalamus are important in the regulation of food intake. Lesions made to more medial areas lead to hyperphagia and obesity (Ranson *et al.*, 1938; Hetherington, 1941; Hetherington & Ranson, 1942; Hetherington, 1944; Brobeck *et al.*, 1943; Brobeck, 1946; Anand & Brobeck, 1951), while bilateral lesions in the lateral hypothalamus lead to cessation of food intake (Anand & Brobeck, 1951). Additionally, the results from studies in which chemical lesions were made to the arcuate nucleus and hypothalamic ventromedial nuclei corroborated the data collected from mechanical lesion studies (Brecher & Waxler, 1949; Marshall *et al.*, 1955a,b; Olney, 1969; Olney *et al.*, 1971). It was clear then that the hypothalamus was a key region involved in regulating metabolism, especially energy balance. Parallel studies using naturally obese (*ob/ob*) or diabetic (*db/db*) mice indicate that this increase in food intake and accumulation of body fat was being promoted by some type of circulating factor (Coleman & Hummel, 1969; Coleman, 1973; for review, Coleman, 1982). Compelling evidence was gathered that signified that this factor was probably acting in the hypothalamus to modulate metabolism. In 1994, a breakthrough discovery revealed that the *obese* (*ob*) gene was encoding a small protein produced mainly by fat tissue, named leptin (Zhang *et al.*, 1994). It was determined that the obese mouse (*ob/ob*) was deficient in leptin (Lep^{ob}; Coleman,

1978; Zhang *et al.*, 1994), whereas the diabetic mouse (*db/db*) was lacking the leptin receptor (*Lepr*^{db}; Chen *et al.*, 1996; Coleman, 1978; Hummel *et al.*, 1966). The massively obese phenotype of these mice and the discovery of leptin as the 'key factor' that is missing in their metabolic signaling pathway helped shed light on the potential mechanisms implicated in human obesity. The possibility of uncovering the central mechanism involved in this condition generated a massive investment on the part of the pharmaceutical industry to develop new treatments based on leptin to solve the problem of obesity. Unfortunately, in humans, mutations in the leptin gene and its receptor were found to account for just a small number of genetically obese patients (Farooqi & O'rahilly, 2008). However, these studies lead to a new era in obesity and feeding research, where newly developed techniques began to be implemented in the study of energy balance. Leptin itself proved to be a powerful modulator of areas important for energy balance, and has been used as a tool to study many of the pathways involved in food intake and energy expenditure.

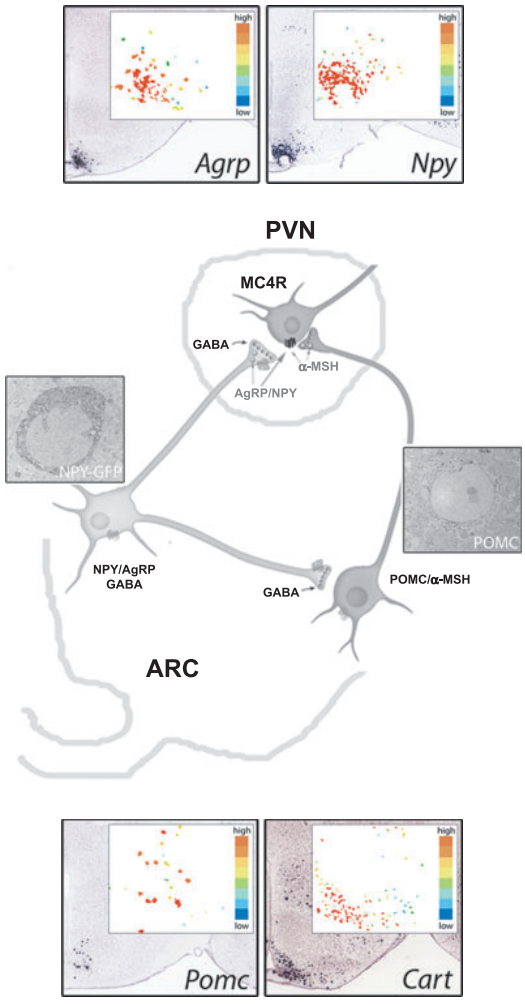

FIG. 1. Schematic diagram showing the two critical neuronal populations in energy metabolism regulation located in the ARC of the hypothalamus with projections to the PVN. (Panels) *In situ* hybridization images showing the expression of different gene trasncripts that characterize the two groups of neurons in the ARC: (bottom) the expression of POMC and CART mRNA characteristic of the neurons that produce α-MSH and provide an anorexigenic tone; (top) expression of Agrp and Npy mRNA characteristic of the Npy/Agrp neurons which promote an orexigenic tone. Inserts: electron micrographs showing AgRP and POMC neurons. Some of the panels were generated and downloaded from the Allen Brain Atlas website (Lein *et al.*, 2007; Allen Atlas Portal, Seattle, WA, USA: Allen Institute for Brain Science. ©2009. Available from: http://www.brain-map.org).

Dissecting the hypothalamic network involved in energy homeostasis

Eating is a complex behavior that involves the instinct to survive, but also entails reward mechanisms. For example, in humans, even though primary areas (such as the midbrain and hypothalamus) are involved in feeding, more superior areas have an important influence on our daily feeding homeostasis. The taste, smell and appearance of food can stimulate sensory areas which project to more 'inferior' sites to drive feeding. Also, psychological components can drive food intake, in part due to projections from the cortex. Even though the signaling network that manages daily energy balance is highly complex, there are several nuclei located in the hypothalamus and midbrain that play an essential role in controlling feeding. Through the use of more advanced techniques, these areas have been examined in higher resolution, revealing elaborate mechanisms of cross-talk. This review will focus on the role of the melanocortin system and two of its components located in the arcuate nucleus (ARC) of the hypothalamus as well as the importance of this system in the regulation of feeding.

The ARC is an area located in the medial–basal hypothalamus and is thought to be a master player in the regulation of energy balance in adult mammals. The ARC is adjacent to the third ventricle, an area that is believed to lack the blood–brain barrier, thus placing it in an ideal location to be a putative brain sensor of humoral and metabolic factors coming from the periphery (Broadwell & Brightman, 1976; Broadwell *et al.*, 1983; Norsted *et al.*, 2008). Moreover, because of its close proximity to the third ventricle, the ARC can also sense the levels of factors found in the cerebrospinal fluid (CSF), which is the main pathway for the entrance of several peptides and hormones into the brain through the blood–CSF barrier.

Within the ARC are housed the two components of the melanocortin system, an elaborate network believed to be at the core of the regulation of energy balance (Cone, 2005). One component consists of the subset of neurons that express neuropeptide-Y (Npy). Npy was first described in 1982, as a novel neuropeptide vastly expressed throughout the brain (Tatemoto *et al.*, 1982). Two years later, Clark *et al.* (1984) and Stanley & Leibowitz (1984) presented the first evidence of the orexigenic effects of Npy. The injection of this peptide into either the cerebral ventricles (Clark *et al.*, 1984) or directly into the hypothalamic paraventricular nucleus (PVN; Stanley & Leibowitz, 1984) promoted a robust increase in food intake. The PVN was found to receive inputs from the Npy neurons in the ARC (Bai *et al.*, 1984, 1985). Subsequently, the expression of the agouti-related protein (Agrp) was found to occur in the same cells that express Npy (Hahn *et al.*, 1998). Dominant mutations in the agouti peptide were known to cause an obese phenotype in mice (Klebig *et al.*, 1995), and this has been proved to be due to the antagonism of melanocortin receptors located in the PVN (Lu *et al.*, 1994; Fan *et al.*, 1997). Additionally, these

Npy/Agrp neurons were found to co-express gamma aminobutyric acid (GABA; Horvath *et al.*, 1997), further confirming the inhibitory nature of these cells in the network. The second component of the melanocortin system within the ARC consists of a neighboring neuronal population that produces proopiomelanocortin (POMC)-derived peptides, such as α-melanocyte stimulating hormone (α-MSH), and cocaine- and amphetamine-regulated transcript (CART) peptides, which promote satiety and positive energy balance (anorexigenic; Zigman & Elmquist, 2003). The interaction between these two sets of neurons is such that the Npy/Agrp neurons maintain a unidirectional tonic inhibition on the POMC neurons (Horvath *et al.*, 1992; Cowley *et al.*, 2001; Pinto *et al.*, 2004). Both groups of cells project to the PVN, an area that expresses particularly high levels of both melanocortin-3 receptors (MC3R) and melanocortin-4 receptors (MC4R). In the PVN, the peptides derived from the breakdown of POMC (mainly α-MSH) are endogenous agonists of MC3R/MC4R, whereas the agouti peptide (Agrp) released from terminals of NPY/Agrp neurons are high-affinity antagonists of these receptors (Fig. 1) (for a more detailed review of the melanocortin signaling, see Cone, 2005). This anatomical and electrophysiological relationship between the Npy/Agrp and POMC neurons is fundamental for survival, a biological truism underscored by experiments showing that selective elimination of the Npy/Agrp neurons leads to cessation of feeding (Bewick *et al.*, 2005; Gropp *et al.*, 2005; Luquet *et al.*, 2005) and death (Luquet *et al.*, 2005). In these reports, the selective elimination of Npy/Agrp was elegantly achieved in mice utilizing transgenic techniques. Mice that expressed the *Cre* recombinase under control of the Agrp promoter were crossed with mice whose expression of the diphteria toxin receptor (DTR) was prevented by a floxed stop cassette (inducible DTR mice). This crossing generates mice in which the DTR is expressed solely in the Agrp neurons, allowing for a selective and inducible ablation of these neurons when the animals are treated with the diphteria toxin. These studies, together with degenerative studies showing that lesions in the ARC do not change energy metabolism, highlight the fact that both groups of cells are essential for a constant cross-talk to occur in order to regulate energy homeostasis. The ablation of one subtype promotes the predominant activity of the other, whereas ablation of both (through ARC lesions) negates the influence of the ARC in the regulation of food intake.

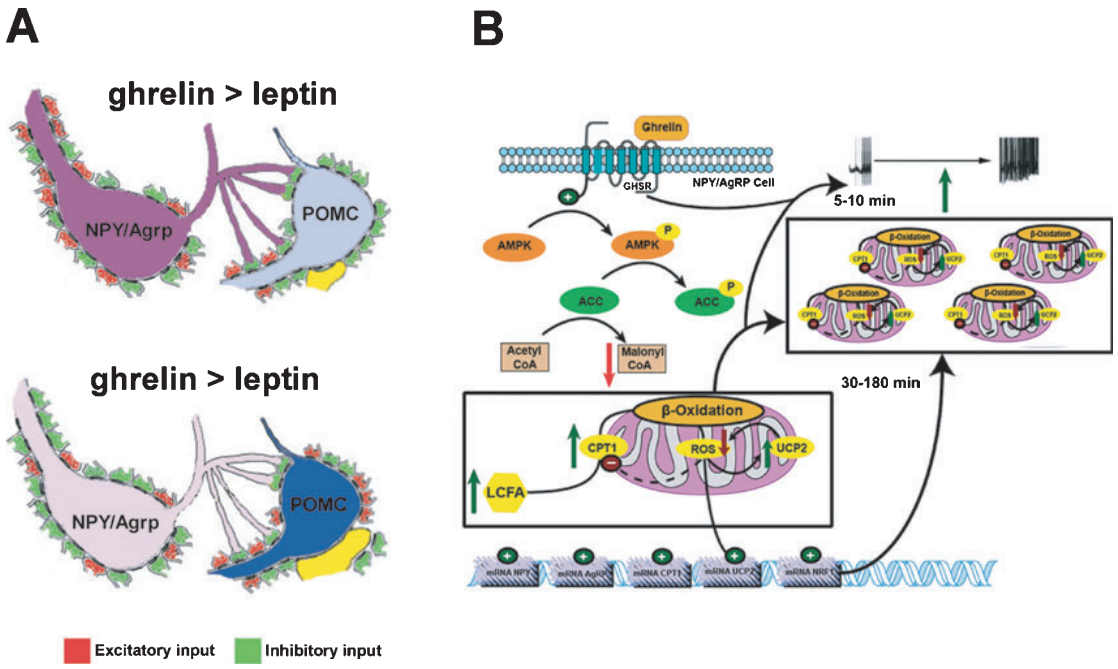

FIG. 2. Schematic drawing illustrating neuronal plasticity in the melanocortin system in response to different hormonal fluctuations. (A, top) When levels of ghrelin, an orexigenic hormone produced by the gut, are high there is an increase in the activity of the Npy/AgRP cells and a concomitant increase in the inhibitory inputs on POMC cells, a synaptological constellation that is in line with the silencing of these anorexigenic neurons. (A, bottom) When the levels of the anorexigenic hormone leptin are high there is an increase in the activity of POMC cells and a decrease in the activity of Npy/AgRP neurons. A related activity-dependent synaptic plasticity also occurs under this condition (Pinto *et al.*, 2004). A putative role for glial cells in this process is shown: prolonged glial end-feet can physically isolate the neuronal plasma membrane from synaptic buttons. When the neuronal cells receive a stimulus to increase synaptic coverage, the glial cells could rapidly shrink their end-feet and expose the neuronal membrane to connect to silent synapses. (B) The activation of the Npy/AgRP neurons by ghrelin is schematically highlighted in this box (adapted from Andrews *et al.*, 2008, with permission). Ghrelin released by the gut enters the ARC and binds to GHSR, increasing Npy/AgRP cell activity. Concomitantly, GHSR signaling increases the activity of 5′ AMP-activated protein kinase, which inhibits acetyl-CoA-carboxylase (ACC). ACC inhibition leads to an increase in the levels of long-chain fatty acids and carnitine palmitoyltransferase 1 (CPT1), and consequently in stimulation of mitochondrial beta-oxidation. Mitochondrial respiration will also increase in response to the metabolic changes occurring in the Npy/AgRP cells during high neuronal activity. This increase in mitochondrial respiration is coupled to increases in ROS production. ROS will increase levels of uncoupling proteins (mainly UCP2) which will buffer the levels of ROS, closing the loop of mitochondrial respiration → ROS production → UCP2 activation → decrease in ROS production → ideal milieu for high mitochondria activity. After 30–180 min of neuronal activation this increase in beta-oxidation and mitochondrial activity will induce mitochondrial proliferation, which will provide appropriated machinery for high levels of cellular energy demand (see Andrews *et al.*, 2008).

Plasticity in brain circuitries involved in feeding

The discovery of the relationship between these two subsets of neurons in the ARC and their projections to the PVN in regulating food intake raised a series of questions about how humoral signals could modulate this system to suppress or induce food intake. In 2004, 10 years after the cloning of the obese gene (*ob*), a striking discovery was reported (Pinto *et al.*, 2004), showing that leptin induces a fast rewiring of POMC and Npy/Agrp cells in the ARC. Through electrophysiological and morphological analyses of POMC and Npy/Agrp cells expressing green-fluorescent protein (GFP) of leptin-deficient mice (POMC-GFP-*Lep*^{ob} and NPY-GFP-*Lep*^{ob}), it was found that peripheral leptin treatment rapidly restored the synaptic inputs in these groups of cells. On the other hand, ghrelin, an orexigenic hormone produced predominantly by the gut, produced the opposite effect on the synaptic arrangement of the POMC cells.

The implications of the rapid rewiring of POMC and Npy/Agrp cells by hormonal stimulus raised the possibility that this mechanism could be used as a target for medical treatments against obesity and hyperphagia. Accordingly, the effects of estradiol administration to obese mice resembled those of leptin on synaptic rearrangements, even in the absence of leptin or its receptor (*Lep*^{ob} and *Lepr*^{db} mice, respectively; Gao *et al.*, 2007). These effects were independent of STAT3 (no effect was seen in Stat3$^{-/-}$ mice), a protein involved in the signaling of leptin and other cytokines (Gao *et al.*, 2007). However, the revelation of an effect of estradiol (and related hormones) on the plasticity of the ARC was nothing new. In the 1980s, research headed by Y. Arai and F. Naftolin (Matsumoto & Arai, 1979, 1981; Garcia-Segura *et al.*, 1986, 1987; Naftolin *et al.*, 1996) presented evidence for rapid rearrangements of the hypothalamic circuitry in response to hormonal fluctuations. In these studies, the authors showed that estrogen has a facilitatory effect on the formation of new spine synapses in the arcuate neurons (Matsumoto & Arai, 1979, 1981), reflecting a circuit remodeling in the ARC after estrogen treatment. In addition to synapse formation, another study showed that 17ß-estradiol administration lead to changes in the neuronal membrane ultrastructure within the ARC (Garcia-Segura *et al.*, 1987), which highlights the importance of the ultramicroscopic analysis in the understanding of the mechanisms implicated in the physiological regulation of neuronal populations.

Subsequently, elegant work developed by D. T. Theodosis further identified a coupled neuron–glia–synaptic remodeling in the adult hypothalamus (Langle *et al.*, 2002; Theodosis *et al.*, 2004, 2006; Panatier *et al.*, 2006). In this model, not only do synaptic inputs change in a rapid fashion but so does the astrocytic coverage of the neuronal surface (for review, see Theodosis *et al.*, 2008). When neuronal activity is enhanced, astrocytic coverage is reduced, thus modifying the extracellular space and increasing the concentration of neurotransmitters in the synaptic cleft due to reduced uptake by glial cells. This mechanism is probably implicated in the formation of synapses in the ARC during feeding regulation, permitting synaptogenesis on neuronal membranes free of astrocytic coverage. However, this model has not yet been tested on the rapid synaptic rearrangements that occur within the melanocortin system (Npy/Agrp and POMC cells; Pinto *et al.*, 2004; Horvath & Diano, 2004) (see Fig. 2A).

Mitochondrial participation in the regulation of the melanocortin system

Classic neurobiology considers the brain a privileged organ that predominantly utilizes glucose for its metabolism and, in some conditions, lactate and ketone bodies. Glucose-sensing neurons were described decades ago but, more recently, POMC cells have been considered as sensors for glucose in the ARC (Ibrahim *et al.*, 2003; Wang *et al.*, 2004; Fioramonti *et al.*, 2007; Parton *et al.*, 2007).

The idea of the use of fatty acids as an energy source has been neglected with regard to neuronal cells. However, a series of findings point to the existence of fatty acid-sensing cells in the hypothalamus. Recently, research headed by T. L. Horvath and collaborators shed light on the possible mechanisms involved in the sensing of fatty acids by neurons (Andrews *et al.*, 2008). Utilizing a myriad of techniques, the authors identify a cascade of events by which ghrelin activates feeding through fatty acid oxidation and free radical buffering in the NPY/Agrp neurons of the ARC. Ghrelin induces feeding by the activation of its receptor, the G-protein-coupled growth hormone secretagogue receptor (GHSR; see below), in the NPY/Agrp neurons, which induces a rapid increase in the firing rate of these cells. Concomitantly, ghrelin activates 5′ AMP-activated protein kinase which in turn suppresses acetyl-CoA-carboxylase (ACC) activity. ACC converts acetyl-CoA into malonyl-CoA, and its inhibition leads to decreased levels of malonyl-CoA, thereby eliminating the inhibition of carnitine palmitoyltransferase 1 (CPT1). CPT1 activation increases the uptake of long-chain fatty acids into the mitochondria, and consequently induces fatty acid beta-oxidation. This process generates reactive oxygen species (ROS) which, together with fatty acids, induces uncoupling protein (UCP) activity, mainly UCP2. The induction of UCP2 neutralizes beta-oxidation-induced ROS production, promoting support for the continuous generation of ATPs through fatty acid oxidation, which enables NPY/Agrp cells to keep their high firing rates. The sustained firing of NPY/Agrp cells induces activity-dependent synaptic plasticity and thus increases the number of inhibitory inputs on POMC cells, thereby promoting the appropriate morphological basis for an increase in feeding to occur. These synaptic rearrangements require mitochondrial uncoupling, as they did not occur in UCP2-knockout mice (see Fig. 2B).

The activity-dependent synaptic plasticity that occurs in the hypothalamus and which is dependent upon mitochondrial UCPs has also been described in other brain areas (Dietrich *et al.*, 2008). These results, together with *in vitro* evidence that there is a dynamic mitochondrial response to neuronal activation (Li *et al.*, 2004), identify putative roles of these organelles in coordinating the response of NPY/Agrp and POMC cells in the regulation of food intake. The activity-dependent induction of mitochondrial migration and division to provide an appropriate milieu for synaptogenesis and spine formation is still an intriguing hypothesis that needs to be fully tested. Because both NPY/Agrp and POMC neurons have shown adaptations in mitochondrial machinery due to cell activation, it is logical to consider that the cellular mechanism involved in the processes of mitochondrial fusion and fission are important in orchestrating feeding behavior.

The mitochondrion is the principal site of production of ATP, which is the main energy substrate for most of the biochemical reactions that occur in eukaryotic cells. To generate ATP, the mitochondrion utilizes metabolic intermediates derived from the breakdown of proteins, lipids and sugars. The oxidation of these substrates generates free energy which is stored in special reduced carriers, mainly $FADH_2$ and NADH. The mitochondrion will utilize these reduced carriers in the respiratory chain to generate ATP through the process of oxidative phosphorylation. Both $FADH_2$ and NADH [or their oxidized forms, flavin adenine dinucleotide (FAD) and nicotinamide adenine dinucleotide (NAD^+)] are co-factors in several biochemical pathways, linking the production of energy inside the mitochondria to the regulation of cellular pathways. Interestingly, two reports have recently described

the putative role of NAD^+ in the regulation of circadian oscillations in mammals (Nakahata *et al.*, 2009; Ramsey *et al.*, 2009). In these articles, research headed by J. Bass (Ramsey *et al.*, 2009) and P. Corsi (Nakahata *et al.*, 2009) shed light on the mechanisms involved in the maintenance of the circadian control of NAD^+ levels. The biosynthesis of NAD^+ can occur through different metabolic pathways. One such classic route is by the *de novo* pathway from amino acids (Magni *et al.*, 1999). However, there is a second mechanism which recycles NAD^+ from nicotinamide and which is called the salvage pathway (Magni *et al.*, 1999). In this scenario, nicotinamide is converted to nicotinamide mononucleotide (NMN) by the rate-limiting enzyme nicotinamide phosphoribosyltransferase (NAMPT), (Revollo *et al.*, 2004). NMN is subsequently transformed into NAD^+ by a group of enzymes called NMN adenylytransferases (NMNAT; Emanuelli *et al.*, 2001; Schweigler *et al.*, 2001). Among the biochemical reactions that utilize NAD^+ as a substrate, the two reports mentioned above highlight the role of SIRT1 in transforming NAD^+ back to nicotinamide, thus closing the cycle ($NAD^+ \rightarrow$ nicotinamide $\rightarrow$ NMN $\rightarrow$ NAD^+; Ramsey *et al.*, 2009; Nakahata *et al.*, 2009). Sirtuin 1 (SIRT1) is a NAD^+-dependent deacetylase of the family of sirtuins (Imai *et al.*, 2000) which senses the cellular redox state (NAD^+/NADH levels; Fulco *et al.*, 2003). SIRT1 has been implicated in several vital functions in mammals, most importantly in the regulation of the effects of calorie restriction on longevity (Cohen *et al.*, 2004). It is known to form a protein complex with CLOCK (Asher *et al.*, 2008; Belden and Dunlap, 2008; Grimaldi *et al.*, 2009; Nakahata *et al.*, 2008). CLOCK is a mammalian protein encoded by the Clock gene that regulates circadian rhythms through the modulation of transcription factors (Vitaterna *et al.*, 1994). This protein complex (CLOCK-SIRT1) was shown to regulate the NAMPT promoter, affecting the levels of NAMPT, and consequently the conversion of nicotinamide to NMN in the salvage pathway (Nakahata *et al.*, 2009; Ramsey *et al.*, 2009). Because CLOCK levels and activity vary during the circadian cycle, this generates a circadian oscillation in NAMPT protein levels related to the CLOCK rhythm. Fluctuations in NAMPT levels produce a concomitant fluctuation in NAD^+ levels. Because NAD^+ is a substrate for the enzymatic activity of SIRT1, the levels of NAD^+ induce oscillatory activity of SIRT1 and, consequently, of the SIRT1-CLOCK complex. This mechanism closes a feedback loop that coordinates the circadian activity of the CLOCK pacemaker with the cellular metabolic machinery (Nakahata *et al.*, 2009; Ramsey *et al.*, 2009). Even though this pathway was revealed in peripheral tissues, a brain correlate is likely. It is important to highlight, however, that NAMPT is virtually absent in brain tissue (Revollo *et al.*, 2007), making the study of the NAD^+ biosynthetic pathways in the brain all the more intriguing. Finally, because mitochondrial activity is dependent on the levels of NAD^+/NADH, the circadian oscillation of these co-enzymes probably generate a circadian fluctuation in mitochondrial activity. This interesting hypothesis still requires further investigation to establish its role in the circadian control of energy metabolism.

The integrated humoral control of food intake

Several peripheral factors have been described as modulating food intake and energy balance. Cholecystokinin (CCK) was one of the first of these to be described. CCK is released by the gastrointestinal system during meals (Liddle *et al.*, 1985) and induces an anorexigenic response. This physiological pathway is believed to be an essential component of postprandial satiety (Chaudhri *et al.*, 2006). CCK activates POMC cells in the nucleus of the solitary tract (NTS), which is located in the brainstem. This effect of peripheral CCK is dependent upon melanocortin signaling, because in the absence of MC4R or by pharmacological inhibition of MC4R in the NTS, the anorexigenic effects of CCK are blocked (Fan *et al.*, 2004). Before the discovery of leptin, CCK was proposed as the factor that was missing in the obese mutant (*ob/ob*) mouse (Straus and Yalow, 1979). However, as stated above, leptin was discovered in 1994 and its role as a fat-derived peptide was unveiled (Zhang *et al.*, 1994). Leptin is produced mostly by adipocytes, and its circulating levels reflect fat storage. It acts in a multitude of tissues that express leptin receptors, including tissues of the reproductive and immune systems. However, its effects in modulating energy balance are mediated primarily by leptin receptors of the brain, because central infusion of leptin into Lep^{ob} mice is sufficient to reverse the metabolic phenotype of these mice (Friedman & Halaas, 1998). In addition to its role in promoting the rewiring of the melanocortin system (see above), leptin also acts in other brain areas to regulate energy intake. This is illustrated by the obese phenotype of mice with an ablated expression of leptin receptors in neurons of the hypothalamic ventromedial nuclei (Dhillon *et al.*, 2006). Additionally, leptin also acts in the ventral tegmental area (VTA), an area containing dopaminergic neurons that are important for the reward aspects of feeding (Fulton *et al.*, 2006; Hommel *et al.*, 2006).

Another peptide produced by the gut that induces an anorexigenic response is peptide YY (PYY). PYY is produced by endocrine cells of the gut, predominantly in the lower portion of the gastrointestinal tract (Adrian *et al.*, 1985; Lundberg *et al.*, 1982; Nilsson *et al.*, 1991; Onaga *et al.*, 2000; see Ekblad & Sundler, 2002 for review) and is released into the circulation in two forms, $PYY_{1\text{-}36}$ and $PYY_{3\text{-}36}$. The short form ($PYY_{3\text{-}36}$) is cleaved from the long form ($PYY_{1\text{-}36}$) by the enzyme dipeptidyl peptidase IV (Mentlein *et al.*, 1993), and decreases food intake when administered peripherally (Batterham *et al.*, 2002; Challis *et al.*, 2003; Adams *et al.*, 2004; Halatchev *et al.*, 2004; Chelikani *et al.*, 2005). The anorectic effect of $PYY_{3\text{-}36}$ requires Y_2 receptors because it fails to inhibit food intake in Y_2 receptor-knockout mice (Batterham *et al.*, 2002). In the same study, $PYY_{3\text{-}36}$ decreased NPY mRNA in the ARC and its direct delivery into the ARC was sufficient to decrease food intake (Batterham *et al.*, 2002), highlighting the probable importance of NPY cells in the anorectic effect of $PYY_{3\text{-}36}$. In contrast, the decrease in food intake by $PYY_{3\text{-}36}$ seems to be independent of the melanocortin system because $Pomc^{-/-}$ (Challis *et al.*, 2004), MC4R-deficient (Halatchev *et al.*, 2004) and agouti (Adams *et al.*, 2004) mice still showed the anorectic response to $PYY_{3\text{-}36}$. Interestingly, $PYY_{3\text{-}36}$ has been shown to decrease the activity of both NPY and POMC cells in the ARC, indicating that $PYY_{3\text{-}36}$ may temporarily decrease the contribution of arcuate cells to the regulation of food intake (Batterham *et al.*, 2002; Acuna-Goycolea & van den Pol, 2005). $PYY_{3\text{-}36}$ also has extra-hypothalamic effects, activating neurons in the area postrema and in the nucleus of solitary tract, which are areas involved in sensing aversive stimuli (Halatchev & Cone, 2005). Thus, it is likely that the effects of $PYY_{3\text{-}36}$ in decreasing food intake are due to a combination of various mechanisms involving different brain areas. Because of the controversial findings about the anorectic effects of $PYY_{3\text{-}36}$ (Tschöp *et al.*, 2004), it is intuitive to postulate that a more complex mechanism could be implicated in its effects. An intriguing hypothesis is that $PYY_{3\text{-}36}$ decreases the contribution of the inhibitory (GABAergic) activity of the NPY cells in extra-hypothalamic nuclei, thus activating other neuronal populations independent of the melanocortin system. In support of this argument is the recent report showing that selective ablation of NPY/Agrp neurons in the ARC induces starvation due to the activation of areas

that are normally being inhibited by GABAergic inputs from the NPY/Agrp cells (Dietrich & Horvath, 2009; Wu *et al.*, 2009). In this report, Wu *et al.* (2009) showed that the parabrachial nucleus of the pons is the main nucleus involved in the anorectic effects seen after NPY/Agrp neuronal ablation. Thus, examining the effects of PYY_{3-36} on these neuronal networks is an interesting line of study that requires further testing.

In opposition to the anorexigenic molecules, ghrelin is the well-studied orexigenic peptide released by the gut. Ghrelin is a 28-amino-acid peptide produced and secreted by enteroendocrine cells in the oxyntic glands of the stomach (Kojima *et al.*, 1999) and upper intestine (Date *et al.*, 2000) in response to negative energy balance. Ghrelin is active when octanoylated, acting as an agonist of the G-protein-coupled growth hormone secretagogue receptor (GHSR) to induce food intake (Wren *et al.*, 2000; Tang-Christensen *et al.*, 2004; Williams & Cummings, 2005). GHSR is highly expressed in the hypothalamus, mainly in the ARC (Howard *et al.*, 1996; Bennett *et al.*, 1997; Willesen *et al.*, 1999; Nogueiras *et al.*, 2004). Indeed, ghrelin has been shown to exert its orexigenic effect by activating NPY/Agrp neurons while inhibiting the anorexigenic POMC neurons (Cowley *et al.*, 2003). However, similar to leptin, ghrelin also acts in other brain regions to modulate food intake (Cowley *et al.*, 2003). For example, ghrelin binds to neurons in the VTA, where it increases dopamine neuronal activity and dopamine turnover in the nucleus accumbens. Direct VTA administration of ghrelin was sufficient to induce food intake, while the blockage of ghrelin's action in the VTA by infusion of a ghrelin antagonist blocked the orexigenic effect of circulating ghrelin (Abizaid *et al.*, 2006). These results indicated that the mesolimbic reward system plays a role in regulating the orexigenic effects of ghrelin.

Future directions

With the advance of techniques in molecular biology, proteomics and bioinformatics, it is expected that the list of hormones, cytokines, peptides, etc., involved in the regulation of energy metabolism will continue to grow, adding more complexity to and understanding of this network. Also, the development of more powerful imaging tools will provide greater in-depth knowledge about the neuronal circuitry involved in energy homeostasis. For example, just recently, an elegant study employing the Cre/lox technology presented a powerful means for elucidating brain circuitry (Livet *et al.*, 2007). Utilizing several fluorescent proteins and different loxP sites in a transgenic mouse, the authors were able to visualize ~ 100 different colors, each color representing one neuron. They were able to track these cells within the brain and establish their projections and connections. Using high-throughput imaging techniques, similar work may be done employing Cre-recombinase driven by different promoters. In the case of energy metabolism, Agrp-cre and POMC-cre mice could be crossed with the multi-fluorescent multi-loxP mice. Then, a better understanding of the anatomy of the connections could be unraveled. Additionally, the combination of cre-lox technology with high-throughput phenotyping will provide more reliable evidence about the role of cell-specific molecules in the circuitry involved in feeding behavior.

During the last several decades, numerous studies have attempted to elucidate the mechanisms involved in feeding behavior and, in the process, have unveiled the highly complex nature of this activity. Thus, the idea of a 'single molecule' therapy to treat obesity and its related disorders is being discarded in favor of a therapy that involves a combination of compounds that will more probably have some success.

Abbreviations

Agrp, agouti-related protein; ARC, arcuate nucleus; CART, cocaine- and amphetamine-regulated transcript; GABA, gamma aminobutyric acid; GHSR, growth hormone secretagogue receptor; MC3R and -4R, melanocortin-3 and -4 receptors; NAD^+, nicotinamide adenine dinucleotide; NMN, nicotinamide mononucleotide; Npy, neuropeptide-Y; POMC, proopiomelanocortin; PVN, hypothalamic paraventricular nucleus; PYY, peptide YY; ROS, reactive oxygen species; SIRT1, sirtuin 1; UCP, uncoupling protein; α-MSH, α-melanocyte stimulating hormone.

Acknowledgements

MOD was partially supported by CNPq/Brazil. TLH was supported by grants from the NIH.

References

Abizaid, A., Liu, Z.W., Andrews, Z.B., Shanabrough, M., Borok, E., Elsworth, J.D., Roth, R.H., Sleeman, M.W., Picciotto, M.R., Tschöp, M.H., Gao, X.B. & Horvath, T.L. (2006) Ghrelin modulates the activity and synaptic input organization of midbrain dopamine neurons while promoting appetite. *J. Clin. Invest.*, **116**, 3229–3239.

Acuna-Goycolea, C. & van den Pol, A.N. (2005) Peptide YY(3-36) inhibits both anorexigenic proopiomelanocortin and orexigenic neuropeptide Y neurons: implications for hypothalamic regulation of energy homeostasis. *J. Neurosci.*, **25**, 10510–10519.

Adams, S.H., Won, W.B., Schonhoff, S.E., Leiter, A.B. & Paterniti ., J.R. Jr (2004) Effects of peptide YY[3-36] on short-term food intake in mice are not affected by prevailing plasma ghrelin levels. *Endocrinology*, **145**, 4967–4975.

Adrian, T.E., Ferri, G.L., Bacarese-Hamilton, A.J., Fuessl, H.S., Polak, J.M. & Bloom, S.R. (1985) Human distribution and release of a putative new gut hormone, peptide YY. *Gastroenterology*, **89**, 1070–1077.

Anand, B.K. & Brobeck, J.R. (1951) Hypothalamic control of food intake in rats and cats. *Yale J. Biol. Med.*, **24**, 123–140.

Andrews, Z.B., Liu, Z.W., Walllingford, N., Erion, D.M., Borok, E., Friedman, J.M., Tschöp, M.H., Shanabrough, M., Cline, G., Shulman, G.I., Coppola, A., Gao, X.B., Horvath, T.L. & Diano, S. (2008) UCP2 mediates ghrelin's action on NPY/AgRP neurons by lowering free radicals. *Nature*, **454**, 846–851.

Asher, G., Gatfield, D., Stratmann, M., Reinke, H., Dibner, C., Kreppel, F., Mostoslavsky, R., Alt, F.W. & Schibler, U. (2008) SIRT1 regulates circadian clock gene expression through PER2 deacetylation. *Cell*, **34**, 317–328.

Bai, F.L., Yamano, M., Inagaki, S., Shiosaka, S., Yamazoe, M., Shibasaki, T., Ling, N., Tachibana, S., Hamaoka, T. & Tohyama, M. (1984) Distribution of neuropeptides in the hypothalamo-hypophyseal system in the rat: an immunohistochemical observation. *Cell. Mol. Biol.*, **30**, 437–452.

Bai, F.L., Yamano, M., Shiotani, Y., Emson, P.C., Smith, A.D., Powell, J.F. & Tohyama, M. (1985) An arcuato-paraventricular and -dorsomedial hypothalamic neuropeptide Y-containing system which lacks noradrenaline in the rat. *Brain Res.*, **331**, 172–175.

Batterham, R.L., Cowley, M.A., Small, C.J., Herzog, H., Cohen, M.A., Dakin, C.L., Wren, A.M., Brynes, A.E., Low, M.J., Ghatzel, M.A., Cone, R.D. & Bloom, S.R. (2002) Gut hormone PYY3-36 physiologically inhibits food intake. *Nature*, **418**, 650–654.

Belden, W.J. & Dunlap, J.C. (2008) SIRT1 is a circadian deacetylase for core clock components. *Cell*, **134**, 212–214.

Bennett, P.A., Thomas, G.B., Howard, A.D., Feighner, S.D., van der Ploeg, L.H., Smith, R.G. & Robinson, I.C. (1997) Hypothalamic growth hormone secretagogue-receptor (GHS-R) expression is regulated by growth hormone in the rat. *Endocrinology*, **138**, 4552–4557.

Bewick, G.A., Gardiner, J.V., Dhillo, W.S., Kent, A.S., White, N.E., Webster, Z., Ghatei, M.A. & Bloom, S.R. (2005) Post-embryonic ablation of AgRP neurons in mice leads to a lean, hypophagic phenotype. *FASEB J.*, **19**, 1680–1682.

Bonanno, A., Schlattl, H. & Paterno, L. (2002) The age of the Sun and the relativistic corrections in the EOS. *Journal reference: Astron. Astrophys.* **390**, 1115–1118.

Brecher, G. & Waxler, S.H. (1949) Obesity in albino mice due to single injections of gold thioglucose. *Proc. Soc. Exp. Biol. Med.*, **70**, 498–501.

Broadwell, R.D. & Brightman, M.W. (1976) Entry of peroxidase into neurons of the central and peripheral nervous systems from extracerebral and cerebral blood. *J. Comp. Neurol.*, **166**, 257–283.
Broadwell, R.D., Balin, B.J., Salcman, M. & Kaplan, R.S. (1983) Brain-blood barrier? Yes and no *Proc. Natl Acad. Sci. USA*, **80**, 7352–7356.
Brobeck, J.R. (1946) Mechanism of the development of obesity in animals with hypothalamic lesions. *Physiol. Rev.*, **26**, 541–559.
Brobeck, J.R., Tepperman, J. & Long, C.N.H. (1943) Experimental hypothalamic hyperphagiainthealbinorat. *Yale J. Biol. Med.*, **15**, 831–853.
Challis, B.G., Pinnock, S.B., Coll, A.P., Carter, R.N., Dickson, S.L. & O'Rahilly, S. (2003) Acute effects of PYY_{3-36} on food intake and hypothalamic neuropeptide expression in the mouse. *Biochem. Biophys. Res. Commun.*, **311**, 915–919.
Challis, B.G., Coll, A.P., Yeo, G.S., Pinnock, S.B., Dickson, S.L., Thresher, R.R., Dixon, J., Zahn, D., Rochford, J.J., White, A., Oliver, R.L., Millington, G., Aparicio, S.A., Colledge, W.H., Russ, A.P., Carlton, M.B. & O'Rahilly, S. (2004) Mice lacking pro-opiomelanocortin are sensitive to high-fat feeding but respond normally to the acute anorectic effects of peptide-YY(3-36). *Proc. Natl Acad. Sci. USA*, **101**, 4695–4700.
Chaudhri, O., Small, C. & Bloom, S. (2006) Gastrointestinal hormones regulating appetite. *Philos. Trans. R. Soc. Lond. B Biol. Sci.*, **361**, 1187–1209.
Chelikani, P.K., Haver, A.C. & Reidelberger, R.D. (2005) Intravenous infusion of peptide YY(3-36) potently inhibits food intake in rats. *Endocrinology*, **146**, 879–888.
Chen, H., Charlat, O., Tartaglia, L.A., Woolf, E.A., Weng, X., Ellis, S.J., Lakey, N.D., Culpepper, J., Moore, K.J., Breitbart, R.E., Duyk, G.M., Tepper, R.I. & Morgenstern, J.P. (1996) Evidence that the diabetes gene encodes the leptin receptor: identification of a mutation in the leptin receptor gene in db/db mice. *Cell*, **84**, 491–495.
Clark, J.T., Kalra, P.S., Crowley, W.R. & Kalra, S.P. (1984) Neuropeptide Y and human pancreatic polypeptide stimulate feeding behavior in rats. *Endocrinology*, **115**, 427–429.
Cohen, H.Y., Miller, C., Bitterman, K.J., Wall, N.R., Hekking, B., Kessler, B., Howitz, K.T., Gorospe, M., De Cabo, R. & Sinclair, D.A. (2004) Calorie restriction promotes mammalian cell survival by inducing the SIRT1 deacetylase. *Science*, **305**, 390–392.
Coleman, D.L. (1973) Effects of parabiosis of obese with diabetes and normal mice. *Diabetologia*, **9**, 294–298.
Coleman, D.L. (1978) Obese and diabetes: two mutant genes causing diabetes-obesity syndromes in mice. *Diabetologia*, **14**, 141–148.
Coleman, D.L. (1982) Diabetes-obesity syndromes in mice. *Diabetes*, **31**, 1–6.
Coleman, D.L. & Hummel, K.P. (1969) Effects of parabiosis of normal with genetically diabetic mice. *Am. J. Physiol.*, **217**, 1298–1304.
Cone, R.D. (2005) Anatomy and regulation of the central melanocortin system. *Nat. Neurosci.*, **8**, 571–578.
Cowley, M.A., Smart, J.L., Rubinstein, M., Cerdán, M.G., Diano, S., Horvath, T.L., Cone, R.D. & Low, M.J. (2001) Leptin activates anorexigenic POMC neurons through a neural network in the arcuate nucleus. *Nature*, **411**, 480–484.
Cowley, M.A., Smith, R.G., Diano, S., Tschöp, M., Pronchuk, N., Grove, K.L., Strasburger, C.J., Bidlingmaier, M., Esterman, M., Heiman, M.L., Garcia-Segura, L.M., Nillni, E.A., Mendez, P., Low, M.J., Sotonyi, P., Friedman, J.M., Liu, H., Pinto, S., Colmers, W.F., Cone, R.D. & Horvath, T.L. (2003) The distribution and mechanism of action of ghrelin in the CNS demonstrates a novel hypothalamic circuit regulating energy homeostasis. *Neuron*, **37**, 649–661.
Date, Y., Kojima, M., Hosoda, H., Sawaguchi, A., Mondal, M.S., Suganuma, T., Matsukura, S., Kangawa, K. & Nakazato, M. (2000) Ghrelin, a novel growth hormone-releasing acylated peptide, is synthesized in a distinct endocrine cell type in the gastrointestinal tracts of rats and humans. *Endocrinology*, **141**, 4255–4261.
Dhillon, H., Zigman, J.M., Ye, C., Lee, C.E., McGovern, R.A., Tang, V., Kenny, C.D., Christiansen, L.M., White, R.D., Edelstein, E.A., Coppari, R., Balthasar, N., Cowley, M.A., Chua, S., Elmquist, J.K. & Lowell, B.B. (2006) Leptin directly activates SF1 neurons in the VMH, and this action by leptin is required for normal body-weight homeostasis. *Neuron*, **49**, 191–203.
Dietrich, M.O. & Horvath, T.L. (2009) GABA keeps up an appetite for life. *Cell*, **137**, 1177–1179.
Dietrich, M., Andrews, Z.B. & Horvath, T.L. (2008) Exercise-induced synaptogenesis in the hippocampus is dependent on UCP2-regulated mitochondrial adaptation. *J. Neurosci.*, **28**, 10766–10771.
Ekblad, E. & Sundler, F. (2002) Distribution of pancreatic polypeptide and peptide YY. *Peptides*, **23**, 251–261.
Emanuelli, M., Carnevali, F., Saccucci, F., Pierella, F., Amici, A., Raffaelli, N. & Magni, G. (2001) Molecular cloning, chromosomal localization, tissue mRNA levels, bacterial expression, and enzymatic properties of human NMN adenylyltransferase. *J. Biol. Chem.*, **276**, 406–412.
Fan, W., Boston, B.A., Kesterson, R.A., Hruby, V.J. & Cone, R.D. (1997) Role of melanocortinergic neurons in feeding and the agouti obesity syndrome. *Nature*, **385**, 165–168.
Fan, W., Ellacott, K.L., Halatchev, I.G., Takahashi, K., Yu, P. & Cone, R.D. (2004) Cholecystokinin-mediated suppression of feeding involves the brainstem melanocortin system. *Nat. Neurosci.*, **7**, 335–336.
Farooqi, I.S. & O'rahilly, S. (2008) Mutations in ligands and receptors of the leptin-melanocortin pathway that lead to obesity. *Nat. Clin. Pract. Endocrinol. Metab.*, **4**, 569–577.
Fioramonti, X., Contié, S., Song, Z., Routh, V.H., Lorsignol, A. & Pénicaud, L. (2007) Characterization of glucosensing neuron subpopulations in the arcuate nucleus: integration in neuropeptide Y and pro-opio melanocortin networks? *Diabetes*, **56**, 1219–1227.
Friedman, J.M. & Halaas, J.L. (1998) Leptin and the regulation of body weight in mammals. *Nature*, **395**, 763–770.
Fulco, M., Schiltz, R.L., Iezzi, S., King, M.T., Zhao, P., Kashiwaya, Y., Hoffman, E., Veech, R.L. & Sartorelli, V. (2003) Sir2 regulates skeletal muscle differentiation as a potential sensor of the redox state. *Mol. Cell*, **12**, 51–62.
Fulton, S., Pissios, P., Manchon, R.P., Stiles, L., Frank, L., Pothos, E.N., Maratos-Flier, E. & Flier, J.S. (2006) Leptin regulation of the mesoaccumbens dopamine pathway. *Neuron*, **51**, 811–822.
Gao, Q., Mezei, G., Nie, Y., Rao, Y., Choi, C.S., Bechmann, I., Leranth, C., Toran-Allerand, D., Priest, C.A., Roberts, J.L., Gao, X.B., Mobbs, C., Shulman, G.I., Diano, S. & Horvath, T.L. (2007) Anorectic estrogen mimics leptin's effect on the rewiring of melanocortin cells and Stat3 signaling in obese animals. *Nat. Med.*, **13**, 89–94.
Garcia-Segura, L.M., Baetens, D. & Naftolin, F. (1986) Synaptic remodelling in arcuate nucleus after injection of estradiol valerate in adult female rats. *Brain Res.*, **366**, 131–136.
Garcia-Segura, L.M., Olmos, G., Tranque, P. & Naftolin, F. (1987) Rapid effects of gonadal steroids upon hypothalamic neuronal membrane ultrastructure. *J. Steroid Biochem.*, **27**, 615–623.
Gehring, W. & Rosbash, M. (2003) The coevolution of blue-light photoreception and circadian rhythms. *J. Mol. Evol.*, **57**(Suppl 1), S286–S289.
Grimaldi, B., Nakahata, Y., Kaluzova, M., Masubuchi, S. & Sassone-Corsi, P. (2009) Chromatin remodeling, metabolism and circadian clocks: the interplay of CLOCK and SIRT1. *Int. J. Biochem. Cell Biol.*, **41**, 81–86.
Gropp, E., Shanabrough, M., Borok, E., Xu, A.W., Janoschek, R., Buch, T., Plum, L., Balthasar, N., Hampel, B., Waisman, A., Barsh, G.S., Horvath, T.L. & Brüning, J.C. (2005) Agouti-related peptide-expressing neurons are mandatory for feeding. *Nat. Neurosci.*, **8**, 1289–1291.
Hahn, T.M., Breininger, J.F., Baskin, D.G. & Schwartz, M.W. (1998) Coexpression of Agrp and NPY in fasting-activated hypothalamic neurons. *Nat. Neurosci.*, **1**, 271–272.
Halatchev, I.G. & Cone, R.D. (2005) Peripheral administration of PYY(3-36) produces conditioned taste aversion in mice. *Cell Metab.*, **1**, 159–168.
Halatchev, I.G., Ellacott, K.L., Fan, W. & Cone, R.D. (2004) Peptide YY3-36 inhibits food intake in mice through a melanocortin-4-receptor-independent mechanism. *Endocrinology*, **145**, 2585–2590.
Hetherington, A.W. (1941) The relation of various hypothalamic lesions to adiposity and other phenomena in the rat. *Amer. J. Physiol.*, **133**, 326–327.
Hetherington, A.W. (1944) Non-production of hypothalamic obesity in the rat by lesions rostral or dorsal to the ventro-medial hypothalamic nuclei. *J. Comp. Neurol.*, **80**, 33–45.
Hetherington, A.W. & Ranson, S.W. (1942) The relation of various hypothalamic lesions to adiposity in the rat. *J. Comp. Neurol.*, **76**, 475–499.
Hommel, J.D., Trinko, R., Sears, R.M., Georgescu, D., Liu, Z.W., Gao, X.B., Thurmon, J.J., Marinelli, M. & DiLeone, R.J. (2006) Leptin receptor signaling in midbrain dopamine neurons regulates feeding. *Neuron*, **51**, 801–810.
Horvath, T.L. & Diano, S. (2004) The floating blueprint of hypothalamic feeding circuits. *Nat. Rev. Neurosci.*, **5**, 662–667.
Horvath, T.L., Naftolin, F., Kalra, S.P. & Leranth, C. (1992) Neuropeptide-Y innervation of beta-endorphin-containing cells in the rat mediobasal hypothalamus: a light and electron microscopic double immunostaining analysis. *Endocrinology*, **131**, 2461–2467.
Horvath, T.L., Bechmann, I., Naftolin, F., Kalra, S.P. & Leranth, C. (1997) Heterogeneity in the neuropeptide Y-containing neurons of the rat arcuate nucleus: GABAergic and non-GABAergic subpopulations. *Brain Res.*, **756**, 283–286.

Howard, A.D., Feighner, S.D., Cully, D.F., Arena, J.P., Liberator, P.A., Rosenblum, C.I., Hamelin, M., Hreniuk, D.L., Palyha, O.C., Anderson, J., Paress, P.S., Diaz, C., Chou, M., Liu, K.K., McKee, K.K., Pong, S.S., Chaung, L.Y., Elbrecht, A., Dashkevicz, M., Heavens, R., Rigby, M., Sirinathsinghji, D.J., Dean, D.C., Melillo, D.G., Patchett, A.A., Nargund, R., Griffin, P.R., DeMartino, J.A., Gupta, S.K., Schaeffer, J.M., Smith, R.G. & Van der Ploeg, L.H. (1996) A receptor in pituitary and hypothalamus that functions in growth hormone release. *Science*, **273**, 974–977.

Hummel, K.P., Dickie, M.M. & Coleman, D.L. (1966) Diabetes, a new mutation in the mouse. *Science*, **153**, 1127–1128.

Ibrahim, N., Bosch, M.A., Smart, J.L., Qiu, J., Rubinstein, M., Rønnekleiv, O.K., Low, M.J. & Kelly, M.J. (2003) Hypothalamic proopiomelanocortin neurons are glucose responsive and express K(ATP) channels. *Endocrinology*, **144**, 1331–1340.

Imai, S., Armstrong, C.M., Kaeberlein, M. & Guarente, L. (2000) Transcriptional silencing and longevity protein Sir2 is an NAD-dependent histone deacetylase. *Nature*, **403**, 795–800.

Klebig, M.L., Wilkinson, J.E., Geisler, J.G. & Woychik, R.P. (1995) Ectopic expression of the agouti gene in transgenic mice causes obesity, features of type II diabetes, and yellow fur. *Proc. Natl Acad. Sci. USA*, **92**, 4728–4732.

Kojima, M., Hosoda, H., Date, Y., Nakazato, M., Matsuo, H. & Kangawa, K. (1999) Ghrelin is a growth-hormone-releasing acylated peptide from stomach. *Nature*, **402**, 656–660.

Langle, S.L., Poulain, D.A. & Theodosis, D.T. (2002) Neuronal-glial remodeling: a structural basis for neuronal-glial interactions in the adult hypothalamus. *J. Physiol. Paris*, **96**, 169–175.

Lein, E.S., Hawrylycz, M.J., Ao, N., Ayres, M., Bensinger, A., Bernard, A., Boe, A.F., Boguski, M.S., Brockway, K.S., Byrnes, E.J., Chen, L., Chen, L., Chen, T.M., Chin, M.C., Chong, J., Crook, B.E., Czaplinska, A., Dang, C.N., Datta, S., Dee, N.R., Desaki, A.L., Desta, T., Diep, E., Dolbeare, T.A., Donelan, M.J., Dong, H.W., Dougherty, J.G., Duncan, B.J., Ebbert, A.J., Eichele, G., Estin, L.K., Faber, C., Facer, B.A., Fields, R., Fischer, S.R., Fliss, T.P., Frensley, C., Gates, S.N., Glattfelder, K.J., Halverson, K.R., Hart, M.R., Hohmann, J.G., Howell, M.P., Jeung, D.P., Johnson, R.A., Karr, P.T., Kawal, R., Kidney, J.M., Knapik, R.H., Kuan, C.L., Lake, J.H., Laramee, A.R., Larsen, K.D., Lau, C., Lemon, T.A., Liang, A.J., Liu, Y., Luong, L.T., Michaels, J., Morgan, J.J., Morgan, R.J., Mortrud, M.T., Mosqueda, N.F., Ng, L.L., Ng, R., Orta, G.J., Overly, C.C., Pak, T.H., Parry, S.E., Pathak, S.D., Pearson, O.C., Puchalski, R.B., Riley, Z.L., Rockett, H.R., Rowland, S.A., Royall, J.J., Ruiz, M.J., Sarno, N.R., Schaffnit, K., Shapovalova, N.V., Sivisay, T., Slaughterbeck, C.R., Smith, S.C., Smith, K.A., Smith, B.I., Sodt, A.J., Stewart, N.N., Stumpf, K.R., Sunkin, S.M., Sutram, M., Tam, A., Teemer, C.D., Thaller, C., Thompson, C.L., Varnam, L.R., Visel, A., Whitlock, R.M., Wohnoutka, P.E., Wolkey, C.K., Wong, V.Y., Wood, M., Yaylaoglu, M.B., Young, R.C., Youngstrom, B.L., Yuan, X.F., Zhang, B., Zwingman, T.A. & Jones, A.R. (2007) Genome-wide atlas of gene expression in the adult mouse brain. *Nature*, **445**, 168–176.

Li, Z., Okamoto, K., Hayashi, Y. & Sheng, M. (2004) The importance of dendritic mitochondria in the morphogenesis and plasticity of spines and synapses. *Cell*, **119**, 873–887.

Liddle, R.A., Goldfine, I.D., Rosen, M.S., Taplitz, R.A. & Williams, J.A. (1985) Cholecystokinin bioactivity in human plasma. Molecular forms, responses to feeding, and relationship to gallbladder contraction. *J. Clin. Invest.*, **75**, 1144–1152.

Livet, J., Weissman, T.A., Kang, H., Draft, R.W., Lu, J., Bennis, R.A., Sanes, J.R. & Lichtman, J.W. (2007) Transgenic strategies for combinatorial expression of fluorescent proteins in the nervous system. *Nature*, **450**, 56–62.

Lu, D., Willard, D., Patel, I.R., Kadwell, S., Overton, L., Kost, T., Luther, M., Chen, W., Woychik, R.P. & Wilkison, W.O. (1994) Agouti protein is an antagonist of the melanocyte-stimulating-hormone receptor. *Nature*, **371**, 799–802.

Lundberg, J.M., Tatemoto, K., Terenius, L., Hellström, P.M., Mutt, V., Hökfelt, T. & Hamberger, B. (1982) Localization of peptide YY (PYY) in gastrointestinal endocrine cells and effects on intestinal blood flow and motility. *Proc. Natl Acad. Sci.*, **79**, 4471–4475.

Luquet, S., Perez, F.A., Hnasko, T.S. & Palmiter, R.D. (2005) NPY/AgRP neurons are essential for feeding in adult mice but can be ablated in neonates. *Science*, **310**, 683–685.

Magni, G., Amici, A., Emanuelli, M., Raffaelli, N. & Ruggieri, S. (1999) Enzymology of NAD^+ synthesis. *Adv. Enzymol. Relat. Areas Mol. Biol.*, **73**, 135–182.

Marshall, N.B., Barrnett, R.J. & Mayer, J. (1955a) Hypothalamic lesions in goldthioglucose injected mice. *Proc. Soc. Exp. Biol. Med.*, **90**, 240–244.

Marshall, N.B., Barrnett, R.J. & Mayer, J. (1955b) Hypothalamic lesions in goldthioglucose injected mice. *Proc. Soc. Exp. Biol. Med.*, **90**, 240–244.

Matsumoto, A. & Arai, Y. (1979) Synaptogenic effect of estrogen on the hypothalamic arcuate nucleus of the adult female rat. *Cell Tissue Res.*, **198**, 427–433.

Matsumoto, A. & Arai, Y. (1981) Neuronal plasticity in the deafferented hypothalamic arcuate nucleus of adult female rats and its enhancement by treatment with estrogen. *J. Comp. Neurol.*, **197**, 197–205.

Mentlein, R., Dahms, P., Grandt, D. & Kruger, R. (1993) Proteolytic processing of neuropeptide Y and peptide YY by dipeptidyl peptidase IV. *Regul. Pept.*, **49**, 133–144.

Naftolin, F., Mor, G., Horvath, T.L., Luquin, S., Fajer, A.B., Kohen, F. & Garcia-Segura, L.M. (1996) Synaptic remodeling in the arcuate nucleus during the estrous cycle is induced by estrogen and precedes the preovulatory gonadotropin surge. *Endocrinology*, **137**, 5576–5580.

Nakahata, Y., Kaluzova, M., Grimaldi, B., Sahar, S., Hirayama, J., Chen, D., Guarente, L.P. & Sassone-Corsi, P. (2008) The NAD^+-dependent deacetylase SIRT1 modulates CLOCK-mediated chromatin remodeling and circadian control. *Cell*, **134**, 329–340.

Nakahata, Y., Sahar, S., Astarita, G., Kaluzova, M. & Sassone-Corsi, P. (2009) Circadian control of the NAD^+ salvage pathway by CLOCK-SIRT1. *Science*, **324**, 654–657.

Nilsson, O., Bilchik, A.J., Goldenring, J.R., Ballantyne, G.H., Adrian, T.E. & Modlin, I.M. (1991) Distibution and immunocytochemical colocalization of peptide YY and enteroglucagon in endocrine cells of rabbit colon. *Endocrinology*, **129**, 139–149.

Nogueiras, R., Tovar, S., Mitchell, S.E., Rayner, D.V., Archer, Z.A., Dieguez, C. & Williams, L.M. (2004) Regulation of growth hormone secretagogue receptor gene expression in the arcuate nuclei of the rat by leptin and ghrelin. *Diabetes*, **53**, 2552–2558.

Norsted, E., Gömüç, B. & Meister, B. (2008) Protein components of the blood-brain barrier (BBB) in the mediobasal hypothalamus. *J. Chem. Neuroanat.*, **36**, 107–121.

Olney, J.W. (1969) Brain lesions, obesity, and other disturbances in mice treated with monosodium glutamate. *Science*, **164**, 719–721.

Olney, J.W., Adamo, N.J. & Ratner, A. (1971) Monosodium glutamate effects. *Science*, **172**, 294.

Onaga, T., Yoshida, M., Inoue, H. & Yokota, H. (2000) Regional distribution and plasma concentration of peptide YY in sheep. *Peptides*, **21**, 655–667.

Panatier, A., Theodosis, D.T., Mothet, J.P., Touquet, B., Pollegioni, L., Poulain, D.A. & Oliet, S.H. (2006) Glia-derived D-serine controls NMDA receptor activity and synaptic memory. *Cell*, **125**, 775–784.

Parton, L.E., Ye, C.P., Coppari, R., Enriori, P.J., Choi, B., Zhang, C.Y., Xu, C., Vianna, C.R., Balthasar, N., Lee, C.E., Elmquist, J.K., Cowley, M.A. & Lowell, B.B. (2007) Glucose sensing by POMC neurons regulates glucose homeostasis and is impaired in obesity. *Nature*, **449**, 228–232.

Pinto, S., Roseberry, A.G., Liu, H., Diano, S., Shanabrough, M., Cai, X., Friedman, J.M. & Horvath, T.L. (2004) Rapid rewiring of arcuate nucleus feeding circuits by leptin. *Science*, **304**, 110–115.

Ramsey, K.M., Yoshino, J., Brace, C.S., Abrassart, D., Kobayashi, Y., Marcheva, B., Hong, H.K., Chong, J.L., Buhr, E.D., Lee, C., Takahashi, J.S., Imai, S. & Bass, J. (2009) Circadian clock feedback cycle through NAMPT-mediated NAD^+ biosynthesis. *Science*, **324**, 351–354.

Ranson, S.W., Fisher, C. & Ingram, W.R. (1938) Diposity and diabetes mellitus in a monkey with hypothalamic lesions. *Endocrinology*, **23**, 175–181.

Revollo, J.R., Grimm, A.A. & Imai, S. (2004) The NAD biosynthesis pathway mediated by nicotinamide phosphoribosyltransferase regulates Sir2 activity in mammalian cells. *J. Biol. Chem.*, **279**, 50754–50763.

Revollo, J.R., Körner, A., Mills, K.F., Satoh, A., Wang, T., Garten, A., Dasgupta, B., Sasaki, Y., Wolberger, C., Townsend, R.R., Milbrandt, J., Kiess, W. & Imai, S. (2007) Nampt/PBEF/Visfatin regulates insulin secretion in beta cells as a systemic NAD biosynthetic enzyme. *Cell Metab.*, **5**, 363–375.

Roenneberg, T. & Merrow, M. (2002) "What watch?... such much!"* Complexity and evolution of circadian clocks. *Cell Tissue Res.*, **309**, 3–9.

Schweigler, M., Hennig, K., Lerner, F., Niere, M., Hirsch-Kauffmann, M., Specht, T., Weise, C., Oei, S.L. & Ziegler, M. (2001) Characterization of recombinant human nicotinamide mononucleotide adenylyl transferase (NMNAT), a nuclear enzyme essential for NAD synthesis. *FEBS Lett.*, **492**, 95–100.

Stanley, B.G. & Leibowitz, S.F. (1984) Neuropeptide Y: stimulation of feeding and drinking by injection into the paraventricular nucleus. *Life Sci.*, **35**, 2635–2642.

Straus, E. & Yalow, R.S. (1979) Cholecystokinin in the brains of obese and nonobese mice. *Science*, **203**, 68–69.

Szymanski, J.S. (1918) Versuche uber die Fahigkeit der Hunde zur Bildung von optischen Association. *Pfluger's Arch. f. d. ges. Physiol.*, **171**, 317–324.

Tang-Christensen, M., Vrang, N., Ortmann, S., Bidlingmaier, M., Horvath, T.L. & Tschöp, M. (2004) Central administration of ghrelin and agouti-related protein (83-132) increases food intake and decreases spontaneous locomotor activity in rats. *Endocrinology*, **145**, 4645–4652.

Tatemoto, K., Carlquist, M. & Mutt, V. (1982) Neuropeptide Y–a novel brain peptide with structural similarities to peptide YY and pancreatic polypeptide. *Nature*, **296**, 659–660.

Theodosis, D.T., Piet, R., Poulain, D.A. & Oliet, S.H. (2004) Neuronal, glial and synaptic remodeling in the adult hypothalamus: functional consequences and role of cell surface and extracellular matrix adhesion molecules. *Neurochem. Int.*, **45**, 491–501.

Theodosis, D.T., Trailin, A. & Poulain, D.A. (2006) Remodeling of astrocytes, a prerequisite for synapse turnover in the adult brain? Insights from the oxytocin system of the hypothalamus *Am. J. Physiol. Regul. Integr. Comp. Physiol.*, **290**, R1175–R1182.

Theodosis, D.T., Poulain, D.A. & Oliet, S.H. (2008) Activity-dependent structural and functional plasticity of astrocyte-neuron interactions. *Physiol. Rev.*, **88**, 983–1008.

Tschöp, M., Castañeda, T.R., Joost, H.G., Thöne-Reineke, C., Ortmann, S., Klaus, S., Hagan, M.M., Chandler, P.C., Oswald, K.D., Benoit, S.C., Seeley, R.J., Kinzig, K.P., Moran, T.H., Beck-sickinger, A.G., Koglin, N., Rodgers, R.J., Blundell, J.E., Ishii, Y., Beattie, A.H., Holch, P., Allison, D.B., Raun, K., Madsen, K., Wulff, B.S., Stidsen, C.E., Birringer, M., Kreuzer, O.J., Schindler, M., Arndt, K., Rudolf, K., Mark, M., Deng, X.Y., Whitcomb, D.C., Halem, H., Taylor, J., Dong, J., Datta, R., Culler, M., Craney, S., Flora, D., Smiley, D., Heiman, M.L. & Withcomb, D.C. (2004) Physiology: does gut hormone PYY3-36 decrease food intake in rodents? *Nature*, **430**, 1.

Vitaterna, M.H., King, D.P., Chang, A.M., Kornhauser, J.M., Lowrey, P.L., McDonald, J.D., Dove, W.F., Pinto, L.H., Turek, F.W. & Takahashi, J.S. (1994) Mutagenesis and mapping of a mouse gene, Clock, essential for circadian behavior. *Science*, **264**, 719–725.

Wang, R., Liu, X., Hentges, S.T., Dunn-Meynell, A.A., Levin, B.E., Wang, W. & Routh, V.H. (2004) The regulation of glucose-excited neurons in the hypothalamic arcuate nucleus by glucose and feeding-relevant peptides. *Diabetes*, **53**, 1959–1965.

Willesen, M.G., Kristensen, P. & Romer, J. (1999) Co-localization of growth hormone secretagogue receptor and NPY mRNA in the arcuate nucleus of the rat. *Neuroendocrinology*, **70**, 306–316.

Williams, D.L. & Cummings, D.E. (2005) Regulation of ghrelin in physiologic and pathophysiologic states. *J. Nutr.*, **135**, 1320–1325.

Wren, A.M., Small, C.J., Ward, H.L., Murphy, K.G., Dakin, C.L., Taheri, S., Kennedy, A.R., Roberts, G.H., Morgan, D.G., Ghatei, M.A. & Bloom, S.R. (2000) The novel hypothalamic peptide ghrelin stimulates food intake and growth hormone secretion. *Endocrinology*, **141**, 4325–4328.

Wu, Q., Boyle, M.P. & Palmiter, R.D. (2009) Loss of GABAergic signaling by AgRP neurons to the parabrachial nucleus leads to starvation. *Cell*, **137**, 1225–1234.

Zhang, Y., Proenca, R., Maffei, M., Barone, M., Leopold, L. & Friedman, J.M. (1994) Positional cloning of the mouse obese gene and its human homologue. *Nature*, **372**, 425–432.

Zigman, J.M. & Elmquist, J.K. (2003) Minireview: from anorexia to obesity – the yin and yang of body weight control. *Endocrinology*, **144**, 3749–3756.

Capítulo IV. GABA Keeps Up an Appetite for Life

Artigo publicado no periódico *Cell*.

Leading Edge
Previews

Cell

GABA Keeps Up an Appetite for Life

Marcelo O. Dietrich[1,2] and Tamas L. Horvath[1,*]
[1]Program on Cell and Neurobiology of Energy Metabolism, Section of Comparative Medicine, Yale University School of Medicine, New Haven, CT 06520, USA
[2]Programa de Pós-graduação em Bioquímica, Department of Biochemistry, Universidade Federal do Rio Grande do Sul, Porto Alegre RS 90035, Brazil
*Correspondence: tamas.horvath@yale.edu
DOI 10.1016/j.cell.2009.06.002

In the arcuate nucleus of the hypothalamus, neurons that produce the neuropeptides NPY and AgRP play a vital role in the maintenance of energy homeostasis. In this issue, Wu et al. (2009) show that these neurons modulate feeding behavior in mice by providing GABAergic input to the parabrachial nucleus in the brainstem.

Neurons that produce the neuropeptides NPY and AgRP (NPY/AgRP neurons) in the arcuate nucleus of the hypothalamus also secrete the inhibitory neurotransmitter GABA (Horvath et al., 1997). An interaction between NPY and GABA in the hypothalamus plays a role in the regulation of feeding behavior in rodents (Pu et al., 1999). In addition, the selective ablation of NPY/AgRP neurons in adult mice induces a rapid decrease in food intake (Gropp et al., 2005; Luquet et al., 2005), leading to starvation (Luquet et al., 2005). Intriguingly, the selective ablation of these neurons also has an effect on their postsynaptic targets outside of the hypothalamus (Wu et al., 2008). In this issue of *Cell*, Wu et al. (2009) further explore the role of the GABAergic outputs of NPY/AgRP neurons in an elegantly designed and executed study in mice. They provide compelling evidence that feeding behavior in mice is regulated by GABAergic input from NPY/AgRP neurons to the parabrachial nucleus.

The parabrachial nucleus is located in the dorsolateral part of the pons (a region of the brainstem) (Figure 1A) and is a relay center for signals from the nucleus tractus solitarius to the forebrain. These autonomic afferent connections to the parabrachial nucleus are responsible for regulating sensory stimuli, including those related to taste and gastric distension (stimuli that modulate feeding behavior). Wu et al. now demonstrate that GABAergic signaling from the NPY/AgRP neurons to the parabrachial nucleus plays a major role in regulating feeding behavior (Figure 1A). The authors observe that in adult mice lacking NPY/AgRP neurons, pharmacological stimulation of $GABA_A$ receptors in the parabrachial nucleus by local injection of bretazenil, a partial $GABA_A$ receptor agonist, is sufficient to maintain feeding and survival. This strongly supports a vital role for GABAergic signaling in the parabrachial nucleus in the regulation of feeding. Wu and colleagues further corroborate these findings by examining the effects of either infusing a GABA antagonist directly into the parabrachial nucleus or selectively ablating NPY/AgRP inputs to this area. Both experiments induce a progressive decrease in feeding (anorexia) in mice, indicating that GABAergic inputs from arcuate nucleus NPY/AgRP neurons to the parabrachial nucleus are required to maintain a critical level of appetite stimulus (orexigenic tone).

These observations also represent a potential shift away from current explanations of energy metabolism regulation. Prior to this work, it had been thought that NPY/AgRP neurons regulated energy metabolism primarily through the pro-opiomelanocortin neurons, also found in the arcuate nucleus (Figure 1B). Wu et al. show that the regulation of feeding through the neural circuit involving the parabrachial nucleus is likely independent of the pro-opiomelanocortin neurons.

In addition to the parabrachial nucleus, Wu and colleagues find that another brain region called the lateral septum is also important, albeit to a lesser extent, in the induction of anorexia stemming from the loss of GABAergic inputs from the NPY/AgRP neurons. Pharmacological manipulation of $GABA_A$ neurotransmission in the lateral septum produces a partial effect on feeding in mice lacking NPY/AgRP neurons. The lateral septum is located in the ventral forebrain, which receives excitatory inputs from the hippocampal formations and the cortex. Like the parabrachial nucleus, the lateral septum also receives a complex network of GABAergic inputs from the hypothalamus, the amygdala, and other areas of the brain that are essential for initiating behavioral responses associated with the limbic system. Thus, both the parabrachial nucleus and lateral septum are positioned to play critical roles in the regulation of complex behaviors associated with higher brain functions. Wu and colleagues propose that the NPY/AgRP neurons of the arcuate nucleus are master regulators of these brain regions and, hence, of complex behaviors. Inferences from their data point to the biological truism that the primary driving force for the emergence of complex organisms and their increasingly sophisticated behaviors is the need to more efficiently acquire resources—primarily energy—from the environment. From this perspective, dual roles for NPY/AgRP neurons in the modulation of energy metabolism and the coordination of higher brain functions seem logical.

Another striking observation of the Wu et al. study is that pharmacological GABA stimulation of adult mice for 10 days after the ablation of NPY/AgRP neurons is sufficient to ensure food intake and survival even after withdrawal of the pharmacological treatment. These results suggest that important adaptive mechanisms are initiated after ablation of the NPY/AgRP neurons.

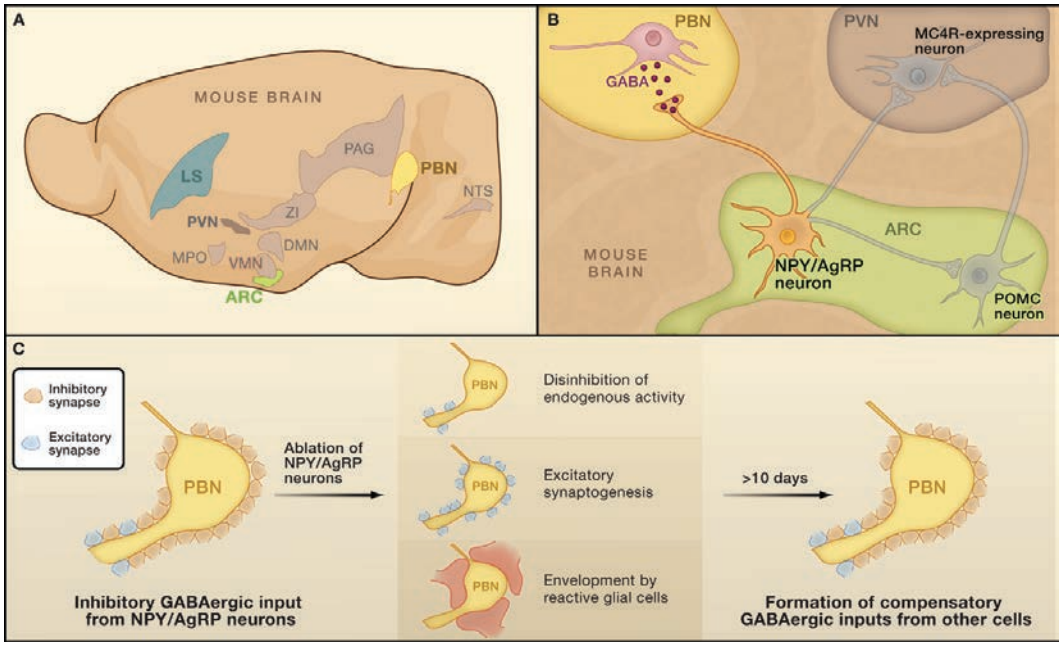

Figure 1. The GABAergic Output of NPY/AgRP Neurons

(A) The NPY/AgRP neurons in the arcuate nucleus (ARC, green) of the hypothalamus send inputs to various nuclei inside and outside the hypothalamus, including the parabrachial nucleus (PBN, yellow) and the lateral septum (LS, blue). MPO, medial preoptic area; ZI, zona incerta; VMN, ventromedial nucleus; DMN, dorsomedial nucleus; ARC, arcuate nucleus; PAG, periaqueductal nucleus; NTS, nucleus tractus solitarius.

(B) Metabolic regulation by GABAergic NPY/AgRP neurons is thought to occur through their interactions with the synaptic output of pro-opiomelanocortin (POMC) neurons or MC4R-expressing neurons in the paraventricular nucleus (PVN). The Wu et al. (2009) study shows that the GABAergic inputs from the NPY/AgRP neurons to the PBN, which are necessary for maintaining feeding behavior, are independent of POMC neurons.

(C) Ablation of NPY/AgRP neurons in the ARC results in the loss of GABAergic inhibitory inputs to target brain regions such as the PBN. One possible mechanistic explanation for the slow adaptive response that occurs after the loss of these neurons is that the ablation first leads to hyperstimulation of the target brain areas due to disinhibition of the activity of the postsynaptic target neurons, an increase in the excitatory inputs to the target cells, and an increase in the envelopment of the target neurons by reactive glia. After this early adaptation, synaptic plasticity allows for modification of the neural circuitry, resulting in the recruitment of new inhibitory inputs on the target cells to compensate for the loss of the GABAergic inputs from the NPY/AgRP neurons.

One intriguing hypothesis for an adaptive mechanism is that the pharmacological stimulation of GABAergic synapses following ablation of NPY/AgRP cells triggers a rewiring of the circuitry in the parabrachial nucleus and lateral septum. This remodeling of neural circuitry then counteracts the loss of GABAergic inputs from the NPY/AgRP neurons. There are reports of neural circuit plasticity triggered by metabolic hormones or manipulation of brain circuits in the hypothalamus (Pinto et al., 2004), the hippocampus (Diano et al., 2006), and the ventral tegmental area of the midbrain (Abizaid et al., 2006). Thus, a similar rearrangement of synaptic inputs to the parabrachial nucleus and lateral septum neurons, as suggested by the work of Wu et al., is likely. However, the precise time after ablation of NPY/AgRP neurons when the GABA agonist must be administered to avoid the anorexic response is unknown. There is also an alternate hypothesis for the adaptive response to GABAergic input. Activation of glial cells following ablation of the NPY/AgRP neurons could be responsible for rescuing feeding behavior. Glial cells are known to respond to insults to the brain through a mechanism termed reactive gliosis. These reactive cells produce a series of factors, including numerous cytokines, that can influence energy balance via the nervous system. The ablation of the NPY/AgRP neurons in the arcuate nucleus does cause glial cell activation in the parabrachial nucleus and lateral septum, but the authors did not examine the role of this activation in the anorexic response. Additionally, Wu et al. did not evaluate whether the partial $GABA_A$ receptor agonist plays a role in regulating glial cell activation.

Notably, the selective ablation of NPY/AgRP neurons in neonatal mice has no obvious effect on body weight and food intake (Luquet et al., 2005). Similarly, the delayed degeneration of NPY/AgRP neurons during adulthood in mice does not produce any robust phenotypes in terms of energy metabolism (Xu et al., 2005). Together, these results suggest that there is a gradual adaptive response on the part of brain networks to replace the inhibition normally maintained by

the GABAergic NPY/AgRP neurons (Figure 1C). However, when the degeneration of these cells is rapid, perhaps no adaptive response can occur to promote survival, thus explaining why ablation of NPY/AgRP neurons in adult mice results in starvation. A thorough comprehension of the molecular, cellular, and morphological adaptations that take place during degeneration of the NPY/AgRP neurons of the arcuate nucleus will bring new insights not only to the regulation of energy metabolism but also to understanding the basic principles of how neural circuits are remodeled.

REFERENCES

Abizaid, A., Liu, Z.-W., Andrews, Z.B., Shanabrough, M., Borok, E., Elsworth, J., Roth, R.H., Sleeman, M., Picciotto, M.R., Tschop, M., et al. (2006). J. Clin. Invest. *116*, 3229–3239.

Diano, D., Farr, S.A., Benoit, S.C., Mcnay, E.C., da Silva, I., Horvath, B., Gaskin, F.S., Nonaka, N., Jaeger, L.B., Xu, L., et al. (2006). Nat. Neurosci. *9*, 381–388.

Gropp, E., Shanabrough, M., Borok, E., Xu, A.W., Janoshek, R., Buch, T., Plum, L., Balthasar, N., Hampel, B., Waisman, A., et al. (2005). Nat. Neurosci. *8*, 1289–1291.

Horvath, T.L., Bechmann, I., Kalra, S.P., Naftolin, F., and Leranth, C. (1997). Brain Res. *756*, 283–286.

Luquet, S., Perez, F.A., Hnasko, T.S., and Palmiter, R.D. (2005). Science *310*, 683–685.

Pinto, S., Roseberry, A.G., Liu, H., Diano, S., Shanabrough, M., Cai, X., Friedman, J.M., and Horvath, T.L. (2004). Science *304*, 110–115.

Pu, S., Jain, M.R., Horvath, T.L., Diano, S., Kalra, P.S., and Kalra, S.P. (1999). Endocrinology *140*, 933–940.

Wu, Q., Howell, M.P., and Palmiter, R.D. (2008). J. Neurosci. *28*, 9218–9226.

Wu, Q., Howell, M.P., and Palmiter, R.D. (2009). Cell, this issue.

Xu, A.W., Kaelin, C.B., Morton, G.J., Ogimoto, K., Stanhope, K., Graham, J., Baskin, D.G., Havel, P., Schwartz, M.W., and Barsh, G.S. (2005). PLoS Biol. *3*, e415. 10.1371/journal.pbio.0030415.

Ironing Out a Midlife Crisis

Sandra Viviana Vergara[1,2,*] and Dennis J. Thiele[1,2]
[1]Department of Pharmacology and Cancer Biology
[2]Duke University Program in Genetics and Genomics
Duke University Medical Center, Durham, NC 27710, USA
*Correspondence: sandra.vergara@duke.edu

DOI 10.1016/j.cell.2009.06.005

There is a strong correlation between age, genomic instability, and the development of cancer. Working in yeast, Veatch et al. (2009) now propose that defects in the biogenesis of iron-sulfur clusters arising as a consequence of mitochondrial dysfunction contribute to the increase in genomic instability as cells age.

As humans approach middle age, the incidence of cancer grows exponentially with a lifetime risk of developing the disease of one in two for men and one in three for women (DePinho, 2000). This increase may be partially explained by the lifetime accumulation of somatic mutations that lead to the inactivation of tumor suppressor genes and activation of oncogenes. However, the number of mutations found in cells from older individuals is higher than would be expected if mutations occur at a constant rate. In addition, the accumulation of spontaneous mutations alone cannot account for the large number of genomic alterations characteristic of cancers, including aneuploidy and other chromosomal aberrations. Instead, a plethora of studies suggest that one or more cellular events lead to a higher-than-normal rate of mutation, thereby increasing the probability of catastrophic genomic alterations. In this issue of *Cell*, Veatch et al. (2009), postulate that damage or loss of mitochondrial DNA (mtDNA) in aging cells precipitates a cellular crisis characterized by a gradual reduction in growth rates, G1 cell cycle arrest, and decreased nuclear genome stability (Figure 1). These findings suggest that genomic instability arises from mitochondrial dysfunction and, more specifically, because of defects in the biogenesis of iron-sulfur (Fe-S) clusters.

Loss of heterozygosity (LOH) typically arises from defects in DNA repair mechanisms, from gross chromosomal rearrangements, or from errors in chromosome segregation. Thus, the frequency of LOH events may be interpreted as a measure of nuclear genomic stability. Using a colony-sectoring method to measure LOH events as a function of daughter cell generation in baker's yeast (McMurray, and Gottschling, 2003), Veatch et al. investigate the role of mitochondrial function in genome stability and identify an important mechanistic link between LOH and mitochondrial dysfunction. The authors find that daughter cells from aging mothers give rise to small colonies that are unable to respire (*petites*), primarily as a consequence of damage to or total loss of mtDNA. Interestingly, the overwhelming fraction of these *petites* also display a dramatically increased frequency of nuclear LOH. As the elimination of mtDNA from young cells, via genetic or pharmacological manipulation, also produces *petite* colonies with a higher frequency of nuclear LOH events, the authors further conclude that mitochondrial dysfunction that is associated with aging, rather than aging itself, leads to increased nuclear genomic instability.

Capítulo V. Synaptic Plasticity of Feeding Circuits: Hormones and Hysteresis

Artigo publicado no periódico *Cell*.

Leading Edge
Previews

Cell

Synaptic Plasticity of Feeding Circuits: Hormones and Hysteresis

Marcelo O. Dietrich[1,4] and Tamas L. Horvath[1,2,3,*]
[1]Section of Comparative Medicine
[2]Department of Obstetrics, Gynecology and Reproductive Sciences
[3]Department of Neurobiology
Yale University School of Medicine, New Haven, CT 06520, USA
[4]Programa de Pós-graduação em Bioquímica, Department of Biochemistry, Universidade Federal do Rio Grande do Sul, Porto Alegre RS 90035, Brazil
*Correspondence: tamas.horvath@yale.edu
DOI 10.1016/j.cell.2011.08.031

The drive to eat is controlled by neuronal circuits in the hypothalamus that respond to hormones signaling hunger or satiety. In this issue of *Cell*, Yang et al. (2011) reveal an AMPK-dependent synaptic pathway that sustains excitatory stimulation of the NPY/AgRP neurons that promote feeding behavior until satiety signals kick in.

Metabolic hormones such a ghrelin, signaling food deprivation, and leptin, signaling satiety, stimulate synaptic activity and plasticity within the neuronal circuits in the hypothalamus that control feeding behavior (Pinto et al., 2004). This process was suggested to play an important role in regulating metabolism (Horvath and Diano, 2004). However, the mechanisms that bring about these rapid changes in synaptic connectivity and activity and how long they persist remain ill defined.

In this issue of *Cell*, Yang et al. (2011) provide a remarkable set of novel findings pinpointing intracellular and intercellular substrates of synaptic plasticity on the orexigenic NPY/AgRP neurons. Their findings demonstrate why the response to a pulse of the appetite-stimulating hormone ghrelin can persist for hours, and how it can be turned off in response to a pulse of leptin. Using in vitro electrophysiological approaches to record from neurons marked by the expression of the neuropeptide NPY, most of which also synthesize the neuropeptide AgRP, the authors found that food deprivation increases the frequency of action potentials in the these neurons (referred to as AgRP neurons by Yang et al.). The increased activity occurs through an AMPA-mediated increase in frequency of miniature excitatory postsynaptic currents (mEPSCs) onto these cells.

This increase in excitatory inputs is driven by AMPK- and ryanodine receptor-mediated calcium release from internal stores in presynaptic sites. Administration of ghrelin mimicked the effect of food deprivation on mEPSCs in in vitro experiments, consistent with ghrelin's previously identified action on midbrain dopamine neurons (Abizaid et al., 2006). The authors demonstrate that calcium/calmodulin-dependent protein kinase kinase (CAMKK) activates AMPK in response to ghrelin to unleash synaptic activity that exhibits hysteresis, i.e., it can persist for hours. The hysteretic nature of this signaling is likely due to the positive feedback loop between calcium release triggered by AMPK activity, which in turn leads to additional AMPK activity promoted by CAMKK. The enhanced synaptic transmission was switched off by the appetite-suppressing hormone leptin, which activates the pro-opiomelanocortin (POMC) neurons. Intriguingly, the authors show that opiods derived from these neurons, most likely β-endorphin, reverse the AMPK-mediated upregulation of excitatory inputs onto AgRP neurons (Figure 1A). The findings thus provide a putative physiological explanation for why mammals no longer feel the drive to eat once satiety is reached.

Changes in synaptic transmission occur within a very short period of time in response to the changing metabolic environment. One of the ingenious aspects of the work of Yang et al. is that the authors recognized that such a physiological phenomenon is virtually impossible to thoroughly investigate with any available transgenic or knockout technology. Thus, the authors used elegantly applied pharmacological tools to test and answer, in a manner not previously attempted, fundamental questions about synaptic transmission governed by metabolic signals.

Conceptually, the work of Yang et al. (2011) builds on previous reports that have proposed mechanisms related to AgRP neuronal plasticity, but the authors excel in providing a refined and unifying framework for synaptic regulation, maintenance, and resetting by metabolic alterations. The AgRP neurons have been considered the primary responders to gut-derived metabolic hormones such as ghrelin. This notion is left in the dust by the study of Yang et al., whose findings point to an AMPK-dependent presynaptic mechanism that kicks off adaptation to ghrelin. This presynaptic mechanism likely acts in synergy with autonomous cell adaptations that occur within the AgRP neurons, allowing them to increase firing rate in a sustained way in response to food deprivation (Takahashi and Cone, 2005) or ghrelin (Kohno et al., 2008) in the absence of synaptic inputs. This cell-autonomous mechanism is also dependent upon AMPK, as well as on downstream mitochondrial factors and Sirtuin 1 activation in AgRP neurons

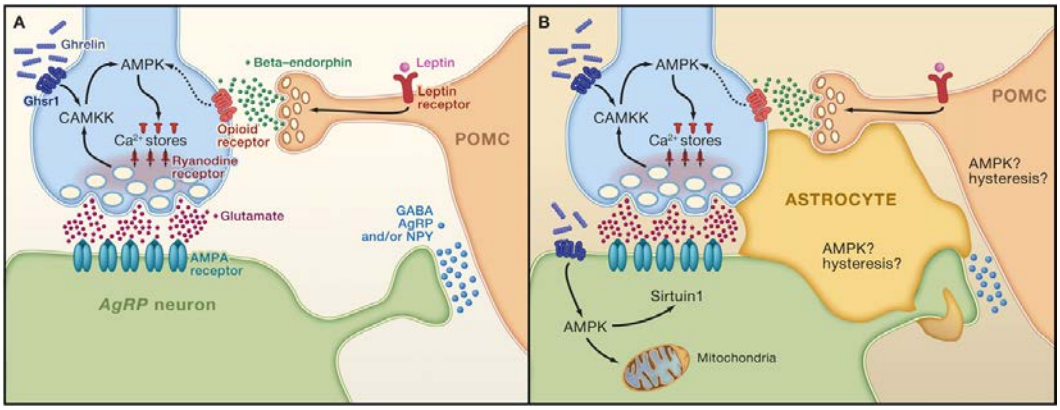

Figure 1. AgRP Neurons Respond to Changing Metabolic States

(A) In response to food deprivation and the ghrelin hormone, a presynaptic pathway involving a positive feedback loop of AMPK-mediated calcium release stimulates the activity of AgRP neurons. The activity of these neurons is known to drive feeding behavior. The hormone leptin signals satiety and induces the POMC neurons to release opioids that turn off the AMPK pathway and, consequently, AgRP neuronal activity. POMC neurons are also known to have an inhibitory synaptic connection with AgRP neurons mediated by GABA, NPY, and/or AgRP.

(B) Under in vivo conditions, a combination of mechanisms likely contributes to the regulation of AgRP neuronal activity. In addition to the presynaptic signaling pathway uncovered by Yang et al., there may be postsynaptic and cell-autonomous intracellular signaling cascades. In addition, the AMPK-dependent presynaptic mechanism could also be located in other cell types, such as the POMC neurons and astrocytes (yellow). Ghrsr1 is the ghrelin receptor.

(Andrews et al., 2008; Kohno et al., 2008; Dietrich et al., 2010) (Figure 1B).

Yang et al. did not identify the presynaptic cells that undergo AMPK-dependent calcium release to stimulate AgRP neurons. The presynaptic nature of the effect was concluded based in part upon comparing the effects of AMPK inhibitors when permitted to affect all cells versus when restricted to AgRP neurons by direct intracellular delivery. Thus the identities of the cells that are mediating the responses to food deprivation and ghrelin remain in question. The data presented by Yang et al. indicate that presynaptic boutons in direct contact with the AgRP neurons might be the site where the intracellular events involving AMPK, calcium mobilization, and opioid action take place to affect release probabilities. This is a very reasonable assumption, and the cells of origin of these terminals will be of interest to pursue. However, other mechanisms may also be in place in support of this process. For example, astrocytes that surround glutamatergic synapses could also contain the AMPK-dependent machinery to modulate synaptic plasticity and neurotransmitter release probability by regulating the synaptic bioenergetics and/or neurotransmitter uptake (Figure 1B). Alternatively, in line with the conclusions of the current study, the opioid factor released by the POMC neurons could diffuse into the arcuate nucleus, a cluster of hypothalamic neurons that are involved in neuroendocrine responses, resulting in local modulatory activity. In addition, although the current report focused on the role of the excitatory projections onto the AgRP neurons, it is also possible that inhibitory synapses may be involved in regulating AgRP neuronal excitability.

Finally, it is worth noting that the experiments performed by Yang et al. were in vitro recordings. In such settings, the milieu is different from physiological situations in which AgRP neurons are active. For example, the media used for recordings contained an 11 mM concentration of glucose. This level of glucose is at least a magnitude above that which occurs during a food-deprived state, and it is substantially higher than that of the fed state. Lower, more physiological levels of glucose in such in vitro conditions were shown to have differential effects on AgRP neurons depending on postsynaptic AMPK content (Claret et al., 2007). Additionally, the effect of the AMPK activator AICAR (used by Yang and colleagues as well) on feeding behavior was blunted in mice lacking mitochondrial uncoupling protein 2 (Andrews et al., 2008), suggesting that AMPK's role in hypothalamic circuit regulation may be more complex.

In summary, the tour-de-force study by Yang et al. highlights a fundamentally novel mechanism that depicts regulatory principles of hypothalamic AgRP neurons in a paradigm-shifting manner. The paper indicates that the current dogma that AgRP neurons represent the first-order neurons in brain sensing peripheral metabolic status may need to be revised.

REFERENCES

Abizaid, A., Liu, Z.-W., Andrews, Z.B., Shanabrough, M., Borok, E., Elsworth, J.D., Roth, R.H., Sleeman, M.W., Picciotto, M.R., Tschöp, M.H., et al. (2006). J. Clin. Invest. *116*, 3229–3239.

Andrews, Z.B., Liu, Z.W., Walllingford, N., Erion, D.M., Borok, E., Friedman, J.M., Tschöp, M.H., Shanabrough, M., Cline, G., Shulman, G.I., et al. (2008). Nature *454*, 846–851.

Claret, M., Smith, M.A., Batterham, R.L., Selman, C., Choudhury, A.I., Fryer, L.G.D., Clements, M.,

Al-Qassab, H., Heffron, H., Xu, A.W., et al. (2007). J. Clin. Invest. *117*, 2325–2336.

Dietrich, M.O., Antunes, C., Geliang, G., Liu, Z.W., Borok, E., Nie, Y., Xu, A.W., Souza, D.O., Gao, Q., Diano, S., et al. (2010). J. Neurosci. *30*, 11815–11825.

Horvath, T.L., and Diano, S. (2004). Nat. Rev. Neurosci. *5*, 662–667.

Kohno, D., Sone, H., Minokoshi, Y., and Yada, T. (2008). Biochem. Biophys. Res. Commun. *366*, 388–392.

Pinto, S., Roseberry, A.G., Liu, H., Diano, S., Shanabrough, M., Cai, X., Friedman, J.M., and Horvath, T.L. (2004). Science *304*, 110–115.

Takahashi, K.A., and Cone, R.D. (2005). Endocrinology *146*, 1043–1047.

Yang, Y., Atasoy, D., Su, H.H., and Sternson, S.M. (2011). Cell *146*, this issue, 992–1003.

Capítulo VI. AgRP Neurons Mediate Sirt1's Action on the Melanocortin System and Energy Balance: Roles for Sirt1 in Neuronal Firing and Synaptic Plasticity

Artigo publicado no periódico *Journal of Neuroscience*.

Behavioral/Systems/Cognitive

Agrp Neurons Mediate Sirt1's Action on the Melanocortin System and Energy Balance: Roles for Sirt1 in Neuronal Firing and Synaptic Plasticity

Marcelo O. Dietrich,[1,4] Catiele Antunes,[1,4] Gan Geliang,[2] Zhong-Wu Liu,[2] Erzsebet Borok,[1] Yongzhan Nie,[1] Allison W. Xu,[5] Diogo O. Souza,[4] Qian Gao,[1] Sabrina Diano,[2] Xiao-Bing Gao,[2] and Tamas L. Horvath[1,2,3]

[1]Program on Cell and Neurobiology of Energy Metabolism, Section of Comparative Medicine and Departments of [2]Obstetrics, Gynecology, and Reproductive Sciences and [3]Neurobiology, Yale University School of Medicine, New Haven, Connecticut 06520, [4]Department of Biochemistry, Universidade Federal do Rio Grande do Sul, Porto Alegre RS 90035, Brazil, and [5]Diabetes Center, University of California, San Francisco, San Francisco, California 94143

Sirt1 has been associated with various effects of calorie restriction, including an increase in lifespan. Here we show in mice that a central regulatory component in energy metabolism, the hypothalamic melanocortin system, is affected by Sirt1, which promotes the activity and connectivity of this system resulting in negative energy balance. In adult mice, the pharmacological inhibition of brain Sirt1 activity decreased Agrp neuronal activity and the inhibitory tone on the anorexigenic POMC neurons, as measured by the number of synaptic inputs to these neurons. When a Sirt1 inhibitor (EX-527) was injected either peripherally (i.p., 10 mg/kg) or directly into the brain (i.c.v., 1.5 nmol/mouse), it decreased both food intake during the dark cycle and ghrelin-induced food intake. This effect on feeding is mediated by upstream melanocortin receptors, because the MC4R antagonist, SHU9119, reversed Sirt1's effect on food intake. This action of Sirt1 required an appropriate shift in the mitochondrial redox state: in the absence of such an adaptation enabled by the mitochondrial protein, UCP2, Sirt1-induced cellular and behavioral responses were impaired. In accordance with the pharmacological results, the selective knock-out of Sirt1 in hypothalamic Agrp neurons through the use of Cre-Lox technology decreased electric responses of Agrp neurons to ghrelin and decreased food intake, leading to decreased lean mass, fat mass, and body weight. The present data indicate that Sirt1 has a central mode of action by acting on the NPY/Agrp neurons to affect body metabolism.

Introduction

Sirtuins are NAD+-dependent class III deacetylases that are highly conserved across species (Brachmann et al., 1995). Sirt1, the mammalian ortholog of Sir2, has been implicated in caloric-restriction-induced longevity (Kaeberlein et al., 1999; Lin et al., 2000; Tissenbaum and Guarente, 2001; Cohen et al., 2004; Rogina and Helfand, 2004; Chen et al., 2005). Nutrient deprivation upregulates Sirt1 in several tissues (Cohen et al., 2004; Ramadori et al., 2008), which is crucial for the metabolic shift that occurs during negative energy balance (Liu et al., 2008), a metabolic state in which the energy expenditure is higher than the energy intake.

Evidence suggests that the effects of sirtuins mimic the beneficial effects of calorie restriction, the only known physiological intervention that promotes a longer, healthier lifespan across species (Kaeberlein et al., 1999; Lin et al., 2000; Tissenbaum and Guarente, 2001; Cohen et al., 2004; Rogina and Helfand, 2004; Chen et al., 2005; Chen and Guarente, 2007). The similarities between the action of sirtuins and calorie restriction raise the possibility that sirtuins may exert their effect, at least in part, by affecting brain circuits controlling negative energy balance, the metabolic state promoted by calorie restriction.

The central melanocortin system located in the arcuate nucleus (ARC) of the hypothalamus is involved in the regulation of energy metabolism (Cone, 2006). This system consists of two components: a neuronal population that produces neuropeptide Y (NPY), agouti-related protein (Agrp), and GABA, which promotes feeding in response to hunger and thus, negative energy balance; and a neighboring cell population producing proopiomelanocortin (POMC)-derived peptides, such as α-melanocyte-stimulating hormone (α-MSH) and cocaine-and-amphetamine-regulated transcript (CART) peptides, which promotes satiety and thus, positive energy balance. The interaction between these two sets of neurons is such that the NPY/Agrp neurons maintain a unidirectional tonic inhibition onto the POMC neurons (Horvath et al., 1992; Cowley et al., 2001; Pinto et al., 2004). The selective elimination of the orexigenic NPY/Agrp neurons in adult mice leads to cessation of feeding (Gropp et al., 2005) and death (Luquet et al., 2005; Wu et al., 2009). The interaction and connectivity of these hypothalamic circuits are not

Received May 1, 2010; revised July 15, 2010; accepted July 16, 2010.

M.O.D. and C.A. were partially supported by Conselho Nacional de Desenvolvimento Científico e Tecnológico (Brazil). T.L.H. and X.-B.G. were supported by grants from the National Institutes of Health (NIH) and American Diabetes Association (ADA). S.D. was supported by grants from the NIH, ADA, and Juvenile Diabetes Research Foundation. D.O.S. was supported by grants from Financiadora de Estudos e Projetos/Ministério da Ciência e Tecnologia and Iniciação Científica for Excitotoxicity and Neuroprotection. Q.G. was supported by a grant from the ADA. We are thankful to Marya Shanabrough for the comments and revisions on the manuscript. T.L.H. dedicates this paper to the memory of his grandfather, Dr. Ferene Ven (1912–2010), who devoted his life to his family and his patients in Hungary during war, oppression, and peace.

Correspondence should be addressed to Tamas L. Horvath, 375 Congress Avenue, LSOG 117, New Haven, CT 06520. E-mail: tamas.horvath@yale.edu.

DOI:10.1523/JNEUROSCI.2234-10.2010

 0270-6474/10/3011815-11$15.00/0

static; they exhibit substantial plasticity depending on the metabolic environment (Pinto et al., 2004; Gao et al., 2007), a process that relies on the redox state and plasticity of the mitochondria (Andrews et al., 2008).

Sirt1 is expressed in the hypothalamus (Ramadori et al., 2008), its function is redox dependent (Prozorovski et al., 2008), and it is induced by negative energy balance (Cohen et al., 2004; Chen et al., 2008; Ramadori et al., 2008). Therefore, Sirt1 may play a role in cellular adaptations in response to negative energy balance. In the brain, the central melanocortin system regulates energy metabolism (Cone, 2006) and its adaptive responses to a changing metabolic environment include synaptic (Pinto et al., 2004; Gao et al., 2007; Andrews et al., 2008) and mitochondrial (Coppola et al., 2007; Andrews et al., 2008) plasticity. Here, we examined whether Sirt1 activity may play a role in these cellular adaptations.

Materials and Methods

Animals. Adult male mice were used in the pharmacological studies. The mice were at least 2 months old when single housed for food intake measurements and they were allowed to habituate to single housing for at least 2 weeks before the start of experiments. All animals were kept in temperature and humidity controlled rooms, in a 12/12 h light/dark cycle, with lights on from 7:00 A.M. to 7:00 P.M. Food and water were provided *ad libitum*, unless otherwise stated. The total number of animals used for these experiments is 247.

Transgenic mice. UCP2 knock-out mice were generated as reported previously (Zhang et al., 2001) and the original breeding pairs were kindly provided by Dr. Bradford Lowell (Beth Israel Deaconess Medical Center and Harvard Medical School, Boston, MA), and have been maintained in our laboratory on a mixed background. This transgenic mouse is available from The Jackson Laboratory: B6.129-Ucp2tm1Lowl/J, stock number 005934). POMC-GFP and NPY-GFP mice were provided by Dr. J. Friedman (Rockefeller University, New York, NY) and have been maintained on a B6 background for >10 generations. Both the NPY-GFP [B6.Cg-Tg(NPY-MAPT/Sapphire)1Rck/J; stock number 008321] and the POMC-GFP [B6.Cg-Tg(Pomc-MAPT/GFP*)1Rck/J, stock number 008322] mice are available from The Jackson Laboratory. Sirt1$^{loxP/loxP}$ mice were purchased from The Jackson Laboratory (B6; 129-Sirt1^{tm1gu}/J; stock number 008041) and have been generated as published (Li et al., 2007). Tg.AgrpCre mice have been maintained in our colony on a mixed background (Kaelin et al., 2004; Xu et al., 2005a,b) and backcrossed to the reporter line Rosa26 mice [B6.129S4-Gt(ROSA)26Sor^{tm1Sor}—originally from The Jackson Laboratory]. All procedures were approved by local committees (Institutional Animal Care and Use Committee from Yale University and from Universidade Federal do Rio Grande do Sul).

Generation of Agrp-Sirt1 KO mice. To evaluate the role of Sirt1 in relation to NPY/Agrp neurons and the regulation of metabolism, we used Cre/Lox technology to knockdown the catalytic domain of Sirt1 in this population of cells. Transgenic mice expressing *Cre* recombinase selectively in the Agrp-expressing cells (Kaelin et al., 2004; Xu et al., 2005a,b) were bred with mice harboring a targeted mutant Sirt1 allele (Sirt1^{loxP}) (Li et al., 2007). The Sirt1$^{loxP/loxP}$ mice contain *loxP* sequences flanking the exon 4 of the Sirt1 gene, which encodes 51 aa of the Sirt1 catalytic domain. When bred with the *AgrpCre*$^{+}$ mice, the deleted Sirt1 allele (Sirt1$^{\Delta ex4}$) transcribes a mutant protein that has no apparent residual Sirt1 activity or dominant negative effects (Cheng et al., 2003; Li et al., 2007). Thus, we used this knockdown model of Sirt1 in the NPY/Agrp neurons to further elucidate the role of this sirtuin in body metabolism. We describe our data by referring to "control" and "Agrp-Sirt1 KO" mice.

To generate Agrp-specific Sirt1 KO mice, we used established breeding strategies similar for this Cre line (Xu et al., 2005a,b; see supplemental Fig. 7, available at www.jneurosci.org as supplemental material). To evaluate the specificity and efficacy of the Cre deletion, we used Rosa26 reporter mice (Soriano, 1999). We found rates of ectopic expression of Cre (~30–40%) similar to those reported previously (Xu et al., 2005a,b). This Cre line has been validated in several previous reports (Xu et al., 2005a,b; Kitamura et al., 2006; Könner et al., 2007).

By breeding Tg.AgrpCre^{+}-Sirt1$^{loxP/+}$ with Sirt1$^{loxP/loxP}$ mice, we were able to get Mendelian ratios of *Cre* and floxed alleles in the offspring. In the first characterization period, we found that the *Cre* deleted heterozygote mice for the Sirt1^{loxP} allele (Tg.AgrpCre^{+}-Sirt1$^{\Delta ex4/+}$) exhibited an intermediate phenotype compared to control littermates and homozygote KO mice (Tg.AgrpCre^{+}-Sirt1$^{\Delta ex4/\Delta ex4}$). The mice carrying the AgrpCre allele and their *Cre*-negative controls showed no differences in phenotype (data not shown), in accordance with previous reports (Xu et al., 2005a,b; Pierce and Xu, 2010). Thus, we pooled the *Cre*-negative mice (control group) and *Cre*-positive mice without the floxed allele.

Metabolic chamber recordings. Adult female mice ($n = 11$) were acclimated in metabolic chambers (TSE Systems—Core Metabolic Phenotyping Center, Yale University) for 4 d before the start of the recordings. Mice were continuously recorded for 3 d with the following measurements being taken every 30 min: water intake, food intake, ambulatory activity (in X and Z axes), and gas exchange (O_2 and CO_2) (using the TSE LabMaster system). VO_2, VCO_2, and energy expenditure were calculated according to the manufacturer's guidelines (PhenoMaster Software, TSE Systems). The respiratory exchange rate was estimated by calculating the ratio of VCO_2/VO_2. Values were adjusted by body weight to the power of 0.75 ($kg^{-0.75}$) where mentioned.

For the fasting response study, the same mice used above were acclimated to the cages for 4 d and then food was removed from the cages 2 h before the dark cycle. The metabolic parameters (cited above) were recorded during zeitgeber time (ZT) 12–18 and the data were analyzed as above.

Body composition. Adult male ($n = 13$) and female ($n = 11$) control and Agrp-Sirt1 KO mice were scanned in a Lunar PIXImus Densitometer (GE Medical Systems) in the Department of Orthopedics at Yale University, and their body composition was estimated based on manufacturer's algorithms. All mice were sedated with a mixture of ketamine and xylazine before scanning.

Food intake measurements. For nocturnal food intake, animals were weighed and injected 30–60 min before the beginning of the dark cycle (ZT 11). Food pellets were weighed and added to the mouse cage at the start of the dark cycle (ZT 12). Food intake was measured after 4 h (ZT 16) and overnight (ZT 0). For ghrelin-induced feeding, mice received the first treatment (i.p., 1 μg/g of body weight) in the middle of the light cycle (ZT 6) and the second injection 30–60 min later (ZT 7). Food pellets were then weighed and added to the mouse cages 30 min after the last injection, and food intake was measured every hour for 4 h. Before the start of the experiments, the home cages were changed to avoid biased results due to mice eating food that may have been deposited in the bedding of the cages. After the experiments, all cages were inspected for food spillage, and those mice in cages with visible food deposits in the bedding were excluded from the studies. However, it is important to note that very few mice had to be excluded from our experiments due to food spillage (2 mice out of 173). We observed that giving mice fewer food pellets (but enough for *ad libitum* feeding) in the cage during the single housing acclimatization period resulted in considerably less food spillage.

For the experiments in which food intake, water intake, and locomotor activity were followed concomitantly, mice were allowed to acclimate to the metabolic chambers (TSE Systems) for 4 d before the start of the recording. Mice were recorded for 24 h before and after EX-527 treatment. For the dose–response and SHU9119 studies, mice were recorded overnight (bin size for all experiments = 30 min). All measurements were taken automatically through the use of the LabMaster Phenotyping system (TSE Systems).

Intracerebroventricular cannulation. Mice were injected with buprenorphine (0.05 mg/kg, s.c.) 30 min before surgery. They were anesthetized using a mixture of ketamine (100 mg/kg) and xylazine (10 mg/kg) given intraperitoneally. Mice were placed in a stereotaxic apparatus (Kopf Instruments), and a small cut was made in the skin above the skull. A drop of a pharmaceutical H_2O_2 solution was placed on the skull for better visualization of bregma and lambda. A small hole was carefully drilled into the skull, enough to insert the cannula (26 ga, Plastics One).

Coordinates were +1.0 mm (lateral), −0.5 mm (posterior), +2.0 mm (caudal) from bregma (Paxinos and Franklin, 2001). Animals were kept warm and proper postsurgical care was taken.

Drug injections. For intraperitoneal injections, 10 ml/kg solution was injected, and for intracerebroventricular injections, 3 μl was slowly injected into the lateral ventricles, using a 5–10 μl Hamilton syringe (Hamilton) connected to a calibrated polyethylene tube. After the experiments, cannula placement was confirmed by injecting methylene blue. Of the 219 mice, 6 were excluded due to misplaced cannulas.

Several compounds have been shown to modulate Sirt1 activity. More recently, synthetic compounds acting directly on Sirt1 have also been developed with higher affinity and specificity (Napper et al., 2005). One of these compounds, EX-527 (Napper et al., 2005) has been extensively studied (Napper et al., 2005; Solomon et al., 2006; Nie et al., 2009; Pacholec et al., 2010); EX-527 is a low-molecular-weight, cell-permeable, biostable molecule that binds directly to the Sirt1 catalytic domain and inhibits its activity (Huhtiniemi et al., 2006; Pacholec et al., 2010). Thus, we have chosen to use this molecule to pharmacologically inhibit Sirt1 activity. EX-527 (Tocris Bioscience) was freshly prepared, dissolved in dimethylsulfoxide (DMSO) to a stock concentration of 50 mM, and then diluted in ultrapure water to a final concentration of between 0.3 and 3.0 nmol/3 μl (with the DMSO final concentration between 1 and 2%); appropriate vehicles were used as controls. Mice were injected with 3 μl (i.c.v.) of drug solution or vehicle. For the SHU9119 experiment, SHU9119 (Sigma-Aldrich—140 pmol/mouse) was injected concomitantly with EX-527 (1.5 nmol/mouse). All solutions were sterile filtered through 0.2 μm syringe filters (Pall).

Immunohistochemistry for GFP and c-fos. GFP and c-fos double immunohistochemistry was performed by sequential addition of primary antibodies. Coronal brain sections (50 μm) were washed several times in phosphate buffer (PB, 0.1 M), pH 7.4, reacted with 1% H_2O_2 in 0.1 M PB solution for 15 min to block endogenous peroxidase activity, and preincubated with Triton X-100 for 30 min. Sections were then washed several times and blocked with 2% normal goat serum and incubated with chicken anti-GFP (1:8000, 4°C, 48 h; Abcam). After, sections were extensively washed and incubated with biotinylated donkey anti-chicken secondary antibody [1:500, 2.5 h at room temperature (RT), Jackson ImmunoResearch Laboratories]. After washing, sections were incubated in ABC and washed, and immunoreactivity was visualized using diaminobenzidine (DAB). Sections were then washed extensively and incubated with rabbit anti-c-fos (1:20,000 at 4°C for 48 h; Oncogene). Following several washes, sections were incubated with biotinylated goat anti-rabbit secondary antibody (1:500, 2.5 h, RT, Vector Laboratories), then washed again and incubated in avidin–biotin complex (Vectastain, ABC Elite kit, Vector Laboratories) for 90 min at RT. Immunoreactivity for c-fos was visualized with nickel diaminobenzidine (Ni-DAB) reaction for 5 min or until desired staining. This approach visualized nuclear c-fos as a black precipitate and NPY-GFP neurons as brown cytoplasmic staining, allowing for easy identification and quantification of NPY/c-fos cells. Sections were then mounted and coverslipped with Depex mounting medium. Unbiased stereology methods were used to quantify NPY/c-fos-immunoreactive cells in the ARC. Cells were visualized by a Zeiss microscope and relayed via a MicroFibre digital camera to a computer, where they were counted using the optical fractionator with the Stereo-Investigator software (MicroBrightField). Two sections, 200 μm apart (−1.50 mm to −1.70 mm from bregma), were collected through the ARC and all NPY, c-fos, and NPY/c-fos cells were counted, using a 63× oil objective, in grids randomly positioned by the software in the outlined counting area through all optical planes, thus creating a three-dimensional counting area. Cells were only counted if they touched the inclusion border or did not touch the exclusion border of the sampling grid. Data are reported as the relative number of double-stained cells (c-fos positive and GFP positive) divided by the total number of GFP-positive cells.

Immunohistochemistry for POMC. In these studies, adult male mice on a mixed background (B6.129) were used. Mice were injected with EX-527 or vehicle before the dark cycle (ZT 11) and were perfused at ZT 17. Mice were deeply anesthetized and the left ventricle of the heart was rapidly cannulated and flushed with 0.9% saline containing heparin followed by freshly prepared fixative (paraformaldehyde 4%, gluteraldehyde 0.1%, picric acid 15%, in PB 0.1 M, pH 7.4). Usually, the time between opening the thoracic cavity and the heart cannulation was <30 s. Brains were then dissected out and postfixed overnight in fixative without gluteraldehyde. After vigorous washing in cold PB (0.1 M), vibratome sections were cut (40–60 μm) containing the ARC of the hypothalamus. Sections were washed in PB several times, cryoprotected, and subsequently frozen and thawed three times in liquid nitrogen. After extensive washing in PB, slices were incubated with H_2O_2 (1%, 20 min, RT, shaking) to block endogenous peroxidase activity. After washing again with PB, sections were incubated with primary antibody (anti-POMC, 1:4000, 48 h, 4°C, gentle shaking). Sections were extensively washed, incubated with secondary antibody (2 h, RT), washed again, put in ABC, and developed with DAB. Sections were then osmicated (15 min in 1% osmium tetroxide in PB) and dehydrated in increasing ethanol concentrations. During the dehydration, 1% uranyl acetate was added to the 70% ethanol to enhance ultrastructural membrane contrast. Dehydration was followed by flat embedding in Durcupan. Ultrathin sections were cut on a Leica ultra microtome, collected on Formvar-coated single-slot grids, and analyzed with a Tecnai 12 Biotwin (FEI) electron microscope. All investigators were blinded to the experimental groups during the entire procedure.

Quantitative synaptology and mitochondria counting. The analysis of synapse number was performed in an unbiased manner (Cowley et al., 2001; Gao et al., 2007) and is presented as number of synapses per 100 μm of cell membrane. For mitochondrial counting, random sections containing POMC cells with a visible nucleus were analyzed. Mitochondria were counted in the POMC cells and the trans-sectional area of each mitochondrion was measured. The data are expressed as number of mitochondria per cell area (in square micrometers) or total mitochondria trans-sectional area (in square micrometers) per cell area (in square micrometers). Therefore, the ratio of the total mitochondria area divided by the cell area can give a very good estimation of the percentage of the cell body occupied by mitochondria. Additionally, the trans-sectional area of each mitochondrion counted and their circularity were measured as indexes of mitochondria morphology. Macnification 1.6 and MatLab R2009a were used for analysis.

Electrophysiology. Four-week-old POMC-GFP male mice were kept in a room with an inverted light/dark cycle (lights on from 8:00 P.M. to 8:00 A.M.) for at least 2 weeks before electrophysiological recordings. Mice were killed at the beginning of the dark cycle, and the ARC was sliced into 250 μm slices (2/mouse), containing the POMC-GFP cells. Slices were then incubated with vehicle or EX-527 at 35°C for 4 h before cells were transferred to recording chambers. For NPY-GFP cell recording, 4- to 7-week-old male NPY-GFP mice were killed at the beginning of the light phase and the ARC was cut into 250 μm slices (2/mouse), containing NPY-GFP cells. After stabilization in ACSF, slices were transferred to the recording chamber and perfused with ACSF plus vehicle or EX-527. For ghrelin-induced cell activation, the basal firing rate was recorded for at least 10 min. The slice was then incubated with ghrelin (0.05 μM) for 8–10 min, followed by a washout (with no ghrelin). Either vehicle or EX-527 (50 μM) was kept in the bath solution during the entire recording period.

Six-week-old Agrp-Sirt1 KO-GFP and control-GFP mice were fasted overnight and killed at the beginning of the light cycle. Whole-cell current-clamp recording was performed using low-resistance (3–4 MΩ) pipettes. The composition of the pipette solution was as follows (in mM): K-gluconate 125, $MgCl_2$ 2, HEPES 10, EGTA 1.1, Mg-ATP 4, Na_2-phosphocreatin 10, and Na_2-GTP 0.5, pH 7.3 with KOH. The composition of the bath solution was as follows (in mM): NaCl 124, KCl 3, $CaCl_2$ 2, $MgCl_2$ 2, NaH_2PO_4 1.23, glucose 2.5, sucrose 7.5, and $NaHCO_3$ 26. After a gigaohm seal and whole-cell access were achieved, membrane potential and action potentials were recorded under current clamp at 0 pA. Ghrelin (0.05 μM) was applied to the bath solution and perfused to the slice. All data were sampled at 3–10 kHz and filtered at 1–3 kHz with an Apple Macintosh computer using Axograph 4.9 (Molecular Devices). Electrophysiological data were analyzed with Axograph 4.9 and plotted with KaleidaGraph 3.6 (Synergy Software) and Igor Pro 5.04 (WaveMetrics). Membrane potential and action potentials were detected and mea-

sured with an algorithm in Axograph 4.9. The frequency of action potential and membrane potential were expressed as mean ± SEM.

Statistical analysis. We used software packages to analyze the data (Matlab R2009a and PASW Statistics 18.0) and plot the figures. First, we tested the homogeneity of variance across the different experimental conditions using Levene's or Bartlett's test.

When the p value was >0.05 in these tests, homogeneity was assumed, and a parametric ANOVA test was used. The Student's t test was used to compare two groups. One-, two-, or three-way ANOVA was used as the other tests unless stated otherwise. Multiple comparisons were performed as described below. For repeated measures analysis we used a mixed-model ANOVA with time as a "within-subject repeated-measures" factor and treatments/genotype as a "between-subject" factor. Significant effects were followed with Fisher's PLSD *post hoc* test with Bonferroni's correction. When homogeneity was not assumed, the Kruskal–Wallis nonparametric ANOVA was used and the Mann–Whitney U test was used to determine *post hoc* significant of differences between groups. Fisher's exact test was used to find differences in the number of cells activated by ghrelin in the electrophysiology recordings. A value of $p < 0.05$ was considered statistically significant. All data are shown as mean ± SEM unless stated otherwise.

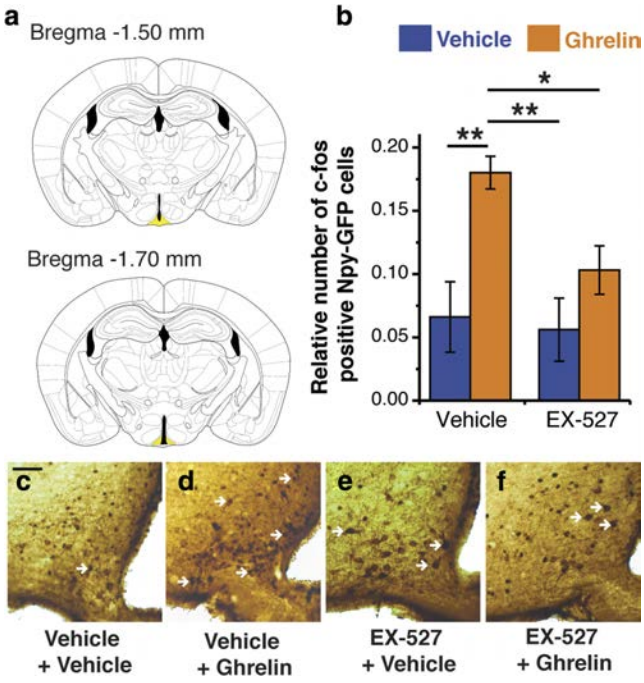

Figure 1. Sirt1 inhibition decreases ghrelin-induced c-fos expression in NPY/Agrp neurons. EX-527 (i.c.v., 1.5 nmol/mouse), a pharmacological inhibitor of Sirt1 (Napper et al., 2005; Pacholec et al., 2010), diminished the number of c-fos labeled NPY-GFP cells after ghrelin treatment (i.p.). ***a***, Slices from the brain highlighting the ARC (in yellow) where the NPY-GFP and c-fos cells were counted (between bregma −1.50 mm to −1.70 mm). ***b***, Histogram showing quantification of double-labeled NPY-GFP/c-fos cells in the ARC of mice injected with vehicle/EX-527 and vehicle/ghrelin. ***c–f***, Representative pictures of double immunohistochemistry for GFP (DAB, brown) and c-fos (nickel DAB, black). White arrows indicate double-stained cells. $n = 4–5$ mice/group. $^*p < 0.05$, $^{**}p < 0.01$.

Results

Sirt1 inhibition decreases the excitability of NPY/Agrp neurons

Negative energy balance is supported by the activity of ARC NPY/Agrp neurons. To test whether sirtuin action affects NPY/Agrp neurons, we evaluated whether Sirt1 inhibition changes the excitability of these cells. First, we measured the membrane potential of NPY/Agrp neurons in acute slices from 4- to 7-week-old male NPY-GFP mice. After an initial stabilization of the slices in ACSF, they were incubated in EX-527 (50 μM) for at least 30 min followed by a washout with ACSF (containing vehicle). We found that Sirt1 inhibition by EX-527 hyperpolarized the neuronal membrane potential of NPY neurons (vehicle = −49.12 ± 1.40; EX-527 = −51.74 ± 1.53; Δ = −2.61 ± 0.56 mV; $n = 4$ cells/4 mice, $t_{(3)} = 4.66$, $p < 0.05$) (see supplemental Fig. 1, available at www.jneurosci.org as supplemental material), while decreasing the firing rate of these cells (vehicle = 100 ± 31%; EX-527 = 46.6 ± 10.8%; $n = 4$ cells/4 mice; $t_{(3)} = 4.20$, $p < 0.05$), indicating a decreased excitability of these neurons.

Next, we sought to determine whether Sirt1 inhibition could also impair the activation of NPY/Agrp neurons induced by ghrelin, a hormone that is elevated during negative energy balance. We found that the pretreatment of slices with EX-527 (50 μM) for 30 min impairs the ghrelin-induced NPY/Agrp cell activation: in the vehicle group, 13 of 14 cells (7 mice) were activated by ghrelin, whereas only 1 of 4 cells (4 mice) were activated in the EX-527-treated group ($p < 0.05$, Fisher's exact test). To understand whether our findings in slice preparation could translate to *in vivo* activation of NPY-GFP cells, we injected mice with EX-527 (i.c.v., 1.5 nmol, 3 μl, according to dose–response below) 30 min before injecting ghrelin (i.p., 1 μg/g body weight). As shown in Figure 1, ghrelin induced the activation of NPY-GFP cells as measured by the number of NPY-GFP neurons that coexpressed c-fos in their nuclei (ANOVA: $F_{(3,15)} = 6.79$, $p < 0.01$; 179 ± 8.33% compared to vehicle control, *post hoc* test $p < 0.01$). EX-527 per se did not change the ratio of c-fos/NPY-GFP cells, but it significantly attenuated the activation of NPY-GFP neurons by ghrelin (61 ± 16.38% compared to ghrelin control, *post hoc* test $p < 0.05$).

Sirt1 inhibition affects synaptic input organization of hypothalamic POMC neurons

A major efferent projection exists from the Agrp neurons to their neighboring POMC cells, and it is an inhibitory, GABAergic projection (see supplemental Fig. 2, available at www.jneurosci.org as supplemental material). Thus, next we studied the effects of EX-527 administered directly into the brain on the synaptic input organization of the POMC neurons in the ARC. Adult male wild-type mice were treated with EX-527 (i.c.v., 1.5 nmol) 30–60 min before the dark cycle and were killed 4 h later to analyze synapses on POMC neurons (by electron microscopy). We found that EX-527 blocked the recruitment of synapses onto POMC perikarya (vehicle = 63.4 ± 9.2, EX-527 = 38.9 ± 6.1 synapses per 100 μm perikarya; Mann–Whitney $U = 83.00$, $p < 0.05$), which was predominantly the result of a decreased number of symmetric synapses (putatively inhibitory—vehicle = 43.4 ± 7.8, EX-527 = 26.8 ± 4.3 synapses per 100 μm perikarya; Mann–Whitney $U = 87.00$, $p < 0.05$) but not asymmetric synapses

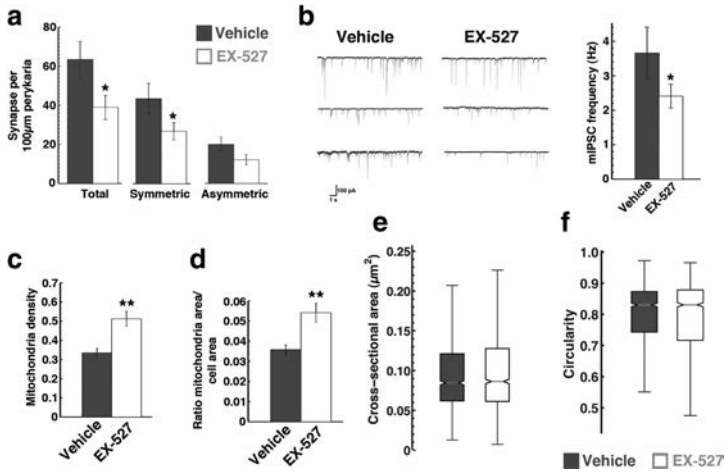

Figure 2. Sirt1 inhibition affects synaptic inputs and mitochondrial number in POMC neurons in the hypothalamus. In ***a***, EX-527 (i.c.v.) was administered to wild-type adult mice at the beginning of the dark cycle and synaptic inputs were measured on POMC neurons 4 h later. EX-527 decreased the recruitment of inputs onto POMC neurons, mainly affecting symmetric, putatively inhibitory, inputs, and not asymmetric, putatively excitatory synapses. Data are mean ± SEM; $n = 15–21$ cells. ***b***, Electrophysiological recordings showing decreased frequency of mIPSCs in POMC-GFP neurons treated with EX-527 (mean ± SEM, $n = 12$ cells). ***c–f***, Sirt1 inhibition by EX-527 affects mitochondrial density in POMC neurons. Sirt1 inhibition increased mitochondrial density (***c***) and relative area (***d***) in POMC cells (mean ± SEM, $n = 13–20$ cells), without affecting indexes of mitochondrial morphology, specifically the cross-sectional mitochondrial area (***e***) and circularity (***f***) (data are median ± interquartile range, $n > 500$). $^{*}p < 0.05$; $^{**}p < 0.01$.

(putatively excitatory—vehicle = 20.0 ± 3.7, EX-527 = 12.1 ± 2.6 synapses per 100 μm perikarya) during the first 4 h of the dark cycle (Fig. 2*a*; see supplemental Fig. 3, available at www.jneurosci.org as supplemental material). An elevated number of inhibitory synapses on POMC neurons in the vehicle control group is consistent with a synaptic arrangement that promotes the suppressed activity of these satiety-signaling cells at the time of increased feeding. To confirm that Sirt1 inhibition blocks the recruitment of inhibitory synapses onto POMC neurons, we also analyzed POMC-GFP cells from acute slices using whole-cell patch electrophysiological recording after incubation with Sirt1 inhibitor (EX-527, 50 μM, 4 h). In corroboration of the morphological data, we found that Sirt1 inhibition blocked the increase in the frequency of miniature IPSCs (mIPSCs) of the POMC-GFP cells [(vehicle = 3.6 ± 0.7, EX-527 = 2.4 ± 0.3 Hz; $n = 12$ cells/4 mice/group; $t_{(12)} = 1.99$, $p < 0.05$ (one-tail) (Fig. 2*b*).

Sirt1 inhibition increases mitochondrial density in POMC neurons of the hypothalamus

Since decreased inhibition of POMC neurons leads to increased melanocortin tone, an adaptation of the mitochondria machinery in these cells may be expected. Indeed, both mitochondrial density (vehicle = 0.33 ± 0.02, EX-527 = 0.51 ± 0.04 mitochondria per cell area; $t_{(31)} = 3.34$, $p < 0.01$) (Fig. 2*c*) and area (vehicle = 0.035 ± 0.002, EX-527 = 0.054 ± 0.005 ∑mitochondria area per cell area; $t_{(31)} = 2.96$, $p < 0.01$) (Fig. 2*d*) were increased in POMC cells after Sirt1 inhibition, an event consistent with increased activity of these cells. However, no changes in mitochondrial morphology were observed as evidenced by the distribution of the cross-sectional area of each mitochondria (Fig. 2*e*) and their circularity (Fig. 2*f*). Together, these data suggest that Sirt1 contributes to the appropriate synaptic and mitochondrial adaptations of the melanocortin system in response to negative energy balance.

Brain Sirt1 inhibition decreases food intake

Our results indicate an acute effect of Sirt1 inhibition on the organization and activity of the melanocortin system in the ARC of the hypothalamus. Because the NPY/Agrp and POMC neurons are the core of the melanocortin system and are implicated in the regulation of food intake, we sought to determine whether the effects we found in the morphological and electrophysiological adaptations due to Sirt1 inhibition could affect food intake. To this end, we first analyzed the effects of peripheral injection of EX-527 on food intake. EX-527 (i.p., 10 mg/kg) inhibited food intake during the dark phase (interaction time × treatment $F_{(1,8)} = 9.33$, $p < 0.05$) (Fig. 3*a*), a period of the circadian cycle during which orexigenic stimuli predominate in nocturnal animals. To further evaluate the acute effects of Sirt1 inhibition in the modulation of food intake, we injected EX-527 (10 mg/kg) daily into adult wild-type mice and measured food intake. In agreement with our acute data, daily peripheral injection of EX-527 given just before the dark cycle induced a robust and consistent decrease in food intake, which persisted until the day after cessation of the treatment (treatment $F_{(1,6)} = 24.53$, $p < 0.05$; time × treatment $F_{(1,6)} = 2.38$, $p < 0.05$) (Fig. 3*b*). In the first 2 d, 24 h food intake was not significantly different. When analyzed closely, it was apparent that EX-527 reduced overnight food intake (e.g., day 1: vehicle = 4.85 ± 0.26, EX-527 = 3.83 ± 0.21 g; $t_{(6)} = 3.06$, $p < 0.05$), without statistical differences in food intake during the light phase (vehicle = 1.04 ± 0.14, EX-527 = 1.61 ± 0.20). On the remaining days (e.g., day 5), EX-527 continued to reduce overnight food intake (vehicle = 5.98 ± 0.50, EX-527 = 4.45 ± 0.28; $t_{(6)} = 2.67$, $p < 0.05$) without causing rebound feeding during the light cycle (vehicle = 0.59 ± 0.17, EX-527 = 0.54 ± 0.07).

Next, we injected EX-527 directly into the cerebral ventricles to evaluate whether the effects we found were due to inhibition of brain Sirt1 activity. Indeed, EX-527 injected directly into the cerebral ventricles also inhibited food intake in a dose-dependent manner (effect of time: $F_{(23,527)} = 228.39$, $p < 0.001$; effect of treatment: $F_{(3,527)} = 4.36$, $p < 0.05$; interaction time × treatment: $F_{(69,527)} = 4.28$, $p < 0.001$) (Fig. 3*c*). We then repeated these experiments using conditions similar to the peripherally administered EX-527 experiment (Fig. 3*a*), injecting the intermediate dose of EX-527 (i.c.v., 1.5 nmol), and found that it inhibited food intake in a manner comparable to the peripheral treatment (supplemental Fig. 5, available at www.jneurosci.org as supplemental material). To further evaluate the effects of central inhibition of Sirt1, we injected mice with EX-527 (i.c.v., 1.5 nmol) and simultaneously monitored food consumption, water intake and ambulatory activity (supplemental Fig. 6, available at www.jneurosci.org as supplemental material). The data obtained on food intake corroborated our previous findings, while no statistical differences in water intake were found. Finally, treatment with central

EX-527 did not statistically change the ambulatory activity of mice (supplemental Fig. 6, available at www.jneurosci.org as supplemental material). Additionally, no overt side effects were observed by central EX-527 treatment (supplemental Table 1, available at www.jneurosci.org as supplemental material). In addition to EX-527, we also found similar results with peripheral and central administration of nicotinamide (data not shown), a natural end product of Sirt1 deacetylase activity, which inhibits Sirt1 in a stoichiometric manner. Together, these data suggest that Sirt1 coordinates neuronal circuit adaptation to negative energy balance to modulate food intake.

To further evaluate the relevance of the melanocortin system in the inhibition of Sirt1 on feeding, we analyzed the effect of the melanocortin 4-receptor antagonist, SHU9119, on EX-527's effect on food intake. SHU9119 was able to reverse the inhibition of food intake promoted by EX-527 (effect of time: $F_{(23,276)} = 495.75$, $p < 0.001$; effect of treatment: $F_{(2,12)} = 4.15$, $p < 0.05$; interaction time × treatment: $F_{(46,276)} = 2.74$, $p < 0.001$; *post hoc*: vehicle × EX-527, $p < 0.05$; EX-527 × EX-527+SHU9119, $p < 0.05$) (Fig. 3*d*), indicating that the effect of Sirt1 inhibition on food intake uses the melanocortin receptors as a downstream effector. In the dose used in this study, we found no changes in food intake when SHU9119 was injected alone (data not shown). These data are in agreement with the results of a recent study (Cakir et al., 2009).

If Sirt1 is intrinsically important for the excitability of NPY/Agrp neurons, then signals that are known to affect food intake via these hypothalamic neurons should have an altered effect on eating when applied concomitantly with the Sirt1 inhibitor, EX-527. Ghrelin affects feeding by activation of the NPY/Agrp neurons. Thus, we injected wild-type mice with ghrelin (30 μg/mouse, i.p.) to induce food intake during the light phase of the circadian cycle, and pretreated the mice with EX-527 (i.c.v., 1.5 nmol, 30–60 min before ghrelin). Feeding induced by the injection of ghrelin (574 ± 21% compared to vehicle control; Mann–Whitney $U = 0.00$, $p < 0.001$) was reversed by pretreatment with the Sirt1 inhibitor EX-527 (52 ± 10% inhibition compared to vehicle plus ghrelin; Mann–Whitney $U = 99.50$, $p < 0.05$), but did not alter normal feeding in vehicle-treated mice (Fig. 3*e*).

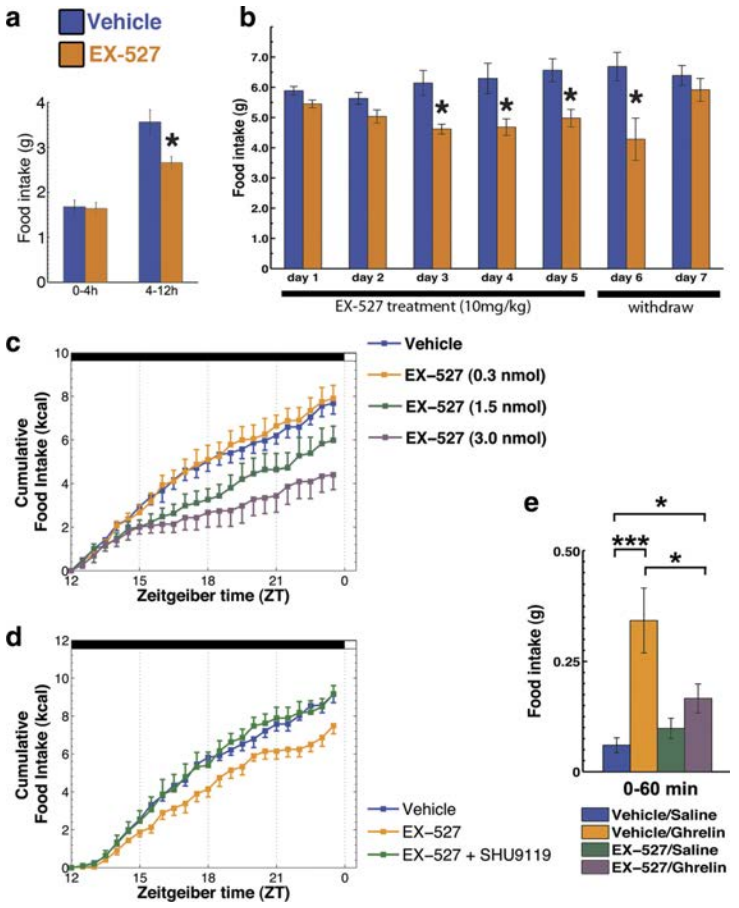

Figure 3. Inhibition of Sirt1 decreases food intake. ***a***, Peripheral injection of a specific Sirt1 inhibitor, EX-527 (10 mg/kg), decreased the overnight food intake with no effect in the first 4 h (mean ± SEM, $n = 5$). ***b***, Daily injection of EX-527 (10 mg/kg) just before the dark cycle produces a robust and consistent decrease in food intake (mean ± SEM, $n = 4$). ***c***, Injection of EX-527 into the cerebral ventricles also inhibited food intake in a dose-dependent manner during the dark cycle (mean ± SEM, $n = 4–7$). ***d***, SHU9119 (140 pmol, i.c.v.), a potent melanocortin receptor antagonist, counteracted the inhibitory effect of EX-527 on food intake (mean ± SEM, $n = 4–6$), highlighting the importance of downstream melanocortin signaling as an effector of Sirt1 inhibition on food intake. ***e***, Brain Sirt1 inhibition by EX-527 (i.c.v.) blunted the orexigenic effect of the gut hormone ghrelin, which depends on redox adaptations in the NPY/Agrp neurons (Andrews et al., 2008) (mean ± SEM, $n = 7–13$ mice). *$p < 0.05$, **$p < 0.01$, ***$p < 0.001$. Scale bars, 50 μm.

The effects of brain Sirt1 inhibition are dependent upon UCP2

Next, we evaluated whether the effects of Sirt1 inhibition on food intake may be altered in mice with an impaired mitochondrial redox adaptation (UCP2 KO mice). The Sirt1 inhibition by any of the three doses of EX-527 used above (data shown for i.c.v., 1.5 nmol dose) failed to show effects in UCP2 KO mice, while it suppressed feeding in wild-type animals (effect of time $F_{(1,31)} = 71.43$, $p < 0.001$; effect of treatment $F_{(1,31)} = 9.22$, $p < 0.01$; interaction time × treatment × genotype $F_{(1,31)} = 4.80$, $p < 0.05$) (Fig. 4). EX-527 also failed to block recruitment of inhibitory synapses onto POMC neurons (total: vehicle = 43.68 ± 5.21, EX-527 = 35.04 ± 5.43; symmetric: vehicle = 28.67 ± 3.89, EX-527 = 27.31 ± 3.64; asymmetric: vehicle = 15.01 ± 2.95, EX-527 = 7.72 ± 2.78 synapses per 100 μm of perikarya) or increase mitochondrial density (vehicle = 0.57 ± 0.05, EX-527 = 0.53 ± 0.06 mitochondria per cell area) or area (vehicle = 0.050 ± 0.004, EX-527 = 0.049 ± 0.005 $\sum$mitochondria area per cell area), nor did it change any of the indexes of mitochondria morphology (data not shown) in these cells during negative energy balance.

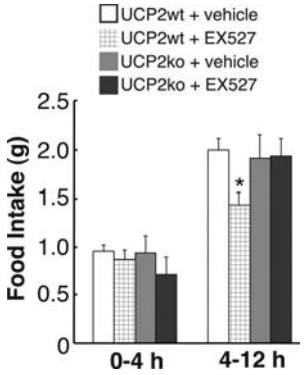

Figure 4. The effect of Sirt1 inhibition on food intake is UCP2 dependent. Inhibition of brain Sirt1 by EX-527 (30 – 60 min before dark cycle, 1.5 nmol, i.c.v.) decreased food intake during the dark cycle in wild-type mice, but not in UCP2 KO mice (mean ± SEM, $n = 5–12$). *$p < 0.05$.

Sirt1 knockdown in Agrp neurons results in decreased feeding and lower body weight

When weaned at 21 d of age, Agrp-Sirt1 KO mice showed no gross abnormalities, and both males and females had body weight similar to that of their control littermates (Fig. 5*a*). However, over time the Agrp-Sirt1 KO gained less weight than their control littermates, and at 11 weeks, both males and females were leaner than controls (Fig. 5*a*). Next, we analyzed the body composition of these transgenic mice using DEXA scanning to estimate lean and fat tissue weight. As presented in Figure 5*a*, females showed a more marked phenotype with reductions in both lean and fat tissue weights, while male Agrp-Sirt1 KO mice showed a consistent reduction in just lean, but not fat, mass (Fig. 5*a*).

Due to the more distinct phenotype of the females, we decided to characterize the metabolic parameters of these mice in metabolic chambers. Coinciding with a decreased body weight, female Agrp-Sirt1 KO mice exhibited a marked reduction in food intake compared to controls (control = 39.85 ± 2.88, KO = 33.91 ± 0.86 kcal/72 h; $t_{(9)} = 2.48$, $p < 0.05$), which was mostly due to decreased nocturnal, and not residual diurnal, food intake (data not shown). Surprisingly, over the same period of time, there was no difference in energy expenditure between control and Agrp-Sirt1 KO mice (control = 27.94 ± 1.26, KO = 26.18 ± 0.68 kcal/72 h). Upon estimation of a relative energy balance (food intake in kcal minus energy expenditure in kcal) for these mice, we found that Agrp-Sirt1 KO animals exhibited a reduced positive energy balance in relation to their littermate controls (control = 11.91 ± 1.83, KO = 7.73 ± 0.088 kcal/72 h; $t_{(9)} = 2.33$, $p < 0.05$), indicating a dysregulation in energy balance in which decreased food intake is not associated with decreased energy expenditure.

We further analyzed the daily metabolism of the Agrp-Sirt1 KO mice by indirect calorimetry, estimating their oxygen consumption (VO_2), VCO_2, energy expenditure, and locomotor activity. We were unable to find statistical differences in any of these parameters (Fig. 5*b–e*). We also estimated the respiratory quotient (VCO_2/VO_2) and found no differences between control and Agrp-Sirt1 KO mice (data not shown).

Altogether, these data indicate that the knockdown of Sirt1 in the NPY/Agrp neurons promotes a decrease in food intake that is not accompanied by a concomitant change in energy expenditure. Moreover, these transgenic mice (Agrp-Sirt1 KO) did not display any gross alteration in any of the metabolic parameters analyzed when fed an *ad libitum* diet.

Agrp-Sirt1 knock-out cells have diminished response to ghrelin

Our observations highlighted an important role of Sirt1 in the NPY/Agrp neuronal regulation of overall metabolism, mainly because the KO mice showed a marked decrease in food intake and body weight gain, which was not associated with reductions in energy expenditure. In an attempt to further understand the physiology of these mutant animals, we bred our Agrp-Sirt1 KO mice with NPY-GFP mice to generate animals that expressed GFP in the NPY/Agrp cells (See material and methods and supplemental Fig. 7, available at www.jneurosci.org as supplemental material for details). In 6- to 7-week-old control-GFP and Agrp-Sirt1 KO-GFP mice, using whole-cell current-clamp recordings, we were able to register the membrane potential and firing rate of the NPY/Agrp neurons.

We administered ghrelin in the incubation chamber to induce NPY/Agrp cell activation and compared the effects in the control and Sirt1 KO cells. In the control-GFP cells, we were able to replicate the effect of ghrelin to increase the excitability of the NPY/Agrp neurons as measured by both a decrease in the membrane potential (vehicle = −52.19 ± 2.92, ghrelin = −41.40 ± 1.14 mV; $n = 6$ cells/6 mice; $t_{(5)} = 3.26$, $p < 0.05$) and an increase in the firing rate of these cells (vehicle = 1.84 ± 0.65, ghrelin = 5.37 ± 1.18 Hz; $n = 6$ cells/6 mice/group; $t_{(5)} = 4.60$, $p < 0.01$). In contrast to this, the Agrp-Sirt1 KO-GFP neurons incubated with ghrelin showed no statistical difference in either the membrane potential (vehicle = −46.62 ± 4.61, ghrelin = −40.99 ± 2.63 mV; $n = 6$ cells/6 mice) or firing rate (vehicle = 2.55 ± 0.62, ghrelin = 2.46 ± 0.49 Hz; $n = 6$ cells/6 mice). Finally, 100% of the recorded neurons in the control group responded to ghrelin, while only 16% of the cells responded in the Sirt1 KO group ($p < 0.01$, Fisher's exact test).

Sirt1 knockdown in Agrp neurons results in impaired responses to fasting

Because NPY/Agrp neurons play an important role in transitioning to negative energy balance, and their excitability was impaired in Agrp-Sirt1 KO mice, we postulated that challenging these mice with food deprivation could exacerbate their phenotype. Thus, we repeated the experiments in the metabolic chambers using identical conditions as before; however, we challenged the mice by fasting them 2 h before the dark cycle and evaluating their response during ZT 12–18 with no food available. Strikingly, the Agrp-Sirt1 KO mice showed a marked increase in ambulatory activity compared to control mice (control = 1954 ± 65, KO = 3115 ± 336 counts; $t_{(9)} = 2.53$, $p < 0.05$), which was concurrent with increased oxygen consumption (VO_2, control = 1552 ± 37, KO = 1783 ± 64 ml · h^{-1} · kg$^{-0.75}$; $t_{(9)} = 2.54$, $p < 0.05$), with no differences in energy expenditure when adjusted for body weight (control = 7.78 ± 0.23, KO = 8.77 ± 0.31 kcal · h^{-1} · kg$^{-0.75}$) or cumulative energy expenditure (control = 2.49 ± 0.04, KO = 2.53 ± 0.08 kcal/6 h).

Discussion

We describe the effects of brain Sirt1 inhibition on NPY/Agrp neuronal excitability and on the synaptic and mitochondrial adaptations of POMC neurons in the ARC of the hypothalamus. Sirt1 inhibition reduced NPY/Agrp neuronal firing and the synaptic input onto the POMC neurons, mainly due to a decrease in the number of inhibitory inputs on these cells. This observation is

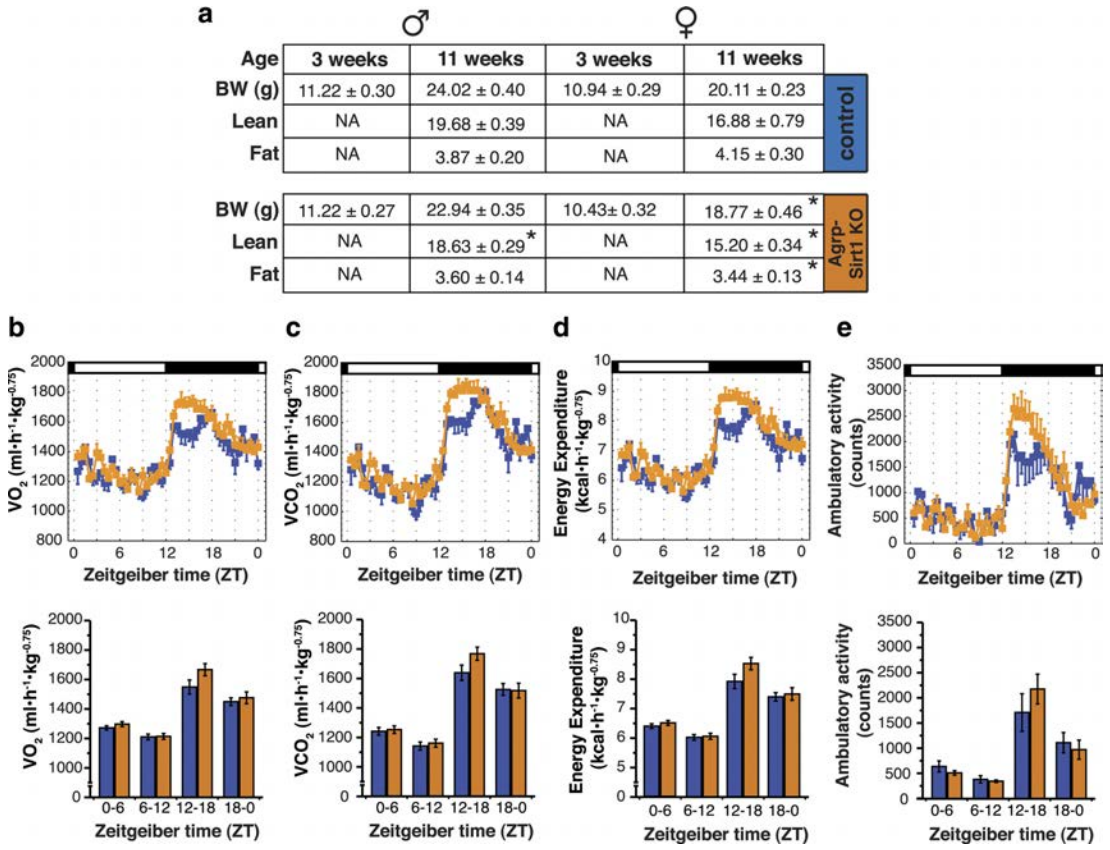

Figure 5. Agrp-Sirt1 KO mice have decreased food intake without concomitant adaptation in energy expenditure. ***a***, Table showing the body weight at weaning and at 11 weeks old in male and female control and Agrp-Sirt1 KO mice. The KO mice gained less weight than controls, which was due mostly to decreased lean mass. Female Agrp-Sirt1 KO mice also showed a diminished fat tissue mass (mean ± SEM, data in grams). ***b–d***, Data from metabolic chambers showing VO_2, VCO_2, and energy expenditure, respectively, adjusted for body mass ($kg^{-0.75}$). There were no statistical differences at any of the time points analyzed. In ***e***, data on ambulatory activity of the same mice in the metabolic chambers showing no statistical differences (mean ± SEM, $n = 4–7$). *$p < 0.05$.

in agreement with the finding of an increase in mitochondrial density, signifying an enhanced activity of POMC cells following brain Sirt1 inhibition. We also found that Sirt1 inhibition decreased food intake during the dark cycle and ghrelin-induced food intake in wild-type mice. The decrease in food intake induced by Sirt1 inhibition was reversed by a melanocortin receptor antagonist, implicating the melanocortin hypothalamic system in the behavioral effects caused by Sirt1 inhibition. The behavioral and physiological effects of inhibition of Sirt1 were not observed in UCP2 KO mice, indicating a role of redox mechanisms involving UCP2 in Sirt1 effects.

Evidence for specificity of brain Sirt1 pharmacological inhibition

In the first set of experiments, we pharmacologically inhibited Sirt1 activity by EX-527, a specific Sirt1 inhibitor. Several lines of evidence support the idea that the effects seen in our experiments were due to Sirt1 inhibition and not to side effects of EX-527: (1) Sirt1 inhibition decreased food intake in a time-delayed manner only during the dark cycle and not during the light cycle (Fig. 3*e*); (2) Sirt1 inhibition did not decrease food intake in UCP2 KO mice (Fig. 4); (3) Sirt1 inhibition did not change symmetric synaptic and mitochondria number in UCP2 KO mice; and (4) Sirt1 inhibition had no effect on water intake and locomotor activity. Also, we have shown that EX-527 increases acetylated forms of Sirt1 target proteins and that this effect is dependent on Sirt1 expression (Nie et al., 2009). Finally, we have also tested the effect of EX-527 on a cell line that resembles the phenotype of NPY/Agrp neurons (N-39), and found an increase in the acetylated levels of Sirt1 target proteins as well (data not shown). However, while we have tested mice injected with central EX-527 acutely in several tests to exclude possible side effects of this compound on feeding, we have not tested for side effects after chronic treatment (Fig. 3*b*).

Participation of the melanocortin system in the effects of brain Sirt1

In mammals, the melanocortin system is central to appetite regulation (Cone, 2006). Negative energy balance, which can be induced by fasting, calorie restriction, or hormones that are active during these situations (e.g., ghrelin) (Ravussin et al., 2001; Kim et al., 2003), promotes the activity of NPY/Agrp neurons over

POMC neurons in the ARC (Hahn et al., 1998; Chen et al., 2004). Several lines of evidence suggest the involvement of Sirt1 in the functioning of the melanocortin system in the ARC. First, Sirt1 is expressed in the ARC and its levels/activity are sensitive to negative energy balance (Ramadori et al., 2008). Recently, it was reported that Sirt1 regulates food intake in rats through the melanocortin system: inhibition of melanocortin receptor signaling by an antagonist reversed the decrease in food intake by a Sirt1 antagonist (Cakir et al., 2009). These data have been replicated in mice in the present study (Fig. 3*d*). A significant component of the effect of inhibition of Sirt1 on feeding was mediated by the melanocortin system: inhibition of MC4R reversed the effect of EX-527. It is important to note, however, that the overall effect of Sirt1 inhibition on feeding was not similar to acute interference with MC4R signaling. Both activation and inactivation of MC4R bring about acute changes in feeding (Cone, 2006). On the other hand, an acute inhibition of Sirt1 (present data) leads to alterations in feeding in a relatively delayed manner. We further investigated the mechanisms implicated in the role of Sirt1 in the regulation of energy metabolism, and found evidence that Sirt1 is important for the synaptic and mitochondrial plasticity that occurs in the melanocortin system. Specifically, pharmacological inhibition of Sirt1 decreases the inhibitory but not excitatory inputs on POMC cells. The effect of Sirt1 inhibition on the synaptic plasticity of POMC neurons was consistent with the food intake data, because it relies on a mechanism that was previously proposed to have an enabling rather than an acute influence on neuronal firing (Pinto et al., 2004; Gao et al., 2007; Andrews et al., 2008). On the other hand, Sirt1 appears to be important for the maintenance of proper cellular machinery that allows the NPY/Agrp neurons to respond to acute ghrelin administration.

Participation of the redox state on the effects of Sirt1

The effect of ghrelin on the hypothalamic melanocortin system is well established. Ghrelin promotes feeding through the activation of NPY/Agrp neurons and inhibition of POMC cells, with a consequent inhibition of MC4R in the paraventricular nucleus (PVN) (Tschöp et al., 2001, 2002; Wang et al., 2002; Chen et al., 2004; Shaw et al., 2005). We showed that ghrelin activates mitochondria respiration and proliferation in NPY/Agrp neurons that are critical for the increase in electrical activity and subsequent increases in food intake (Andrews et al., 2008). The acute feeding response to ghrelin as well as the synaptic plasticity and mitochondrial adaptation in the hypothalamus (Coppola et al., 2007; Andrews et al., 2008) and hippocampus (Dietrich et al., 2008) rely on UCP2-regulated shifts in oxidative processes. Intriguingly, oxidative conditions (in contrast to reducing conditions) have been shown to upregulate Sirt1 activity in neurons (Prozorovski et al., 2008). The present results indicate that Sirt1 participates in the signaling involved in feeding, linking the redox state of the hypothalamic melanocortin system to the activity of Sirt1 and its participation in the mechanisms of synaptic and mitochondrial plasticity. This assumption is reinforced by the facts that Sirt1 inhibition (1) reversed the orexigenic effects of ghrelin (Fig. 3*e*) and (2) did not decrease feeding UCP2 KO mice (Fig. 4).

Impaired response to food deprivation in Agrp-Sirt1 KO mice

In addition to the pharmacological data, we developed a transgenic mouse model of Sirt1 deficiency in the NPY/Agrp neurons of the hypothalamus that resembles the phenotype of wild-type mice after pharmacological Sirt1 inhibition in the brain. These Agrp-Sirt1 KO mice were leaner and had reduced food intake and impaired adaptation of metabolic parameters to decreased energy intake.

Sirt1 has been linked to shifts in metabolism that occur during food deprivation (Rodgers and Puigserver, 2007). During fasted states, Sirt1 maintains hepatic gluconeogenesis and fatty acid oxidation (Rodgers and Puigserver, 2007; Nie et al., 2009), and the knockdown of Sirt1 in hepatocytes diminishes β-oxidation in this tissue (Rodgers and Puigserver, 2007; Purushotham et al., 2009). Our present data are in agreement with the notion that Sirt1 activity contributes to a shifting from positive to negative energy balance, because Agrp-Sirt1 KO mice showed an impaired response to food deprivation by demonstrating increased locomotor activity and oxygen consumption compared to their control littermates.

Additionally, the impaired excitability of the Agrp-Sirt1 KO NPY/Agrp cells in response to ghrelin supports the involvement of Sirt1 in shifting from positive to negative energy balance. The role of Sirt1 in modulating the transition to fatty acid metabolism during periods of negative energy balance (Rodgers and Puigserver, 2007; Purushotham et al., 2009), together with the fact that the Agrp-Sirt1 KO mice had impaired energy balance and adaptation to food deprivation, corroborates our previous data, indicating that β-oxidation contributes to NPY/Agrp neuronal activation, which regulates energy balance (Andrews et al., 2008).

Comparisons between Agrp-specific Sirt1 KO and whole-body Sirt1 KO mice

Our results contrast with those from previous studies showing that whole-body Sirt1 KO mice are hyperphagic (Chen et al., 2005; Pani et al., 2006). However, the data from studies using Sirt1 KO mice are difficult to interpret, because these mice have profound developmental problems, and only a small number of pups reach adulthood (Cheng et al., 2003; McBurney et al., 2003). Once the knock-out mice reach adulthood, they gain ~60% more body weight than their littermates (Chen et al., 2005). Thus, the hyperphagic behavior of the Sirt1 KO mice is likely caused by complex compensatory developmental mechanisms that have little to do with Sirt1 normal physiological mechanisms in the adult brain. In our studies, we used an acute inhibition of or chronic knockdown of Sirt1 specifically in the Agrp neurons (Agrp-Sirt1 KO mice). In contrast to the whole-body Sirt1 KO mice, the Agrp-Sirt1 KO mice were born in Mendelian rates, had no gross developmental problems compared to their littermates, and demonstrated decreased feeding.

Concluding remarks

Our data on hypothalamic neurobiological events indicate that Sirt1 activation in NPY/Agrp neurons is a determinant of their excitability, which consequently is important for appropriate shifts in behavioral, autonomic, and endocrine processes to occur for adaptation to negative energy balance. These findings reveal a novel mechanism by which the selective activation of Sirt1 within the NPY/Agrp neurons promotes negative energy balance that is characteristic of calorie restriction, which promotes a longer, healthier lifespan.

References

Andrews ZB, Liu ZW, Walllingford N, Erion DM, Borok E, Friedman JM, Tschöp MH, Shanabrough M, Cline G, Shulman GI, Coppola A, Gao XB,

Horvath TL, Diano S (2008) UCP2 mediates ghrelin's action on NPY/AgRP neurons by lowering free radicals. Nature 454:846–851.
Brachmann CB, Sherman JM, Devine SE, Cameron EE, Pillus L, Boeke JD (1995) The SIR2 gene family, conserved from bacteria to humans, functions in silencing, cell cycle progression, and chromosome stability. Genes Dev 9:2888–2902.
Cakir I, Perello M, Lansari O, Messier NJ, Vaslet CA, Nillni EA (2009) Hypothalamic Sirt1 regulates food intake in a rodent model system. PLoS One 4:e8322.
Chen D, Guarente L (2007) SIR2: a potential target for calorie restriction mimetics. Trends Mol Med 13:64–71.
Chen D, Steele AD, Lindquist S, Guarente L (2005) Increase in activity during calorie restriction requires Sirt1. Science 310:1641.
Chen D, Bruno J, Easlon E, Lin SJ, Cheng HL, Alt FW, Guarente L (2008) Tissue-specific regulation of SIRT1 by calorie restriction. Genes Dev 22:1753–1757.
Chen HY, Trumbauer ME, Chen AS, Weingarth DT, Adams JR, Frazier EG, Shen Z, Marsh DJ, Feighner SD, Guan XM, Ye Z, Nargund RP, Smith RG, Van der Ploeg LH, Howard AD, MacNeil DJ, Qian S (2004) Orexigenic action of peripheral ghrelin is mediated by neuropeptide Y and agouti-related protein. Endocrinology 145:2607–2612.
Cheng HL, Mostoslavsky R, Saito S, Manis JP, Gu Y, Patel P, Bronson R, Appella E, Alt FW, Chua KF (2003) Developmental defects and p53 hyperacetylation in Sir2 homolog (SIRT1)-deficient mice. Proc Natl Acad Sci U S A 100:10794–10799.
Cohen HY, Miller C, Bitterman KJ, Wall NR, Hekking B, Kessler B, Howitz KT, Gorospe M, de Cabo R, Sinclair DA (2004) Calorie restriction promotes mammalian cell survival by inducing the SIRT1 deacetylase. Science 305:390–392.
Cone RD (2006) Studies on the physiological functions of the melanocortin system. Endocr Rev 27:736–749.
Coppola A, Liu ZW, Andrews ZB, Paradis E, Roy MC, Friedman JM, Ricquier D, Richard D, Horvath TL, Gao XB, Diano S (2007) A central thermogenic-like mechanism in feeding regulation: an interplay between arcuate nucleus T3 and UCP2. Cell Metab 5:21–33.
Cowley MA, Smart JL, Rubinstein M, Cerdán MG, Diano S, Horvath TL, Cone RD, Low MJ (2001) Leptin activates anorexigenic POMC neurons through a neural network in the arcuate nucleus. Nature 411:480–484.
Dietrich MO, Andrews ZB, Horvath TL (2008) Exercise-induced synaptogenesis in the hippocampus is dependent on UCP2-regulated mitochondrial adaptation. J Neurosci 28:10766–10771.
Gao Q, Mezei G, Nie Y, Rao Y, Choi CS, Bechmann I, Leranth C, Toran-Allerand D, Priest CA, Roberts JL, Gao XB, Mobbs C, Shulman GI, Diano S, Horvath TL (2007) Anorectic estrogen mimics leptin's effect on the rewiring of melanocortin cells and Stat3 signaling in obese animals. Nat Med 13:89–94.
Gropp E, Shanabrough M, Borok E, Xu AW, Janoschek R, Buch T, Plum L, Balthasar N, Hampel B, Waisman A, Barsh GS, Horvath TL, Brüning JC (2005) Agouti-related peptide-expressing neurons are mandatory for feeding. Nat Neurosci 8:1289–1291.
Hahn TM, Breininger JF, Baskin DG, Schwartz MW (1998) Coexpression of Agrp and NPY in fasting-activated hypothalamic neurons. Nat Neurosci 1:271–272.
Horvath TL, Naftolin F, Kalra SP, Leranth C (1992) Neuropeptide-Y innervation of beta-endorphin-containing cells in the rat mediobasal hypothalamus: a light and electron microscopic double immunostaining analysis. Endocrinology 131:2461–2467.
Huhtiniemi T, Wittekindt C, Laitinen T, Leppänen J, Salminen A, Poso A, Lahtela-Kakkonen M (2006) Comparative and pharmacophore model for deacetylase SIRT1. J Comput Aided Mol Des 20:589–599.
Kaeberlein M, McVey M, Guarente L (1999) The SIR2/3/4 complex and SIR2 alone promote longevity in *Saccharomyces cerevisiae* by two different mechanisms. Genes Dev 13:2570–2580.
Kaelin CB, Xu AW, Lu XY, Barsh GS (2004) Transcriptional regulation of agouti-related protein (Agrp) in transgenic mice. Endocrinology 145:5798–5806.
Kim MS, Yoon CY, Park KH, Shin CS, Park KS, Kim SY, Cho BY, Lee HK (2003) Changes in ghrelin and ghrelin receptor expression according to feeding status. Neuroreport 14:1317–1320.
Kitamura T, Feng Y, Kitamura YI, Chua SC Jr, Xu AW, Barsh GS, Rossetti L, Accili D (2006) Forkhead protein FoxO1 mediates Agrp-dependent effects of leptin on food intake. Nat Med 12:534–540.
Könner AC, Janoschek R, Plum L, Jordan SD, Rother E, Ma X, Xu C, Enriori P, Hampel B, Barsh GS, Kahn CR, Cowley MA, Ashcroft FM, Brüning JC (2007) Insulin action in AgRP-expressing neurons is required for suppression of hepatic glucose production. Cell Metab 5:438–449.
Li H, Rajendran GK, Liu N, Ware C, Rubin BP, Gu Y (2007) SirT1 modulates the estrogen-insulin-like growth factor-1 signaling for postnatal development of mammary gland in mice. Breast Cancer Res 9:R1.
Lin SJ, Defossez PA, Guarente L (2000) Requirement of NAD and SIR2 for life-span extension by calorie restriction in *Saccharomyces cerevisiae*. Science 289:2126–2128.
Liu Y, Dentin R, Chen D, Hedrick S, Ravnskjaer K, Schenk S, Milne J, Meyers DJ, Cole P, Yates J 3rd, Olefsky J, Guarente L, Montminy M (2008) A fasting inducible switch modulates gluconeogenesis via activator/coactivator exchange. Nature 456:269–273.
Luquet S, Perez FA, Hnasko TS, Palmiter RD (2005) NPY/AgRP neurons are essential for feeding in adult mice but can be ablated in neonates. Science 310:683–685.
McBurney MW, Yang X, Jardine K, Hixon M, Boekelheide K, Webb JR, Lansdorp PM, Lemieux M (2003) The mammalian SIR2alpha protein has a role in embryogenesis and gametogenesis. Mol Cell Biol 23:38–54.
Napper AD, Hixon J, McDonagh T, Keavey K, Pons JF, Barker J, Yau WT, Amouzegh P, Flegg A, Hamelin E, Thomas RJ, Kates M, Jones S, Navia MA, Saunders JO, DiStefano PS, Curtis R (2005) Discovery of indoles as potent and selective inhibitors of the deacetylase SIRT1. J Med Chem 48:8045–8054.
Nie Y, Erion DM, Yuan Z, Dietrich M, Shulman GI, Horvath TL, Gao Q (2009) STAT3 inhibition of gluconeogenesis is downregulated by SirT1. Nat Cell Biol 11:492–500.
Pacholec M, Bleasdale JE, Chrunyk B, Cunningham D, Flynn D, Garofalo RS, Griffith D, Griffor M, Loulakis P, Pabst B, Qiu X, Stockman B, Thanabal V, Varghese A, Ward J, Withka J, Ahn K (2010) SRT1720, SRT2183, SRT1460, and resveratrol are not direct activators of SIRT1. J Biol Chem 285:8340–8351.
Pani G, Fusco S, Galeotti T (2006) Smaller, hungrier mice. Science 311:1553–1554; author reply 1553–1554.
Paxinos G, Franklin KBJ (2001) The mouse brain in stereotaxic coordinates, Ed 2. San Diego: Academic.
Pierce AA, Xu AW (2010) De novo neurogenesis in adult hypothalamus as a compensatory mechanism to regulate energy balance. J Neurosci 30:723–730.
Pinto S, Roseberry AG, Liu H, Diano S, Shanabrough M, Cai X, Friedman JM, Horvath TL (2004) Rapid rewiring of arcuate nucleus feeding circuits by leptin. Science 304:110–115.
Prozorovski T, Schulze-Topphoff U, Glumm R, Baumgart J, Schröter F, Ninnemann O, Siegert E, Bendix I, Brüstle O, Nitsch R, Zipp F, Aktas O (2008) Sirt1 contributes critically to the redox-dependent fate of neural progenitors. Nat Cell Biol 10:385–394.
Purushotham A, Schug TT, Xu Q, Surapureddi S, Guo X, Li X (2009) Hepatocyte-specific deletion of SIRT1 alters fatty acid metabolism and results in hepatic steatosis and inflammation. Cell Metab 9:327–338.
Ramadori G, Lee CE, Bookout AL, Lee S, Williams KW, Anderson J, Elmquist JK, Coppari R (2008) Brain SIRT1: anatomical distribution and regulation by energy availability. J Neurosci 28:9989–9996.
Ravussin E, Tschöp M, Morales S, Bouchard C, Heiman ML (2001) Plasma ghrelin concentration and energy balance: overfeeding and negative energy balance studies in twins. J Clin Endocrinol Metab 86:4547–4551.
Rodgers JT, Puigserver P (2007) Fasting-dependent glucose and lipid metabolic response through hepatic sirtuin 1. Proc Natl Acad Sci U S A 104:12861–12866.
Rogina B, Helfand SL (2004) Sir2 mediates longevity in the fly through a pathway related to calorie restriction. Proc Natl Acad Sci U S A 101:15998–16003.
Shaw AM, Irani BG, Moore MC, Haskell-Luevano C, Millard WJ (2005) Ghrelin-induced food intake and growth hormone secretion are altered in melanocortin 3 and 4 receptor knockout mice. Peptides 26:1720–1727.
Solomon JM, Pasupuleti R, Xu L, McDonagh T, Curtis R, DiStefano PS, Huber LJ (2006) Inhibition of SIRT1 catalytic activity increases p53 acetylation but does not alter cell survival following DNA damage. Mol Cell Biol 26:28–38.
Soriano P (1999) Generalized lacZ expression with the ROSA26 Cre reporter strain. Nat Genet 21:70–71.

Tissenbaum HA, Guarente L (2001) Increased dosage of a sir-2 gene extends lifespan in *Caenorhabditis elegans*. Nature 410:227–230.

Tschöp M, Wawarta R, Riepl RL, Friedrich S, Bidlingmaier M, Landgraf R, Folwaczny C (2001) Post-prandial decrease of circulating human ghrelin levels. J Endocrinol Invest 24:RC19–21.

Tschöp M, Statnick MA, Suter TM, Heiman ML (2002) GH-releasing peptide-2 increases fat mass in mice lacking NPY: indication for a crucial mediating role of hypothalamic agouti-related protein. Endocrinology 143:558–568.

Wang L, Saint-Pierre DH, Taché Y (2002) Peripheral ghrelin selectively increases Fos expression in neuropeptide Y-synthesizing neurons in mouse hypothalamic arcuate nucleus. Neurosci Lett 325:47–51.

Wu Q, Boyle MP, Palmiter RD (2009) Loss of GABAergic signaling by AgRP neurons to the parabrachial nucleus leads to starvation. Cell 137:1225–1234.

Xu AW, Kaelin CB, Takeda K, Akira S, Schwartz MW, Barsh GS (2005a) PI3K integrates the action of insulin and leptin on hypothalamic neurons. J Clin Invest 115:951–958.

Xu AW, Kaelin CB, Morton GJ, Ogimoto K, Stanhope K, Graham J, Baskin DG, Havel P, Schwartz MW, Barsh GS (2005b) Effects of hypothalamic neurodegeneration on energy balance. PLoS Biol 3:e415.

Zhang CY, Baffy G, Perret P, Krauss S, Peroni O, Grujic D, Hagen T, Vidal-Puig AJ, Boss O, Kim YB, Zheng XX, Wheeler MB, Shulman GI, Chan CB, Lowell BB (2001) Uncoupling protein-2 negatively regulates insulin secretion and is a major link between obesity, beta cell dysfunction, and type 2 diabetes. Cell 105:745–755.

Supplementary Material

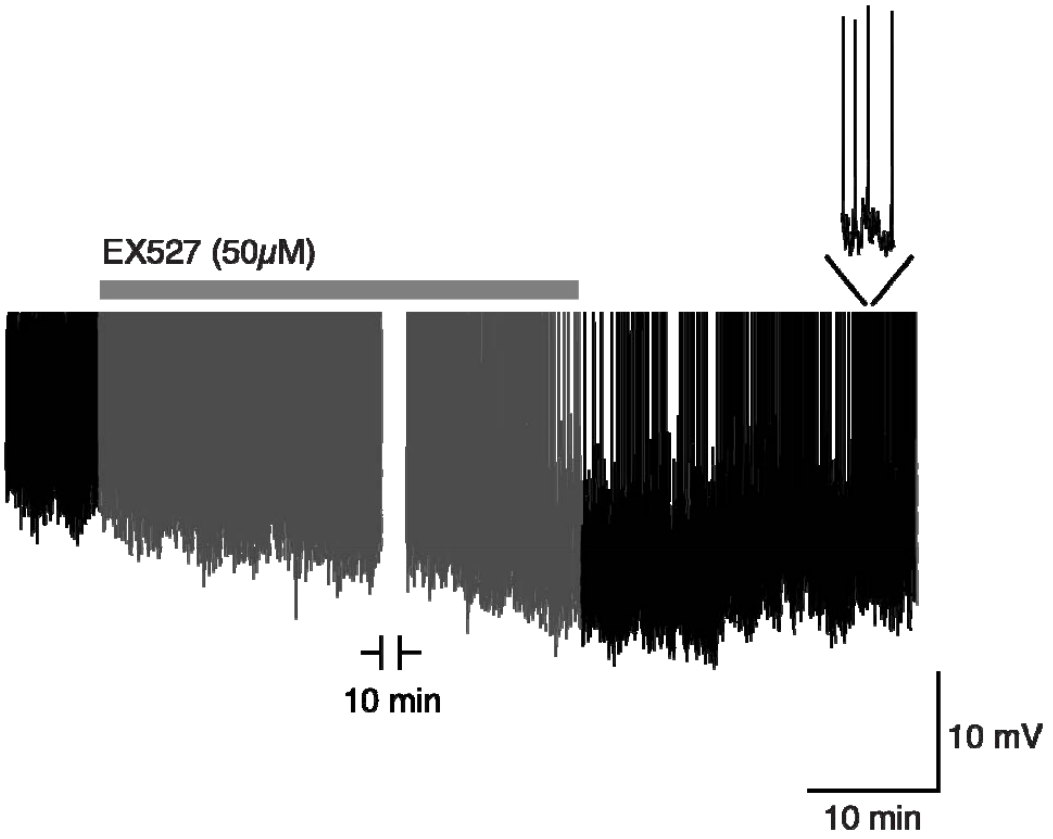

Supplementary Figure 1 Representative trace of membrane potential of NPY-GFP neurons treated with EX-527 in the recording chamber.
The membrane potential of the NPY-GFP cells was recorded after EX-527 application to the recording chamber and showed a hyperpolarization of the membrane (shown in gray). Before and after the application of EX-527, the incubation chamber was perfused with vehicle in ACSF. In the insert, it is shown in more details the membrane potential and action potentials (during 3 seconds).

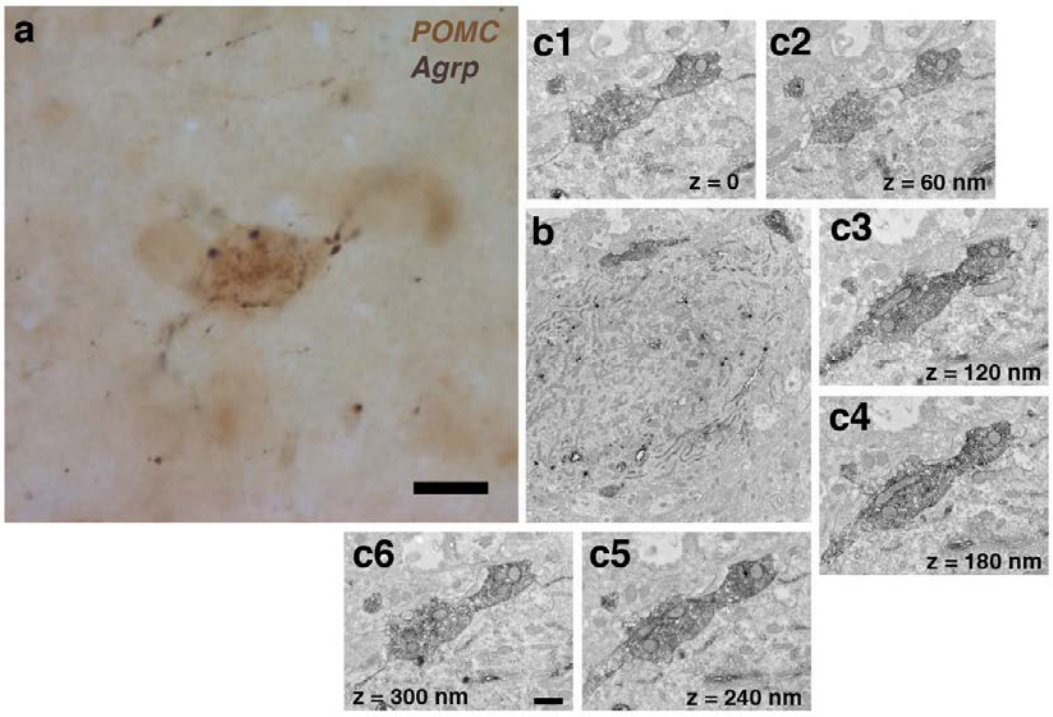

Supplementary Figure 2 NPY/AgRP neurons send inhibitory projections to their neighbor POMC neurons

Correlated light (**a**) and electron microscopy (**b-c**) with micrographs showing double immunostaining for POMC and Agrp. (**a**) Light microscopy image showing a POMC cell stained with DAB (light brown color) and Agrp developed with Nickel-DAB (brown-black dots). Several buttons covers the POMC cell membrane, highlighting the importance of this network in the regulation of neuronal function and metabolism. In (**b**), a low magnification electron micrograph showing the appearance of the POMC cell under the electron microscope with at least 3 Agrp buttons touching the membrane of the POMC cell. Note that the POMC staining is concentrated almost exclusively in the endoplasmatic reticulum of the POMC cell. (**c**) High magnification serial sectioning images (60 nm apart) where it is possible to visualize the Agrp button touching the membrane of the POMC cell. Morphologically, the synapse between the Agrp button and the POMC cell is symmetric, which is putatively inhibitory (GABAergic) synapse. Scale bars = 10 μm (in **a**), and 500 nm (in **c**).

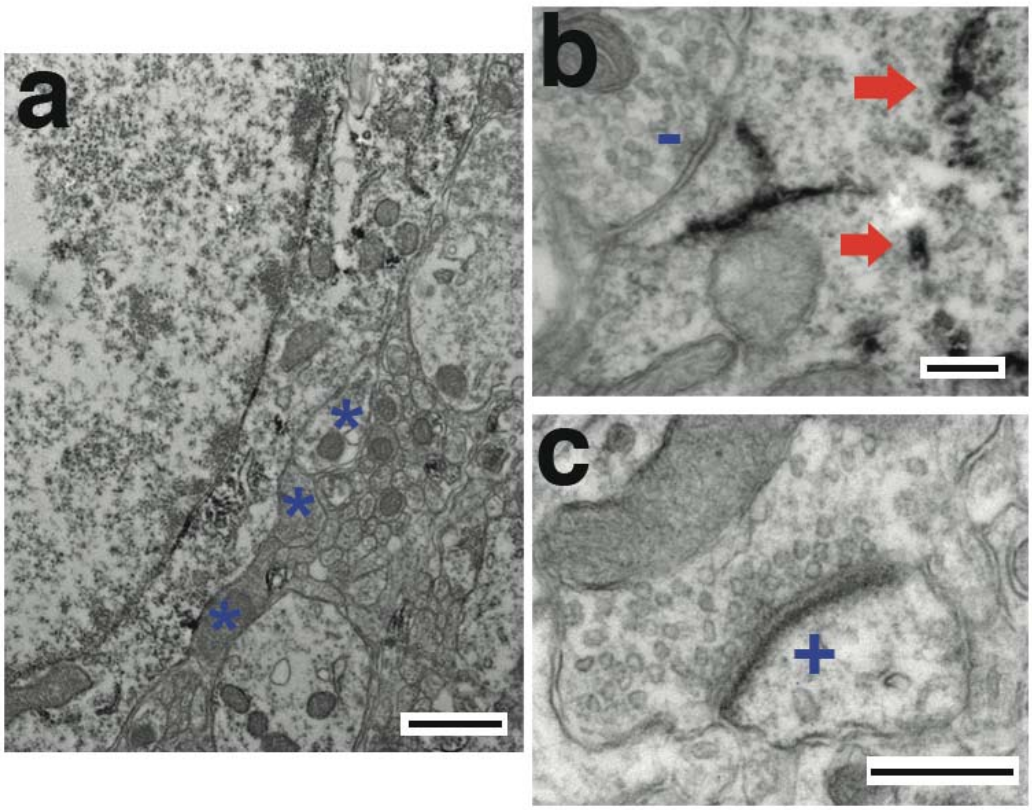

Supplementary Figure 3 Synaptic coverage of POMC neurons in the arcuate nucleus
Electron micrograph showing examples of typical symmetric and asymmetric synapses in POMC neurons. We count the number of synapses surrounding the cell membrane of the POMC cells and classify the synapses in symmetric or asymmetric. In (**a**), a POMC cell with 3 synapses marked with blue stars (blue *), scale bar represents 500 nm. (**b**) Symmetric, putative inhibitory synapse marked with blue minus (blue -), scale bar represents 100 nm. The POMC staining, developed with DAB is marked with red arrows. (**c**) Asymmetric, putative excitatory synapse with a blue plus sign (blue +). Scale bar denotes 100 nm.

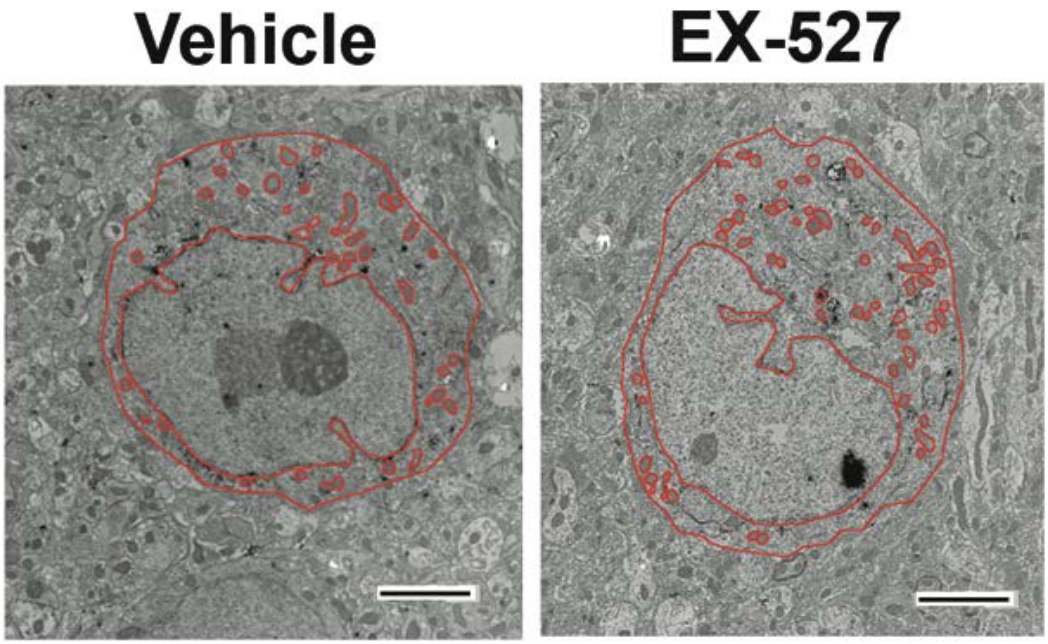

Supplementary Figure 4 Mitochondria distribution in POMC neurons
Electron micrographs showing mitochondria outlined in red in POMC neurons from the arcuate nucleus after treatment with vehicle or EX-527 (i.c.v., 1.5 nmol). Mice were injected before dark cycle (30-60 min) and perfused 4 hours later to identify synaptical and mitochondrial changes in the POMC neurons. We evaluate different parameters of mitochondria morphology and distribution, as the number of mitochondria in the cross-section area divided by the cell area, the total area of the cross-sectional mitochondria divided by the cell area. Additionally, we also computed the distribution of the cross-sectional mitochondria area and circularity as indexed of mitochondria morphology. Cell, nuclei and mitochondrial membranes are highlighted in red. Scale bar represents 2 μm.

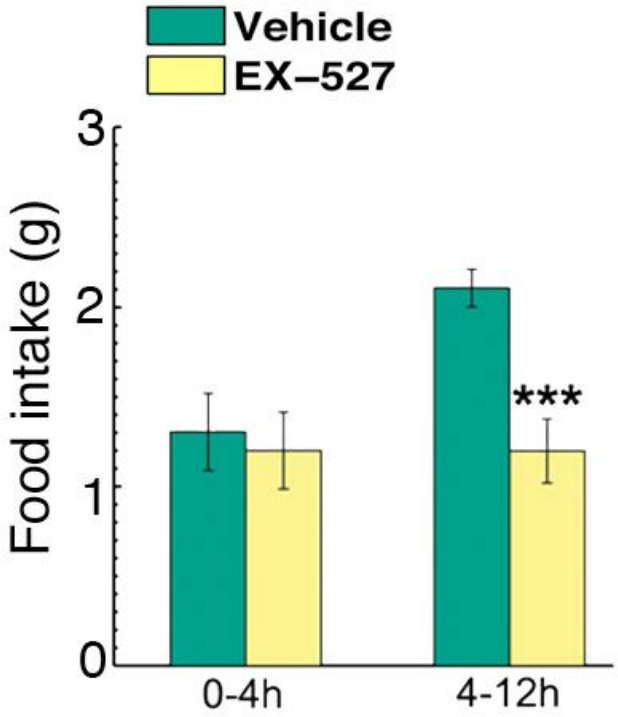

Supplementary Figure 5 EX-527 injected in the brain decreases food intake similarly to peripheral injection of the compound

EX-527 was injected in the lateral cerebral ventricle of mice 30-60 minutes before dark cycle and food intake was evaluated manually 4h and 12h later by measuring the food pellet on the cage. Injection of EX-527 into the cerebral ventricles (1.5 nmol) inhibited food intake during the dark cycle (effect of treatment: $F_{1,26} = 7.98$, $p < 0.01$; time x treatment: $F_{1,26} = 4.56$, $p < 0.05$ - mean ± s.e.m., n = 14) in a manner similar to peripheral EX-527 (see Figure 2a, main text). We repeated this experiment identically to the peripheral injection of EX-527 to be able to compare the response of the animals to both forms of treatment. *** $p < 0.001$.

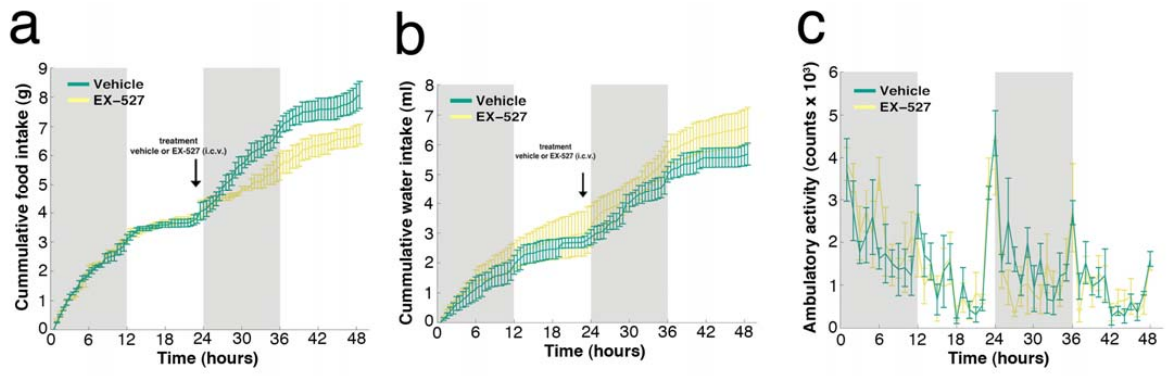

Supplementary Figure 6 Pharmacological inhibition of brain Sirt1 decreases food intake independently of major changes in locomotor activity and water intake
The intermediate dose of EX-527 found in our dose-response studies (Figure 2c, main text) to inhibit food intake was used to evaluate the effects of Sirt1 inhibition on locomotor activity and water intake. Mice were acclimatized to home cages equipped with an electronic system to measure locomotor activity, water intake and food intake (TSE Systems, Germany), and data were collected during 24h before and 24h after EX-527 treatment (i.c.v.) (mean ± s.e.m., n = 3-4). (**a**) Replicating our previous data, EX-527 (i.c.v., 1.5 nmol) inhibited food intake (effect of treatment: $F_{1,235} = 6.14$, $p > 0.05$; time x treatment: $F_{47,235} = 4.02$, $p < 0.001$), with no major effects on (**b**) water intake and (**c**) locomotor activity. It is noteworthy that there is a trend to decrease locomotor activity in the first hours after the injection of EX-527, a time when food consumption is still in normal range. Black arrows indicate time of EX-527 injection. Shadows indicate dark cycle.

Supplementary Figure 6

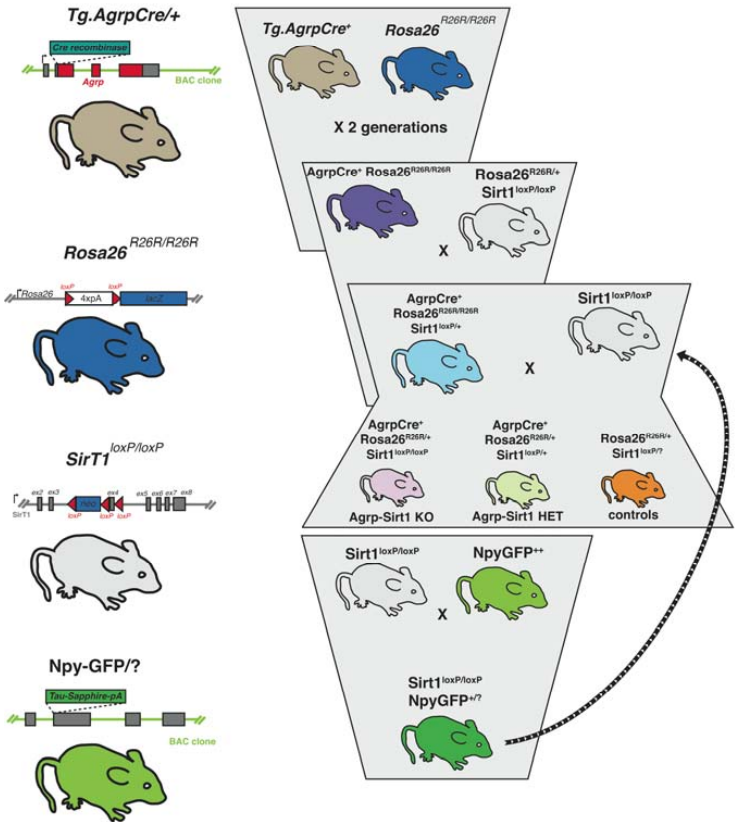

Supplementary Figure 7 Constructs and breeding scheme used to generate the Agrp-Sirt1 KO mice.
On the left side is illustrated four different transgenic mouse lines used in this study to generate the Agrp-Sirt1 KO mice. On the right side it is drawn a schematic of the crossings to obtain our final experimental mice. First, transgenic *AgrpCre*$^{+}$ mice were bred with *Rosa26* homozygote mice to generate *AgrpCre*$^{+}$-*Rosa26*$^{R26R/R26R}$ (we keep these mice as founders in our laboratory). We then crossed Sirt1$^{loxP/loxP}$ with *Rosa26* homozygote mice to obtain a Sirt1 floxed mouse carrying the *Rosa26* reporter locus. These animals were crossed with AgrpCre^{+}-Rosa26$^{R26R/R26R}$ to obtain final breeders (*AgrpCre*$^{+}$-*Rosa26*$^{R26R/R26R}$-Sirt1$^{loxP/+}$). These mice were then bred against Sirt1 floxed mice or NpyGFP-Sirt1$^{loxP/loxP}$ mice to obtain final experimental mice. All experimental mice were paired to control littermates of same age and sex. Preliminary experiments (not shown) and data published elsewhere[38,39] showed that the *AgrpCre*$^{+}$ were indistinguishable phenotypically of their *Cre* controls. Thus, we pooled as controls all mice that were *Cre* negative. Heterozygote mice for the Sirt1 floxed allele that were *AgrpCre*$^{+}$ showed intermediate phenotype compared to controls and Agrp-Sirt1 KO mice.

Supplementary Table 1:

Time after treatment	30-90 minutes			4-5 hours		
Treatment	**Open-field[a]**	**Rota-rod[b]**	**Rectal temperature[c]**	**Open-field[a]**	**Rota-rod[b]**	**Rectal temperature[c]**
Central (i.c.v.)						
Vehicle	504 ± 58	60 ± 0	35.85 ± 0.44	218 ± 29	58 ± 2	37.12 ± 0.45
EX-527 1.5 nmol	369 ± 79	60 ± 0	35.59 ± 0.28	232 ± 44	60 ± 0	37.28 ± 0.31

[a] Data expressed in arbitrary counts, mean ± s.e.m.
[b] Latency to fall in seconds, mean ± s.e.m.
[c] Data expressed in ºC, mean ± s.e.m.
NA, data not available.

Mice were injected with EX-527 (i.c.v., 1.5 nmol) or vehicle and were analyzed in the different tasks in the following sequence: open-field, rota-rod, rectal temperature. Measurements were repeated 30 minutes after injection and 4 hours later to indentify both short time and delayed side effects/toxicity.

Open-field behavior
Mice were individually placed in 40 x 40 x 40 cm boxes, recorded and analyzed by automatic software (Mousetracker©, designed by Adriano B. Tort). For more information, visit http://mousetrackers.com/Site/Home.html. Total recording time was 10 minutes. The data is expressed as locomotor counts (arbitrary units).

Rota-rod test
Mice were individually put in an electronically motorized wheel and the latency to fall was measured. A cut off time of 60 seconds was set up.

Rectal temperature measurements
After behavioral measurements, mice were held and a rectal probe was inserted into the anus and allowed to stabilize before recording the rectal temperature. If the mice were evacuating, the measurements were not considered since fecal evacuation promotes a temporary increase in rectal temperature.

Capítulo VII. Sirt1 in AgRP neurons is necessary for exploratory behavior during calorie restriction

Artigo em preparação; periódico ainda não definido.

Sirt1 in AgRP neurons is necessary for exploratory behavior during calorie restriction

Marcelo O. Dietrich[1, 2] Diogo O. Souza[2], and Tamas L. Horvath[1, *]

[1]Section of Comparative Medicine, Yale University, New Haven CT 06520, USA and [5]Department of Biochemistry, UFRGS, Porto Alegre RS 90035, Brazil. * tamas.horvath@yale.edu.

Abstract (online only):

Calorie restriction can prolong healthy life span in mammals. The underlying mechanisms involved in this process are ill-defined. We show here that CR promotes the activity of NPY/AgRP neurons in the brain, and that disrupting Sirt1 (a deacetylase that senses NAD+) in these cells lead to impaired behavioral but not metabolic responses to CR. These findings highlight the pivotal role of the NPY/AgRP neurons during CR in regulation of complex behaviors.

Calorie restriction (CR) promotes complex behavioral and metabolic adaptations and can lead to a prolonged healthy lifespan in mammals (*1*). The regulatory principles that underlie the effect of CR on integrative physiology are unresolved. The molecular machinery involved in the effects of CR on whole body physiology involves sirtuins, including Sirt1. Sirt1 is a deacetylase that requires NAD+ as a substrate for its enzymatic reaction, linking its activity to the metabolic state of the cell. It has been shown that Sirt1 mediates several effects of CR (*2-5*). The arcuate nucleus (ARC) in the hypothalamus integrates metabolic signals to regulate energy balance. POMC neurons produce alpha-melanocyte-stimulating hormone, which activates the melanocortin receptors (MCRs), promoting satiety. NPY/AgRP neurons produce agouti-related peptide (AgRP), which acts as an endogenous antagonist of the MCRs, and promote appetite. NPY/AgRP neurons are activated by orexigenic signals and mediate metabolic shifts during periods of negative energy balance, including fasting. The involvement of AgRP neurons in starvation-like states points to a potential role of these cells in promoting adaptation to CR. To address this prospectively, first, we characterized the adaptive response of NPY/AgRP neurons to CR. As expected, *npy* and *agrp* mRNA levels in the ARC were highly increased by CR, while *pomc* was decreased (Fig.1A). This result is consistent with an increase c-fos labeling in the NPY/AgRP neurons (Fig.1A) and an increase GFP fluorescence in the ARC in NPY-GFP reporter mice under CR (Fig.1A). The switch towards NPY/AgRP neuronal function and POMC inhibition is also in line with the changes observed in the synaptic coverage of these cells (Fig.1B and Table S1). Altogether, these results highlight that CR promotes a robust adaptation of the melanocortin system in ARC, promoting NPY/AgRP neuronal function while inhibiting POMC cells.

Next, we sought to determine whether Sirt1 in the NPY/AgRP neurons might be important for the adaptive response of mice to CR as Sirt1 knockdown in these cells was shown to affect AgRP neuronal responses to ghrelin and adiposity in ad libitum-fed animals (*6*). Ten months exposure to CR resulted in similar changes in body weight, lean and fat mass, and blood lipid profile of control and AgRP-Sirt1 KO mice (Table S2). Indirect calorimetry also revealed no differences in responses to CR of control and Agrp-Sirt1 animals (Fig.S1).

CR has a major impact on behavior. For example, CR increases locomotor activity in mice, a behavior adaptation that has been linked to Sirt1 expression (*3, 4*). To test whether the AgRP-Sirt1 KO mice have altered locomotor response to CR, first we monitored their home-cage activity. CR strongly induced ambulatory activity in all animals (Fig.1C), an effect that was significantly enhanced in the AgRP-Sirt1 KO mice (Fig.1C). Next we tested the animals in a novel environment. In parallel with elevated home-cage activity, control animals exposed to CR had increased exploratory activity in an open-field compared to their ad libitum counterparts (Fig.1D and Fig.S2). In striking contrast however, AgRP-Sirt1 KO exposed to CR showed a significant decrease in exploratory activity in the novel environment compared to their ad libitum fed counterparts (Fig.1D and Fig.S2) unrelated to motor coordination (Fig.S3). Intriguingly, we found that AgRP-Sirt1 KO in CR explored the open-field exclusively close to the walls, avoiding the center of the box (Fig.1D). These results appear to be independent of anxiety-related behaviors as AgRP-Sirt1 KO animals did not show altered behavior in elevated plus maze test compared to controls (Fig.S4).

Taken together, these results show that Sirt1 in AgRP neurons are critical for complex behavioral adaptations but not metabolic responses to CR.

References

1. L. Fontana, L. Partridge, V. D. Longo, Extending healthy life span--from yeast to humans. *Science* **328**, 321 (Apr 16, 2010).
2. H. Cohen *et al.*, Calorie restriction promotes mammalian cell survival by inducing the SIRT1 deacetylase. *Science* **305**, 390 (Jul, 2004).
3. D. Cohen, A. Supinski, M. Bonkowski, G. Donmez, L. Guarente, Neuronal SIRT1 regulates endocrine and behavioral responses to calorie restriction. *Genes Dev* **23**, 2812 (Dec, 2009).
4. D. Chen, A. Steele, S. Lindquist, L. Guarente, Increase in activity during calorie restriction requires Sirt1. *Science* **310**, 1641 (Dec, 2005).
5. A. Satoh *et al.*, SIRT1 promotes the central adaptive response to diet restriction through activation of the dorsomedial and lateral nuclei of the hypothalamus. *Journal of Neuroscience* **30**, 10220 (Jul 28, 2010).
6. M. Dietrich *et al.*, Agrp neurons mediate Sirt1's action on the melanocortin system and energy balance: roles for Sirt1 in neuronal firing and synaptic plasticity. *J Neurosci* **30**, 11815 (Sep, 2010).

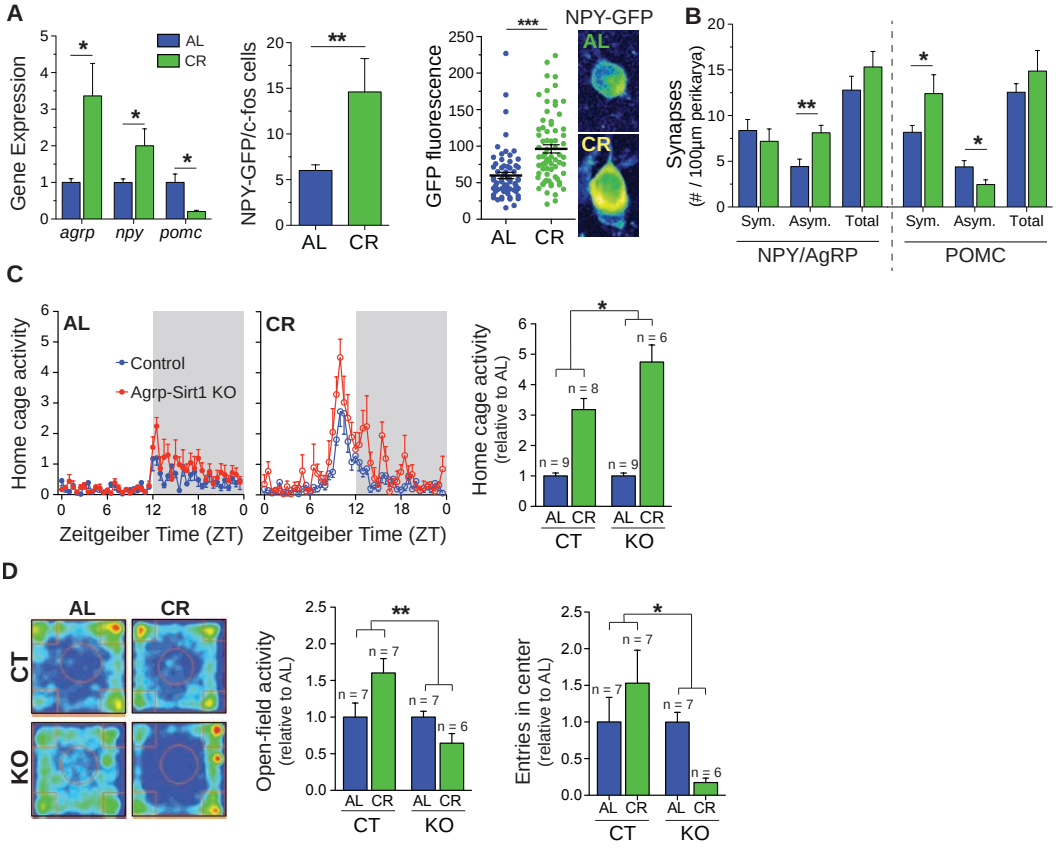
A
Gene Expression
AL
CR
agrp
npy
pomc
NPY-GFP/c-fos cells
AL
CR
GFP fluorescence
NPY-GFP
AL
CR
B
Synapses
(# / 100μm perikarya)
Sym.
Asym.
Total
NPY/AgRP
POMC
C
Home cage activity
AL
CR
Control
Agrp-Sirt1 KO
Zeitgeiber Time (ZT)
Home cage activity
(relative to AL)
CT
KO
D
AL
CR
CT
KO
Open-field activity
(relative to AL)
Entries in center
(relative to AL)

Fig.1:

(**A**) CR promotes NPY/AgRP neuronal function while inhibits POMC neurons. Left, CR increases *agrp* and *npy*, and decreases *pomc* mRNA in the ARC; middle, the number of c-fos labeled NPY/AgRP neurons increases after CR; right, green fluorescence is increased in NPY-GFP reported mice under CR. Representative cells are shown in pseudo-color. (**B**) CR promotes changes in the synaptic input organization in the ARC. CR increases putative excitatory inputs (asymmetric) onto NPY/AgRP neuronal perikarya with concomitant increase in putative inhibitory (symmetric) and decrease excitatory inputs onto POMC perikarya (SOM for more details). (**C**) CR increases home-cage activity in control mice, an effect that is enhanced in AgRP-Sirt1 KO mice (diet x genotype: $F_{(1,28)} = 7.365$). (**D**) Open-field exploratory behavior is increased in CR mice; such effect is abrogated in AgRP-Sirt1 KO mice. Left, group average occupancy plots (lower -> higher, blue -> red); middle, locomotor activity in the open-field; right, entries in the center of the open-field. In (C) and (D), the data are related to AL mice from the same genotype. * $p < 0.05$, ** $p < 0.01$, *** $p < 0.001$.

Materials and Methods

Animals

All animals were kept in temperature and humidity controlled rooms, in a 12/12h light/dark cycle, with lights on from 7:00AM-7:00PM. NPY-GFP mice were provided by Dr. J. Friedman (Rockefeller University, New York, NY – B6.Cg-Tg(NPY-MAPT/Sapphire)1Rck/J; stock number 008321 in The Jackson Laboratory repository) and have been maintained on a B6 background for more than 10 generations. Sirt1$^{loxP/loxP}$ mice were purchased from The Jackson Laboratory (B6; 129-Sirt1^{tm1gu}/J; stock number 008041). Tg.AgrpCre mice have been maintained in our colony on a mixed background and backcrossed to the reporter line Rosa26-LSL-lacz mice (B6.129S4-Gt(ROSA)26Sor^{tm1Sor} - originally from The Jackson Laboratory). All procedures were approved by local committees (Institutional Animal Care and Use Committee from Yale University). The Agrp-Sirt1 KO mice were generated as previously described (*6*).

Calorie restriction (CR) protocol:

Adult mice (older than 9 weeks) were used in these studies. Mice were single housed two weeks before starting the protocol to avoid changes in food intake and body weight due to the stress of single housing. After two weeks, daily food intake was monitored by manually measuring the food in the cage at ZT 11 (6:00 PM). Body weight was monitored weekly. After a stable baseline food intake, mice were divided in AL and CR groups. Both groups have similar food intake at baseline. The CR groups, received 10% of the food of the AL group in the first week, 20% less in the second week, 30% less in the third week, and then were kept in a 35-40% CR diet. The animals used for qRT-PCR, c-fos staining, EM, GFP fluorescence were CR for 8 weeks. The Agrp-Sirt1 mice were CR for 10 months for behavioral analysis.

Quantitative real-time PCR:

Freshly dissected media-basal hypothalamuses were stored in RNAlater Stabilization reagent (Cat. # 76104, Qiagen) at 4ºC. RNA was extracted using RNeasy Mini Kit (Cat. # 74104, Qiagen). Transcript detection and relative quantification was done using TaqMan Gene Expression Assays (Applied Biosystems), using the following assays: agrp (Mm00475829_g1), npy (Mm03048253_m1), and pomc (Mm00435874_m1) in a Roche 480 Lightcycler. Differences between AL and CR were tested using *t* test. A *p* value less than 0.05 was considered statistically significant.

Immunohistochemistry for c-fos and GFP:

We used similar techniques as reported elsewhere (*6*).

Quantitative GFP fluorescence analysis:

Transgenic mice carrying the tau (MAPT)-sapphire green fluorescent protein (GFP) under the *npy* promoter were used for this analysis. Mice were deeply anesthetized and the left ventricle of the heart was rapidly cannulated and flushed with 0.9% saline containing heparin followed by freshly prepared fixative (paraformaldehyde 4%, gluteraldehyde 0.1%, picric acid 15%, in Phosphate Buffer (PB) 0.1M, pH=7.4). The same perfusion method was used for electron microscopy and c-fos immunostaining. Brain slices (50 µm) containing the ARC were immediately mounted on slides using PB 0.1M and scanned in a confocal microscope

using fixed settings for GFP detection. After collecting all images from all mice, the fluorescence intensity was measured using ImageJ. The whole procedure was blinded, from perfusion to data analysis. 11 cells from each mouse in the AL group and 12 cells from each mouse in the CR were used for analysis (6 mice/group). Statistical differences were tested using two-tailed *t* test. A p value less than 0.05 was considered significant.

Electron microscopy:

We used similar techniques as reported elsewhere (*6*). For NPY/AgRP labeling, transgenic mice carrying the tau (MAPT)-sapphire green fluorescent protein (GFP) under the *npy* promoter were used. A primary antibody against GFP was used for immunolabeling - chicken anti-GFP (1:8000, 4ºC, 48h; ABCAM). All the other procedures were carried as described (*6*).

Body composition:

Mice were scanned in the EchoMRI-100 machine (no anesthesia) or, alternatively, in the Lunar PIXImus Densitometer (GE Medical Systems) (ketamine plus xylazine mixture was used to anesthetize mice).

Blood analysis:

Mice were fasted overnight (6:00 PM to 8:00 AM), and eye bled. CR mice received a food pellet as usual just before the night cycle, and were fasted overnight. Serum was collected by centrifugation and aliquots were stored at -80ºC until analyzed. NEFA was measured using a kit from Wako Diagnostics (HR Series NEFA-HR). Total cholesterol was measured using a kit from Cayman Chemical (Cat. #10007640). Triglycerides were measure using a kit from Sigma (Cat. #TR0100). Statistical analyses were performed in SPSS 18.0 for Mac using two-way ANOVA. A *p* value less than 0.05 was considered statistically significant.

Indirect calorimetry and home-cage activity:

Mice were acclimated in metabolic chambers (TSE Systems, Germany) for 4 days before the start of the recordings. Mice were continuously recorded for at least 3 days with the following measurements being taken every 30 minutes: water intake, food intake, ambulatory activity (in X and Z axes), and gas exchange (O_2 and CO_2) (using the TSE LabMaster system, Germany). VO_2, VCO_2 and energy expenditure were calculated according to the manufacturer's guidelines (PhenoMaster Software, TSE Systems). The respiratory exchange rate (RER) was estimated by calculating the ratio of VCO_2/VO_2.

Open-field:

This test was used to investigate exploratory behavior in a new environment. We used two different paradigms to test the mice in different environments. First, we placed the mice in standard rat cages without bedding, connected to a computerized system that measured the number of beam brakes along the X-axis of the cage. For this experiment, mice were let to explore the cage for 60 minutes. In the second experiment, the apparatus consist of a squared open-field (37 cm × 37 cm × 37 cm) covered with a synthetic grey cover to provide enough contrast for video tracking. Mice were automatically recorded using the software ANY-maze Video Tracking System (version 4.72, Stoelting Co., Wood Dale, IL, USA). In the software, the open-field was virtually divided in two main zones, the center (circle around the center of

the apparatus with a diameter of 14 cm) and the walls (a 6 cm strip along the walls of the apparatus). Four similar apparatus were recorded simultaneously. Mice were put in the open-field for 5 minutes and let to explore the new environment. The apparatus was cleaned with an alcohol solution (70%) and water to avoid olfactory clues before placing the next animal. For the center of the open-field, the animal's head was considered when analyzing the time in the zone. Occupancy plots were generated by the ANY-maze software and consist of the group occupancy plot of the animal's head position. The maximum occupancy is the maximum value found in any of the plots, thus the plots can be compared between them, but cannot be used to direct comparisons to other plots from different experiments. The raw data obtained in the video tracking software was exported to SPSS 18.0. Data were first tested for homogeneity of variances using Levene's test. After assuming homogeneity of variances ($p > 0.05$), differences were tested using two-way ANOVA.

Plus-maze:

All mice were brought to the testing room at least 2 hours before initiating the tests to acclimate the mice. The apparatus consisted of four elevated arms (40 cm from the floor, 25 cm long and 5.2 cm wide) arranged at right angles (cross-like disposition). Two opposite arms were enclosed by 15-cm high walls, and the other two were open (no walls). The maze had a central 5.2 cm × 5.2 cm square platform that gave access to all arms. The floor of the maze was covered with a gray synthetic cover glued to the apparatus to provide enough contrast for automatic video tracking. Each mouse was placed in the central square facing an open arm. The apparatus was cleaned with an alcohol solution (70%) and water to avoid olfactory clues before placing the next animal. Number of entries in each arm and time spent in each arm were recorded for 5 min. The number of alternations was considered as the total number of entries in the open arms plus the entries in the closed arms. For one entry to occur, at least 50% of the total animal area had to be inside the zone. One exit from the zone was not counted until less than 30% of the total animal area was in the zone. All data was automatically recorded and analyzed using the software ANY-maze Video Tracking System (version 4.72, Stoelting Co., Wood Dale, IL, USA). Occupancy plots were generated by the ANY-maze software and consist of the group occupancy plot of the animal's centre position. The maximum occupancy is the maximum value found in any of the plots, thus the plots can be compared between them, but cannot be used to direct comparisons to other plots from different experiments. The raw data obtained in the video tracking software was exported to SPSS 18.0. Data were first tested for homogeneity of variances using Levene's test. After assuming homogeneity of variances ($p > 0.05$), differences between control and Agrp-Sirt1 KO mice were tested using two-way ANOVA.

Rota-rod:

The apparatus consist of a rolling bar located 20 cm above the floor, divided in 4 compartments. The floor of the apparatus contained an automatic dispositive to record when the mice felt from the rolling bar. Mice were acclimated to the behavior room for at least 2 hours before the test. On days 1-4, all mice were trained in the rota-rod (2 trials/day) using the following parameters: initial speed = 4 rpm, maximum speed = 60 rpm, time to reach maximum speed = 300 seconds. The cut off time on the rota-rod was 600 seconds. The latency to fall from the rotating bar was recorded. After finishing the first trial, mice were returned to the home cage. A group of 4 mice were tested at the same time in the apparatus. When all 4 mice finished one section of

training, they were put back in the rota-rod for the second trial, which was identical to the first trial. All experiments started at ZT 4.5. Data analysis was performed by averaging the latency of both trials in each day, and utilizing mixed model ANOVA with time as a repeated measure. Sphericity was tested using the Mauchly's test of sphericity. If the P value of the Mauchly's test was lower than 0.05, the degrees of freedom were adjusted using the epsilon calculated by the Greenhouse-Geisser procedure. PASW Statistics 18.0 software was used for the analysis.

SOM Text

Acknowledgements

We thank to Catiele Antunes for helping with the Agrp-Sirt1 project and immunohistochemistry. Erszebet Borok for helping with electron microscopy. Jeremy Bober and Marya Shanabrough for technical support. Esther de la Fuente for helping with blood analysis. This work was supported by the NIH Pioneer Award to TLH. MOD was partially supported by a fellowship from CNPq-Brazil.

Fig. S1.

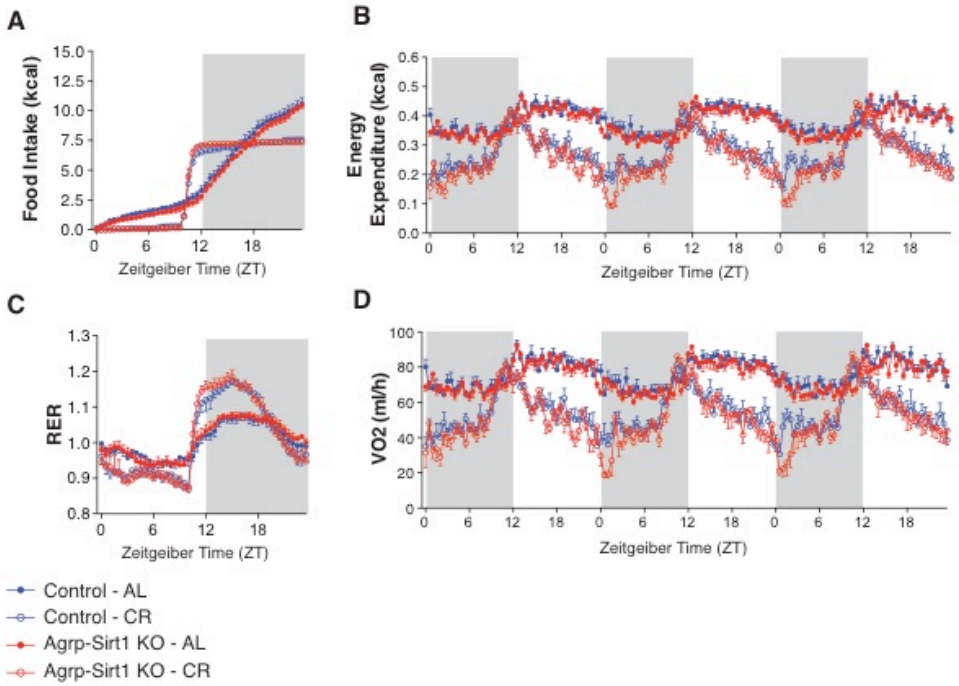

Agrp-Sirt1 KO male (AL n = 9, CR n = 6) mice and their littermate controls (AL n = 9, CR n = 8) show similar metabolic phenotype during indirect calorimetry when fed an AL or a CR diet for at least 10 months. (**A**) Representative 1 day cumulative food intake. (**B**) Energy expenditure during 3 representative days. (**C**) RER (see methods) during 1 representative day. And (**D**) VO2 during 3 representative days. Shadow areas indicate dark cycle. There were no statistical differences in any of the parameters showed here in addition to VCO2 and water intake (not shown).

Fig. S2

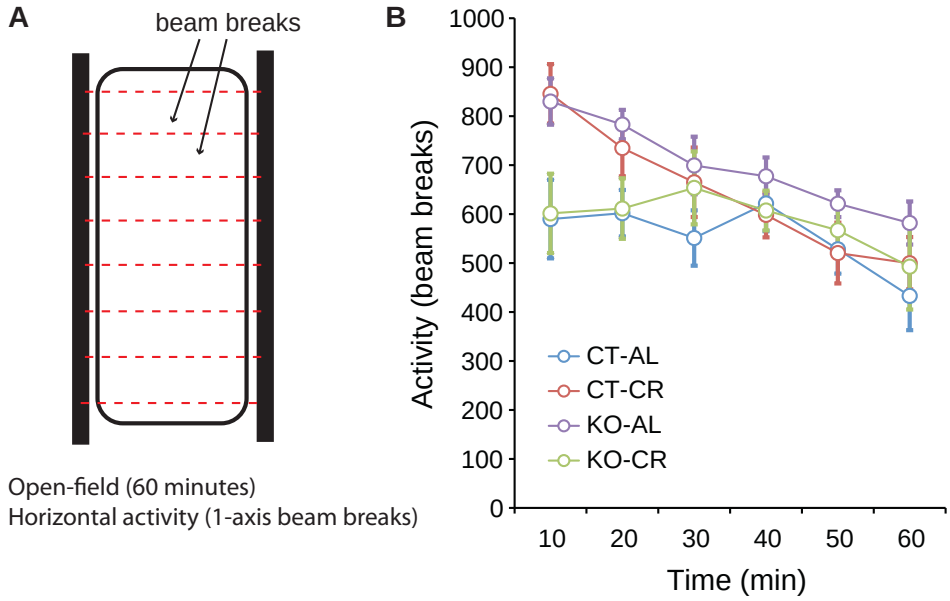

Exploratory behavior in an open-field test during 60 minutes. (**A**) Diagram of the open-
field used in this test: a clear standard rat cage without bedding was used to measure 1-axis activity using a computerized beam breaks system. (**B**) While control mice in CR have increased exploratory activity during the first 20 minutes in a novel environment, the Agrp-Sirt1 KO in CR have decreased activity when compared to their AL controls. See full statistics below. CT-AL n = 7, CT-CR n = 7, KO-AL n = 7, KO-CR n = 6.

Statistical analysis: mixed model ANOVA with time as a repeated measure and genotype and diet as factors.
Mauchly's test of Sphericity: W = 0.239, chi-square = 30.161, df = 14, p = 0.008.
Greenhouse-Geisser epsilon = 0.651.
Effect of time: $F_{(3.256,\ 74.879)} = 13.449$, $p < 0.001$.
Effect of time x genotype: $F_{(3.256,\ 74.879)} = 0.478$, $p = 0.714$.
Effect of time x diet: $F_{(3.256,\ 74.879)} = 0.467$, $p = 0.722$.
Effect of time x diet x genotype: $F_{(3.256,\ 78.879)} = 3.800$, $p = 0.012$.
Effect of genotype: $F_{(1,23)} = 1.116$, $p = 0.302$.
Effect of diet: $F_{(1,23)} = 0.057$, $p = 0.814$.
Effect of diet x genotype: $F_{(1,23)} = 5.567$, $p = 0.027$.

Fig. S3

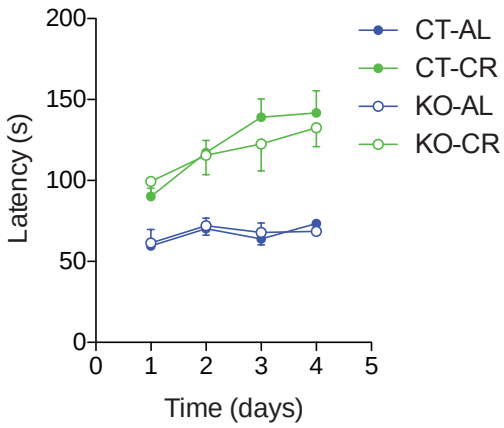

Latency to fall from the rotating bar in a rota-rod test (see methods for details). CR increases the latency in both control and Agrp-Sirt1 KO mice, with no differences between the two genotypes. See full statistics below. CT-AL n = 7, CT-CR n = 7, KO-AL n = 7, KO-CR n = 6.

Statistical analysis: mixed model ANOVA with time as a repeated measure and genotype and diet as factors.
Mauchly's test of Sphericity: W = 0.432, chi-square = 18.224, df = 5, p = 0.003.
Greenhouse-Geisser epsilon = 0.681.
Effect of time: $F_{(2.042,\ 46.968)} = 18.344$, $p < 0.001$.
Effect of time x genotype: $F_{(2.042,\ 46.968)} = 1.242$, $p = 0.299$.
Effect of time x diet: $F_{(2.042,\ 46.968)} = 8.607$, $p < 0.001$.
Effect of time x diet x genotype: $F_{(2.042,\ 46.968)} = 1.180$, $p = 0.317$.
Effect of genotype: $F_{(1,23)} = 0.069$, $p = 0.796$.
Effect of diet: $F_{(1,23)} = 55.395$, $p < 0.001$.
Effect of diet x genotype: $F_{(1,23)} = 0.134$, $p = 0.718$.

Fig. S4

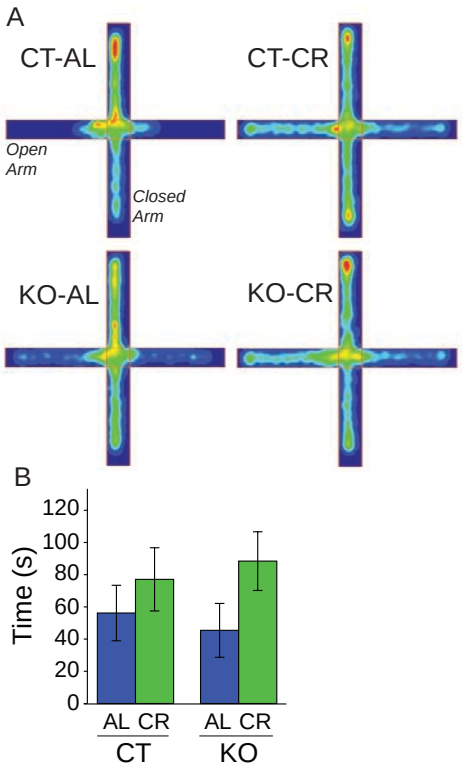

Agrp-Sirt1 KO and their littermate controls did not show statistically significant differences in the time spend in the open arms in a plus-maze anxiety test.
CT-AL n = 7, CT-CR n = 7, KO-AL n = 7, KO-CR n = 6.

Statistical analysis: two-way ANOVA with genotype and diet as factors.
Effect of genotype: $F_{(1,22)} = 0.000$, $p = 0.987$.
Effect of diet: $F_{(1,22)} = 3.087$, $p = 0.093$.
Effect of diet x genotype: $F_{(1,22)} = 0.369$, $p = 0.550$.

Table S1.

Morphological data and statistical analysis on NPY/AgRP and POMC neurons in the ARC of mice fed a CR diet and their AL controls.

Supplementary Table 1:

	NPY-GFP			POMC		
	AL	**CR**	**Stat**	**AL**	**CR**	**Stat**
Cell morphology:	**(n = 34)**	**(n = 34)**		**(n = 33)**	**(n = 27)**	
Perikarya (μm)	34.07 ± 1.10	36.92 ± 1.20	t = 1.745, df = 66 p = 0.085 (2-tail)	34.15 ± 0.98	32.76 ± 1.05	t = 0.9629, df = 58 p = 0.3396 (2-tail)
Cellular area (μm^2)	75.88 ± 4.36	88.72 ± 5.12	t = 1.909, df = 66 p = 0.060 (2-tail)	78.29 ± 3.70	73.26 ± 3.96	t = 0.9237, df = 58 p = 0.3595 (2-tail)
Nuclear area (μm^2)	37.11 ± 2.84	42.04 ± 2.76	t = 1.245, df = 66 p = 0.217 (2-tail)	30.91 ± 2.096	34.14 ± 2.626	t = 0.9742, df = 58 p = 0.3340 (2-tail)
Citosol area (μm^2)	38.77 ± 3.54	46.68 ± 4.00	t = 1.478, df = 66 p = 0.144 (2-tail)	47.39 ± 3.29	39.12 ± 2.62	t = 1.901, df = 58 p = 0.0623 (2-tail)
Ratio Nuclear/cell area	0.488 ± 0.028	0.482 ± 0.023	t = 0.155, df = 66 p = 0.877 (2-tail)	0.407 ± 0.024	0.461 ± 0.026	t = 1.512, df = 58 p = 0.1360 (2-tail)
Synaptic coverage:	**(n = 27-29)**	**(n = 22)**		**(n = 33)**	**(n = 22-24)**	
Symmetric [A]	8.37 ± 1.19	7.18 ± 1.35	t = 0.6597, df = 49 p = 0.2563 (1-tail)	8.17 ± 0.74	12.41 ± 2.06	t = 2.157, df = 55 p = 0.0177 (1-tail)
Asymmetric [A]	4.42 ± 0.81	8.13 ± 0.81	t = 3.151, df = 49 p = 0.0014 (1-tail)	4.38 ± 0.69	2.46 ± 0.50	t = 2.089, df = 55 p = 0.0207 (1-tail)
Total [A]	12.80 ± 1.50	15.32 ± 1.70	t = 1.107, df = 49 p = 0.2737 (2-tail)	12.56 ± 0.92	14.88 ± 2.24	t = 1.055, df = 55 p = 0.2960 (2-tail)
% Symmetric	66.30 ± 6.41	43.34 ± 6.62	t = 2.471, df = 47 p = 0.0086 (1-tail)	67.78 ± 4.66	82.03 ± 4.02	t = 2.159, df = 53 p = 0.0177 (1-tail)
% Asymmetric	33.70 ± 6.41	56.66 ± 6.62	t = 2.471, df = 47 p = 0.0086 (1-tail)	32.22 ± 4.66	17.97 ± 4.02	t = 2.159, df = 53 p = 0.0177 (1-tail)

Notes:
In red: data statistically significant (alpha < 0.05).
In blue: data not statistically significant but with alpha close to significance (0.05 < alpha < 0.10).
[A] Units: number of synapses per 100 μm of perykarya.

Table S2.

Body composition and blood analysis in Agrp-Sirt1 KO mice and their littermate controls fed an AL or a CR diet for at least 10 months.

	Controls		Agrp-Sirt1 KO		2-way ANOVA		
	AL	CR	AL	CR	Genotype	Diet	Interaction
Body composition:	**(n = 9)**	**(n = 8)**	**(n = 9)**	**(n = 6)**			
Body weight (g)	29.76 ± 1.14	20.81 ± 1.26	27.22 ± 1.14	18.54 ± 0.51	$F_{(1,28)} = 4.391$, $p = 0.045$	$F_{(1,28)} = 59.18$, $p < 0.001$	$F_{(1,28)} = 0.013$, $p = 0.907$
Lean mass (g)	20.52 ± 0.55	15.42 ± 0.77	19.55 ± 0.57	14.13 ± 0.29	$F_{(1,28)} = 3.407$, $p = 0.075$	$F_{(1,28)} = 74.06$, $p < 0.001$	$F_{(1,28)} = 0.071$, $p = 0.791$
Fat mass (g)	5.40 ± 0.58	2.23 ± 0.45	4.25 ± 0.64	1.38 ± 0.09	$F_{(1,28)} = 3.287$, $p = 0.080$	$F_{(1,28)} = 29.88$, $p < 0.001$	$F_{(1,28)} = 0.076$, $p = 0.784$
% Fat	17.78 ± 1.43	10.24 ± 1.23	15.07 ± 1.70	7.43 ± 0.34	$F_{(1,28)} = 3.723$, $p = 0.063$	$F_{(1,28)} = 28.11$, $p < 0.001$	$F_{(1,28)} = 0.001$, $p = 0.973$
Blood Analysis:	**(n = 8-9)**	**(n = 6-7)**	**(n = 9)**	**(n =5-6)**			
NEFA (mEq/L)	0.768 ± 0.040	0.927 ± 0.164	0.696 ± 0.031	0.978 ± 0.226	$F_{(1,27)} = 0.007$, $p = 0.930$	$F_{(1,27)} = 3.479$, $p = 0.073$	$F_{(1,27)} = 0.276$, $p = 0.603$
Total Cholesterol	156.42 ± 9.24	107.89 ± 7.62	142.56 ± 5.60	111.69 ± 13.60	$F_{(1,27)} = 0.313$, $p = 0.580$	$F_{(1,27)} = 19.52$, $p < 0.001$	$F_{(1,27)} = 0.964$, $p = 0.334$
Tryglicerydes (mg/dl)	133.79 ± 32.22	17.04 ± 8.68	85.70 ± 17.96	21.59 ± 6.28	$F_{(1,27)} = 0.940$, $p = 0.340$	$F_{(1,27)} = 16.22$, $p < 0.001$	$F_{(1,27)} = 1.375$, $p = 0.251$

Notes:

In red: data statistically significant (alpha < 0.05).

In blue: data not statistically significant but with alpha close to significance (0.05 < alpha < 0.10).

Capítulo VIII. AgRP neurons regulate the development of dopamine neuronal plasticity and non food-associated behaviors

Artigo submetido ao periódico *Nature Neuroscience*.

AgRP neurons regulate the development of dopamine neuronal plasticity and non food-associated behaviors

Marcelo O. Dietrich[1,6], Jeremy Bober[1], Jozélia G. Ferreira[4,5], Luis A. Tellez[4,5], Yann Mineur[4], Ivan Araújo[4,5], Marina Picciotto[4], Zhong-Wu Liu[1] and Tamas L. Horvath[1,2,3]

[1]Program in Integrative Cell Signaling and Neurobiology of Metabolism, Section of Comparative Medicine and Departments of [2]Obstetrics, Gynecology and Reproductive Sciences, [3]Neurobiology and [4]Psychiatry, Yale University School of Medicine, New Haven CT 06520, USA. [5]The John B. Pierce Laboratory, New Haven CT 06520, USA. [6]Department of Biochemistry, Universidade Federal do Rio Grande do Sul, Porto Alegre RS 90035, Brazil.

Correspondence and requests for materials should be addressed to T.L.H. (tamas.horvath@yale.edu).

Abstract

It is not known whether motivational behaviors not related to feeding are affected by primary regulators of energy balance located in the hypothalamus. Here we show that impairment of AgRP neuronal function by knockdown of Sirt1, a NAD+-dependent deacetylase, increases exploratory behavior of mice unrelated to feeding. Behavioral responses to cocaine, were also altered in these transgenic mice. As a neurobiological substrate of these altered behaviors, in Agrp-Sirt1 KO mice, ventral tegmental (VTA) dopamine (DA) neurons, which targeted by AgRP efferents, exhibited enhanced spike-timing-dependent long-term potentiation (STD-LTP), decreased amplitude of mIPSCs, and increased DA levels in basal forebrain. Early postnatal ablation of AgRP neurons led to a phenotype resembling that of Agrp-Sirt1 KO mice, with enhanced LTP in VTA-DA cells and altered response to novelty. These observations reveal a fundamental regulatory role of AgRP neurons in determining the set point of the DA reward circuitry and associated behaviors during development.

Hypothalamic neurons that co-produce neuropeptide Y (NPY), Agouti-related protein (AgRP) and GABA[1] are fundamental for eliciting feeding behavior[2-4]: when these hypothalamic neurons are selectively ablated in adult mice, feeding behavior is diminished[2-4], and unless artificially fed, these animals die[2, 4, 5]. On the other hand, the selective activation of these neurons using optogenetic[6] or DREAD[7] technologies led to a robust acute increase in feeding. The critical role of the AgRP neurons in maintenance of life[2, 4, 5] gave us the impetus to test whether, beyond feeding, these hypothalamic neurons also coordinate other complex motivated behaviors.

We analyzed behavioral responses of mice in which AgRP neuronal excitability is selectively altered[8]. We have shown that cell autonomous deletion of Sirt1, a NAD+-dependent deacetylase, rendered AgRP cells less responsive to peripheral metabolic signals and that these transgenic mice developed a mild metabolic phenotype, resembling that of a low AgRP neuronal function[8]. Sirt1 functions as a metabolic sensor within the cell, and is up-regulated during states of negative energy balance[9, 10], when AgRP neurons are also active. We showed that Sirt1 expression in AgRP neurons plays a role in the appropriate adaptation of these neurons and their efferents to cues of negative energy balance[8].

To address the effects of impaired AgRP neuronal function on motivated behaviors other than feeding, we first analyzed the behavior of Agrp-Sirt1 KO mice and their control littermates in an open-field test. This analysis addresses exploratory behavior in a novel environment[11, 12]. Agrp-Sirt1 KO mice exhibited increased activity compared to littermate controls during both exploratory and novelty stages (Fig.1a,b – Supplementary Fig. 1), a result consistent with previous studies on the effect of AgRP on locomotion[13]. During the exploratory phase, no differences were observed in time spent in the center of the open-field (Fig.1c). However, in the novelty stage, Agrp-Sirt1 KO mice explored the novel object significantly more than their littermate controls (Fig.1c). Next, we tested another cohort of

mice in a different open-field during 60 minutes, and we observed similar results with increased activity in the Agrp-Sirt1 KO mice (Fig.1d). These findings were not due to differences in motor coordination/skills (Supplementary Fig. 2) or due to altered level of anxiety (Supplementary Fig. 3). Moreover, intrinsic differences in leptin levels, adiposity and body weight did not seem to directly account for this phenotype either (Supplementary Table 1, Supplementary Fig. 4 and 5).

Motivation to explore a novel environment/object relies, at least in part, on the activity of the midbrain dopamine system. This dopaminergic system is also a critical regulator of other motivated behaviors not related to food, for example, responses to drugs of abuse. To further interrogate the effect of lower AgRP neuronal excitability on non-food related behaviors, we tested the responses of Agrp-Sirt1 KO and control mice to cocaine. First, we analyzed locomotor responses of these animals to cocaine. Agrp-Sirt1 KO mice showed increased response to cocaine, with the greatest differences appearing upon administration of larger doses (Fig.1e and Supplementary Fig. 6). Next, we tested the response of Agrp-Sirt1 KO mice to cocaine sensitization. After sensitization of control and Agrp-Sirt1 KO to cocaine (Supplementary Fig. 7 - see Methods for details), all mice were challenged with saline and cocaine to test for contextual and drug sensitization, respectively. Agrp-Sirt1 KO mice had elevated cocaine sensitization responses compared to controls (Fig.1f).

Increased sensitization of locomotor activity in response to cocaine does not confirm an increase in motivation in the Agrp-Sirt1 KO mice. To address motivational aspects of cocaine exposure, we tested the mice in a conditioned place preference test (CPP). While both control and Agrp-Sirt1 KO animals developed a preference for cocaine, Agrp-Sirt1 KO mice showed a significantly increased preference for cocaine compared to control mice (Fig.1g). Taken together, the results above show that impaired AgRP neuronal excitability

results in increased levels of motivational behaviors unrelated to feeding, and that these behavioral adaptations may be supported by increased sensitivity of the midbrain dopamine neurons.

Intriguingly, it has been shown that AgRP fibers innervate the VTA[14, 15]. Using the *Agrp-Cre:R26-LSL-tdTomato* reporter mice (Supplementary Fig. 8) and immunohistochemistry, we confirmed moderate innervation of the VTA by AgRP fibers in adult mice (Supplementary Fig. 9 and 10), suggesting that AgRP neurons may exert a direct influence on VTA dopamine neurons.

To address whether intrinsic differences exist in VTA dopamine neurons between control and Agrp-Sirt1 KO animals, first we evaluated the synaptic input organization of the VTA DA cells using patch clamp analysis of mPSCs. While we found no differences in the frequency of mIPSCs and mEPSCs (data not shown), there was a marked decrease in the average peak amplitude of mIPSCs (Fig.2a insert) with no statistical changes in the average peak amplitude of mEPSCs (Fig.2b insert). When analyzing the probability distribution of the amplitude of mPSCs, we found an increased probability of lower amplitudes in the mIPSCs (Fig.2a), with marginal increases in the probability of events of higher amplitude for mEPSCs (Fig.2b). We then revealed that GABA, the neurotransmitter present in AgRP neurons[1], but not melanocortin signaling contributed to these changes in the mIPSCs. First we showed that bicuculline, a GABA antagonist, abolished the synaptic responses in both control and Agrp-Sirt1 KO mice (Supplementary Fig. 11). On the other hand, when we recorded mIPSCs in the presence of the melanocortin receptor agonist, MT-II, or the melanocortin receptor antagonist, SHU9119, we did not observe any statistical changes in the frequency (Fig.2c) or amplitude (not shown) of mini-events in the VTA DA neurons. These latter data are in agreement with a previous report that showed lack of effect of AgRP in triggering electric responses of VTA dopamine cells[16]. Utilizing electron microscopy, we

further assessed the synaptic input organization of the dopamine neurons in the VTA of control and Agrp-Sirt1 KO mice. We found no differences in synaptic number (Supplementary Table 2) arguing that it is the efficacy of synaptic transmission that is changed, a notion that is consistent with lower excitability of AgRP neurons in Agrp-Sirt1 KO mice[8]. Together, these data indicate that due to a lower inhibitory tone, there may be an increased excitability of the VTA DA cells in the Agrp-Sirt1 KO mice in response to stimuli. To test that, next, we analyzed a form of synaptic plasticity, long-term potentiation (LTP) induced by a spike-timing dependent protocol (STD-LTP). Neurons recorded from control mice did not display LTP, while VTA DA neurons of AgRP-Sirt1 KO mice had enhanced LTP induction (Fig.2d). Corroborating the behavioral and electrophysiological data, dopamine levels in the basal forebrain, a target site of the midbrain dopamine system, was more than 3 times higher in Agrp-Sirt1 KO mice compared to littermate controls (Fig.2e).

The GENSTAT database revealed that AgRP fibers innervate the VTA more robustly during the first postnatal week compared to adult age (Supplementary Fig. 12). This information suggests that AgRP neurons may exert an organizational effect on VTA dopamine neurons during development, in addition to a direct effect in the adult mice. To test for developmental changes in synaptic plasticity in the VTA dopamine cells, we elicited LTP in these neurons at different ages in control and Agrp-Sirt1 KO mice in the presence of $GABA_A$ blocker, which is known to facilitate LTP in the VTA DA cells[17]. A mild induction of LTP was observed in neurons from control mice at 30 and 45 days old, but not in 15 days old mice (Fig.3a-d). More strikingly, in the Agrp-Sirt1 KO mice a robust increased in the amplitude of EPSCs after STD-LTP protocol was observed in all ages tested (Fig.3a-d). These results indicate that AgRP neurons influence the development of the VTA dopamine cells from early postnatal age. To further examine the effect of the AgRP neurons on VTA dopamine cell development, we used transgenic mice that express diphtheria toxin receptor

under the control of the AgRP promoter[2]. We hypothesized that if the AgRP neurons were important to the development of the VTA dopamine cells, ablation of the AgRP neurons during the early postnatal age would mimic the findings in the Agrp-Sirt1 KO mice. We injected transgenic and wild type controls with diphtheria toxin at postnatal day 5 (P5), and analyzed synaptic plasticity and behavioral responses later in development (Fig.3e). While we observed only a modest (not statistically significant) increase in the LTP in control cells, there was a marked facilitation in the induction of LTP in the VTA dopamine cells from AgRP ablated mice (Fig.3f). Finally, we aimed to test if ablating the AgRP neuron in the early postnatal age could lead to behavioral changes in the adult. We tested control and AgRP ablated mice in the open-field with novelty stage. During exploratory stage, control and AgRP ablated mice did not differ in their activity and time spent in the center of the open-field (Fig.3g-i and Supplementary Fig. 13). These data are in agreement with no changes in the home cage activity between control and AgRP ablated mice (Supplementary Figure 14). However, during the novelty stage of the open-field test, the AgRP ablated mice had increased activity and time exploring the new object (Fig.3g-i and Supplementary Fig. 13), revealing an increased motivational behavior to explore novelty. Noteworthy, however, the AgRP ablated mice had normal food intake (Supplementary Fig.14) demonstrating that these mice compensate for the lack of AgRP neurons regarding feeding. In contrast, female Agrp-Sirt1 KO mice have decreased food intake[8] reinforcing the critical role of the AgRP neurons in setting midbrain dopaminergic tone despite of metabolic adaptations.

In summary, the above results unmasked a previously unsuspected role of hypothalamic hunger-promoting neurons in setting midbrain dopamine neuronal function and associated behaviors. Our data also provide evidence for an inverse relationship between hypothalamus-driven motivated behaviors that relate to feeding and those driven by the

reward circuitry that do not relate to energy metabolism. These observations are of relevance because the reward circuitry and associated behaviors have been emphasized as possible contributors to obesity. The data presented here reveals a critical role for the AgRP neurons in regulating VTA dopamine circuitry during development. This as well as other possible indirect routes of communication between AgRP and VTA needs further investigation.

Acknowledgements

We thank Marya Shanabrough, Catiele Antunes and Melissa Taylor for assistance, and Yun You for helping with animal management. We also thank Patricia Cirillo and Nicole Dangelo for technical support with the animal colony. We are thankful to Vanessa Kazlauckas for discussing the behavioral experiments. We thank Esther de la Fuente for the leptin assay. A special thank to Laura Kus from the GENSTAT Project that provided important information on the Agrp-EGFP mouse (MT25). We thank Allison Xu for providing breeding pairs of Agrp-Cre mice. We thank Richard Palmiter for providing breeding pairs of the Agrp-DTR mice. This work was supported by an NIH Director's Pioneer Award to TLH. MP was supported by NIH grants. IEA was supported by NIDCD (NIH) grants. MOD was partially supported by Conselho Nacional de Desenvolvimento Científico e Tecnológico (CNPq-Brazil).

Author contributions

M.O.D. designed, executed, collected, and analyzed all the data (except executing the electrophysiology experiments). Z.W.L. designed, executed and analyzed the electrophysiology experiments. J.B. help to design and execute the experiments that involved dopamine measurements and immunohistochemistry, and with animal

maintenance/genotyping. Y.M. helped with the CPP experiment. M.P. helped to design and discuss the experiments and results of the cocaine experiments. J.F. and L.T. helped in the microdialysis experiment. I.A. designed, discussed and helped analyzing the dopamine measurement experiment. T.L.H. designed and analyzed the experiments. M.O.D. and T.L.H. wrote the manuscript.

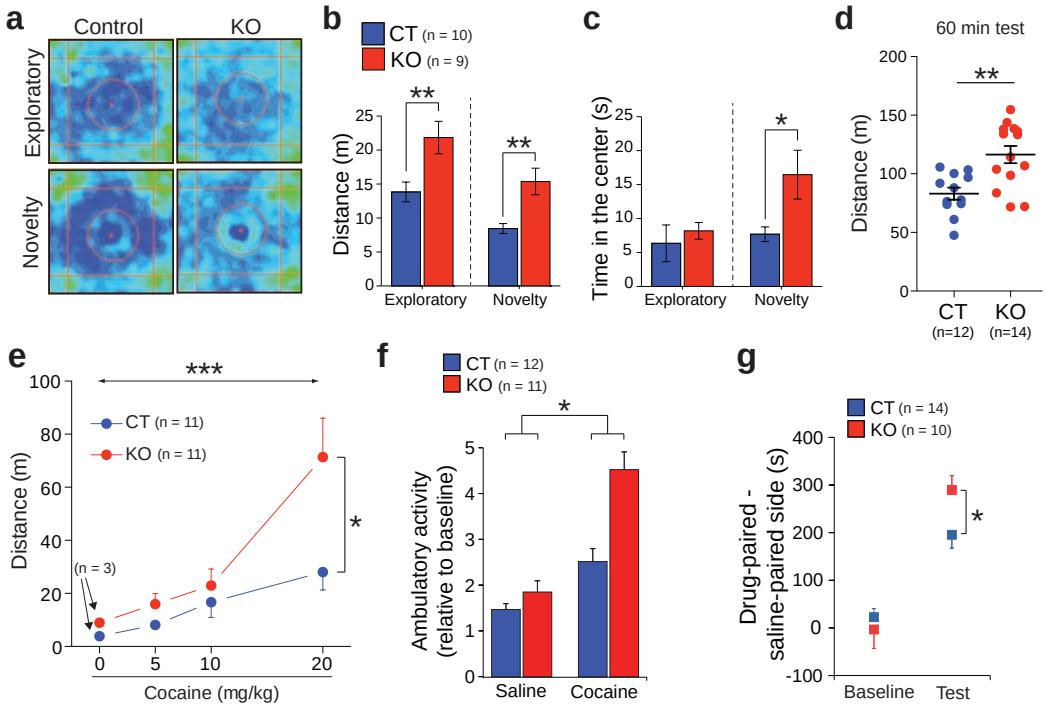
a
Control
KO
Exploratory
Novelty
b
CT (n = 10)
KO (n = 9)
Distance (m)
Exploratory
Novelty
c
Time in the center (s)
Exploratory
Novelty
d
60 min test
Distance (m)
CT
(n=12)
KO
(n=14)
e
CT (n = 11)
KO (n = 11)
Distance (m)
(n = 3)
Cocaine (mg/kg)
f
CT (n = 12)
KO (n = 11)
Ambulatory activity
(relative to baseline)
Saline
Cocaine
g
CT (n = 14)
KO (n = 10)
Drug-paired -
saline-paired side (s)
Baseline
Test

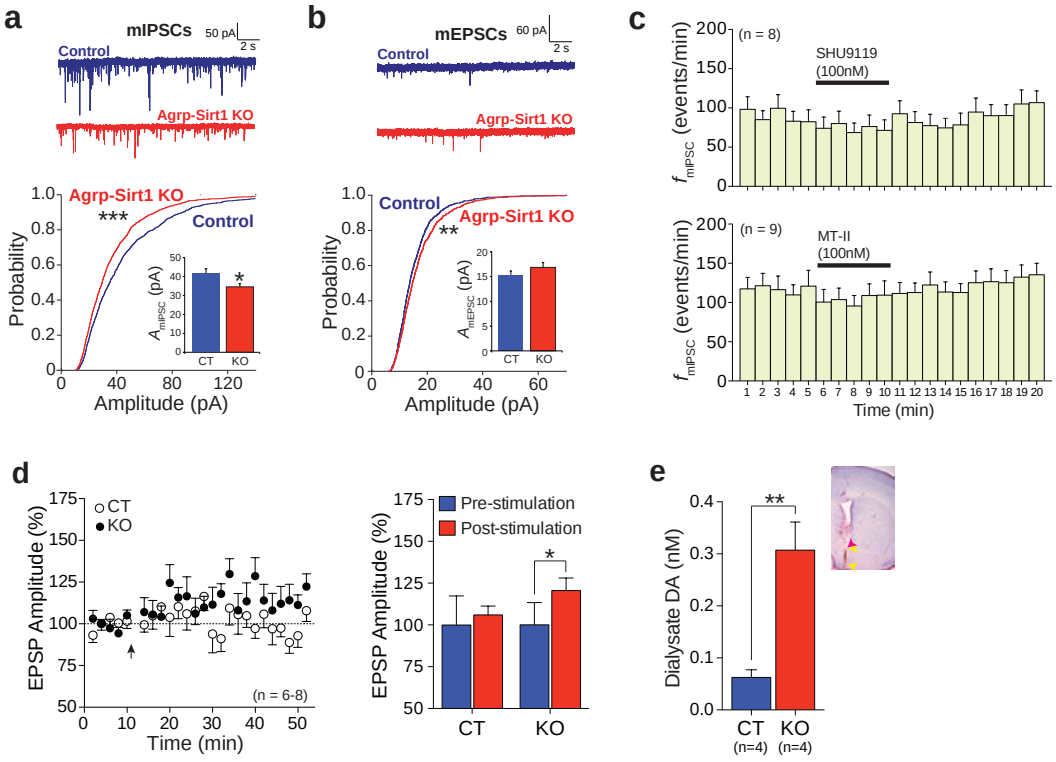
a
mIPSCs
50 pA
2 s
Control
Agrp-Sirt1 KO
Agrp-Sirt1 KO
Control
***
Probability
Amplitude (pA)
CT
KO
b
mEPSCs
60 pA
2 s
Control
Agrp-Sirt1 KO
Control
Agrp-Sirt1 KO
**
Probability
Amplitude (pA)
CT
KO
c
(n = 8)
SHU9119
(100nM)
(events/min)
(n = 9)
MT-II
(100nM)
(events/min)
Time (min)
d
CT
KO
EPSP Amplitude (%)
(n = 6-8)
Time (min)
Pre-stimulation
Post-stimulation
EPSP Amplitude (%)
CT
KO
e
Dialysate DA (nM)
CT
KO
(n=4)
(n=4)

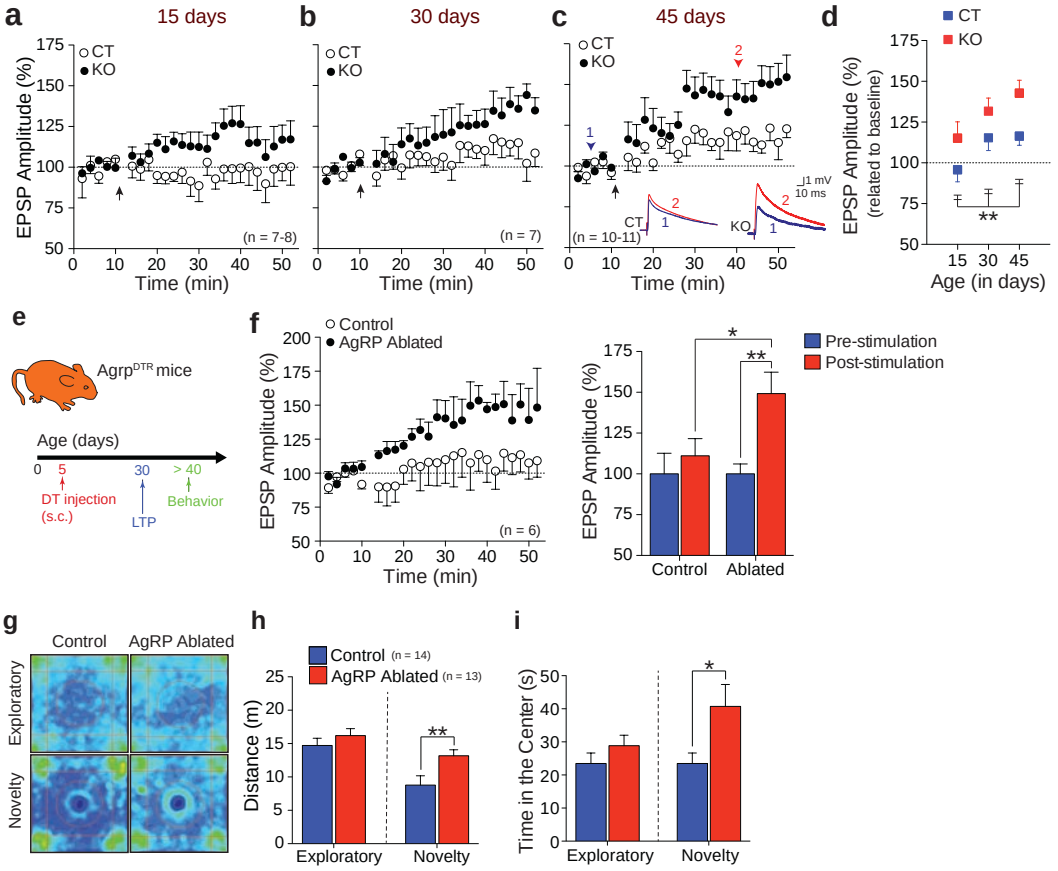
a
15 days
b
30 days
c
45 days
d
CT
KO
EPSP Amplitude (%)
Time (min)
(n = 7-8)
(n = 7)
(n = 10-11)
1 mV
10 ms
EPSP Amplitude (%)
(related to baseline)
Age (in days)
**
e
Agrp^DTR mice
Age (days)
0
5
30
> 40
DT injection
(s.c.)
LTP
Behavior
f
Control
AgRP Ablated
(n = 6)
Pre-stimulation
Post-stimulation
*
**
Control
Ablated
g
Control
AgRP Ablated
Exploratory
Novelty
h
Control (n = 14)
AgRP Ablated (n = 13)
Distance (m)
Exploratory
Novelty
i
Time in the Center (s)
Exploratory
Novelty

Figure Legends

Figure 1

AgRP neurons determine the behavioral response to novelty and cocaine. A two-stage open-field exploratory test was used to study motivational behavior in control and Agrp-Sirt1 KO mice. Animals were allowed to explore a novel environment without (exploratory stage) and with an object (novelty stage) in the center of the box as a novel stimulus. Generally, animals spend most of their time in the corner of the open-field, moving primarily close to the walls, while they explore, to a lesser extent, the center. (**a**) Occupancy plots of the averaged position of the head of the group during both exploratory (no object) and novelty (novel object in the center) stages. (**b**) Agrp-Sirt1 KO mice show increased exploratory activity in the open-field during both exploratory ($F_{(1, 17)} = 8.566$, $P = 0.009$) and novelty stages ($U = 11.00$, $P = 0.004$). (**c**) In the exploratory phase, Agrp-Sirt1 KO mice spent similar time in the center of the arena ($F_{(1, 17)} = 2.435$, $P = 0.137$); when a new object was inserted in the middle of the field as a stimulus, Agrp-Sirt1 KO mice spent more time exploring the new object compared to control mice ($U = 18.00$, $P = 0.028$). (**d**) The increased activity of Agrp-Sirt1 KO mice in the open-field last for at least 60 minutes, as shown in different cohort of mice ($t_{24} = 3.604$, $P = 0.001$). To test the behavioral response of Agrp-Sirt1 KO and control mice to cocaine, we first tested the response of the animals to an acute injection of cocaine. (**e**) Agrp-Sirt1 KO mice displayed increased locomotor response to cocaine (dose: $F_{(3,64)} = 10.85$, $P < 0.001$; genotype: $F_{(1,64)} = 5.304$, $P = 0.024$; interaction: $F_{(3,64)} = 2.793$, $P = 0.047$). (**f**) Agrp-Sirt1 KO mice showed stronger sensitization response to cocaine compared to their littermate controls (challenge: $F_{(1, 21)} = 58.155$, $P < 0.001$; genotype: $F_{(1, 21)} = 3.373$, $P = 0.080$; interaction: $F_{(1, 21)} = 5.386$, $P = 0.030$). (**g**) Another group of mice were tested in a conditional place preference task, with saline injected in one

side chamber and cocaine in the other. While both control (χ^2 = 10.286, P = 0.001) and Agrp-Sirt1 KO mice (χ^2 = 10.000, P = 0.002) showed strong preference for the cocaine chamber in the test day (0 indicates no preference), Agrp-Sirt1 KO mice had increased response compared to control mice (baseline: U = 53.50, P = 0.334; test: U = 106.00, P = 0.017 (1-tail)). * P < 0.05, ** P < 0.01, and *** P < 0.001. Bars and symbols represent mean ± s.e.m.

Figure 2

AgRP neuronal excitability determines synaptic plasticity of VTA dopamine neurons. VTA dopamine neurons were identified by a characteristic large I_h current in midbrain horizontal slices. (**a**) Representative traces, probability plot and average peak amplitude (insert) show marked decrease in the amplitude of mIPSCs in the DA cells from Agrp-Sirt1 KO mice compared to littermate controls (k = 0.125, P < 0.001 (probability plot); t_{64} = 2.499, P = 0.015 (insert); n = 33 cells/group). (**b**) Representative traces, probability plot and average peak amplitude (insert) show increase in the probability distribution of mEPSCs of higher amplitude in the DA cells from Agrp-Sirt1 KO mice compared to littermate controls (k = 0.079, P < 0.01; n = 28-29 cells/group). (**c**) The melanocortin agonist (MT-II, 100 nM) and the antagonist (SHU9119, 100 nM) did not change the frequency of mIPSCs in the VTA DA neurons. STD-LTP protocol was applied to 45 days old control and Agrp-Sirt1 KO mice. The evoked postsynaptic currents (EPSCs) were monitored using whole-cell recordings of the VTA DA cells at -60 mV, and an extracellular stimulation was applied to the rostral region of the VTA. (**d**) LTP was not induced in control cells (106 ± 5.3%) but was evident in VTA DA neurons from Agrp-Sirt1 KO mice (120.6 ± 7.5%, t_6 = 2.765, P = 0.016). Arrow indicates when the STD-LTP stimulation was applied. (**e**) Microdialysis measurements of extracellular dopamine in basal forebrain of control and Agrp-Sirt1 KO mice show a marked increased in

dopamine levels in transgenic mice (t_6 = 4.353, P = 0.004). *Insert*, histology showing representative location of a probe. Yellow arrowheads delineate the probe's location; pink arrowhead points the tip of the guide cannula. * P < 0.05, ** P < 0.01, *** P < 0.001. Bars and symbols represent mean ± s.e.m.

Figure 3

AgRP neurons influence the development of synaptic characteristics of VTA dopamine neurons and the behavioral response to novelty. In the presence of a $GABA_A$ blocker, STD-LTP protocol was applied to (**a**) 15 days old, (**b**) 30 days old, and (**c**) 45 days old control and Agrp-Sirt1 KO mice. (**d**) Agrp-Sirt1 KO mice displayed enhanced LTP facilitation compared to control mice, as early as 15 days of age (time: $F_{(2,44)}$ = 5.091, P = 0.01; genotype: $F_{(1,44)}$ = 10.04, P = 0.002). (**e**) To test for a direct impact of AgRP neuronal function on the development of synaptic plasticity in the VTA DA cells and behavioral changes in the adult mice, we ablated the AgRP neurons using diphtheria toxin injection in transgenic mice that ectopically express the diphtheria toxin receptor in the AgRP neurons[2]. (**f**) In 30 days old mice, STD-LTP protocol was applied in the VTA DA cells; while no statistically significant increase in LTP was observed in control mice (111.1 ± 10.4%), there was a significant facilitation of LTP in the AgRP ablated mice (baseline: 100.0 ± 6.1%, STD-LTP: 149.2 ± 13.1%; t_{10} = 3.399, P = 0.003 – 1-tail). In (**a-c, f**), arrows indicate the time of stimulation (STD-LTP). In (**c**), arrowheads indicate the time where representative episodes are illustrated. Blue arrowheads indicate a time before the stimulation, and red arrowheads after stimulation (LTP). Control and AgRP ablated mice were tested in the open-field to examine their behavioral response to novelty. While no statistically significant differences were observed in the (**h**) distance and (**i**) time spend in the center of the open-field during the exploratory stage, AgRP ablated mice had (**h**) increased activity (t_{25} = 2.591, P = 0.007 – 2-

tail) and (**i**) increased time exploring the new object (t_{25} = 2.393, P = 0.012 – 2-tail) when compared to littermate controls during the novelty stage. * P < 0.05, ** P < 0.01. Bars and symbols represent mean ± s.e.m.

References

1. Horvath, T.L., Bechmann, I., Naftolin, F., Kalra, S.P. & Leranth, C. *Brain Research* **756**, 283-286 (1997).

2. Luquet, S., Perez, F., Hnasko, T. & Palmiter, R. *Science* **310**, 683-685 (2005).

3. Gropp, E., *et al. Nature Neuroscience* **8**, 1289-1291 (2005).

4. Wu, Q., Boyle, M. & Palmiter, R. *Cell* **137**, 1225-1234 (2009).

5. Dietrich, M.O. & Horvath, T.L. *Cell* **137**, 1177-1179 (2009).

6. Aponte, Y., Atasoy, D. & Sternson, S.M. *Nature neuroscience* **14**, 351-355 (2011).

7. Krashes, M.J., *et al. The Journal of Clinical Investigation* **121**, 1424-1428 (2011).

8. Dietrich, M., *et al. J Neurosci* **30**, 11815-11825 (2010).

9. Cohen, H., *et al. Science* **305**, 390-392 (2004).

10. Liu, Y., *et al. Nature* **456**, 269-273 (2008).

11. Dulawa, S.C., Grandy, D.K., Low, M.J., Paulus, M.P. & Geyer, M.A. *J Neurosci* **19**, 9550-9556 (1999).

12. Kazlauckas, V., *et al. Behav Brain Res* **162**, 272-278 (2005).

13. Tang-Christensen, M., *et al. Endocrinology* **145**, 4645-4652 (2004).

14. Broberger, C., Johansen, J., Johansson, C., Schalling, M. & Hokfelt, T. *P Natl Acad Sci USA* **95**, 15043-15048 (1998).

15. Wu, Q., Howell, M.P. & Palmiter, R.D. *Journal of Neuroscience* **28**, 9218-9226 (2008).

16. Korotkova, T.M., Brown, R.E., Sergeeva, O.A., Ponomarenko, A.A. & Haas, H.L. *Eur J Neurosci* **23**, 2677-2685 (2006).

17. Liu, Q., Pu, L. & Poo, M. *Nature* **437**, 1027-1031 (2005).

AgRP neurons regulate the development of dopamine neuronal plasticity and non food-associated behaviors

Marcelo O. Dietrich[1,6], Jeremy Bober[1], Jozélia G. Ferreira[4,5], Luis A. Tellez[4,5], Yann Mineur[4], Ivan Araújo[4,5], Marina Picciotto[4], Zhong-Wu Liu[1] and Tamas L. Horvath[1,2,3]

[1]Program in Integrative Cell Signaling and Neurobiology of Metabolism, Section of Comparative Medicine and Departments of [2]Obstetrics, Gynecology and Reproductive Sciences, [3]Neurobiology and [4]Psychiatry, Yale University School of Medicine, New Haven CT 06520, USA. [5]The John B. Pierce Laboratory, New Haven CT 06520, USA. [6]Department of Biochemistry, Universidade Federal do Rio Grande do Sul, Porto Alegre RS 90035, Brazil.

Correspondence and requests for materials should be addressed to T.L.H. (tamas.horvath@yale.edu).

Supplementary Figures 1-14.

Supplementary Tables 1-2.

Supplementary Methods.

Supplementary References.

Supplementary Figure 1:

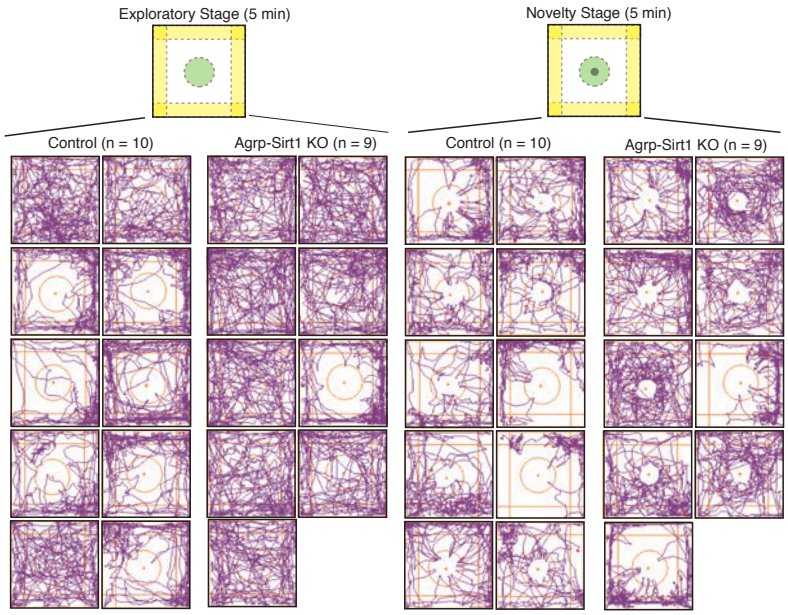

Individual tracks illustrating the behavior of Agrp-Sirt1 KO and littermate control mice in the open-field test. A total of 10 littermate controls and 9 Agrp-Sirt1 KO female mice were used in the experiment. *Left*, mice were allowed to explore an open-field for 5 minutes, and were returned to the home cage for 2 minutes for an inter-test interval. *Right*, mice were then re-tested in the open-field containing a new object in the middle of the box as a new stimulus to induce exploration (exploratory stage - 5 minutes). The red dot represents the position of the mouse when the recording ended.

Supplementary Figure 2:

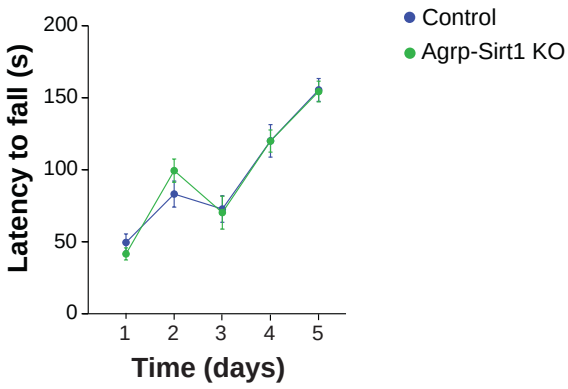

Rota-rod performance of control (n = 12) and Agrp-Sirt1 KO (n = 12) female mice. Both groups of mice presented similar latency to fall off the rota-rod and similar learning curves during the 5 days of experiments (ε = 0.603; time: $F_{(2.412, 53.064)} = 55.847$, $P < 0.001$; time x genotype: $F_{(2.412, 53.064)} = 0.555$, $P = 0.610$; genotype: $F_{(1, 22)} = 0.004$, $P = 0.948$). These data reinforce the changes in activity observed in the Agrp-Sirt1 KO mice and are not related to changes in motor coordination or motor learning skills.

Supplementary Figure 3:

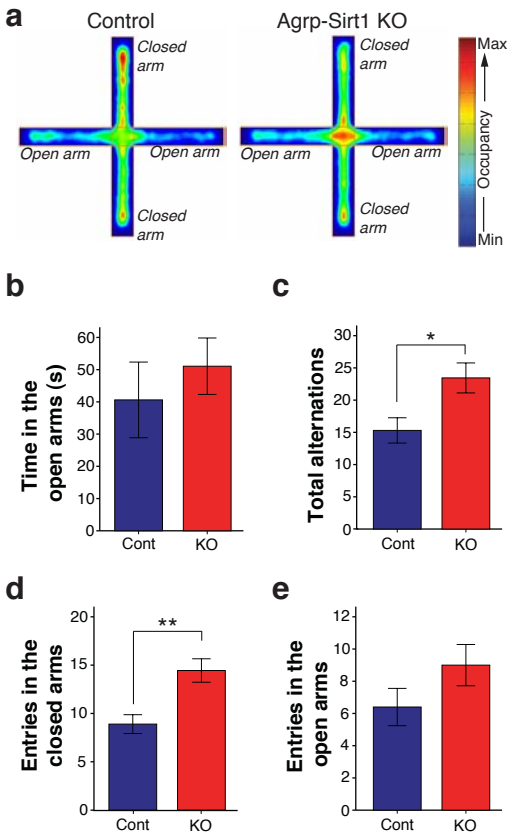

Agrp-Sirt1 KO mice did not display changes in anxiety in the plus-maze test. (**a**) Occupancy plots of the averaged position of the body of littermate controls (left) and Agrp-Sirt1 KO mice (right) in a plus-maze test. Mice tend to spend the majority of their time in the closed arms and in the center of the apparatus, while making some attempts to explore the open arms. (**b**) The time spent in the open arms was not significantly different between controls and Agrp-Sirt1 KO mice. (**c**) Agrp-Sirt1 KO mice explore the apparatus more as measured by the number of alternations, which was mainly due to alternations in the closed arms (**d**), but not into the open arms (**e**). * $P < 0.05$, ** $P < 0.01$. Control (n = 10) and Agrp-Sirt1 KO (n = 9). Bars represent mean ± s.e.m.

Supplementary Figure 4:

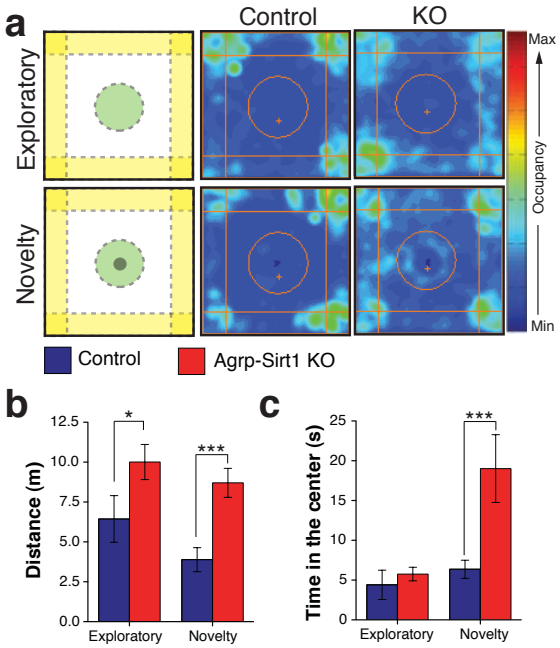

Leptin replacement did not revert the response of Agrp-Sirt1 KO mice to novelty. The altered excitability of the Agrp neurons in the Agrp-Sirt1 KO mice leads to decreased adiposity[1], and an expected decrease in blood leptin levels (Supplementary Table 1). Leptin has been shown to directly modulate the VTA dopamine neuronal activity, and locomotor activity in mice[2, 3]. Thus, one possibility is that the decreased leptin levels in the Agrp-Sirt1 KO mice could lead to the behavioral alterations in the response of these mice to novelty. We replaced leptin in the Agrp-Sirt1 KO mice, and we found no changes in the behavioral response to novelty. The same mice tested in Figure 1 (main text), were re-tested in the open-field after an injection of leptin (5 mg/kg, i.p.). (**a**) Occupancy plots of the average position of the head for each group during both exploratory (no object) and novelty (novel object in the center) stages. (**b**) Agrp-Sirt1 KO mice show increased exploratory activity in the open-field, and (**c**) spent more time in the center of the arena when the object was inserted as a stimulus. * $P < 0.05$, *** $P < 0.001$. Control (n = 10) and Agrp-Sirt1 KO (n = 9). Bars represent mean ± s.e.m.

Supplementary Figure 5:

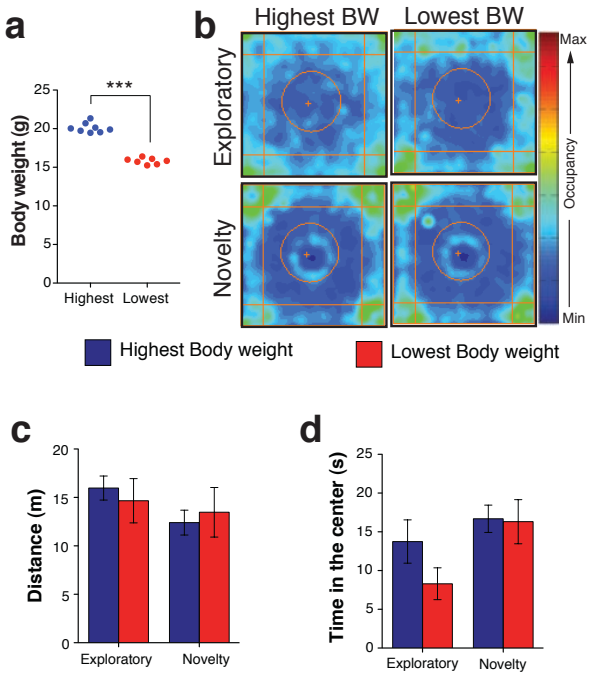

Mice selected to show natural differences in body weight have similar response to novelty in the open-field test. We selected mice with high and low body weights from a pool of 40 random C57B6/J female mice, to test whether the differences in body weight and adiposity between control and Agrp-Sirt1 KO mice could be mimicked in mice that show natural differences in body mass. (**a**) Differences in body weight between the two groups. (**b**) Occupancy plots of the average position of the head for each group during both exploratory (no object) and novelty (novel object in the center) stages. (**c**) No differences were observed between the two groups in the exploratory activity in the open-field, and (**d**) in the time spent in the center of the arena. *** $P < 0.001$. Lowest BW (n = 7) and Highest BW (n = 8). Bars represent mean ± s.e.m.

Supplementary Figure 6:

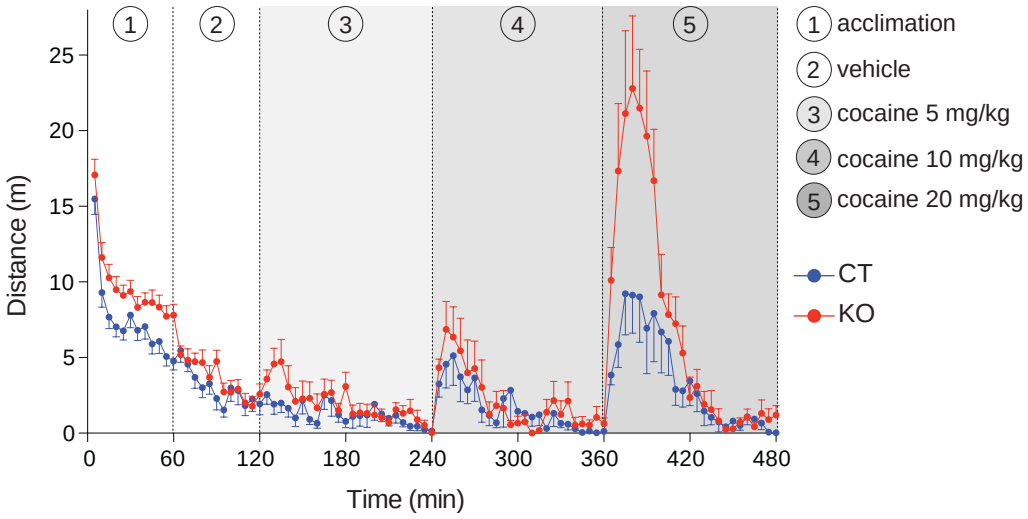

Locomotor activity in an open-field, and cocaine dose-response. Control and Agrp-Sirt1 KO mice were allowed to explore a novel environment for 60 minutes before receiving an injection of vehicle (PBS, i.p.). After vehicle treatment, mice were allowed to explore the new environment for 60 minutes before cocaine dose-response. Every 120 minutes thereafter, mice received an injection of cocaine (5, 10 and 20 mg/kg, i.p. – total volume 10 ml/kg) and locomotor activity was recorded using video tracking and data were plotted in 5-min bins.

Supplementary Figure 7:

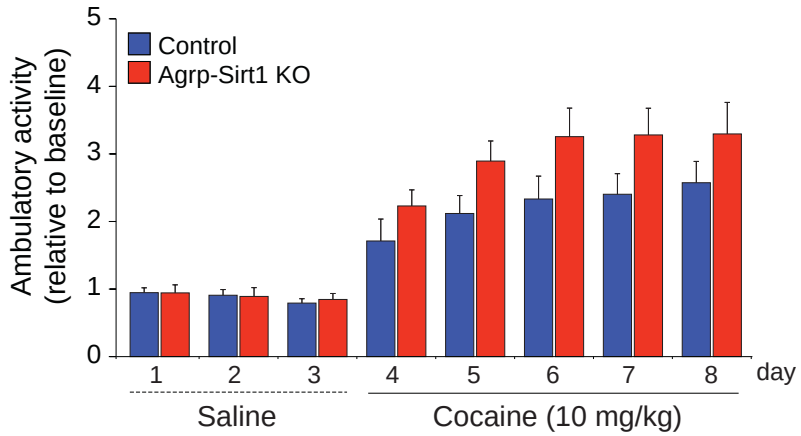

Response of control and Agrp-Sirt1 KO to a cocaine sensitization protocol. Control and Agrp-Sirt1 KO were challenged with saline or cocaine injections to induce locomotor sensitization. Despite a higher baseline activity (day 0 – data no shown), these mice did not show any major differences in their response to saline or cocaine treatments, as measured by relative changes related to baseline activity (day 0). Mice were first acclimated in the locomotor activity chamber for 60 minutes on day 0 (data not shown). On days 1-3, all mice received a saline injection (i.p.) and their activity was recorded for 20 minutes (data are related to individual mouse locomotor activity on day 0 to normalize for differences in baseline activity). There was no difference in the locomotor response to saline acclimation between control and Agrp-Sirt1 KO mice (time: $F_{(2, 42)} = 3.694$, $P = 0.033$; time x genotype: $F_{(2, 42)} = 0.325$, $P = 0.725$; genotype: $F_{(1, 21)} = 0.008$, $P = 0.930$). From days 4-8, mice received one daily injection of cocaine (10 mg/kg, i.p.) to elicit sensitization of their locomotor response. Both control and Agrp-Sirt1 KO mice had a similar response to the cocaine sensitization protocol ($\varepsilon = 0.493$; time: $F_{(1.974, 41.453)} = 11.966$, $p < 0.001$; time x genotype: $F_{(1.974, 41.453)} = 0.490$, $P = 0.613$; genotype: $F_{(1, 21)} = 3.035$, $P = 0.096$). Next, cocaine treatment was withdrawn for 4 days, and all mice were challenged with saline on day 13 and cocaine on day 14 to test for contextual and drug sensitization respectively (see Fig. 1f).

Supplementary Figure 8:

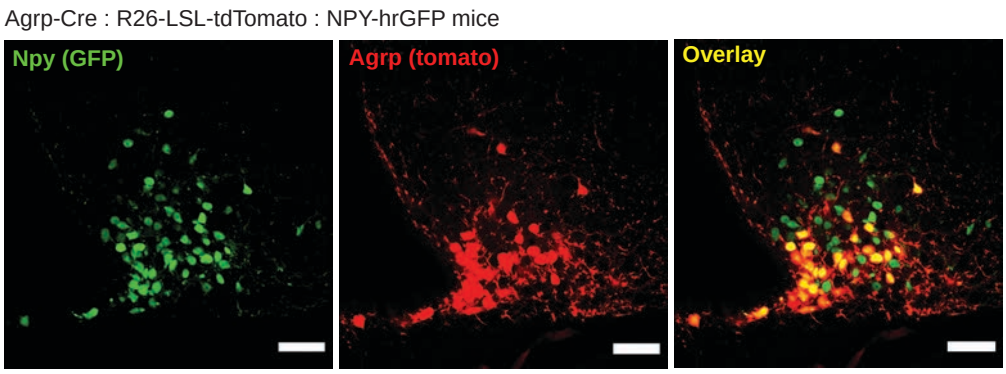

Characterization of Agrp-Cre:R26-LSL-tdTomato:hrNPY-GFP reporter mice. Transgenic mice expressing Cre recombinase in AgRP neurons were crossed with mice carrying the reporter Rosa26-loxP-STOP-loxP-tdTomato allele and the NPY-hrGFP reporter transgene. *Left panel*, GFP fluorescence labeling of NPY neurons in the ARC. *Middle panel*, tdTomato fluorescence labeling of AgRP neurons. *Right panel*, overlay showing in yellow the neurons that co-express NPY/AgRP and a population of neurons that express NPY but do not express AgRP. Scale bars = 50 μm.

Supplementary Figure 9:

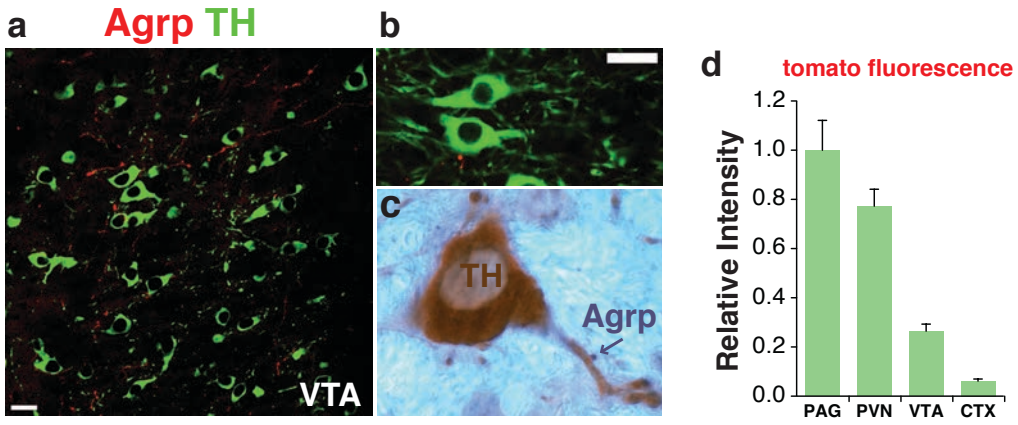

AgRP neurons from the ARC nucleus send weak to moderate projections to the VTA. (**a**) Confocal scan from the VTA of Agrp-Cre:R26-LSL-tdTomato mice, showing AgRP fibers (red) located in the vicinity of the dopamine cells (green – TH immunostaining). (**b**) Close-up showing an AgRP terminal in close proximity to the TH neuron. (**c**) Double-immunohistochemistry showing AgRP terminals (Nickel-DAB – bluish) in close proximity to TH neurons (regular DAB – brownish). (**d**) Quantification of red fluorescence intensity in diverse brain areas of Agrp-Cre:R26-LSL-tdTomato mice. Altogether, the available data suggest that there is a direct innervation of the DA cells in the VTA by AgRP fibers. The moderate innervation of the VTA by AgRP fibers resembles that of orexin/hypocretin innervations of the same brain region[4, 5]. Orexin neurons projecting from the lateral hypothalamus have a major impact on the dopaminergic system within the VTA, and consequent behavior[6, 7]. Unexpectedly, the orexin projecting fibers to the VTA are sparse and synapse infrequently in this area[5]. Thus, even though the AgRP neurons do not project massively to the VTA, it is not unlikely that they promote an important neurobiological effect on this region.

Supplementary Figure 10:

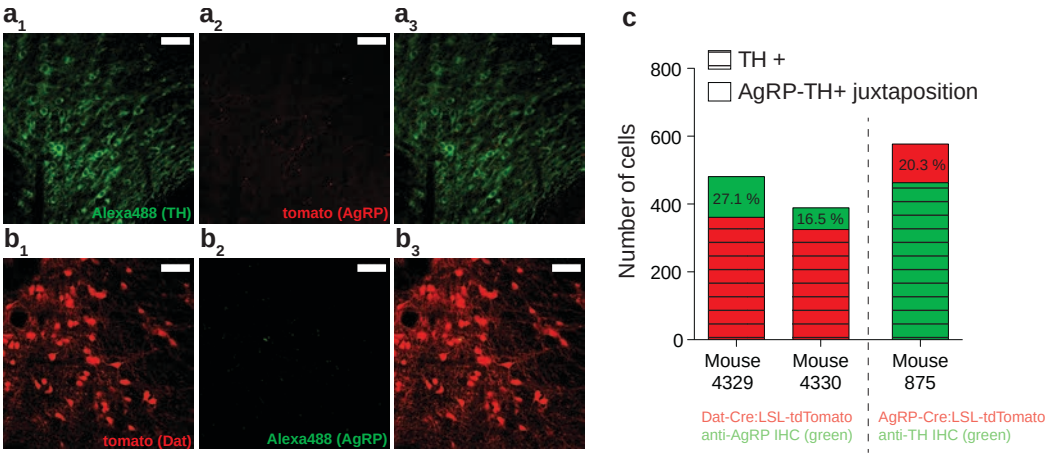

AgRP neuronal fibers from the ARC are juxtaposed to dopamine cells in the VTA. We used Dat-Cre:R26-LSL-tdTomato and Agrp-Cre:R26-LSL-tdTomato combined with IHC to track the interaction of AgRP fibers with dopamine neurons in the VTA. (**a**) Slice containing the VTA of Agrp-Cre:R26-LSL-tdTomato mice stained against TH and labeled with Alexa488 secondary antibody. (**a$_1$**) Green channel (Alexa488) showing TH+ neurons in the VTA; (**a$_2$**) red channel showing endogenous tomato fluorescence from the AgRP fibers; (**a$_3$**) merged channel. (**b**) Slice containing the VTA of Dat-Cre:R26-LSL-tdTomato mice stained against AgRP and labeled with Alexa488 secondary antibody. (**b$_1$**) red channel showing endogenous tomato fluorescence from the dopamine neurons in the VTA and their fibers; (**b$_2$**) green channel showing AgRP fibers innervating the VTA of adult mice, as labeled by an antibody against AgRP and a secondary antibody coupled to Alexa488; (**b$_3$**) merged channel. (**c**) Quantification of the interaction (close proximity) between AgRP fibers and dopamine cells in the VTA from three mice. More than 1400 dopamine cells were visualized, and – on average – at least 1 interaction every 6 cells was seen in a 40x confocal slice of the VTA of adult mice. Scale bars = 50 µm.

Supplementary Figure 11:

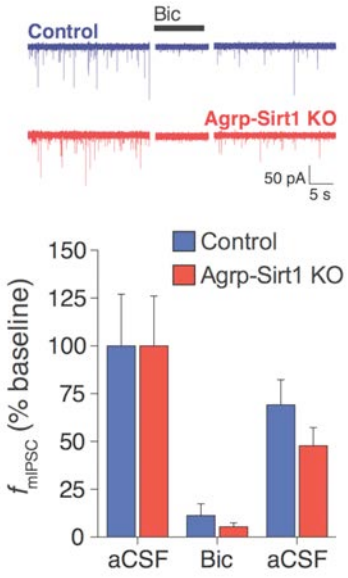

Miniature IPSCs are GABA mediated in the dopamine cells of the VTA. We confirmed the mIPSCs recorded from the VTA DA cells were GABA mediated by blocking the appearance of such events by adding bicuculline (Bic), a $GABA_A$ antagonist, in the recording chamber. Bic abolished the mIPSCs events in both VTA DA cells from control and Agrp-Sirt1 KO mice.

Supplementary Figure 12:

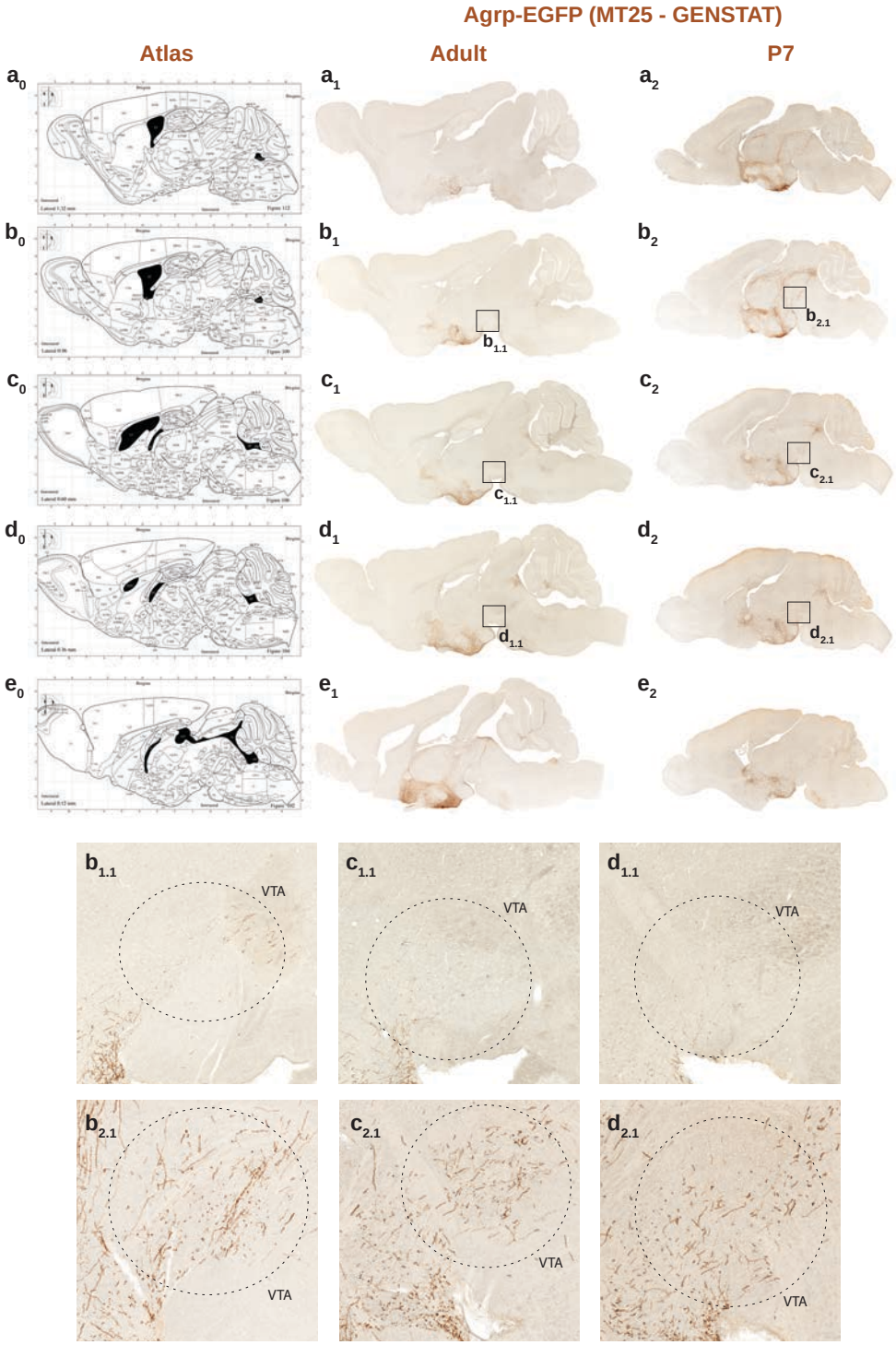

Legend for Supplementary Figure 12:

AgRP projections to the VTA during development. (**a-e**) Sagittal slices of the mouse brain showing the localization of Agrp. These images correspond to a transgenic mouse generated by the GENSTAT Project, in which EGFP is expressed under the promoter of Agrp (Agrp-EGFP mouse line – MT25). The brain is stained against GFP and developed with DAB. (**a-e$_0$**) Sagittal slices from the adult mice Paxinus brain atlas. (**a-e$_1$**) Slices from adult Agrp-EGFP mice, and (**a-e$_2$**) from postnatal day 7 (P7) mice. (**b-d$_{1.1}$**) show inserts from adult mice VTA, and (**b-d$_{2.1}$**) show inserts from P7 mice VTA. While there is a weak to moderate innervation of the VTA by Agrp fibers in adult mice, there is a strong innervation of this midbrain nucleus in P7 mice. These images are courtesy of NCBI, and are found online in the GENSTAT database – "The Gene Expression Nervous System Atlas (GENSAT) Project, NINDS Contracts N01NS02331 & HHSN271200723701C to The Rockefeller University (New York, NY)"[8].

Supplementary Figure 13:

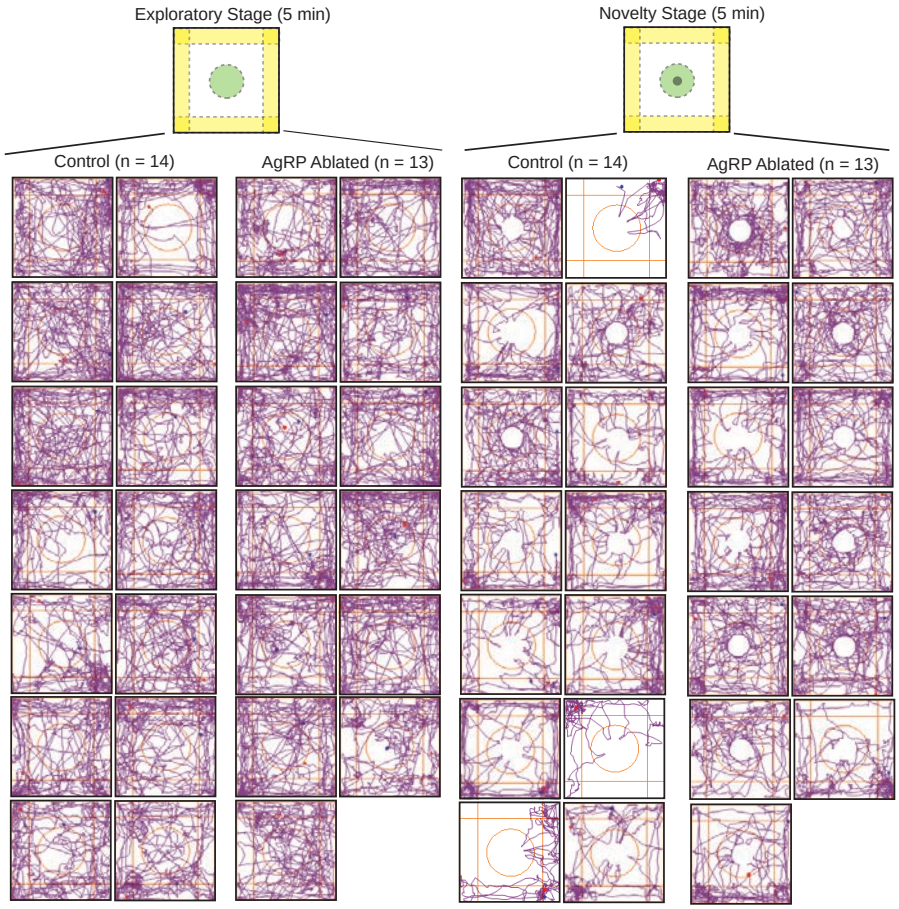

Individual tracks illustrating the behavior of AgRP Ablated and littermate control mice in the open-field test. A total of 14 controls and 13 AgrpDTR female mice that were injected with diphtheria toxin at postnatal age of 5 days (P5) were used in the experiment. *Left*, mice were allowed to explore an open-field for 5 minutes, and were returned to the home cage for 2 minutes for an inter-test interval. *Right*, mice were then re-tested in the open-field containing a new object in the middle of the box as a new stimulus to induce exploration (exploratory stage - 5 minutes). The red dot represents the position of the mouse when the recording ended.

Supplementary Figure 14:

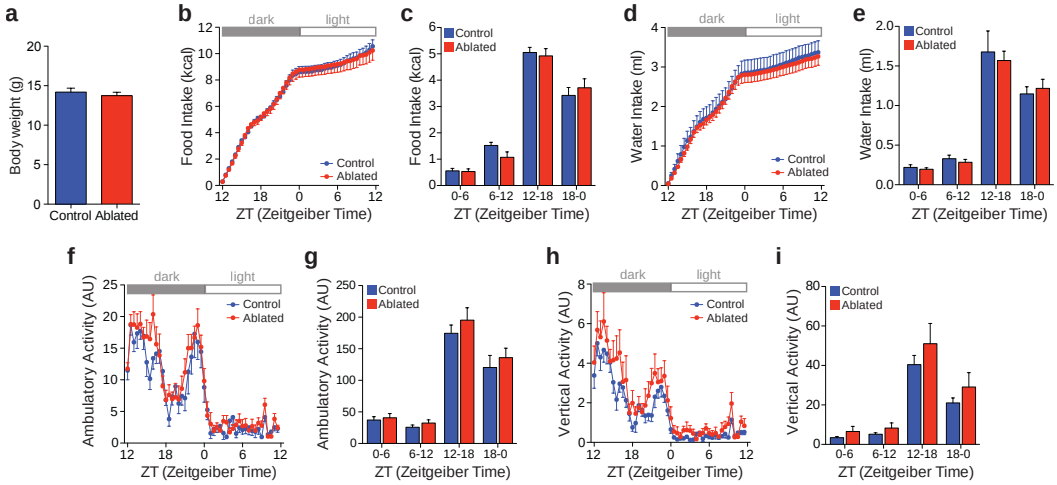

Phenotypic characterization of control and AgRP ablated mice. A total of 8 controls and 8 AgrpDTR female mice that were injected with diphtheria toxin at postnatal age of 5 days (P5), were phenotypically characterized in their home cages. Ablation of AgRP neurons in early postnatal age (P5) did not significantly change (**a**) body weight, (**b-c**) food intake, (**d-e**) water intake, (**f-g**) ambulatory activity, and (**h-i**) vertical activity when compared to littermate control mice.

Supplementary Table 1:

	Control (n = 9)	Agrp-Sirt1 KO (n = 8)
Leptin (ng/ml)	**3.86 ± 0.55**	**2.33 ± 0.29***
Fat mass (g)	**3.94 ± 0.20**	**3.00 ± 0.17****
Fat (%)	**17.45 ± 0.83**	**13.24 ± 0.81****

* $P < 0.05$.

* $P < 0.01$.

Supplementary Table 2:

Data from the analysis of electron microscopic pictures of TH positive cells in the ventral tegmental area of the midbrain from control and Agrp-Sirt1 KO adult female mice.

	Control (n = 33 cells/5 mice)	**Agrp-Sirt1 KO (n = 33 cells/5 mice)**	***P* value**
Average area (μm^2):			
Cell	123.67 ± 5.50	122.07 ± 5.41	0.836
Nucleus	57.19 ± 3.51	58.12 ± 2.97	0.841
Cytosol	66.48 ± 4.33	63.95 ± 3.96	0.668
Ratio nucleus/cell area	0.468 ± 0.022	0.478 ± 0.018	0.731
Cell perimeter (μm)	46.25 ± 1.48	47.27 ± 1.29	0.603
Synaptic density (number of synapses per 100 μm perikarya):			
Asymmetric	1.54 ± 0.31	1.75 ± 0.37	0.675
Symmetric	5.80 ± 0.71	5.62 ± 0.62	0.851
Total	7.34 ± 0.90	7.37 ± 0.83	0.982
Mitochondria number:			
Number per cell area	0.346 ± 0.016	0.341 ± 0.019	0.840
Number per cytosol area	0.661 ± 0.026	0.653 ± 0.029	0.841

Methods

Animals:

Female transgenic mice were used in these studies. Littermate controls and Agrp-Sirt1 KO mice were generated as described[1]. All animals were kept in temperature and humidity controlled rooms, in a 12/12h light/dark cycle, with lights on from 7:00AM-7:00PM. Food and water were provided ad libitum unless otherwise stated. All procedures were approved by the Institutional Animal Care and Use Committee from Yale University.

The following transgenic mice were used in this study: Agrp-Cre mice donated by Allison Xu (UCSF, San Francisco, CA – USA); Agrp-DTR mice donated by Richard Palmiter (University of Washington School of Medicine, Seattle, WA – USA); Dat-Cre mice donated by Nils-Goran Larssons (Karolinska Institute, Sweden). Agrp-Cre mice (Strain: Agrp<tm1(cre)Lowl1>/J, Stock number: 012899), $Sirt1^{loxP/loxP}$ mice (Strain: B6;129-*Sirt1*^{tm1Ygu}/J, Stock Number: 008041), R26-LSL-LacZ reporter mice (Strain: 129-Gt(ROSA)26Sor/J, Stock number: 002292), R26-LSL-tdTomato reporter mice (B6.Cg-Gt(ROSA)26Sortm14(CAG-tdTomato)Hze/J, Stock number: 007914), and NPY-hrGFP mice (Strain: B6.FVB-Tg(Npy-hrGFP)1Lowl/J, Stock number: 006417) were from The Jackson Laboratories.

Ablation of the AgRP neurons:

AgrpDTR or wild type mice (in a B6 background) from the same litter received injection of diphtheria toxin (DT) at postnatal age of 5 days (P5). DT was injected

utilizing the same method as published elsewhere[9]. We confirmed that DT ablated the AgRP neurons by performing immunohistochemistry using an anti-AgRP antibody in a group of adult mice that received the DT injection at P5. In AgRP ablated mice, the amount of AgRP residual fibers was less than 10% of those present in wild type mice. For behavioral analyzes, mice received DT injection at P5 and were tested when older than 40 days old. Ablation of the AgRP neurons was also predicted by testing ghrelin-induced food intake in these mice, as it is known to be abrogated in AgRP ablated mice. For electrophysiology, AgrpDTR mice were crossed with Dat-Cre:R26-LSL-tdTomato reporter mice to allow easier identification of the dopamine cells in the VTA.

Elevated plus-maze test:

All mice were brought to the testing room at least 2 hours before initiating the tests to acclimate the mice. The apparatus consisted of four elevated arms (40 cm from the floor, 25 cm long and 5.2 cm wide) arranged at right angles (cross-like disposition). Two opposite arms were enclosed by 15-cm high walls, and the other two were open (no walls). The maze had a central 5.2 cm × 5.2 cm square platform that gave access to all arms. The floor of the maze was covered with a gray synthetic cover glued to the apparatus to provide enough contrast for automatic video tracking. Each mouse was placed in the central square facing an open arm. The apparatus was cleaned with an ethanol solution (70%) and water to avoid olfactory clues before placing the next animal. Number of entries in each arm and time spent in each arm were recorded for 5 min. The number of alternations was considered as the total number of entries in the open arms plus the entries in the closed arms. For one entry to occur, at least 50% of the total animal

area had to be inside the zone. One exit from the zone was not counted until less than 30% of the total animal area was in the zone. Data were automatically recorded and analyzed using the software ANY-maze Video Tracking System (version 4.72, Stoelting Co., Wood Dale, IL, USA). Occupancy plots were generated by the ANY-maze software and consist of the group occupancy plot of the animal's center position. The maximum occupancy is the maximum value found in any of the plots, thus the plots can be compared between themselves, but cannot be used as comparisons to other plots from different experiments. The raw data obtained in the video tracking software was exported to SPSS 18.0. Data were first tested for homogeneity of variances using Levene's test. After assuming homogeneity of variances ($P > 0.05$), differences between control and Agrp-Sirt1 KO mice were tested using one-way ANOVA.

Open-field:

The same mice used in the plus-maze test were used the next day in the open-field test. This test was used to investigate exploratory behavior in a new environment which is a task not motivated by feeding. The apparatus consists of an open-field (37 cm × 37 cm × 37 cm) covered with a synthetic grey cover to provide enough contrast for video tracking. Mice were automatically recorded using the software ANY-maze Video Tracking System (version 4.72, Stoelting Co., Wood Dale, IL, USA). In the software, the open-field was virtually divided in two main zones, the center (circle around the virtual object with a diameter of 14 cm – green area in Supplementary Fig.1) and the walls (a 6 cm strip along the walls of the apparatus – yellow area in Supplementary Fig.1). Four similar apparatus were recorded simultaneously. Mice were first put in the open-field for

5 minutes and allowed to freely explore the new environment. This stage was called ‘exploratory stage’. Immediately after finishing this stage, mice were returned to their home cages for 2 minutes. A new object (a cylinder of 5 cm radius and 10 cm high) was placed in the center of the arena to stimulate exploration. Mice were then returned to the open-field for an additional 5 minutes (‘novelty stage’). The apparatus was cleaned with an ethanol solution (70%) and water to avoid olfactory clues before placing the next animal. Seven weeks later, the same mice were injected with murine leptin (5 mg/kg, i.p., 3-4 h before test – PreproTech Inc, Rocky Hill, NJ – Cat #450-31, Lot #101076) and were re-tested in the open-field using a different object as a novel stimulus. The time between the walls was computed when the animal’s center was inside the zone. For the center of the open-field, the animal’s head was considered when analyzing the time in the zone. Immobility detection was set at 85% sensitivity and a 2000 ms minimum immobility period. Occupancy plots were generated by the ANY-maze software and consist of the group occupancy plot of the animal’s head position. The maximum occupancy is the maximum value found in any of the plots, thus the plots can be compared between themselves, but cannot be used as comparisons to other plots from different experiments. The individual track plots were obtained by showing the position of the animal’s center. The raw data obtained in the video tracking software was exported to SPSS 18.0. Data were first tested for homogeneity of variances using Levene’s test. After assuming homogeneity of variances ($P > 0.05$), differences between control and Agrp-Sirt1 KO mice were tested using one-way ANOVA. If homogeneity of variances were not assured ($P < 0.05$ in Levene’s test), the Mann-Whitney U non-parametric test was used to compare groups. For the experiment using low and high body weight mice,

we purchased 40 C57B6/J female mice (8 weeks old) from The Jackson Laboratory (Bar Harbor, Maine, USA). The mice were acclimated to the Yale University Animal Facilities for 2 weeks prior to the behavioral experiments. When the mice were 10 weeks old, their body weight was measured and the 8 heaviest and 8 lowest mice were selected for the open-field test. One mouse in the low body weight group was not used because it had malocclusion. Similar procedures as described above were used to test these mice in the open-field test. For the experiment using AgRP ablated mice, female adult (45-55 days old) mice were used, and all tests were performed in the same way as described above.

Open-field acclimation and cocaine dose-response:

Female control (n = 14) and Agrp-Sirt1 KO (n = 14) were allowed to explore a novel environment (45 × 24 × 20 cm clear plastic cages covered with white paper bedding, which differs from the corn bedding in the regular housing condition) for 60 minutes before receiving an injection of vehicle (PBS, i.p.). Sixty minutes after the PBS injection, 11 mice in each group received cocaine injections (5, 10 and 20 mg/kg, every 120 minutes, i.p.), while 3 mice in each group (control and Agrp-Sirt1 KO) received PBS injections. The total volume of injected fluid was 10 ml/kg, i.p. Fourteen mice were tracked at the same time using ANY-Maze video tracking system (see more details above). For the cocaine dose-response plot, the first 20 min of each block were considered for analyses. 5-min bin locomotor activity plots are shown in Supplementary Fig. 6. The software did not appropriately track two mice during the acclimation stage, which were subsequently excluded from the analysis of this stage. For 60 min locomotor

activity analysis (Fig.1d), an unpaired t test was used to find statistical differences. For the cocaine dose-response a two-way ANOVA, with cocaine dose and genotype as factors, was used for analysis. In both cases a $P < 0.05$ was considered statistically significant.

Cocaine sensitization:

Female control (n = 12) and Agrp-Sirt1 KO (n = 11) mice (between 10-14 weeks old) were used in this experiment. On day 0, mice were placed in 45 × 24 × 20 cm clear plastic cages between two rows of photocells (16 total, 2 cm apart, Columbus Instruments, Columbus, OH, USA) for 60 min. to acclimate to the behavioral chamber. Locomotor activity was assessed by measuring the number of beam breaks per minute and recorded by a Dell computer using Opto-max software (Columbus Instruments). Beam breaks were compiled into four 5-min bins for analysis. On each of the next three days (days 1, 2, 3), mice received an injection of saline (0.9% NaCl, sterile, i.p.) just before being placed in the recording chambers, and activity was recorded for 20 minutes. Cages were cleaned with ethanol (70%) and washed with water before testing the next mouse. On days 4-8, mice received an injection of cocaine (10 mg/kg, i.p.), and activity was recorded for 20 minutes in the same way as before. After 4 days of treatment withdrawal, mice were challenged again with saline (day 13) and cocaine (day 14) to test for contextual and drug sensitization respectively. Due to differences in baseline activity between control and Agrp-Sirt1 KO mice, the data during the sensitization protocol (saline acclimation and cocaine injections) were normalized by the individual's activity on day 0. For statistical analysis, homogeneity of variances was tested by Levene's test.

A two-way mixed model ANOVA, with genotype as a between groups factor and time as a repeated measures, was used to find differences in the saline and cocaine sensitization protocol. In the challenge protocol (days 13 and 14), a two-way ANOVA (challenge x genotype) was used for statistical analysis. Sphericity was tested using the Mauchly's test of sphericity. If the *P* value of the Mauchly's test was lower than 0.05, the degrees of freedom were adjusted using the epsilon calculated by the Greenhouse-Geisser procedure. The difference in the ratio (locomotor response in the cocaine challenge divided by the response in the saline challenge) was tested using one-way ANOVA. PASW Statistics 18.0 software was used for the analysis.

Rota-rod:

A total of 12 control (age = 10.36 ± 0.27 weeks old) and 12 Agrp-Sirt1 KO (age = 10.20 ± 0.28 weeks old) female mice were used in this test. The apparatus consists of a rolling bar located 20 cm above the floor, divided into 4 compartments. The floor of the apparatus contained an automatic dispositive to record when the mice fell from the rolling bar. Mice were acclimated to the behavior room for at least 2 hours before the test. On days 1-5, all mice were trained in the rota-rod (2 trials/day) using the following parameters: initial speed = 4 rpm, maximum speed = 60 rpm, time to reach maximum speed = 300 seconds. The cut off time on the rota-rod was 600 seconds. The latency to fall from the rotating bar was recorded. After finishing the first trial, mice were returned to their home cage. A group of 4 mice was tested at the same time in the apparatus. When all 4 mice finished one section of training, they were put back in the rota-rod for the second trial, which was identical to the first trial. All experiments started at ZT 4.5. Data

analysis was performed by averaging the latency of both trials in each day and utilizing mixed model ANOVA with time as a repeated measure and genotype as the between groups factor. Sphericity was tested using the Mauchly's test of sphericity. If the *P* value of the Mauchly's test was lower than 0.05, the degrees of freedom were adjusted using the epsilon calculated by the Greenhouse-Geisser procedure. PASW Statistics 18.0 software was used for the analysis.

Cocaine Place Preference:

A total of 34 female adult mice were used in this study. All mice were transported to the facility where the behavioral training would take place two weeks prior to behavioral testing. Conditioning place preference (CPP) boxes (ENV-256C Med Associates Inc, St. Albans, VT) were modified for a non-biased CPP procedure. Two conditioning chambers (side-chambers, named A and C) with retractable doors were separated by a grey neutral chamber (middle-chamber, named B) with a grey Plexiglass floor. Chamber A had a wire mesh floor, and chamber C had a grid floor. The location of the mouse in the chamber was recorded by photocell beam breaks and time spent in each chamber was automatically recorded using Med-PC IV software (Med Associates Inc, St. Albans, VT).

Mice were transferred to the testing room at ZT 1.5 and the behavior testing started at ZT 3.0. The testing room was illuminated with dim light. Mice were injected with saline or cocaine (10 mg/kg, i.p.) just prior to placement in the CPP chamber. On day 1, baseline preference was assessed by injecting all mice with saline and they were placed inside chamber B and allowed to explore both sides (A and C) for 15 minutes.

One mouse was excluded from the study due to high preference for one of the conditioning chambers in the baseline preference (the threshold for preference was arbitrarily pre-defined as 70%-30% ratio). Four CPP boxes were used simultaneously to record 4 mice, and there was no significant box differences in the preference for one of the side chambers (ANOVA: $F_{(3, 34)} = 1.783$, $P = 0.171$).

During the conditioning phase of the experiment (days 2, 3, and 4), mice received two conditioning sessions per day during 3 consecutive days. During the AM session (beginning at ZT 3.0), mice were isolated in one conditioning chamber (A or C) for 30 minutes following injection of saline or cocaine. During the PM session (beginning at ZT 6.5) animals were isolated in the opposite conditioning chamber (C or A) following a second injection (saline or cocaine, the opposite of the AM treatment). Mice were randomly scheduled to receive different AM-PM treatments, and all groups had counterbalanced numbers of animals in each schedule. Additionally, mice were counterbalanced for drug-paired chamber according to genotype and baseline preference. On day 5, mice were tested again for their preference of the conditioning chambers A and C, identical to the baseline preference testing. Both baseline and test sessions were assessed at an intermediate time between the AM and PM sessions (ZT 5.0). Total time spent in each conditioning chamber during the baseline and test sessions was recorded and cocaine CPP was measured as the amount of time spent in the drug-paired chamber minus the time spent in the saline-paired chamber. A total of 14 mice were analyzed in the control group and 10 mice in the Agrp-Sirt1 KO group. Additionally, a third group of mice received saline in both AM and PM sessions and was used as a control group for the

conditioning chambers. No preference for either chamber A or C was seen in the saline-saline group (baseline = -47.25 ± 40.51, test = -70.38 ± 72.11; Wilcoxon Signed Ranks Test: $T = 17.00$, $P = 0.889$). To test for place preference, differences within the same group (baseline x test) were analyzed by Friedman's non-parametric test. The differences between control and Agrp-Sirt1 KO mice were analyzed using Mann-Whitney U test. Because the previous data suggested that the Agrp-Sirt1 KO mice have a higher response to cocaine when compared to littermate controls, we used one-tailed statistics to find differences between the two groups in the test session.

Home cage monitoring:

AgRP ablated mice and their littermate controls were let to acclimate in TSE LabMaster home cages for at least 5 days before recording food intake, water intake and activity. The same mice were injected with ghrelin to test for ghrelin-induced food intake, which predicts the ablation of the AgRP neurons.

Agrp reporter mice:

We bred Agrp-Cre mice (Jax 012899) to R26-LSL-tdTomato mice to study the projections of the Agrp neurons to the VTA (Supplementary Fig. 8). The advantage of this method is that tdTomato is a very soluble and bright fluorescent protein allowing high sensitivity and specificity to trace neuronal projections. Also, because Agrp neurons express GABA and NPY, it is possible that the Agrp fibers that innervate some of the target areas of these neurons lack Agrp, thus decreasing the sensitivity of immunohistochemistry as a method to detect neuronal projections. We further crossed

these mice (Agrp-Cre:R26-LSL-tdTomato) to NPY-hrGFP mice to confirm that the Agrp neurons in the ARC expressing tdTomato were also NPY neurons. Adult mice (about 3 months old) were perfused (see protocol below) and the brain was kept in PB 0.1M at 4ºC. Vibratome sections (50µm) containing the ARC and the VTA were cut and vigorously washed in PB 0.1M to wash out residues of PFA. Slices were mounted using Vectashield Mounting Medium for Fluorescence (Vector Laboratories Inc., Burlingame, CA – Cat # H-100) and scanned in a confocal microscope.

Immunohistochemistry for TH and Agrp

Mice were deeply anesthetized and the left ventricle of the heart was rapidly cannulated and flushed with 0.9% saline containing heparin followed by freshly prepared fixative (paraformaldehyde 4%, gluteraldehyde 0.1%, picric acid 15%, in PB 0.1M, pH=7.4). Usually, the time between opening the thoracic cavity and the heart cannulation was less than 30 seconds. Brains were then dissected out and post-fixed overnight in fixative without gluteraldehyde. After vigorous washing in cold phosphate buffer (0.1M), vibratome sections were cut (50µm) containing the VTA of the midbrain. Sections were washed in PB several times, cryo-protected and subsequently frozen and thawed 3 times in liquid nitrogen. After extensive washing in PB, slices were incubated with H_2O_2 (1%, 20 minutes, room temperature, shaking) to block endogenous peroxidase activity. After washing again with PB, sections were incubated with primary antibody (guinea pig anti-Agrp, 1:3000, 48 hours, 4°C, gentle shaking – donated by Kevin Grove) in PB 0.1M plus 3% normal serum. Sections were extensively washed, incubated with secondary antibody (anti-Guinea Pig, 1:500, from Jackson Laboratories, Cat #706-065-148, Lot #85820 - 2

hours, room temperature), washed again, put in ABC and developed with Nickel-DAB. Sections were then extensively washed in PB 0.1M, and incubated in primary antibody again (mouse anti-TH antisera, 1:5000, 24 h, 4ºC) and developed with DAB after incubation with secondary antibody and ABC. Alternatively, slices were incubated with secondary antibodies coupled to Alexa488 (molecular probes) to visualize AgRP – TH positive cell juxtaposition in a confocal microscope.

Microdialysis

Females adult mice were administered the analgesic buprenorphine (0.1 mg/kg) 30 minutes prior to surgery. They then were anesthetized with a solution of 30 mg/kg ketamine and 6 mg/kg xylazine and loaded into a stereotaxic frame. Two openings were made into the skull using a hand drill with a 0.7 mm burr. An anchor screw (CMA, #7431021) was seated into one hole at approximately the following coordinates in relation to bregma: ap -2.5, lateral -1.7 (hole locations were sometimes slightly adjusted to avoid damaging any clearly visible blood vessels). CMA-7 microdialysis guide cannulas, with dummy cannulas within (CMA, #P000137), were inserted and slowly lowered into the following coordinates in relation to bregma: anterior-posterior +1.3 mm, lateral -0.6 mm and dorsal-ventral -3.6 mm. The cannulas were secured in place with Cerebond Adhesive Skull (Plastics One), which was built up around the cannula and bonded to the anchor screw. Mice were administered saline post-surgery to prevent dehydration and were given moist chow for 2 days. Animals were allowed a minimum of 5 days for postoperative recovery before further experimentation.

Mice were placed into the testing cages and acclimated to the environment for 2 hours prior to the initiation of the experiment. CMA/7 microdialysis probes with 1 mm membrane length (CMA, #P000082) were attached through FEP tubing to a PHD-Ultra syringe pump (Harvard Apparatus). Probes were prepared by washing with artificial cerebrospinal fluid at a rate of 1.2 µl/min. Dummy cannulas were removed and microdialysis probes were inserted into the implanted guide cannulas mounted on the mice. Artificial cerebrospinal fluid was then continuously pumped through the probes at 1.2 µl/min for the remainder of the experiment. Mice were allowed 1.5 hours for aCSF washing before samples were collected. Thereafter, samples were collected every 15 minutes and kept on ice for later dopamine measurements. A total of 8 samples were collected at the 15 min intervals to establish baseline levels of dopamine. After the conclusion of the experiment, mice were perfused (as described above) and brains were sectioned at a thickness of 100 µm to check for probe and cannula location and orientation. Dopamine concentrations were measured in the microdialysate samples from each mouse using an HPLC (Eicom, USA).

TH staining, quantitative synaptology and mitochondria counting:

Electron microscopy analysis of the dopamine (TH positive) neurons in the VTA was performed as previously described[10].

Body composition:

A group of control and Agrp-Sirt1 mice were scanned in the EchoMRI-100 machine to measure their whole body fat mass.

Mouse leptin assay:

Mice were fasted overnight (6:00 PM to 8:00 AM), and eye bled. Serum was collected by centrifugation and aliquots were stored at -80ºC until analyzed. Leptin serum levels were measured using the Mouse Leptin ELISA kit (Millipore, Billerica, MA, USA – Cat #EZML-82K).

Electrophysiology:

Horizontal brain slices containing the VTA were cut from female control and Agrp-Sirt1 KO mice, and were freshly prepared for electrophysiology recordings as reported[10, 11]. For the LTP measurements, mice were between 13-16 days old for the 15 day old group; 27-31 days old for the 30 day old group; and 44-55 days old for the 45 day old group. mIPSCs and mEPSCs were recorded in ~45 day old mice. For the recordings in the AgRP ablated mice, all mice were 29-31 days old, and dopamine cells were identified by the red fluorescence in Dat-Cre:R26-LSL-tdTomato:AgrpDTR mice.

Statistical Analysis: For all tests, a *P* value below 0.05 was considered statistically significant. Data distribution was first tested for homogeneity of variances using Levene's test. If homogeneity was assumed, then one- or two- way ANOVA was used. For two-way ANOVA with repeated measures, sphericity was tested using the Mauchly's test of sphericity, and the degrees of freedom were adjusted using the epsilon calculated by the Greenhouse-Geisser procedure when necessary. To test for LTP response, a paired *t* test (one-tail) was used between pre- and post-stimulation values. When homogeneity

was not assumed, Mann-Whitney *U* test or Friedman's test was used. The n, df, *t*, *F*, *U*, χ^2 and *P* values are reported in the text. Details for the tests used in each individual experiment are described in the appropriated section above. PASW Statistics 18.0 for Mac software was used for all analysis.

Supplementary References

1. Dietrich, M., *et al. J Neurosci* **30**, 11815-11825 (2010).
2. Hommel, J.D., *et al. Neuron* **51**, 801-810 (2006).
3. Fulton, S., *et al. Neuron* **51**, 811-822 (2006).
4. Fadel, J. & Deutch, A.Y. *Neuroscience* **111**, 379-387 (2002).
5. Balcita-Pedicino, J.J. & Sesack, S.R. *J Comp Neurol* **503**, 668-684 (2007).
6. Borgland, S.L., Taha, S.A., Sarti, F., Fields, H.L. & Bonci, A. *Neuron* **49**, 589-601 (2006).
7. Nakamura, T., *et al. Brain Res* **873**, 181-187 (2000).
8. Gong, S., *et al. Nature* **425**, 917-925 (2003).
9. Luquet, S., Perez, F., Hnasko, T. & Palmiter, R. *Science* **310**, 683-685 (2005).
10. Abizaid, A., *et al. J Clin Invest* **116**, 3229-3239 (2006).
11. Liu, Q., Pu, L. & Poo, M. *Nature* **437**, 1027-1031 (2005).

Capítulo IX. Physiological roles of hunger-promoting neurons and implications for anti-obesity drugs

Artigo submetido ao periódico *Nature Reviews Drug Discovery*.

Physiological roles of hunger-promoting neurons and implications for anti-obesity drugs

Marcelo O. Dietrich[1,2] and Tamas L. Horvath[1]

[1]Program in Integrative Cell Signaling and Neurobiology of Metabolism, Section of Comparative Medicine, Yale University School of Medicine, New Haven CT 06520, USA. [2]Department of Biochemistry, Universidade Federal do Rio Grande do Sul, Porto Alegre RS 90035, Brazil.

Correspondence should be addressed to T.L.H. (tamas.horvath@yale.edu).

Abstract

Emerging evidence indicates that the hypothalamus is a key regulator in the coordination of the central nervous system (CNS) to adapt to the changing environment in support of survival, with subsets of hypothalamic neurons acting upstream to control brain regions classically considered as master determinants of CNS function, such as the cortex and hippocampus. The regulatory role of the hypothalamus in cortical and hippocampal functions is mediated by classic neuronal pathways and by the management of peripheral tissue output in the form of hormones and nutrients. Here, an argument is made that when the relationships between these brain regions and peripheral tissues are reconsidered based upon the driving principles of health and survival, it is hard to envision that long-lasting successful strategies to combat obesity can emerge from drugs that simply promote satiety and energy expenditure. We discuss how this knowledge could help understand failures in the development of successful obesity drugs and could aid the discovery of new drugs with greater effectiveness and an acceptable benefit/risk profile.

Introduction

Efficient and safe pharmacological options for the prevention and cure of obesity remain elusive. One of the reasons for this failure perhaps is that our understanding of the pathogenesis of obesity (an excessive growth of adipose tissue in response to overnutrition) is still incomplete. Alternatively, the molecular underpinning of biological processes that underlie the emergence of obesity may not lend themselves to selective manipulations that successfully reduce adipose tissue stores without impairing long term health and survival. The availability of nutrients (energy) to fuel biological reactions is the fundamental principle of life. It is plausible that living organisms evolved in an environment in which they struggled to acquire energy and metabolize it efficiently. A lack in the availability of energy or a switch towards negative energy balance (as in starvation, cachexia or anorexia) leads to a life threatening state. The growing obesity epidemic, which is characterized by a continuous overnutrition (positive energy balance in which the absorption of energy surpasses its metabolism by the body, i.e., intake higher than expenditure). The propagation of such a metabolic state leads to accumulation of fat, which physiologically serves to generate energy supplies for periods of famine. In modern societies, not only is it highly unlikely to have a period of starvation which would serve to deplete the fat stores, but the accessibility of food (energy) is abundant and cheep, thus fat accumulates and obesity develops. The levels of obesity are growing worldwide, and are reaching epidemic proportions in several countries, affecting almost 40% of the population in the United States[1]. The economic and social burden that this poses are enormous, particularly since obesity is a high risk factor for several other chronic diseases (e.g., cardiovascular disorders, diabetes, cancer). Thus, finding an effective treatment for obesity is a priority for the society and consequently for the pharmaceutical industry.

Despite the growing amount of resources being applied to research in the field, the development of anti-obesity drugs has been plagued by failures[2-5]. A great number of the putative new drug targets for obesity do not reach the effectiveness advocated by the FDA, while the few that are effective enough to bring some hope end up having severe side effects that preclude long-term use in patients (see table 1). The number and diversity of side effects indicate that the pathways targeted thus far are ubiquitously important in several tissues, and not in just those directly implicated in the regulation of energy balance/obesity. Most (if not all) of the

pharmaco-therapies for obesity attempt to suppress food intake, by either curbing appetite or suppressing the craving for food. Thus, the basic principle behind the development of these drugs has been to target pathways to promote satiety. This review will evaluate the evidence that promote the notion that anti-obesity drugs that focus on the satiety pathways may be destined to fail due to "side effects". Some aspects of why such side effects occur will be discussed.

Hunger drives mnemonic functions

The adaptive response to the need for higher energy levels for cellular metabolism is hunger (or appetite). Since the primordial ages, hunger has been the driving force for creativity and for the development of civilization in general. The evolution of human society has been characterized by innovations associated with seeking and securing resources in support of survival. Besides these common truisms, there is an irrefutable amount of scientific evidence accumulated in the last century that supports the idea of hunger as a primary driver of higher brain functions. Experimental neuroscience has vastly utilized approaches of positive reinforcement that hinge upon hunger or appetite as the motivational force to learn new tasks. While there are many other methods for the study of mnemonic functions, the profound role that hunger plays in promoting complex brain functions is evident from these studies. More recently, the humoral, neuronal and molecular fingerprints of this phenomenon have emerged and suggest a fundamental role of the hypothalamus and peripheral tissues in coordinating these processes[6-8]. Because hunger has such notable effects in determining cognitive functions, it is likely that whatever intervention is designed to interfere with hunger will ultimately also interfere with cognition.

Hunger drives longevity

Late onset chronic diseases, including obesity, dementias, diabetes, CV disorders and cancer, are leading causes of mortality and morbidity creating the greatest emotional and financial burden on society. As the aging population grows, it is expected that chronic diseases will further dominate our civilization. Guided by the idea that late onset chronic diseases, including obesity, are a consequence of prolonged overworking of various tissues that have certain vulnerabilities (e.g., genetic, epigenetic), it is possible that the cellular energy metabolism of the different tissues will determine health and longevity. In support of this idea is the finding

of a positive effect of calorie restriction on a healthy lifespan in a broad range of animal models, including the worm, fruit fly, rodents and non-human primates[9-11]. To date, this is the only physiological intervention known to have a consistent and predictable effect to maintain health and prolong life in all species studied. The robust effects of calorie restriction, a form of protracted negative energy balance, on chronic diseases lends support to the argument that late onset disorders are the consequence of sustained high levels of substrate oxidation by the various tissues. Negative energy balance is thought to promote the activity of specific populations of neurons in the hypothalamus, which drive hunger. Thus, the evidence that comes from the calorie restriction studies point to hunger, and the promotion of the activity of these specific populations of cells (see below), as the promoter of a healthier and longer life, while satiety does just the opposite in that it promotes metabolic overload in tissues leading to chronic disease.

The role of the hypothalamus in hunger (Fig. 1)

More than six decades ago, lesion studies identified specific areas in the hypothalamus as central regulators of feeding[12-18]. Certain hypothalamic lesions lead to the cessation of feeding and subsequent death by starvation[17,18]. In the past two decades, two peptidergic systems were discovered in the lateral hypothalamus where lesions cause aphasia and death[17,18]: the hypocretin/orexin neurons[19,20] and the melanin-concentrating hormone (MCH)-producing cells[21,22]. Both of these neuronal systems, when activated, promote feeding. Lesions in the more medial-basal part of the hypothalamus, the arcuate nucleus (ARC), did not affect feeding. However, later studies found that chemical lesions targeted to selective populations of neurons within the ARC could disturb energy balance[23]. Strikingly, selective ablation of a small subset of inhibitory neurons in this region of the brain recapitulated the effects of classic lesion studies, leading to cessation of feeding in a few days and death by starvation[24-28]. These neurons are those that co-produce neuropeptide Y (NPY), agouti-related protein (AgRP), and gamma amino butyric acid (GABA)[29-32].

The involvement of the hypothalamic NPY/AgRP neurons in the regulation of feeding has been suspected for more than twenty-five years. First, in 1984, NPY was found to be the most potent inducer of appetitive and feeding ever described[33-35]. Second, NPY neurons were anatomically and functionally tied to the hypothalamic melanocortin producing neurons[30], which

play a fundamental role in satiety[36]. The latter are the POMC neurons, which produce alpha-MSH, an agonist of the melanocortin receptors.

Consensus exists that the NPY/AgRP/GABA neurons serve as critical suppressors of the melanocortin system, a tonic inhibitory relationship supported by both hard wiring and pre- and postsynaptic actions[32,37,38]. This tonic inhibition is the underlying cause for appetite and feeding stimulation being set as the default signaling of the brain, an obvious necessity from the perspective of survival. Because of this, it was surprising that neither the removal of NPY nor AgRP by means of knockout technology lead to major alterations in energy balance[39]. However, with new techniques to selectively eliminate this population of neurons, it became evident that the NPY/AgRP neurons were major regulators of feeding[24,26,27], since the acute elimination of these cells in the adult lead to cessation of feeding, and ultimately death[24,25,40]. This effect was not an artifact of acute neuronal degeneration within the ARC as asserted by studies that showed that when the neighboring POMC neurons were eliminated in a similar manner, the animals ate more and even gained weight[26]. The moribund state of the AgRP neuron-ablated mice is characterized by an overall disinterest in the environment and the lack of a desire for food for days preceding death. The lethal effect of this intervention (AgRP neuronal ablation) can be blocked by site-selective administration of an agonist of GABA receptor[25,28]. Figure 2 shows an overview of the melanocortin system in the ARC, and intracellular mechanisms related to NPY/AgRP and POMC neuronal activity.

Box 1: The hypothalamic melanocortin system

The central melanocortin system resides in the medial-basal hypothalamus, more precisely in the arcuate nucleus (ARC) where the NPY/AgRP and the POMC neurons are located. The latter produce a series of different peptides that are encoded by the pro-opiomelanocortin gene (*pomc*), including α-MSH. Melanocortin peptides are endogenous agonists of melanocortin receptors, a family of G-protein coupled receptors with at least 5 members in the family (MC1R-MC5R). In the brain, MC3R and MC4R are the most abundant receptors for melanocortins, and they mediate the effects of α-MSH. POMC expressing neurons are not exclusive to the ARC, but also reside in the nucleus of the solitary tract (NTS) in the brainstem. The second population of

neurons that form the central melanocortin system is the NPY/AgRP neurons, which produce NPY and AgRP peptides plus GABA[31]. AgRP peptide acts as a strong endogenous antagonist of the MC3/4R[38], and is thought to regulate the signaling of these receptors by blocking the activity of α-MSH. Indeed, most of the areas of projection of the POMC and AgRP neurons overlap, emphasizing the crosstalk between these two populations of cells. A series of gene alterations in the melanocortin system leads to obesity, in both mice[41-44] and humans[45-52]. In addition to obesity and food intake, the central melanocortin system has also been implicated in several different homeostatic functions, including the control of insulin levels[53], cholesterol homeostasis[54,55], thyroid function[56,57], among others.

One of the unique properties of the ARC melanocortin system is that the NPY/AgRP neurons send inhibitory projections to the neighboring POMC neurons[30]. This unidirectional synaptic organization of the circuitry allows the NPY/AgRP neurons to coordinate feeding by direct inhibition of target areas, and/or by inhibiting POMC neurons, thereby releasing target areas of the excitatory inputs from the POMC cells. Accordingly, selective knockdown of GABA release by the AgRP neurons led to weight gain and an increased POMC tone in mice[58]. However, the melanocortin signaling does not seem to be essential to sustain feeding in AgRP ablated mice[59,60], while GABA signaling is[25,59]. Indeed, it has been known for decades[61-64] that GABA promotes feeding and recent evidence indicates that it is the AgRP/GABA tone that is essential for feeding to occur in adult mice[25,28,59].

Hypothalamic principles of obesity (Fig. 3)

The central melanocortin system is believed to be the key regulator of energy metabolism[7,65]. Leptin is a hormone produced by the adipocytes, which is lacking in the naturally occurring obese mice (ob/ob)[66,67]. Leptin and leptin receptor deficiencies lead to obesity in both mice and humans[66,68-73]. The discovery of this hormone[66] created hope that it could be used to treat obesity, however, only a small subset of genetically deficient (obese) patients are helped by leptin treatment[74,75]. Interestingly, it has been found that leptin levels are actually high in obese individuals (both rodents and humans)[76,77] and its administration has little effect in reducing body weight[78,79]. This scenario has been described as “leptin resistance,” and the mechanisms

that lead to such a situation in obese subjects are still largely unknown although several recent discoveries have shed light on this subject (see below). Leptin is thought to mediate its effects on energy metabolism regulation mainly by targeting the melanocortin circuitry in the brain[37,80]. Along this line, it has been proposed that leptin resistance occurs primarily in the hypothalamus. For example, high levels of leptin in obese states might lead to chronic activation of suppressor of cytokine signaling 3 (SOCS3), which in turn inhibits leptin signaling in the hypothalamus, leading to local leptin resistance[81]. More recently it was shown that an increase in endoplasmic reticulum (ER) stress and activation of the unfolded protein response (UPR; activated in response to an accumulation of unfolded or misfolded proteins in the lumen of the endoplasmic reticulum) occur in the hypothalamus of obese subjects, and leads to inhibition of leptin receptor signaling locally[82]. Various treatments of mice with chemical chaperones, which decrease ER stress, have a leptin-sensitizing activity, thus providing an important mechanism with possible translation to humans[82]. Notoriously, ER stress seems to be a common trait in chronic metabolic disorders[83], such as obesity and type 2 diabetes, and chemicals that decrease ER stress have shown benefits in both conditions[82,84].

The metabolic overload that takes place during obesity in the hypothalamus leading to ER stress[82] correlates with increased peroxisome proliferation in POMC neurons[85], which is consistent with the idea that peroxisomes are formed from the ER[86-88]. This increased peroxisome proliferation during diet-induced obesity is regulated by peroxisome proliferator-activated receptor gamma (PPARg), and is an adaptive response to control reactive oxygen species (ROS) levels in the POMC cells[85]. ROS are critical regulators of hypothalamic neuronal activity[85,89,90], and their levels within the hypothalamus correlate with circulating leptin amounts in lean mice[85]. The sustained increase in ROS production that occurs during positive energy balance (e.g., obesity), and the concomitant increase in peroxisome proliferation to control ROS levels, is likely another important hub in the mechanism(s) involved in leptin resistance in the hypothalamus. Additionally, this sustained increase in ROS linked to satiety states (positive energy balance) is consistent with the occurrence of increased degenerative processes under such conditions. Thus, chronic positive energy balance promotes the metabolic intracellular state related to satiety with increased ROS production that contributes to chronic disorders.

Box 2: Humoral determinants of brain function during metabolic shifts: implications for psychiatric and neurological disorders

Signals from the periphery initiate a brain response to declining energy availability. These signals arise from various peripheral tissues in the form of hormones and nutrients. Among the various hormones, only one to date has been shown to trigger feeding behavior, and that is the gut-derived acylated polypeptide, ghrelin[91,92]. This hormone not only triggers feeding behavior by activation of the arcuate nucleus NPY/AgRP neurons[93], but exerts action in extra-hypothalamic sites as well[94,95]. Ghrelin was originally discovered as a regulator of growth hormone release[91], and subsequently was identified as an appetite stimulating, adipogenic hormone[92]. Ghrelin is secreted from the stomach when the stomach is empty. Numerous studies revealed that the effect of ghrelin to promote feeding is mediated by the arcuate nucleus AgRP neurons[89,93,96]. In slice preparations, AgRP neurons were activated by ghrelin directly, while the anorexigenic pro-opiomelanocortin (POMC) neurons were inhibited indirectly by ghrelin[89,93]. Intriguingly, besides the acute electrophysiological effects of ghrelin on these neurons, peripheral ghrelin administration also rapidly re-organized the synaptic inputs on POMC neurons[37]. The resultant synaptic rewiring of the POMC neurons further promoted the suppression of these arcuate cells, which is consistent with the observation of an overall orexigenic influence of ghrelin. More recently, ghrelin has been shown to modulate the activity of the NPY/AgRP neurons by modulating pre-synaptic excitatory inputs onto these cells[97,98], in a mechanism similar to what has been described in other neuronal populations[98,99]. The possibility that ghrelin modulates feeding by acting both directly on the NPY/AgRP neurons[100,101] and indirectly through other cells that regulate pre-synaptic inputs onto these neurons[97], opens the possibility for other major players in the regulation of appetite[98].

However, in addition to the regulation of feeding, ghrelin also controls higher brain functions and may represent a molecular link between learning capabilities and energy metabolism. For example, circulating ghrelin enters the hippocampal formation and midbrain where it binds to neurons, and promotes the formation of synapses in both of these areas[102,103]. Ghrelin-regulated synapse formation and long-term potentiation of synapses in the hippocampus have a positive correlation with spatial memory and learning[102]. Beyond the alteration of these mnemonic

functions, hippocampal administration of ghrelin also promoted feeding[94]. The interference of ghrelin signaling in the midbrain also suppressed feeding triggered by peripheral ghrelin administration, which argues for a role of the midbrain reward circuitry in feeding regulation. However, the dopamine system within this area also projects to the pre-frontal cortex suggesting a direct role for ghrelin in motivated behavior resulting from cortical modulation and in working memory as well.

The ventral tegmental area is in the immediate vicinity of the substantia nigra, where dopamine neurons play a critical role in the regulation of motor functions. The loss of this dopamine system is the underlying cause of Parkinson's disease, and ghrelin was recently found to have a robust action on these cells in which it promotes and protects the activity of the dorso-striatal dopamine system[104]. Elegant experiments have also revealed that besides the well-known effect of this dorso-striatal dopamine system in the regulation of movement, dopamine signaling in this pathway has direct relevance to feeding behavior as well[105-107].

The preceding examples of ghrelin action highlight the emerging view that humoral signals associated with energy metabolism have profound and direct effects on brain areas that have not classically been associated with behavioral, endocrine and autonomic regulation of peripheral tissue functions.

Like ghrelin, the adipose hormone, leptin, has also been shown to impact these structures and associated brain functions, such as motivated behavior, learning and memory[108]. Functional imaging studies of the human brain confirm that these effects of the peripheral metabolic hormones do target the same brain sites that were unmasked in experimental animal models[95,109,110]. All and all, these seemingly novel and interesting findings serve to emphasize the relevance of the assertion that the function of all aspects of the central nervous system is under the control of the metabolic needs of the body and that peripheral tissues exert their requirements by shifting the activity of various brain regions, in part, by humoral signals. Thus, it is plausible that modulation of hormonal or nutrient signals important for these metabolic shifts will affect higher level brain functions and, consequently, generate psychiatric and neurological responses with likely implications to the etiology of correlated disorders. See Figure 4 for a

schematic illustration of integrative physiology and the role of the hypothalamus governing higher brain functions.

Mechanism of action of obesity therapeutics (Fig. 5)

Obesity therapies currently on the market

The great majority of the anti-obesity therapies are aimed towards combating appetite. History has shown that the development of successful drug treatments has been plagued by failure. A few drugs have been kept on the market, the longest example of which is phentermine, an amphetamine, approved by the FDA in 1959. At that time, clinical trials and rigorous safety tests were not requested by the FDA, thus phentermine has not been subjected to that type of scrutiny. However, it is known from the long usage of this drug that it causes a vast number of side effects, all related to those of the amphetamine family, but thought to be milder than the other compounds of the same family. In 2001, phentermine was withdrawn from the European market following litigation. Another amphetamine approved by the FDA at about the same time (1959) was diethylpropion (amfepramone), and it is still on the market today. Both drugs act by increasing the release of serotonin, dopamine, and norepinephrine, with higher specificity for the latter. At least two other drugs are available with mechanisms of action similar to phentermine and diethylpropion: benzphetamine (approved in 1960) and phendimetrazine (approved in 1982). All of these compounds are approved for short usage only, less than three months and all act to promote satiety through the release of serotonin and catecholamines in the brain. The action of these compounds is not selective and it is thought that their anorectic effect is due to increased levels of monoamines in several hypothalamic nuclei that leads to a sympathetic response. A myriad of other functions controlled by the brain may be altered by these drugs, such as sexual behavior, hormonal secretion, mood, cognition, and sleep. Therefore, although they remain on the market, these drugs are of limited usage.

The only drug available for long-term treatment of obesity is orlistat, a lipase inhibitor that results in decreased fat absorption in the GI tract[111]. Because orlistat inhibits fat absorption,

it causes major gastrointestinal side effects (e.g., flatulence, fatty stools, etc.), and is more tolerated in combination with a low fat diet[111-114]. A new compound called Cetilistat[115,116] (Table 1) is under development and is thought to have less severe GI side effects compared to Orlistat[115-119]. The FDA approved Orlistat in 1999, and its relatively safe profile predicts that it is likely to have a long run. When compared to all other developments in the anti-obesity pharmacopeia, orlistat may be the only compound that is not aimed at promoting satiety, but rather promotes malabsorption with theoretical promotion of appetite due to impaired absorption of nutrients. Paradoxically, the effectiveness of orlistat may be due to its side effects that motivate the patient to ingest a low fat diet. Because the severity of the side effects increases if the diet deviates from the goal of being low fat, the patients may sense the GI distress as a sort of punishment and this in turn may help them to maintain the "healthier" diet and thus, result in an effective treatment. In agreement with the fact that orlistat does not promote satiety (the state of cellular overload), it has other potential benefits besides weight loss, such as improving diabetes and cardiovascular outcomes[120-124].

Obesity therapies recently withdrawn from the market

Several agents were developed to promote serotonin signaling in the brain, which is thought to promote an anorectic response[125]. Earlier studies identified an inverse correlation between brain serotonin levels and appetite[126,127]. The administration of serotoninergic compounds to rodents increased the levels of POMC and decreased NPY mRNA in the hypothalamus[128], indicating that the promotion of serotonin signaling inhibits appetite through the hypothalamic melanocortin system. Later, it was established that serotonin agonists activate the 5-HT2c receptors in the POMC neurons[22,129,130], to promote the activity of these cells, while activating 5-HT1b receptors in the NPY/AgRP neurons[129], to inhibit their activity. The promotion of these changes in the ARC melanocortin system was dependent upon downstream melanocortin signaling[129,130] to bring about weight loss.

The first compounds approved by the FDA as appetite suppressants based upon the aforementioned mechanisms were fenfluramine (approved in 1973) and dexfenfluramine (1996), which significantly decreased body weight alone or in combination with phentermine[131,132]. In 1997, the FDA finally withdrew these drugs from the market due to increased evidence of

valvular heart disease and primary pulmonary hypertension[23,32,133-136]. These side effects were thought to be due to widespread effects of serotonin on 5-HT receptors, other than those located in the ARC and important for metabolic regulation. During the same time period (1997), the FDA approved another serotoninergic drug to reduce body weight in obese individuals called Sibutramine. This is a serotonin and noradrenaline reuptake inhibitor that has minor effects on dopamine uptake and neurotransmitter release. Besides the serotoninergic mechanism, sibutramine is also thought to decrease body weight and appetite through central alpha-1 and beta-1 adrenergic receptors, and peripheral beta-3 receptors. For a period of time, sibutramine was the standard in anti-obesity therapies to which newly developed drugs would be compared, and it was effective in reducing body weight in patients with a variety of underlying pathological conditions [137-146]. However, in 2010, the FDA withdrew sibutramine of the market due to concerns over the increased risk of cardiovascular events (heart attack and stroke). Serotoninergic drugs are developed to promote satiety by inhibiting appetite in brain centers that express serotonin receptors. There are at least two main drawbacks to the effective treatment of obesity by serotoninergic compounds that act through these pathways: (i) serotonin receptors are not, in principle, -area specific and any drug developed to act in one region will have an effect somewhere else in the body, and likely with detrimental results; (ii) by promoting satiety, these drugs shift metabolic and behavioral adaptations to a homeostatic state that lead to chronic disease; thus, despite ameliorating obesity, it leads to other undesirable consequences such as cardiovascular disorders, cancer etc. This data gives impetus to the idea that the promotion of pathways that are involved with appetite (towards negative energy balance) rather than to those pathways mentioned above will lead to more successful outcomes to health, instead of failures such as those seen thus far with anti-obesity agents (other than orlistat).

More recently, the cannabinoid system has been described to play an important role in brain function by modulating synaptic transmission. Endogenous cannabinoid neurotransmitters, like anandamide, activate G-coupled cannabinoid-1 receptors (CB1), located throughout the brain and the peripheral nervous system. CB1 receptor-inverse agonist treatment in both humans and animals inhibits food intake and increase energy expenditure, leading to a more negative energy balance, which was thought to be beneficial in the treatment of obesity and correlated disorders[147,148].

In 2006, rimonabant[149,150] was the first CB1 receptor inverse agonist to enter the market to treat obesity. But it was approved only in the European market, and did not pass FDA scrutiny. Four large Rimonabant in Obesity and Related metabolic disorders (RIO) phase III trials were run, and subsequently included in several meta-analyses and systematic reviews[151-155]. It was a promising drug since it not only decreased food intake, but also increased energy expenditure and promoted other beneficial outcomes, as improved glycemic control and lipid profile[151-153]. However, the meta-analyses and systematic reviews later showed that rimonabant increased the likelihood that patients would develop severe side effects, specifically related to brain function[154-156]. Rimonabant-treated subjects were at an increased risk for anxiety and depression, including a high risk of suicide. The number of patients needed to harm (NNH) for psychiatric adverse effects was 30. The evidence of major psychiatric side effects led to the withdrawal of rimonabant from the European market in late 2008, and the permanent suspension of all clinical studies. Taranabant[148,157,158], another CB1 receptor inverse agonist, was also under investigation to treat obesity, but failed to pass phase III trials[159-162] and was also discontinued[163]. The ubiquitous expression of CB1 receptors in the brain led to the hypothesis that antagonist (or inverse agonists) that acted solely on the periphery could promote weight loss without the psychiatric side effects. Research on this subject is under way and is showing some promise[147,164,165].

Obesity therapies recently reviewed by the FDA

As already stated, the role of serotonin signaling in the regulation of appetite has been a target of anti-obesity therapies for a long time. The non-specific side effects of these compounds have ultimately led to their failure and withdrawal from the market. Experimental evidence has revealed the 5-HT2c receptors in the brain as a more specific target to promote satiety[22,125,129,130,166], with the potential to avoid undesirable side effects. Lorcaserin is a selective 5-HT2c agonist[167,168] with a 15- to 100-fold selectivity over 5-HT2a and 5-HT2b receptors, respectively[168]. The selectivity of lorcaserin and the observed lack of effect in the release of serotonin and other monoamines in *in vitro* assays[168] represented an important difference from previous drugs such as dexfenfluramine. Three large-scale clinical trials with lorcaserin demonstrated an effective weight loss when compared to placebo: BLOOM (Behavioral

modification and Lorcaserin for Overweight and Obesity Management)[169], BLOOSSOM (Behavioral modification and Lorcaserin Second Study for Obesity Management)[170], and BLOOM-DM (in patients with type 2 diabetes mellitus)[171]. In 2009, after completing two phase III trials (BLOOM and BLOOSSOM), a new drug application was submitted to the FDA. In October 2010, the FDA issued a complete response letter stating that lorcaserin could not be approved for clinical use citing concerns about the possibility of increased malignancy in rats treated with lorcaserin, along with its modest effects in reducing body weight, thus giving lorcaserin a poor benefit-risk profile. A final report of the BLOOM-DM trial and a response to the FDA's CRL is expected shortly. Lorcaserin is thought to reduce body weight by acting as an agonist of 5-HT2c receptors in POMC neurons, however, it is noteworthy that 5-HT2c receptors are expressed in other brain areas, for example, the choroid plexus, hippocampus, hypothalamus, cerebral cortex, striatum, brainstem, spinal cord and midbrain (in rat tissues); in humans, 5-HT2c receptors were identified in the cerebral cortex, substantia nigra and cerebellum[172-175] to name a few. Thus, despite the promising effects of lorcaserin to reduce body weight, it may take longer to prove that it is a safe, specific and effective drug in the treatment of obesity.

In addition to monotherapies to treat obesity, it has been proposed that combined therapies could provide additional benefits in terms of weight reduction and improved co-morbidities, with decreased incidence of undesirable side effects, leading to a more acceptable benefit-risk profile. Two examples of combined therapies that are in advanced stages of research are Contrave© (bupropion plus naltrexone) and Qnexa© (phentermine plus topiramato).

Contrave© (Orexigen Therapeutics, Inc.) is a combination of bupropion and naltrexone, two drugs that have been approved by the FDA to treat disorders other than obesity for a long period of time. Bupropion is an atypical antidepressant that is believed to act by inhibiting both norepinephrine (NE) and dopamine reuptake in the synapse. It also reduces body weight[176,177] by a mechanism proposed to be dependent upon dopaminergic/noradrenergic signaling in the POMC neurons[178]. However, the evidence supporting this mechanism of action is weak. Indeed, the effects of NE on feeding are much more complex, and it can elicit feeding behavior by acting in other hypothalamic areas, mainly the paraventricular nucleus (PVN)[179]. The role of dopamine on the regulation of food intake is also evolving, and definitely not restricted to the regulation of

POMC neuronal activity[180-183]. On the other hand, naltrexone (and its metabolites) is a long acting opioid receptor antagonist (mainly μ- and κ-receptors), which has been used for many years in clinics to treat alcohol and opioid dependences. It is thought to act synergistically with bupropion to release POMC neurons from the inhibitory feedback mechanism that limits their activity[178]. Despite the rather non-specific mechanism of action, the bupropion/naltrexone combination has shown efficacy in reducing body weight in clinical trials without presenting major side effects[184-186]. The profile of this drug combination led to a favorable position on the part of the FDA towards Contrave© approval. In a press release[187], Orexigen Therapeutics informed the public that a reasonable and feasible cardiovascular outcomes trial (CVOT) was discussed with the FDA, and it could lead to approval for Contrave©[188].

Qnexa© (Vivus, Inc.) is a pharmacological combination of controlled-release phentermine (see above) plus topiramate. While phentermine is a long-lasting approved drug for the short-term treatment of obesity (approved by the FDA in 1959), it has not been studied in long-term clinical trials as a monotherapy. At the doses usually employed to manage obesity, phentermine is thought to act mainly through norepinephrine signaling in the brain[189]. Its counterpart, topiramate, has several mechanisms of action, and little is known about where and how it works. The FDA approved topiramate for the treatment of epilepsy (in 1996) and the prevention of migraine (in 2004). Clinical trials showed that topiramate as a monotherapy induced weight loss in obese subjects with concomitant benefits in other metabolic markers[190-192]. Despite weight reduction, topiramate has a significant number of side effects mainly related to brain function. Additionally, topiramate also inhibits carbonic anhydrase, which can account for the parestesia, taste alteration, decreased serum concentrations of bicarbonate and potassium, and increased risk of nephrolithiasis experienced in patients taking it. Qnexa© aims to combine two effective therapies that decrease body weight, utilizing lower doses compared to those used in the monotherapy to maximize weight loss and minimize side effects. Three large randomized clinical trials have been completed using different doses of Qnexa© against placebo (EQUATE, EQUIP, CONQUER)[193,194]. Qnexa© was highly effective in reducing body weight and surpassed the FDA's criteria for an anti-obesity pharmacotherapy. However, an FDA expert panel voted against approval of Qnexa© due to concerns about its side effects. Of particular note, the occurrence of psychiatric events, cognitive dysfunction, increased heart rate and the teratogenic

potential of this formulation were not welcome by the FDA panel, despite the fact that lower doses of Qnexa© have a much safer profile.

Figure 5 illustrates the mechanism of action of some of the anti-obesity drugs available in the market and the most recent withdraws.

The risk of anti-obesity drugs: side effects or unavoidable outcome?

There is an inherent "catch 22" in the promotion of satiety as a means to fight obesity. Satiety promotion hinges upon the activation of POMC neurons in the hypothalamus, which in turn supports the suppression of feeding and an increase in energy expenditure[65]. The fundamental and long-term problem of such a process is that it relies on glucose metabolism within the hypothalamus and it promotes glucose utilization in the periphery. At first glance, this may seem to be a good thing (for example lowering circulating glucose), but when the cellular consequences of these processes are considered, it becomes evident that maintaining satiety in the long run can be detrimental for tissue integrity and survival.

The ROS Paradox: POMC neurons utilize glucose as the main fuel to generate action potentials. Whether the fuel for neuronal firing is glucose (POMC neurons) or fatty acids (NPY/AgRP cells), the by-products of substrate oxidation are free radicals. However, recent data argues that ROS generation is not a simple by-product of substrate oxidation, but rather plays a critical role in the promotion of POMC neuronal firing[85]. For example, when NPY/AgRP neurons are activated during negative energy balance and they utilize long-chain fatty acids, ROS levels are not increased in these cells despite increased firing and substrate utilization[100]. However, if ROS generation is uncontrolled in the NPY/AgRP cells, neuronal firing of these cells is impaired[100]. In contrast, during positive energy balance, when glucose-utilizing POMC neurons are firing at high levels, ROS is accumulating in these cells[85]. Thus, sustained ROS levels in POMC neurons appear to favor satiety. It was recently reported that glucose-induced ROS generation in POMC neurons is actually fundamental to the promotion of satiety[85].

The involvement of ROS in support of POMC neuronal function has immediate implications for the long-term consequences of satiety promotion. The fact that satiety relies on continuous ROS production in the hypothalamus associated with glucose-triggered ROS

production in the periphery as well, argues that sustained satiety, by default, will result in ROS-induced damage in central and peripheral tissues. One of the more vulnerable peripheral tissues to increased glucose load is the heart. The preferred fuel for cardiomyocytes is fatty acids[195]. When the fuel source shifts from fatty acids to glucose in cardiomyocytes, their ability to function properly in the long run is impaired. Indeed, the reason for the most recent withdrawal of the obesity drug, sibutramine (the serotonin and noradrenaline reuptake inhibitor), was due to cardiovascular "side" effects. Therefore, it will be a daunting, if not counterproductive task to attempt to promote satiety as a means to fight obesity. Weight loss will be achieved in the short term, but at the expense of long-term health and survival.

Targeting central versus peripheral modes of action by obesity therapies: does it make a difference?

The evidence is overwhelming to stipulate that it is virtually impossible to alter behavioral aspects of feeding or energy expenditure from within the central nervous system without having a major impact on many other brain regions associated with higher brain functions. When specific neurotransmitter systems are affected, such as the serotonin or norepinephrine circuits, the intervention, by default, will affect higher brain functions, emotional states, sleep/wake cycles, etc. On the other hand, even if very specific circuits in the hypothalamus that govern feeding, the NPY/AgRP or POMC neurons, could be selectively manipulated, similar effects could be expected: the promotion of satiety will lead to a metabolic state of increased levels of circulating glucose, insulin and leptin with a concomitant decrease in the levels of circulating ghrelin and glucocorticoid. In turn, each of these metabolic signals generated from the periphery can have major direct effects on multiple sites of the central nervous system[99,104,196-202]. In the same vein, selective manipulation of the periphery by any means to promote weight loss will result in an altered constellation of circulating metabolic signals, which will consequently affect the central nervous system. Thus, from the perspective of long-term intervention, it is reasonable to conclude that either central or peripheral interventions will impact both the brain and peripheral tissues.

Anticipation and alteration of benefit/risk ratio for future obesity therapies

As the obesity epidemic continues to grow and the development of associated chronic disorders increases concomitantly, the need for some alternative to the treatment of obesity has become all the more evident. The lack of pharmacological options and the persistent failure of anti-obesity drugs to promote weight lost without significant side effects, raise the flag as to how to discern the benefit-risk profile. Currently, the FDA's criteria for the effectiveness of an anti-obesity drug are two-fold: (i) the treatment leads to a mean reduction of body weight of 5% (compared to placebo); and/or (ii) at least 35% of the subjects receiving the treatment (compared to placebo) maintain at least a 5% reduction in body weight compared to the baseline weight. These factors highlight the emphasis that the FDA places on weight reduction in the search for drugs to treat obesity. One possible problem in applying such a paradigm to assess anti-obesity drugs is that it narrows the clinical evaluation of compounds to just those that do promote weight loss. However, weight gain in obese patients usually occurs over a long period of time, leading to complex metabolic adaptations. The majority of the investigational studies evaluate the acute or short-term effect of drugs in reducing appetite/food intake or promoting weight loss. However, it is possible that the metabolic and behavioral changes that will lead to a sustained reduction in body weight may take longer to occur, thus leading to a biased investigational approach. Additionally, the criteria proposed by the FDA do not take into account the improvements in morbidity/mortality, which may be even more important than weight reduction per se. It is possible that some treatments might help to treat/delay co-morbidities related to obesity, but not obesity itself. Thus, it seems imperative that the FDA consider additional and/or alternative factors (besides weight loss) in their approval process of new treatments for obesity.

Obesity levels in the U.S. continue to climb with the expectation that not only a larger portion of the population will reach obese levels, but that obese subjects will become even heavier. This, in turn, would lead to an increased risk of co-morbidities, and consequent stratification of risk of obese patients in accordance with the level of obesity. Thus, it is also anticipated that the FDA might evaluate the benefit-risk profile of distinct anti-obesity treatments based on the degree of obesity of the patients, and eventually vote in favor of compounds with a higher risk, but which can be beneficial to extremely obese individuals. Finally, two recent reports highlight the fact that behavioral interventions may be highly effective in reducing body weight in a subpopulation of obese individuals[203,204]. For obvious reasons, an increase in exercise

and decrease in calorie intake is the most efficient way to combat obesity. These two studies just emphasized that behavioral interventions can reach this goal in some patients with efficiency similar to the best pharmacological interventions available on the market. Thus, there is still plenty of room to address new ways to pursue behavioral changes in obese patients with the aim of increasing physical activity and decreasing calorie intake.

Outlook/conclusion

Overnutrition associated with obesity is a major contributor to the propagation of chronic diseases. Suppression of obesity will benefit long-term health and survival. Thus, the need to develop medications to fight obesity is understandable from a pragmatic and conceptual perspective. However, when the biological underpinnings of behavioral and metabolic correlates of obesity are interrogated closely, it becomes less clear what paths should be taken by the pharmaceutical industry to develop therapeutics without undesired "side" effects. Weight loss can be accomplished by many different ways using individual or combination of compounds. Whether chemically it will ever be possible to shift energy balance by decreasing appetite without negatively impacting long-term tissue function and survival is a question that will continue to hunt both the pharmaceutical industry and the public.

Figure legends:

Figure 1: Humoral and nutritional cross talk between peripheral tissues and the brain. To adapt to daily variations in energy balance (intake and expenditure), our bodies sense and integrate information about energy availability that is conveyed to the brain by hormones and nutrients from the periphery. These molecules regulate feeding behavior by acting on neurons in the hypothalamus and the brainstem. During periods of satiety, the body works towards storage of the acquired nutrients. Satiety is associated with increased sympathetic activity, which promotes both insulin release by the pancreas (and thus stimulates glucose storage in the liver and muscle) and fat deposition (which leads to a rise in leptin levels). Food ingestion results in a release of incretins by the gut. These include GLP1, which stimulates the pancreas to secrete insulin; both GLP1 and insulin are thought to reduce food intake by acting directly in the brain. In pancreatic β-cells, the hormone amylin is co-released with insulin in response to a meal. It is a potent satiety signal, inhibits digestive secretion and slows gastric emptying. The precise brain targets of amylin are not known, but include the area postrema (AP) in the brainstem and the lateral hypothalamus. Conversely, during periods of hunger, the hypothalamus regulates the activity of the autonomic nervous system to promote fat release from white adipose tissue and trigger gluconeogenesis in the liver. These changes in peripheral nutrient levels lead to a decrease in the levels of thyroid hormones, insulin and leptin, and to an increase in the level of ghrelin and corticosteroids, which increase food-seeking behavior through their effect on the brain. The hormones and peptides mentioned above are only a few among a myriad of molecules thought to be involved in the regulation of energy balance. Research into this complex system continues to identify new candidates that could be pharmacologically targeted to regulate energy balance.

Figure 2: The hypothalamic melanocortin system

Top panel: In the brain, the hypothalamus (boxed area in mid saggital view of the brain) contains two critical subsets of neurons (blow up of boxed area): the NPY/AgRP/GABA cells, which when activated due to decreasing glucose and leptin levels and elevating ghrelin levels, promoter hunger and appetite, in part by suppressing the activity of neighboring POMC neurons, and antagonizing MC4 receptors in target areas. Elevating glucose and leptin levels with

subsiding ghrelin availability inhibit NPY/AgRP neurons and activate POMC cells, which in turn lead to satiety.

Lower left panel: During low glucose levels, fatty acid metabolism is increased. FA metabolism, promoted by UCP2 activity, reduces intracellular ROS levels leading to the elevated firing of NPY/AgRP neurons and decreased activity of POMC neurons.

Lower right panel: The firing of POMC neurons during elevated glucose levels (satiety) relies on cellular glucose metabolism and signaling pathways activated by leptin and insulin receptors. It appears that a fundamental signaling event that affects action potential generation in these cells is glucose-derived ROS. The same event, however, hyperpolarizes NPY/AgRP neurons and suppresses their firing.

Figure 3: Central role of the hypothalamus in integrative physiology.
The hypothalamus senses hormonal signals and metabolites from the periphery and also integrates inputs from other brain areas. Hypothalamic neurons command hormonal axes by projecting to the pituitary, and also influence the sympathetic neural output from the brainstem to peripheral organs. Both hormonal and neural outputs from the brain are important to regulate peripheral tissues function, and consequently the feedback release of hormones, nutrients and metabolites in circulation. All those, in turn, become important regulators of brain function, and different metabolic states will lead to concomitant changes in brain activity/plasticity. Hnece, higher brain areas, as for example the cortex, are also under the influence of peripheral factors that are closely related to metabolic state. Additionally, the hypothalamus projects to several subcortical structures (and in some cases, projects directly to cortical areas) as well as the cortex itself. The metabolic, nutritional, hormonal and neural integration that occurs in the hypothalamus is fundamental to govern whole body homeostasis.

Figure 4: Summary of known hypothalamic mechanisms involved in obesity in Humans.
In the ARC, NPY/AgRP/GABA neurons project to target areas to regulate energy balance; AgRP peptide is a potent endogenous antagonist of the melanocortin receptors, promoting appetite. POMC/CART neurons, on the other hand, synthesize alpha-MSH through the breakdown of POMC. Alpha-MSH is an endogenous agonist of the MC3/4R in the brain, and promotes satiety. Red dots indicate pathways that have been linked to obesity in Humans. Leptin mutant

individuals develop severe obesity that can be treated with recombinant leptin replacement. Leptin binds to its receptor and, in the POMC neurons, leads to enhance POMC transcription. Several mutations in leptin receptor have been described and are related to obesity. Rare mutations in POMC gene have also been described in clinical syndromes accompanied by obesity. The breakdown of POMC to alpha-MSH (and all the other POMC-derived peptides) depends on enzymatic cleavage of POMC by, for example, PC1. Mutations in this pathway are also linked to obesity. Finally, MC4R is the most common target of mutations related to obesity in humans, and these mutations lead to impaired signaling through the receptor and consequent satiety signals to occur.

Figure 5: Mechanism of action of the main anti-obesity drugs currently in the market or withdrawn recently.
Phentermine is a non-specific drug that increases brain levels of serotonin (5HT), noradrenaline (NE) and dopamine (DA). Its anti-obesity activity is thought to occur mainly by increasing NE levels in the hypothalamus leading to increased sympathetic tone. The effects of phentermine are not specific to the hypothalamus and most of its side effects are related to drugs from the same pharmacological family (amphetamine). Orlistat is the only anti-obesity drug approved by the FDA for long-term treatment of obesity. In the intestinal mucosa, orlistat binds to endogenous lipases released by the pancreas in response to fat intake, blocking the activity of this enzyme. Lipase is involved in the breakdown of large fat molecules (triglycerides) in small fat acids that can be absorbed by the duodenal mucosa. Thus, orlistat decreases the breakdown of fat molecules and their absorption, leading to decrease calorie intake due to malabsorption. The main side effects related to orlistat are gastrointestinal, and are close related to the amount of fat in the diet. Two drugs have recently been withdrawn from the market due to potential serious side effects related to brain function. These two exemplify that pharmacological compounds designed to target the hypothalamic feeding circuitry will inexorably lead to life threatening side effects. First, sibutramine was the gold standard in anti-obesity drug therapy for several years, and its success was related to its better specificity as a blocker of 5-HT and NE reuptake in the synapse. The blockage of neurotransmitter reuptake leads to sustained increase in neurotransmitter levels in the synaptic clef. Rimonabant is a cannabinoid receptor inverse agonist (CB1 receptor), which blocks the signaling of endogenous cannabinoids (as 2-AG). The ubiquitous expression of CB1 receptors throughout the brain and the peripheral nervous system indicated that this pharmacological manipulation was not specific to feeding circuits. The withdrawn of rimonabant from the European market (it was never approved by the FDA) was due to concerns about increased depression and suicide behavior in patients taking rimonabant.

References

1 Finucane, M. M. *et al.* National, regional, and global trends in body-mass index since 1980: systematic analysis of health examination surveys and epidemiological studies with 960 country-years and 9.1 million participants. *Lancet* **377**, 557-567 (2011).

2 Ioannides-Demos, L. L., Piccenna, L. & McNeil, J. J. Pharmacotherapies for obesity: past, current, and future therapies. *J Obes* **2011**, 179674 (2011).

3 Jones, D. Suspense builds on anti-obesity rollercoaster ride. *Nat Rev Drug Discov* **10**, 5-6 (2011).

4 Huntington, M. K. & Shewmake, R. A. Anti-obesity drugs: are they worth it? *Future Med Chem* **3**, 267-269 (2011).

5 Powell, A. G., Apovian, C. M. & Aronne, L. J. New drug targets for the treatment of obesity. *Clin Pharmacol Ther* **90**, 40-51 (2011).

6 Seeley, R. J. & Woods, S. C. Monitoring of stored and available fuel by the CNS: Implications for obesity. *Nature Reviews Neuroscience* **4**, 901-909 (2003).

7 Cone, R. Studies on the physiological functions of the melanocortin system. *Endocr Rev* **27**, 736-749 (2006).

8 Gao, Q. & Horvath, T. L. Neurobiology of feeding and energy expenditure. *Annu Rev Neurosci* **30**, 367-398 (2007).

9 Fontana, L. Modulating human aging and age-associated diseases. *Bba-Gen Subjects* **1790**, 1133-1138 (2009).

10 Piper, M. D. W. & Bartke, A. Diet and aging. *Cell Metabolism* **8**, 99-104 (2008).

11 Fontana, L., Partridge, L. & Longo, V. D. Extending healthy life span--from yeast to humans. *Science* **328**, 321-326 (2010).

12 Hetherington, A. W. & Ranson, S. W. Hypothalamic lesions and adiposity in the rat. *Anat Rec* **78**, 149-172 (1940).

13 Hetherington, A. W. & Ranson, S. W. The relation of various hypothalamic lesions to adiposity in the rat. *Journal of Comparative Neurology* **76**, 475-499 (1942).

14 Hetherington, A. W. Non-production of hypothalamic obesity in the rat by lesions rostral or dorsal to the ventro-medial hypothalamic nuclei. *Journal of Comparative Neurology* **80**, 33-45 (1944).

15 Nutrition Classics. The Anatomical Record, Volume 78, 1940: Hypothalamic lesions and adiposity in the rat. *Nutr Rev* **41**, 124-127 (1983).

16 Hetherington, A. W. & Ranson, S. W. Hypothalamic-Lesions and Adiposity in the Rat. *Nutrition Reviews* **41**, 124-127 (1983).

17 Anand, B. K. & Brobeck, J. R. Hypothalamic Control of Food Intake in Rats and Cats. *Yale J Biol Med* **24**, 123-140 (1951).

18 Anand, B. K. & Brobeck, J. R. Localization of a Feeding Center in the Hypothalamus of the Rat. *P Soc Exp Biol Med* **77**, 323-324 (1951).

19 De Lecea, L. *et al.* The hypocretins: Hypothalamus-specific peptides with neuroexcitatory activity. *P Natl Acad Sci USA* **95**, 322-327 (1998).

20 Sakurai, T. *et al.* Orexins and orexin receptors: A family of hypothalamic neuropeptides and G protein-coupled receptors that regulate feeding behavior (vol 92, pg 573, 1998). *Cell* **92**, U29-U29 (1998).

21 Qu, D. Q. *et al.* A role for melanin-concentrating hormone in the central regulation of feeding behaviour. *Nature* **380**, 243-247 (1996).

22 Heisler, L. K. *et al.* Activation of central melanocortin pathways by fenfluramine. *Science* **297**, 609-611 (2002).

23 Jick, H. *et al.* A population-based study of appetite-suppressant drugs and the risk of cardiac-valve regurgitation. *N Engl J Med* **339**, 719-724 (1998).

24 Luquet, S., Perez, F., Hnasko, T. & Palmiter, R. NPY/AgRP neurons are essential for feeding in adult mice but can be ablated in neonates. *Science* **310**, 683-685 (2005).

25 Wu, Q., Boyle, M. & Palmiter, R. Loss of GABAergic signaling by AgRP neurons to the parabrachial nucleus leads to starvation. *Cell* **137**, 1225-1234 (2009).

26 Gropp, E. *et al.* Agouti-related peptide-expressing neurons are mandatory for feeding. *Nat Neurosci* **8**, 1289-1291 (2005).

27 Bewick, G. *et al.* Post-embryonic ablation of AgRP neurons in mice leads to a lean, hypophagic phenotype. *FASEB J* **19**, 1680-1682 (2005).

28 Dietrich, M. O. & Horvath, T. L. GABA keeps up an appetite for life. *Cell* **137**, 1177-1179 (2009).

29 Hahn, T., Breininger, J., Baskin, D. & Schwartz, M. Coexpression of Agrp and NPY in fasting-activated hypothalamic neurons. *Nat Neurosci* **1**, 271-272 (1998).

30 Horvath, T., Naftolin, F., Kalra, S. & Leranth, C. Neuropeptide-Y innervation of beta-endorphin-containing cells in the rat mediobasal hypothalamus: a light and electron microscopic double immunostaining analysis. *Endocrinology* **131**, 2461-2467 (1992).

31 Horvath, T. L., Bechmann, I., Naftolin, F., Kalra, S. P. & Leranth, C. Heterogeneity in the neuropeptide Y-containing neurons of the rat arcuate nucleus: GABAergic and non-GABAergic subpopulations. *Brain Research* **756**, 283-286 (1997).

32 Loke, Y. K., Derry, S. & Pritchard-Copley, A. Appetite suppressants and valvular heart disease - a systematic review. *BMC Clin Pharmacol* **2**, 6 (2002).

33 Clark, J. T., Kalra, P. S., Crowley, W. R. & Kalra, S. P. Neuropeptide-Y and Human Pancreatic-Polypeptide Stimulate Feeding-Behavior in Rats. *Endocrinology* **115**, 427-429 (1984).

34 Horvath, T. L. *et al.* GPA protects the nigrostriatal dopamine system by enhancing mitochondrial function. *Neurobiology of disease* **43**, 152-162 (2011).

35 Mineur, Y. S. *et al.* Nicotine decreases food intake through activation of POMC neurons. *Science (New York, NY)* **332**, 1330-1332 (2011).

36 Cowley, M. *et al.* Leptin activates anorexigenic POMC neurons through a neural network in the arcuate nucleus. *Nature* **411**, 480-484 (2001).

37 Pinto, S. *et al.* Rapid rewiring of arcuate nucleus feeding circuits by leptin. *Science* **304**, 110-115 (2004).

38 Ollmann, M. M. *et al.* Antagonism of central melanocortin receptors in vitro and in vivo by Agouti-related protein. *Science* **278**, 135-138 (1997).

39 Qian, S. *et al.* Neither agouti-related protein nor neuropeptide Y is critically required for the regulation of energy homeostasis in mice. *Molecular and Cellular Biology* **22**, 5027-5035 (2002).

40 Wu, Q., Howell, M. P. & Palmiter, R. D. Ablation of neurons expressing agouti-related protein activates Fos and gliosis in postsynaptic target regions. *Journal of Neuroscience* **28**, 9218-9226 (2008).

41 Yaswen, L., Diehl, N., Brennan, M. B. & Hochgeschwender, U. Obesity in the mouse model of pro-opiomelanocortin deficiency responds to peripheral melanocortin. *Nature medicine* **5**, 1066-1070 (1999).

42 Yen, T. T., Gill, A. M., Frigeri, L. G., Barsh, G. S. & Wolff, G. L. Obesity, diabetes, and neoplasia in yellow A(vy)/- mice: ectopic expression of the agouti gene. *The FASEB journal : official publication of the Federation of American Societies for Experimental Biology* **8**, 479-488 (1994).

43 Huszar, D. *et al.* Targeted disruption of the melanocortin-4 receptor results in obesity in mice. *Cell* **88**, 131-141 (1997).

44 Butler, A. A. *et al.* A unique metabolic syndrome causes obesity in the melanocortin-3 receptor-deficient mouse. *Endocrinology* **141**, 3518-3521 (2000).

45 Krude, H. *et al.* Severe early-onset obesity, adrenal insufficiency and red hair pigmentation caused by POMC mutations in humans. *Nature genetics* **19**, 155-157 (1998).

46 Clément, K. *et al.* Unexpected endocrine features and normal pigmentation in a young adult patient carrying a novel homozygous mutation in the POMC gene. *The Journal of clinical endocrinology and metabolism* **93**, 4955-4962 (2008).

47 Vaisse, C., Clement, K., Guy-Grand, B. & Froguel, P. A frameshift mutation in human MC4R is associated with a dominant form of obesity. *Nature genetics* **20**, 113-114 (1998).

48 Yeo, G. S. *et al.* A frameshift mutation in MC4R associated with dominantly inherited human obesity. *Nature genetics* **20**, 111-112 (1998).

49 Farooqi, I. S. *et al.* Dominant and recessive inheritance of morbid obesity associated with melanocortin 4 receptor deficiency. *The Journal of clinical investigation* **106**, 271-279 (2000).

50 Vaisse, C. *et al.* Melanocortin-4 receptor mutations are a frequent and heterogeneous cause of morbid obesity. *The Journal of clinical investigation* **106**, 253-262 (2000).

51 Farooqi, I. S. *et al.* Clinical spectrum of obesity and mutations in the melanocortin 4 receptor gene. *The New England journal of medicine* **348**, 1085-1095 (2003).

52 Branson, R. *et al.* Binge eating as a major phenotype of melanocortin 4 receptor gene mutations. *The New England journal of medicine* **348**, 1096-1103 (2003).

53 Fan, W. *et al.* The central melanocortin system can directly regulate serum insulin levels. *Endocrinology* **141**, 3072-3079 (2000).

54 Wiedmer, P. *et al.* The HPA axis modulates the CNS melanocortin control of liver triacylglyceride metabolism. *Physiol Behav* **105**, 791-799 (2011).

55 Perez-Tilve, D. *et al.* Melanocortin signaling in the CNS directly regulates circulating cholesterol. *Nature neuroscience* **13**, 877-882 (2010).

56 Vella, K. R. *et al.* NPY and MC4R Signaling Regulate Thyroid Hormone Levels during Fasting through Both Central and Peripheral Pathways. *Cell Metabolism* (2011).

57 Preston, E. *et al.* Central neuropeptide Y infusion and melanocortin 4 receptor antagonism inhibit thyrotropic function by divergent pathways. *Neuropeptides* **45**, 407-415 (2011).

58 Tong, Q., Ye, C. P., Jones, J. E., Elmquist, J. K. & Lowell, B. B. Synaptic release of GABA by AgRP neurons is required for normal regulation of energy balance. *Nature neuroscience* **11**, 998-1000 (2008).

59 Wu, Q. & Palmiter, R. D. GABAergic signaling by AgRP neurons prevents anorexia via a melanocortin-independent mechanism. *European journal of pharmacology* **660**, 21-27 (2011).

60 Wu, Q., Howell, M. P., Cowley, M. A. & Palmiter, R. D. Starvation after AgRP neuron ablation is independent of melanocortin signaling. *P Natl Acad Sci USA* **105**, 2687-2692 (2008).

61 Grandison, L. & Guidotti, A. Stimulation of food intake by muscimol and beta endorphin. *Neuropharmacology* **16**, 533-536 (1977).

62 Kelly, J., Alheid, G. F., Newberg, A. & Grossman, S. P. GABA stimulation and blockade in the hypothalamus and midbrain: effects on feeding and locomotor activity. *Pharmacology, biochemistry, and behavior* **7**, 537-541 (1977).

63 Przewlocka, B., Stala, L. & Scheel-Kruger, J. Evidence that GABA in the nucleus dorsalis raphe induces stimulation of locomotor activity and eating behavior. *Life sciences* **25**, 937-945 (1979).

64 Kelly, J., Rothstein, J. & Grossman, S. P. GABA and hypothalamic feeding systems. I. Topographic analysis of the effects of microinjections of muscimol. *Physiol Behav* **23**, 1123-1134 (1979).

65 Cone, R. D. Anatomy and regulation of the central melanocortin system. *Nature neuroscience* **8**, 571-578 (2005).

66 Zhang, Y. *et al.* Positional cloning of the mouse obese gene and its human homologue. *Nature* **372**, 425-432 (1994).

67 Halaas, J. L. *et al.* Weight-reducing effects of the plasma protein encoded by the obese gene. *Science* **269**, 543-546 (1995).

68 Farooqi, I. S. Genetic aspects of severe childhood obesity. *Pediatric endocrinology reviews : PER* **3 Suppl 4**, 528-536 (2006).

69 Farooqi, I. S. Monogenic human obesity syndromes. *Progress in brain research* **153**, 119-125 (2006).

70 Farooqi, I. S. *et al.* Clinical and molecular genetic spectrum of congenital deficiency of the leptin receptor. *The New England journal of medicine* **356**, 237-247 (2007).

71 Hummel, K. P., Dickie, M. M. & Coleman, D. L. Diabetes, a new mutation in the mouse. *Science* **153**, 1127-1128 (1966).

72 Tartaglia, L. A. *et al.* Identification and expression cloning of a leptin receptor, OB-R. *Cell* **83**, 1263-1271 (1995).

73 Chen, H. *et al.* Evidence that the diabetes gene encodes the leptin receptor: identification of a mutation in the leptin receptor gene in db/db mice. *Cell* **84**, 491-495 (1996).

74 Montague, C. T. *et al.* Congenital leptin deficiency is associated with severe early-onset obesity in humans. *Nature* **387**, 903-908 (1997).

75 Farooqi, I. S. *et al.* Effects of recombinant leptin therapy in a child with congenital leptin deficiency. *The New England journal of medicine* **341**, 879-884 (1999).

76 Considine, R. V. *et al.* Serum immunoreactive-leptin concentrations in normal-weight and obese humans. *The New England journal of medicine* **334**, 292-295 (1996).

77 Maffei, M. *et al.* Leptin levels in human and rodent: measurement of plasma leptin and ob RNA in obese and weight-reduced subjects. *Nature medicine* **1**, 1155-1161 (1995).

78 Halaas, J. L. *et al.* Physiological response to long-term peripheral and central leptin infusion in lean and obese mice. *P Natl Acad Sci USA* **94**, 8878-8883 (1997).

79 Cusin, I., Rohner-Jeanrenaud, F., Stricker-Krongrad, A. & Jeanrenaud, B. The weight-reducing effect of an intracerebroventricular bolus injection of leptin in genetically obese fa/fa rats. Reduced sensitivity compared with lean animals. *Diabetes* **45**, 1446-1450 (1996).

80 Vaisse, C. *et al.* Leptin activation of Stat3 in the hypothalamus of wild-type and ob/ob mice but not db/db mice. *Nature genetics* **14**, 95-97 (1996).

81 Bjorbaek, C., Elmquist, J. K., Frantz, J. D., Shoelson, S. E. & Flier, J. S. Identification of SOCS-3 as a potential mediator of central leptin resistance. *Molecular cell* **1**, 619-625 (1998).

82 Ozcan, L. *et al.* Endoplasmic reticulum stress plays a central role in development of leptin resistance. *Cell Metabolism* **9**, 35-51 (2009).

83 Ozcan, U. *et al.* Endoplasmic reticulum stress links obesity, insulin action, and type 2 diabetes. *Science* **306**, 457-461 (2004).

84 Ozcan, U. *et al.* Chemical chaperones reduce ER stress and restore glucose homeostasis in a mouse model of type 2 diabetes. *Science* **313**, 1137-1140 (2006).

85 Diano, S. *et al.* Peroxisome proliferation-associated control of reactive oxygen species sets melanocortin tone and feeding in diet-induced obesity. *Nature medicine* **17**, 1121-1127 (2011).

86 Toro, A. A. *et al.* Pex3p-dependent peroxisomal biogenesis initiates in the endoplasmic reticulum of human fibroblasts. *J Cell Biochem* **107**, 1083-1096 (2009).

87 Titorenko, V. I. & Mullen, R. T. Peroxisome biogenesis: the peroxisomal endomembrane system and the role of the ER. *The Journal of cell biology* **174**, 11-17 (2006).

88 Schluter, A. *et al.* The evolutionary origin of peroxisomes: an ER-peroxisome connection. *Mol Biol Evol* **23**, 838-845 (2006).

89 Andrews, Z. *et al.* UCP2 mediates ghrelin's action on NPY/AgRP neurons by lowering free radicals. *Nature* **454**, 846-851 (2008).

90 Horvath, T. L., Andrews, Z. B. & Diano, S. Fuel utilization by hypothalamic neurons: roles for ROS. *Trends Endocrin Met* **20**, 78-87 (2009).

91 Kojima, M. *et al.* Ghrelin is a growth-hormone-releasing acylated peptide from stomach. *Nature* **402**, 656-660 (1999).

92 Tschop, M., Smiley, D. L. & Heiman, M. L. Ghrelin induces adiposity in rodents. *Nature* **407**, 908-913 (2000).

93 Cowley, M. A. *et al.* The distribution and mechanism of action of ghrelin in the CNS demonstrates a novel hypothalamic circuit regulating energy homeostasis. *Neuron* **37**, 649-661 (2003).

94 Carlini, V. P. *et al.* Differential role of the hippocampus, amygdala, and dorsal raphe nucleus in regulating feeding, memory, and anxiety-like behavioral responses to ghrelin. *Biochem Bioph Res Co* **313**, 635-641 (2004).

95 Malik, S., McGlone, F., Bedrossian, D. & Dagher, A. Ghrelin modulates brain activity in areas that control appetitive behavior. *Cell Metabolism* **7**, 400-409 (2008).

96 Horvath, T. L. *et al.* Synaptic input organization of the melanocortin system predicts diet-induced hypothalamic reactive gliosis and obesity. *P Natl Acad Sci USA* **107**, 14875-14880 (2010).

97 Yang, Y., Atasoy, D., Su, H. H. & Sternson, S. M. Hunger states switch a flip-flop memory circuit via a synaptic AMPK-dependent positive feedback loop. *Cell* **146**, 992-1003 (2011).

98 Dietrich, M. O. & Horvath, T. L. Synaptic plasticity of feeding circuits: hormones and hysteresis. *Cell* **146**, 863-865 (2011).

99 Abizaid, A. *et al.* Ghrelin modulates the activity and synaptic input organization of midbrain dopamine neurons while promoting appetite. *The Journal of clinical investigation* **116**, 3229-3239 (2006).

100 Andrews, Z. B. *et al.* UCP2 mediates ghrelin's action on NPY/AgRP neurons by lowering free radicals. *Nature* **454**, 846-851 (2008).

101 Kohno, D., Sone, H., Minokoshi, Y. & Yada, T. Ghrelin raises [Ca2+]i via AMPK in hypothalamic arcuate nucleus NPY neurons. *Biochem Bioph Res Co* **366**, 388-392 (2008).

102 Diano, S. *et al.* Ghrelin controls hippocampal spine synapse density and memory performance. *Nature Neuroscience* **9**, 381-388 (2006).

103 Abizaid, A. *et al.* Ghrelin modulates the activity and synaptic input organization of midbrain dopamine neurons while promoting appetite. *J Clin Invest* **116**, 3229-3239 (2006).

104 Andrews, Z. B. *et al.* Ghrelin Promotes and Protects Nigrostriatal Dopamine Function via a UCP2-Dependent Mitochondrial Mechanism. *Journal of Neuroscience* **29**, 14057-14065 (2009).

105 Szczypka, M. S. *et al.* Dopamine production in the caudate putamen restores feeding in dopamine-deficient mice. *Neuron* **30**, 819-828 (2001).

106 Szczypka, M. S. *et al.* Feeding behavior in dopamine-deficient mice. *P Natl Acad Sci USA* **96**, 12138-12143 (1999).

107 Szczypka, M. S., Rainey, M. A. & Palmiter, R. D. Dopamine is required for hyperphagia in Lep(ob/ob) mice. *Nat Genet* **25**, 102-104 (2000).

108 Morrison, C. D. Leptin signaling in brain: A link between nutrition and cognition? *Bba-Mol Basis Dis* **1792**, 401-408 (2009).

109 Farooqi, I. S. *et al.* Leptin regulates striatal regions and human eating Behavior. *Science* **317**, 1355-1355 (2007).

110 Batterham, R. L. *et al.* PYY modulation of cortical and hypothalamic brain areas predicts feeding behaviour in humans. *Nature* **450**, 106-+ (2007).

111 Guerciolini, R. Mode of action of orlistat. *Int J Obes Relat Metab Disord* **21 Suppl 3**, S12-23 (1997).

112 Hartmann, D., Hussain, Y., Guzelhan, C. & Odink, J. Effect on dietary fat absorption of orlistat, administered at different times relative to meal intake. *Br J Clin Pharmacol* **36**, 266-270 (1993).

113 Drent, M. L. *et al.* Orlistat (Ro 18-0647), a lipase inhibitor, in the treatment of human obesity: a multiple dose study. *Int J Obes Relat Metab Disord* **19**, 221-226 (1995).

114 James, W. P., Avenell, A., Broom, J. & Whitehead, J. A one-year trial to assess the value of orlistat in the management of obesity. *Int J Obes Relat Metab Disord* **21 Suppl 3**, S24-30 (1997).

115 Padwal, R. Cetilistat, a new lipase inhibitor for the treatment of obesity. *Curr Opin Investig Drugs* **9**, 414-421 (2008).

116 Yamada, Y., Kato, T., Ogino, H., Ashina, S. & Kato, K. Cetilistat (ATL-962), a novel pancreatic lipase inhibitor, ameliorates body weight gain and improves lipid profiles in rats. *Horm Metab Res* **40**, 539-543 (2008).

117 Kopelman, P. *et al.* Cetilistat (ATL-962), a novel lipase inhibitor: a 12-week randomized, placebo-controlled study of weight reduction in obese patients. *Int J Obes (Lond)* **31**, 494-499 (2007).

118 Bryson, A., de la Motte, S. & Dunk, C. Reduction of dietary fat absorption by the novel gastrointestinal lipase inhibitor cetilistat in healthy volunteers. *Br J Clin Pharmacol* **67**, 309-315 (2009).

119 Kopelman, P. *et al.* Weight loss, HbA1c reduction, and tolerability of cetilistat in a randomized, placebo-controlled phase 2 trial in obese diabetics: comparison with orlistat (Xenical). *Obesity (Silver Spring)* **18**, 108-115 (2010).

120 Hollander, P. A. *et al.* Role of orlistat in the treatment of obese patients with type 2 diabetes. A 1-year randomized double-blind study. *Diabetes Care* **21**, 1288-1294 (1998).

121 Heymsfield, S. B. *et al.* Effects of weight loss with orlistat on glucose tolerance and progression to type 2 diabetes in obese adults. *Arch Intern Med* **160**, 1321-1326 (2000).

122 Kelley, D. E. *et al.* Clinical efficacy of orlistat therapy in overweight and obese patients with insulin-treated type 2 diabetes: A 1-year randomized controlled trial. *Diabetes Care* **25**, 1033-1041 (2002).

123 Miles, J. M. *et al.* Effect of orlistat in overweight and obese patients with type 2 diabetes treated with metformin. *Diabetes Care* **25**, 1123-1128 (2002).

124 Hanefeld, M. & Sachse, G. The effects of orlistat on body weight and glycaemic control in overweight patients with type 2 diabetes: a randomized, placebo-controlled trial. *Diabetes Obes Metab* **4**, 415-423 (2002).

125 Garfield, A. S. & Heisler, L. K. Pharmacological targeting of the serotonergic system for the treatment of obesity. *J Physiol* **587**, 49-60 (2009).

126 Saller, C. F. & Stricker, E. M. Hyperphagia and increased growth in rats after intraventricular injection of 5,7-dihydroxytryptamine. *Science* **192**, 385-387 (1976).

127 Fletcher, P. J. & Paterson, I. A. A comparison of the effects of tryptamine and 5-hydroxytryptamine on feeding following injection into the paraventricular nucleus of the hypothalamus. *Pharmacol Biochem Behav* **32**, 907-911 (1989).

128 Choi, S., Blake, V., Cole, S. & Fernstrom, J. D. Effects of chronic fenfluramine administration on hypothalamic neuropeptide mRNA expression. *Brain Res* **1087**, 83-86 (2006).

129 Heisler, L. K. *et al.* Serotonin reciprocally regulates melanocortin neurons to modulate food intake. *Neuron* **51**, 239-249 (2006).

130 Lam, D. D. *et al.* Serotonin 5-HT2C receptor agonist promotes hypophagia via downstream activation of melanocortin 4 receptors. *Endocrinology* **149**, 1323-1328 (2008).

131 Guy-Grand, B. *et al.* International trial of long-term dexfenfluramine in obesity. *Lancet* **2**, 1142-1145 (1989).

132 Mathus-Vliegen, E. M., van de Voorde, K., Kok, A. M. & Res, A. M. Dexfenfluramine in the treatment of severe obesity: a placebo-controlled investigation of the effects on weight loss, cardiovascular risk factors, food intake and eating behaviour. *J Intern Med* **232**, 119-127 (1992).

133 Abenhaim, L. *et al.* Appetite-suppressant drugs and the risk of primary pulmonary hypertension. International Primary Pulmonary Hypertension Study Group. *N Engl J Med* **335**, 609-616 (1996).

134 Devereux, R. B. Appetite suppressants and valvular heart disease. *N Engl J Med* **339**, 765-766 (1998).

135 From the Centers for Disease Control and Prevention. Cardiac valvulopathy associated with exposure to fenfluramine or dexfenfluramine: US Department of Health and Human Services interim public health recommendations, November 1997. *JAMA* **278**, 1729-1731 (1997).

136 Delcroix, M., Kurz, X., Walckiers, D., Demedts, M. & Naeije, R. High incidence of primary pulmonary hypertension associated with appetite suppressants in Belgium. *Eur Respir J* **12**, 271-276 (1998).

137 Weintraub, M., Rubio, A., Golik, A., Byrne, L. & Scheinbaum, M. L. Sibutramine in weight control: a dose-ranging, efficacy study. *Clin Pharmacol Ther* **50**, 330-337 (1991).

138 Bray, G. A. *et al.* A double-blind randomized placebo-controlled trial of sibutramine. *Obes Res* **4**, 263-270 (1996).

139 Rolls, B. J., Shide, D. J., Thorwart, M. L. & Ulbrecht, J. S. Sibutramine reduces food intake in non-dieting women with obesity. *Obes Res* **6**, 1-11 (1998).

140 Seagle, H. M., Bessesen, D. H. & Hill, J. O. Effects of sibutramine on resting metabolic rate and weight loss in overweight women. *Obes Res* **6**, 115-121 (1998).

141 Hanotin, C., Thomas, F., Jones, S. P., Leutenegger, E. & Drouin, P. A comparison of sibutramine and dexfenfluramine in the treatment of obesity. *Obes Res* **6**, 285-291 (1998).

142 Bray, G. A. *et al.* Sibutramine produces dose-related weight loss. *Obes Res* **7**, 189-198 (1999).

143 Tambascia, M. A. *et al.* Sibutramine enhances insulin sensitivity ameliorating metabolic parameters in a double-blind, randomized, placebo-controlled trial. *Diabetes Obes Metab* **5**, 338-344 (2003).

144 Sanchez-Reyes, L. *et al.* Use of sibutramine in overweight adult hispanic patients with type 2 diabetes mellitus: a 12-month, randomized, double-blind, placebo-controlled clinical trial. *Clin Ther* **26**, 1427-1435 (2004).

145 Garcia-Morales, L. M. *et al.* Use of sibutramine in obese mexican adolescents: a 6-month, randomized, double-blind, placebo-controlled, parallel-group trial. *Clin Ther* **28**, 770-782 (2006).

146 Lindholm, A. *et al.* Effect of sibutramine on weight reduction in women with polycystic ovary syndrome: a randomized, double-blind, placebo-controlled trial. *Fertil Steril* **89**, 1221-1228 (2008).

147 Cota, D. *et al.* The endogenous cannabinoid system affects energy balance via central orexigenic drive and peripheral lipogenesis. *The Journal of clinical investigation* **112**, 423-431 (2003).

148 Addy, C. *et al.* The acyclic CB1R inverse agonist taranabant mediates weight loss by increasing energy expenditure and decreasing caloric intake. *Cell Metabolism* **7**, 68-78 (2008).

149 Rinaldi-Carmona, M. *et al.* SR141716A, a potent and selective antagonist of the brain cannabinoid receptor. *FEBS letters* **350**, 240-244 (1994).

150 Rinaldi-Carmona, M. *et al.* Biochemical and pharmacological characterisation of SR141716A, the first potent and selective brain cannabinoid receptor antagonist. *Life sciences* **56**, 1941-1947 (1995).

151 Després, J.-P., Golay, A., Sjöström, L. & Group, R. i. O.-L. S. Effects of rimonabant on metabolic risk factors in overweight patients with dyslipidemia. *The New England journal of medicine* **353**, 2121-2134 (2005).

152 Van Gaal, L. F. *et al.* Effects of the cannabinoid-1 receptor blocker rimonabant on weight reduction and cardiovascular risk factors in overweight patients: 1-year experience from the RIO-Europe study. *Lancet* **365**, 1389-1397 (2005).

153 Pi-Sunyer, F. X. *et al.* Effect of rimonabant, a cannabinoid-1 receptor blocker, on weight and cardiometabolic risk factors in overweight or obese patients: RIO-North America: a randomized controlled trial. *JAMA : the journal of the American Medical Association* **295**, 761-775 (2006).

154 Curioni, C. & André, C. Rimonabant for overweight or obesity. *Cochrane database of systematic reviews (Online)*, CD006162 (2006).

155 Christensen, R., Kristensen, P. K., Bartels, E. M., Bliddal, H. & Astrup, A. Efficacy and safety of the weight-loss drug rimonabant: a meta-analysis of randomised trials. *Lancet* **370**, 1706-1713 (2007).

156 Nathan, P. J., O'Neill, B. V., Napolitano, A. & Bullmore, E. T. Neuropsychiatric Adverse Effects of Centrally Acting Antiobesity Drugs. *CNS neuroscience & therapeutics* (2010).

157 Addy, C. *et al.* Multiple-dose pharmacokinetics, pharmacodynamics, and safety of taranabant, a novel selective cannabinoid-1 receptor inverse agonist, in healthy male volunteers. *Journal of clinical pharmacology* **48**, 734-744 (2008).

158 Addy, C. *et al.* Safety, tolerability, pharmacokinetics, and pharmacodynamic properties of taranabant, a novel selective cannabinoid-1 receptor inverse agonist, for the treatment of obesity: results from a double-blind, placebo-controlled, single oral dose study in healthy volunteers. *Journal of clinical pharmacology* **48**, 418-427 (2008).

159 Wadden, T. A. *et al.* A randomized trial of lifestyle modification and taranabant for maintaining weight loss achieved with a low-calorie diet. *Obesity (Silver Spring, Md.)* **18**, 2301-2310 (2010).

160 Proietto, J. *et al.* A clinical trial assessing the safety and efficacy of the CB1R inverse agonist taranabant in obese and overweight patients: low-dose study. *International journal of obesity (2005)* **34**, 1243-1254 (2010).

161 Kipnes, M. S. *et al.* A one-year study to assess the safety and efficacy of the CB1R inverse agonist taranabant in overweight and obese patients with type 2 diabetes. *Diabetes, obesity & metabolism* **12**, 517-531 (2010).

162 Aronne, L. J. *et al.* A clinical trial assessing the safety and efficacy of taranabant, a CB1R inverse agonist, in obese and overweight patients: a high-dose study. *International journal of obesity (2005)* **34**, 919-935 (2010).

163 Koch, L. Obesity: Taranabant no longer developed as an antiobesity agent. *Nature reviews. Endocrinology* **6**, 300 (2010).

164 Nogueiras, R. *et al.* Peripheral, but not central, CB1 antagonism provides food intake-independent metabolic benefits in diet-induced obese rats. *Diabetes* **57**, 2977-2991 (2008).

165 Son, M.-H. *et al.* Peripherally acting CB1-receptor antagonist: the relative importance of central and peripheral CB1 receptors in adiposity control. *International journal of obesity (2005)* **34**, 547-556 (2010).

166 Heisler, L. K. *et al.* Central serotonin and melanocortin pathways regulating energy homeostasis. *Annals of the New York Academy of Sciences* **994**, 169-174 (2003).

167 Smith, B. M. *et al.* Discovery and structure-activity relationship of (1R)-8-chloro-2,3,4,5-tetrahydro-1-methyl-1H-3-benzazepine (Lorcaserin), a selective serotonin 5-HT2C receptor agonist for the treatment of obesity. *Journal of medicinal chemistry* **51**, 305-313 (2008).

168 Thomsen, W. J. *et al.* Lorcaserin, a novel selective human 5-hydroxytryptamine2C agonist: in vitro and in vivo pharmacological characterization. *J Pharmacol Exp Ther* **325**, 577-587 (2008).

169 Smith, S. R. *et al.* Multicenter, placebo-controlled trial of lorcaserin for weight management. *The New England journal of medicine* **363**, 245-256 (2010).

170 Fidler, M. C. *et al.* A one-year randomized trial of lorcaserin for weight loss in obese and overweight adults: the BLOSSOM trial. *The Journal of clinical endocrinology and metabolism* **96**, 3067-3077 (2011).

171 Arena Pharmaceuticals, I. *Lorcaserin Phase 3 Clinical Trial in Patients with Type 2 Diabetes Shows Statistically Significant Weight Loss*, <http://invest.arenapharm.com/releasedetail.cfm?releaseid=528113> (2010).

172 Clemett, D. A., Punhani, T., Duxon, M. S., Blackburn, T. P. & Fone, K. C. Immunohistochemical localisation of the 5-HT2C receptor protein in the rat CNS. *Neuropharmacology* **39**, 123-132 (2000).

173 Abramowski, D., Rigo, M., Duc, D., Hoyer, D. & Staufenbiel, M. Localization of the 5-hydroxytryptamine2C receptor protein in human and rat brain using specific antisera. *Neuropharmacology* **34**, 1635-1645 (1995).

174 Abramowski, D. & Staufenbiel, M. Identification of the 5-hydroxytryptamine2C receptor as a 60-kDa N-glycosylated protein in choroid plexus and hippocampus. *Journal of neurochemistry* **65**, 782-790 (1995).

175 Sharma, A., Punhani, T. & Fone, K. C. Distribution of the 5-hydroxytryptamine2C receptor protein in adult rat brain and spinal cord determined using a receptor-directed antibody: effect of 5,7-dihydroxytryptamine. *Synapse* **27**, 45-56 (1997).

176 Gadde, K. M. *et al.* Bupropion for weight loss: an investigation of efficacy and tolerability in overweight and obese women. *Obesity research* **9**, 544-551 (2001).

177 Anderson, J. W. *et al.* Bupropion SR enhances weight loss: a 48-week double-blind, placebo- controlled trial. *Obesity research* **10**, 633-641 (2002).

178 Greenway, F. L. *et al.* Rational design of a combination medication for the treatment of obesity. *Obesity* **17**, 30-39 (2009).

179 Wellman, P. J. Norepinephrine and the control of food intake. *Nutrition* **16**, 837-842 (2000).

180 Hnasko, T. S., Szczypka, M. S., Alaynick, W. A., During, M. J. & Palmiter, R. D. A role for dopamine in feeding responses produced by orexigenic agents. *Brain research* **1023**, 309-318 (2004).

181 Sotak, B. N., Hnasko, T. S., Robinson, S., Kremer, E. J. & Palmiter, R. D. Dysregulation of dopamine signaling in the dorsal striatum inhibits feeding. *Brain research* **1061**, 88-96 (2005).

182 Hnasko, T. S. *et al.* Cre recombinase-mediated restoration of nigrostriatal dopamine in dopamine-deficient mice reverses hypophagia and bradykinesia. *P Natl Acad Sci USA* **103**, 8858-8863 (2006).

183 Domingos, A. I. *et al.* Leptin regulates the reward value of nutrient. *Nature neuroscience* (2011).

184 Ornellas, T. & Chavez, B. Naltrexone SR/Bupropion SR (Contrave): A New Approach to Weight Loss in Obese Adults. *P T* **36**, 255-262 (2011).

185 Wadden, T. A. *et al.* Weight loss with naltrexone SR/bupropion SR combination therapy as an adjunct to behavior modification: the COR-BMOD trial. *Obesity* **19**, 110-120 (2011).

186 Greenway, F. L. *et al.* Effect of naltrexone plus bupropion on weight loss in overweight and obese adults (COR-I): a multicentre, randomised, double-blind, placebo-controlled, phase 3 trial. *Lancet* **376**, 595-605 (2010).

187 Orexigen® Therapeutics, I. *Orexigen and FDA Identify a Clear and Feasible Path to Approval for Contrave®*, <http://ir.orexigen.com/phoenix.zhtml?c=207034&p=irol-newsArticle&ID=1608571&highlight=> (2011).

188 Ledford, H. Slim spoils for obesity drugs. *Nature* **468**, 878 (2010).

189 Rothman, R. B. & Baumann, M. H. Appetite suppressants, cardiac valve disease and combination pharmacotherapy. *Am J Ther* **16**, 354-364 (2009).

190 Wilding, J., Van Gaal, L., Rissanen, A., Vercruysse, F. & Fitchet, M. A randomized double-blind placebo-controlled study of the long-term efficacy and safety of topiramate in the treatment of obese subjects. *International journal of obesity and related metabolic disorders : journal of the International Association for the Study of Obesity* **28**, 1399-1410 (2004).

191 Bray, G. A. *et al.* A 6-month randomized, placebo-controlled, dose-ranging trial of topiramate for weight loss in obesity. *Obesity research* **11**, 722-733 (2003).

192 Tonstad, S. *et al.* Efficacy and safety of topiramate in the treatment of obese subjects with essential hypertension. *Am J Cardiol* **96**, 243-251 (2005).

193 Gadde, K. M. *et al.* Effects of low-dose, controlled-release, phentermine plus topiramate combination on weight and associated comorbidities in overweight and obese adults (CONQUER): a randomised, placebo-controlled, phase 3 trial. *Lancet* **377**, 1341-1352 (2011).

194 Allison, D. B. *et al.* Controlled-Release Phentermine/Topiramate in Severely Obese Adults: A Randomized Controlled Trial (EQUIP). *Obesity* (2011).

195 Lopaschuk, G. D. & Jaswal, J. S. Energy metabolic phenotype of the cardiomyocyte during development, differentiation, and postnatal maturation. *J Cardiovasc Pharmacol* **56**, 130-140 (2010).

196 Andrews, Z. B. *et al.* Ghrelin promotes and protects nigrostriatal dopamine function via a UCP2-dependent mitochondrial mechanism. *Journal of Neuroscience* **29**, 14057-14065 (2009).

197 Diano, S. *et al.* Ghrelin controls hippocampal spine synapse density and memory performance. *Nature neuroscience* **9**, 381-388 (2006).

198 Perry, M. L. *et al.* Leptin promotes dopamine transporter and tyrosine hydroxylase activity in the nucleus accumbens of Sprague-Dawley rats. *Journal of neurochemistry* **114**, 666-674 (2010).

199 Opland, D. M., Leinninger, G. M. & Myers, M. G. Modulation of the mesolimbic dopamine system by leptin. *Brain research* **1350**, 65-70 (2010).

200 Fulton, S. *et al.* Leptin regulation of the mesoaccumbens dopamine pathway. *Neuron* **51**, 811-822 (2006).

201 Hommel, J. D. *et al.* Leptin receptor signaling in midbrain dopamine neurons regulates feeding. *Neuron* **51**, 801-810 (2006).

202 Muller, A. P. *et al.* Exercise increases insulin signaling in the hippocampus: physiological effects and pharmacological impact of intracerebroventricular insulin administration in mice. *Hippocampus* **21**, 1082-1092 (2011).

203 Appel, L. J. *et al.* Comparative effectiveness of weight-loss interventions in clinical practice. *The New England journal of medicine* **365**, 1959-1968 (2011).

204 Wadden, T. A. *et al.* A two-year randomized trial of obesity treatment in primary care practice. *The New England journal of medicine* **365**, 1969-1979 (2011).

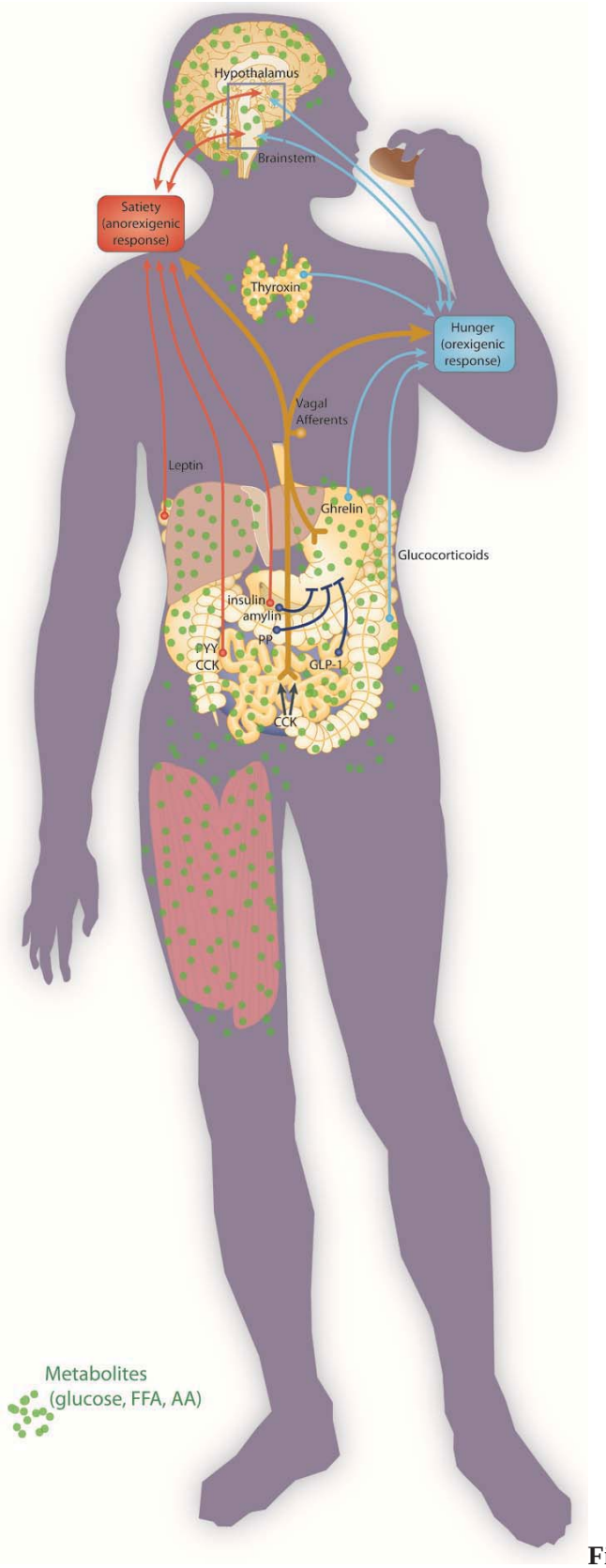
Hypothalamus
Brainstem
Satiety
(anorexigenic
response)
Thyroxin
Hunger
(orexigenic
response)
Vagal
Afferents
Leptin
Ghrelin
Glucocorticoids
insulin
amylin
PP
PYY
CCK
GLP-1
CCK
Metabolites
(glucose, FFA, AA)

Fig. 1

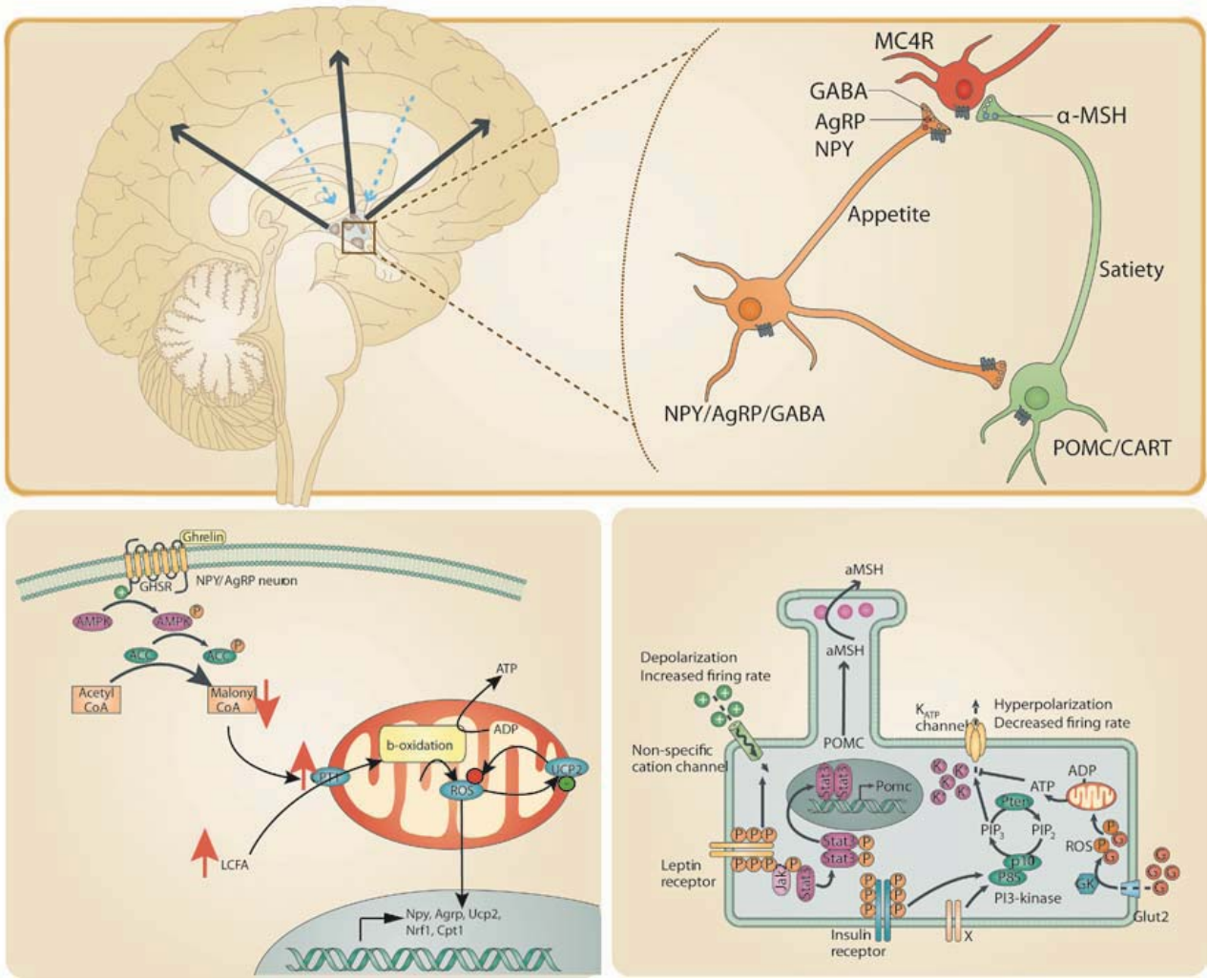
MC4R
GABA
AgRP
NPY
α-MSH
Appetite
Satiety
NPY/AgRP/GABA
POMC/CART
Ghrelin
GHSR
NPY/AgRP neuron
AMPK
ACC
Acetyl CoA
Malonyl CoA
CPT1
b-oxidation
ATP
ADP
ROS
UCP2
LCFA
Npy, Agrp, Ucp2, Nrf1, Cpt1
aMSH
Depolarization
Increased firing rate
Non-specific cation channel
POMC
Pomc
Hyperpolarization
Decreased firing rate
Leptin receptor
Jak
Stat3
PIP3
PIP2
Pten
P110
P85
PI3-kinase
GK
Glut2
Insulin receptor
X

Fig. 2

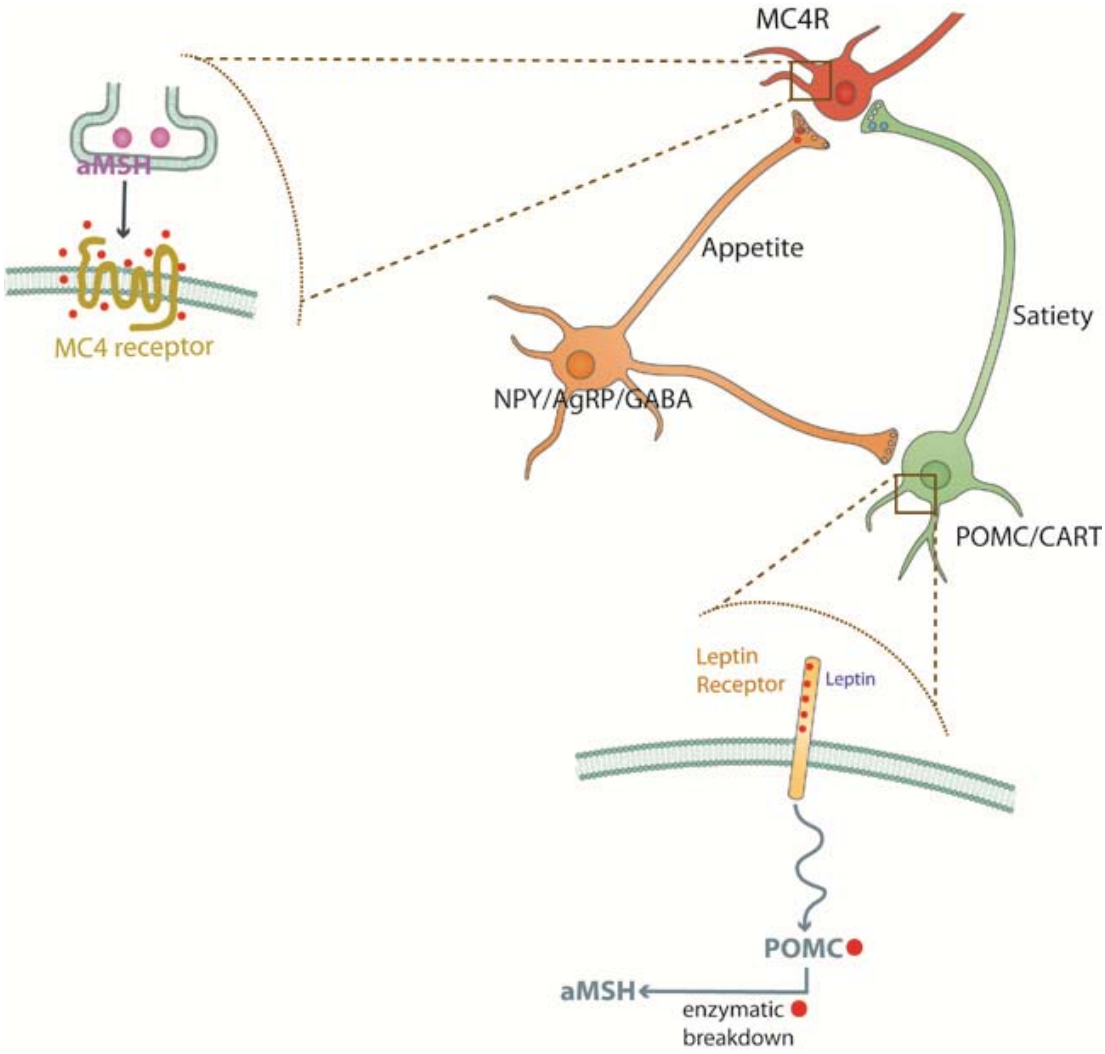
MC4R
aMSH
MC4 receptor
Appetite
Satiety
NPY/AgRP/GABA
POMC/CART
Leptin
Receptor
Leptin
POMC
aMSH
enzymatic
breakdown

Fig. 3

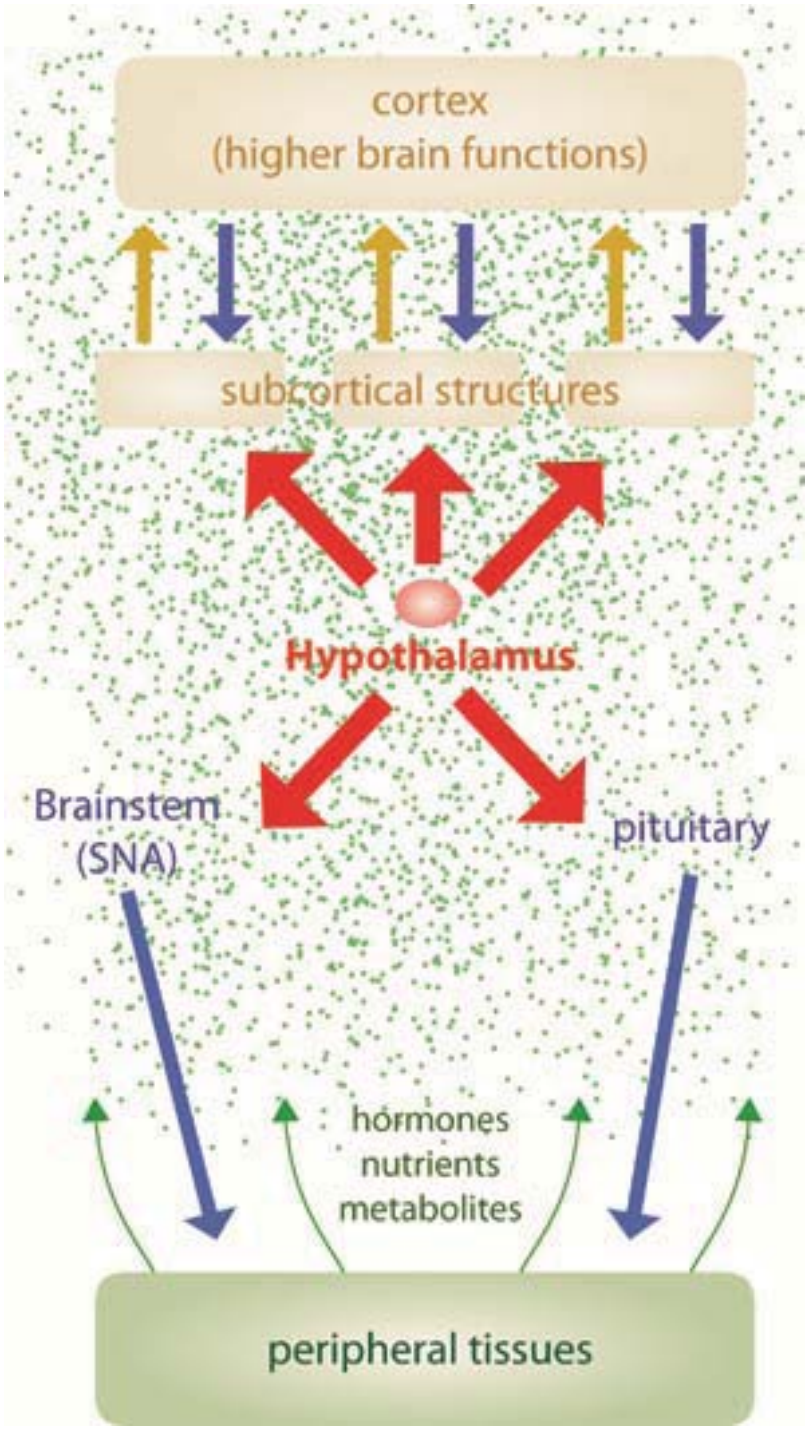
cortex
(higher brain functions)
subcortical structures
Hypothalamus
Brainstem
(SNA)
pituitary
hormones
nutrients
metabolites
peripheral tissues

Fig. 4

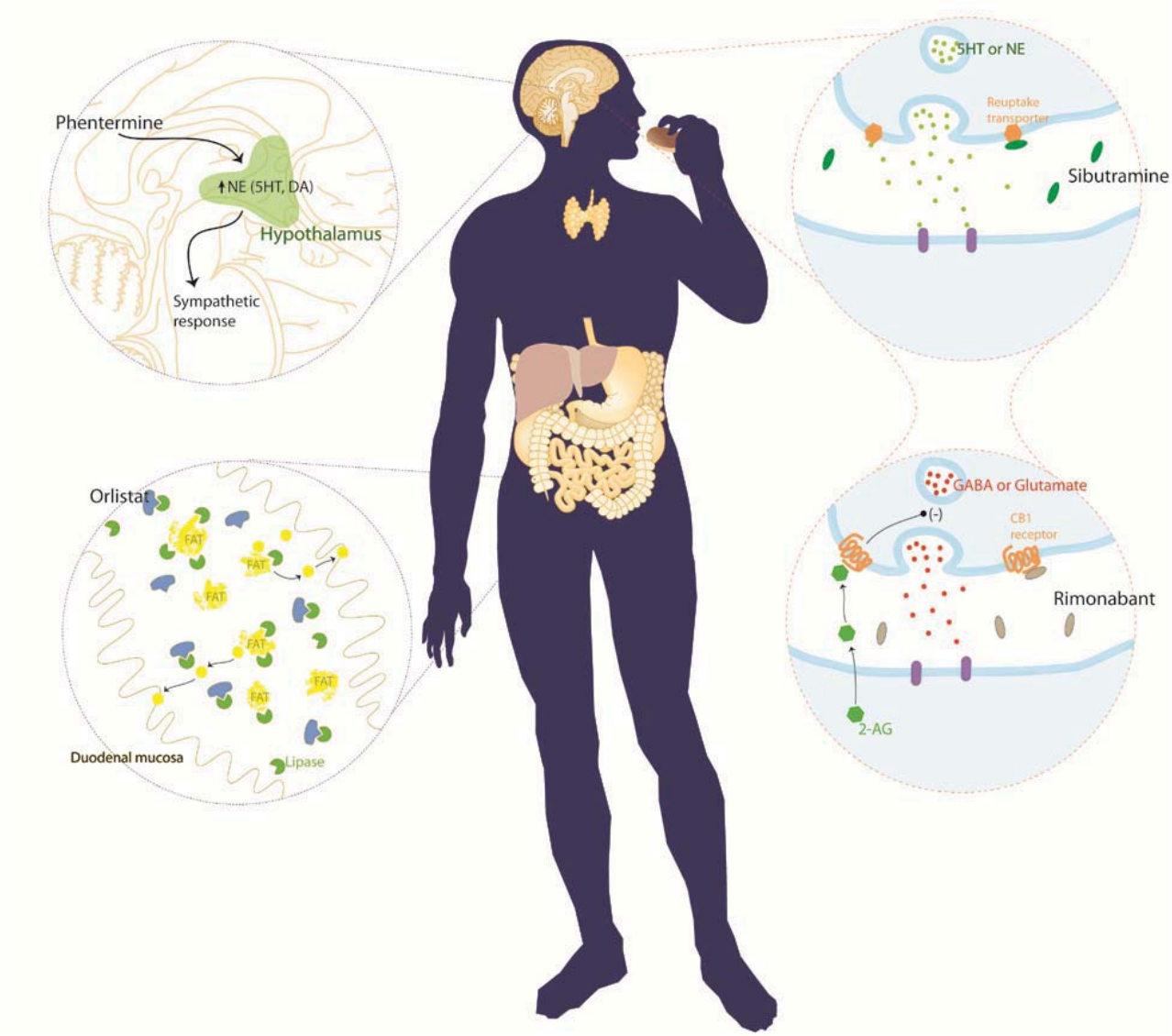
Phentermine
NE (5HT, DA)
Hypothalamus
Sympathetic response
5HT or NE
Reuptake transporter
Sibutramine
Orlistat
FAT
Duodenal mucosa
Lipase
GABA or Glutamate
(-)
CB1 receptor
Rimonabant
2-AG

Fig. 5

PARTE III

Onde os resultados apresentados nesta tese são discutidos.

Discussão

No corpo principal desta tese, apresentamos várias evidências que examinaram os mecanismos envolvidos (i) nos efeitos do exercício físico no cérebro e (ii) no controle do balanço energético pelo hipotálamo. Além disso, funções previamente não relacionadas com áreas classicamente envolvidas na regulação do apetite foram descritas. Aqui serão discutidas algumas das implicações desses estudos.

Primeiramente, mostramos que o exercício regular em camundongos leva a adaptações no hipocampo cerebral que são dependentes de uma adequada modulação da plasticidade mitocondrial (Ver capítulo I, parte II "Exercise-induced synaptogenesis in the hippocampus is dependent on UCP2-regulated mitochondrial adaptation"). Exercício aumentou o número de mitocôndrias nos neurônios hipocampais e também a respiração mitocondrial medida em homogenato do hipocampo de camundongos. O número de sinapses no DG e CA1 também aumentaram após exercício, sendo que todos estes efeitos foram dependentes da expressão da proteína desacopladora do fluxo de prótons, UCP2 (Dietrich *et al.*, 2008). Os animais deficientes de UCP2 tiveram uma diminuição no número de sinapses em DG e CA1 após exercício, enfatizando a função crítica da bioenergética mitocondrial na adaptação dos neurônios ao aumento da atividade tecidual. Este dado reforça a noção de que o exercício regular pode aumentar a produção de radicais livres no cérebro que são tamponados pela presença de UCPs (Echtay *et al.*, 2002; Produit-Zengaffinen *et al.*, 2007; Giardina *et al.*, 2008); na ausência de tais proteínas (como nos camundongos deficientes de UCP2), os efeitos benéficos do exercício podem levar a dano tecidual, devido a produção de radicais livres. Esses resultados mostram que a prática de atividade física regular pode gerar efeitos benéficos atuando

no SNC, sendo necessários mecanismos intactos de proteção tecidual contra radicais livres, como as UCPs. No capítulo II, parte II ("The role of mitochondrial uncoupling proteins in lifespan") revisamos mais extensivamente os papel das UCPs com vista nos mecanismos supracitados (Dietrich & Horvath, 2010).

Na sequência da apresentação desta tese mostramos, através de um estudo de revisão e de dois comentários críticos de artigos publicados, que a regulação da plasticidade sináptica envolvida nas adaptações necessárias para o controle do balanço energético dependem, provavelmente, de células inter-neuronais chamadas de astrócitos (Dietrich & Horvath, 2009a; Dietrich & Horvath, 2009b; 2011). Primeiramente, baseado na evidência de que a eliminação dos neurônios NPY/AgRP em animais adultos leva a morte por inanição (Luquet *et al.*, 2005; Wu *et al.*, 2009; Wu & Palmiter, 2011) e o fato de haver um período crítico de aproximadamente 10 dias - em que a manutenção do tônus GABAérgico é suficiente para reverter o desfecho fatal desta manipulação (Wu *et al.*, 2009) - nos fez concluir que um dos mecanismos possivelmente implicados em tal adaptação seja a plasticidade astrocitária (Dietrich & Horvath, 2009b). Esse mecanismo abre portas para pesquisas que visem influir sobre esse grupo de células neuronais para manipular o balanço energético ou outras funções neurais. Subsequentemente, um outro trabalho foi publicado mostrando que a modulação da plasticidade sináptica no hipotálamo é responsável pelos efeitos do balanço energético negativo na atividade dos neurônios NPY/AgRP (Yang *et al.*, 2011). Esse segundo artigo reforça nossa hipótese de que astrócitos estão associados com a plasticidade sináptica envolvida na adaptação cerebral a estímulos metabólicos (Dietrich & Horvath, 2011). Esse possível papel dos astrócitos hipotalâmicos (e extra-hipotalâmicos) na regulação da plasticidade sináptica relacionada ao balanço energético e ao status metabólico do animal é tema

atual do nosso grupo de pesquisa. Através de diversas manipulações específicas nos astrócitos estamos atualmente testando a hipótese de que estas células são capazes (e necessárias) de modular a resposta neuronal a diferentes estímulos. As vias de sinalização entre astrócitos e neurônios neste contexto são perguntas que também estamos buscando responder e são consequências diretas desta tese.

O papel crucial dos neurônios NPY/AgRP na regulação do apetite pode ser visto pelo fenótipo dos animais que têm esses neurônios eliminados na idade adulta, levando a perda de peso, diminuição do apetite e, finalmente, morte (Bewick *et al.*, 2005a; Gropp *et al.*, 2005; Luquet *et al.*, 2005). Esse mecanismo não parece ser devido a um processo inflamatório ou de resposta neurodegenerativa no hipotálamo, visto que a eliminação dos neurônios POMC – que estão localizados na mesma região - leva ao ganho de peso (Gropp *et al.*, 2005). A ativação dos neurônios NPY/AgRP agudamente no animal adulto leva a um aumento imediato da ingesta alimentar (Aponte *et al.*, 2011; Krashes *et al.*, 2011). Este papel fundamental dos neurônios NPY/AgRP na regulação do apetite acabou por direcionar nossos estudos subsequentes nesta população de células e sua implicação para fisiologia integrada do organismo.

Os neurônios NPY/AgRP são ativados em momentos de balanço energético negativo, por exemplo durante jejum ou após o tratamento com grelina (Hahn *et al.*, 1998; Takahashi & Cone, 2005; Luquet *et al.*, 2007; Andrews *et al.*, 2008; Yang *et al.*, 2011). Grelina é um hormônio produzido principalmente por células do estômago (Kojima *et al.*, 1999) que é liberado na circulação e induz uma resposta orexigênica atuando nos neurônios NPY/AgRP do ARC (Ravussin *et al.*, 2001; Tschöp *et al.*, 2001; Wang *et al.*, 2002; Cowley *et al.*, 2003; Kim *et al.*, 2003; Chen *et al.*, 2004).

Sirt1 é uma proteína com atividade deacetilase que também está relacionada com adaptações metabólicas em períodos de balanço energético negativo, como restrição calórica e jejum (Kaeberlein *et al.*, 1999; Lin *et al.*, 2000; Cohen *et al.*, 2004; Nemoto *et al.*, 2004; Chen *et al.*, 2005b; Rodgers *et al.*, 2005; Rodgers & Puigserver, 2007). Essa semelhança entre os neurônios NPY/AgRP e Sirt1, ambos sendo importantes durante balanço energético negativo, nos levou a estudar em mais detalhes o papel desta proteína neste grupo especifico de neurônios.

No capitulo VI, parte II ("AgRP neurons mediate Sirt1's action on the melanocortin system and energy balance: roles for Sirt1 in neuronal firing and synaptic plasticity"), nós mostramos que a inibição de Sirt1 nos neurônios NPY/AgRP leva a diminuição da atividade destas células. Além disso, células deficientes de Sirt1 não responderam ao tratamento com grelina. Tratamento de camundongos com inibidor de Sirt1 levou a diminuição do apetite, sem efeitos colaterais significativos. Essa diminuição do apetite foi acompanhada por uma diminuição significativa das sinapses inibitórias nos neurônios POMC e aumento do número de mitocôndrias nestas células, significando um aumento na atividade dessa população de neurônios após inibição de Sirt1. Os efeitos da inibição de Sirt1 no apetite foram dependentes do sistema de melanocortinas e da presença de UCP2. Um achado importante desse estudo foi o efeito tardio da inibição de Sirt1 na diminuição do apetite. Quando os camundongos foram tratados com o inibidor de Sirt1, a diminuição da ingesta alimentar ocorreu aproximadamente 4 horas após o tratamento. Esse efeito comportamental correlaciona-se com mudanças na inervação sináptica dos neurônios POMC, evidenciando o papel fundamental da plasticidade sináptica nas adaptações metabólicas que ocorrem no sistema de melanocortinas (ver também capítulos "Feeding signals and brain circuitry", "GABA keeps up an appetite for life",

e “Synaptic plasticity of feeding circuits: hormones and hysteresis”). No capítulo I, parte II (“Exercise-induced synaptogenesis in the hippocampus is dependent on UCP2-regulated mitochondrial adaptation”) nós mostramos que a plasticidade sináptica no hipocampo é dependente da presença de UCP2 e, portanto, das adaptações no status redox celular em momentos de atividade celular aumentada. Este mecanismo foi corroborado no capitulo VI, parte II (“AgRP neurons mediate Sirt1’s action on the melanocortin system and energy balance: roles for Sirt1 in neuronal firing and synaptic plasticity”), onde mostramos que as mudanças sinápticas (e comportamentais) decorrentes da inibição de Sirt1 não acontecem em camundongos deficientes de UCP2. Nossos resultados mostram que Sirt1 nos neurônios NPY/AgRP é importante para manutenção da atividade fisiológica dessas células. Animais deficientes de Sirt1 seletivamente nestes neurônios apresentam diminuição da ingesta alimentar e são mais magros.

O envolvimento de Sirt1 nos efeitos da restrição calórica (Cohen *et al.*, 2004; Chen *et al.*, 2005a; Chen *et al.*, 2008; Cohen *et al.*, 2009; Satoh *et al.*, 2010) e o papel dos neurônios NPY/AgRP em períodos de balanço energético negativo nos levaram a estudar os efeitos metabólicos e comportamentais de animais deficientes de Sirt1 especificamente neste grupo neuronal (Dietrich *et al.*, 2010). Apesar de o déficit de Sirt1 nos neurônios NPY/AgRP não ter um efeito pronunciado no metabolismo dos camundongos em restrição calórica, nossos resultados mostraram um efeito crucial de Sirt1 neste grupo neuronal no comportamento locomotor (ver capítulo VII, parte II “Sirt1 in AgRP neurons is necessary for exploratory behavior during calorie restriction”). Animais deficientes de Sirt1 apresentaram aumento da atividade locomotora quando analisados nas caixas onde são criados; entretanto, quando esses animais são testados em um ambiente novo, os animais deficientes de Sirt1

apresentam uma diminuição da atividade locomotora quando mantidos em restrição calórica. Dramaticamente, os animais deficientes de Sirt1 nos neurônios NPY/AgRP praticamente não exploram o centro da nova arena onde são testados. Esse déficit no comportamento exploratório chama muito a atenção, porque mostra que um comportamento não relacionado a ingesta de alimentos é afetado por uma manipulação seletiva dos neurônios NPY/AgRP. Uma vez que comportamentos motivacionais, como atividade exploratória em um ambiente novo, estão fortemente relacionados com o sistema dopaminérgico, buscamos estudar se os neurônios NPY/AgRP poderiam ter algum efeito na modulação desse sistema.

Efetivamente, mostramos no capítulo VIII, parte II ("AgRP neurons regulate the development of dopamine neuronal plasticity and non-food associated behaviors") que os neurônios NPY/AgRP são importantes na regulação de diversos comportamentos motivacionais em camundongos. Animais com atividade dos neurônios NPY/AgRP comprometida devido ao déficit de Sirt1 tiveram aumento da atividade exploratória em um novo ambiente, além de apresentarem uma resposta aumentada a drogas de abuso, como cocaína. Mostramos também que os neurônios NPY/AgRP projetam para uma região no cérebro rica em neurônios dopaminérgicos (zona tegmental ventral – VTA); animais deficientes de Sirt1 nos neurônios NPY/AgRP apresentaram mudanças sinápticas nos neurônios dopaminérgicos na VTA, além de um aumento na plasticidade sináptica medida com um protocolo de LTP (potenciação de longo prazo). Finalmente, mostramos que os neurônios AgRP são importantes para o desenvolvimento do circuito envolvido na resposta dopaminérgica, uma vez que a morte dos neurônios NPY/AgRP no período neonatal levou a um efeito similar ao déficit de Sirt1 nesses neurônios no animal adulto. Esses resultados mostram pela primeira vez na literatura um papel crucial dos neurônios

NPY/AgRP na modulação de comportamento motivacional relacionado ao uso de cocaína. Além disso, nossos resultados mostram pela primeira vez a implicação dos neurônios NPY/AgRP no desenvolvimento de outras regiões cerebrais, durante o período neonatal. Esses resultados têm implicação imediata no delineamento de futura pesquisa médica na área de desenvolvimento cerebral. Por exemplo, devido aos fatos de os neurônios NPY/AgRP serem críticos durante esse período do desenvolvimento cerebral e destes neurônios serem responsivos ao status metabólico do animal, é de se esperar que diferentes dietas durante períodos de desenvolvimento cerebral possam afetar os neurônios NPY/AgRP e, consequentemente, o desenvolvimento de diversas outras áreas. Gestantes que possuem déficit alimentar podem gerar, por exemplo, um balanço energético negativo que vai ter um impacto nos neurônios NPY/AgRP e no desenvolvimento cerebral, com possível comprometimento do comportamento do filho(a) na idade adulta. A importância dessa descoberta é singular para políticas de saúde publica e atualmente estamos interrogando com mais detalhes as perguntas levantadas por tal descoberta. Uma das consequências diretas de tais resultados seria a distinção entre diferentes tipos de dieta que mimetizariam diferentes status metabólicos para gestantes em desnutrição, visando aquelas que propiciem melhor desenvolvimento cerebral baseado no efeito destas nos neurônios NPY/AgRP. Obviamente, no estágio atual de pesquisa, tais conclusões e hipóteses são puramente especulativas visto que nossos resultados foram testados em roedores e ainda não temos evidências de que tais efeitos ocorram também em humanos.

Na última parte desta tese, utilizamos o conhecimento adquirido nos capítulos anteriores para propor novas estratégias de busca de medicamentos efetivos para combater obesidade. Interpretamos criticamente os medicamentos atualmente sendo estudados contra obesidade e aqueles disponíveis no mercado. Nossa conclusão com

esse estudo de revisão é que drogas que visem combater o apetite (logo, promover saciedade) estão fadadas a gerar efeitos colaterais graves, como já vistos com uma série de drogas aprovadas para obesidade que tiveram que ser retiradas do mercado. Esse efeito indesejado de tais drogas deve-se ao fato de que promovendo saciedade se está promovendo um mecanismo contrário àquele responsável pela promoção de saúde. É através da restrição calórica e exercício que se promove saúde; estes ativam vias envolvidas na indução do apetite. Atuando em direção oposta pode levar a perda de peso, mas levará consequentemente a diversas outras doenças crônicas decorrentes da promoção de saciedade. A perda de peso, baseada em nossa proposição, pode não ser o efeito principal esperado para a melhoria da saúde de pessoas obesas, ao menos não a curto prazo. Talvez a promoção de saúde deva ser obtida pela promoção daqueles mecanismos celulares e teciduais envolvidos nos efeitos da restrição calórica. A promoção de balanço energético negativo pode efetivamente levar a melhoria da qualidade de vida e consequente diminuição de doenças neste grupo de pacientes. Tal mecanismo pode ser exemplificado, a principio, pelo efeito positivo da droga orlistat (Xenical) em pacientes obesos. Essa droga, que promove mal absorção de lipídios no intestino, leva a um estado de “restrição calórica” que traz diversos benefícios ao paciente.

O último estudo contido no corpo desta tese poderá ter um efeito crucial na indústria farmacêutica e na pesquisa biomédica relacionada à regulação do balanço energético. O gasto bilionário da indústria na tentativa de isolar compostos com efeito positivo em pacientes obesos tem se mostrado um fracasso constante. Se nossa hipótese está correta, se a questão da promoção de saúde for olhada sob a perspectiva proposta poderemos ver um avanço significativo na pesquisa biomédica nesta área nos próximos anos.

Conclusão

Os resultados desta tese mostram que o exercício físico modifica a morfologia e a atividade mitocondrial no cérebro, com relevância para a plasticidade sináptica. Nossos resultados também sugerem que o hipotálamo é importante para o desenvolvimento cerebral, com possível impacto em diversas funções cerebrais não classicamente relacionadas ao hipotálamo. Tais descobertas podem ser relevantes na pesquisa translacional. Conclusões especificas de cada capitulo da parte II e também dos anexos podem ser encontradas nos mesmos.

Referências Bibliográficas

Anand, B.K. & Brobeck, J.R. (1951a) Hypothalamic Control of Food Intake in Rats and Cats. *Yale J Biol Med*, **24**, 123-140.

Anand, B.K. & Brobeck, J.R. (1951b) Localization of a Feeding Center in the Hypothalamus of the Rat. *P Soc Exp Biol Med*, **77**, 323-324.

Andrews, Z.B., Diano, S. & Horvath, T.L. (2005) Mitochondrial uncoupling proteins in the CNS: in support of function and survival. *Nature reviews. Neuroscience*, **6**, 829-840.

Andrews, Z.B., Erion, D., Beiler, R., Liu, Z.-W., Abizaid, A., Zigman, J., Elsworth, J.D., Savitt, J.M., DiMarchi, R., Tschoep, M., Roth, R.H., Gao, X.-B. & Horvath, T.L. (2009) Ghrelin promotes and protects nigrostriatal dopamine function via a UCP2-dependent mitochondrial mechanism. *Journal of Neuroscience*, **29**, 14057-14065.

Andrews, Z.B. & Horvath, T.L. (2009) Uncoupling protein-2 regulates lifespan in mice. *American journal of physiology Endocrinology and metabolism*, **296**, E621-627.

Andrews, Z.B., Liu, Z.W., Walllingford, N., Erion, D.M., Borok, E., Friedman, J.M., Tschop, M.H., Shanabrough, M., Cline, G., Shulman, G.I., Coppola, A., Gao, X.B., Horvath, T.L. & Diano, S. (2008) UCP2 mediates ghrelin's action on NPY/AgRP neurons by lowering free radicals. *Nature*, **454**, 846-851.

Aponte, Y., Atasoy, D. & Sternson, S.M. (2011) AGRP neurons are sufficient to orchestrate feeding behavior rapidly and without training. *Nature neuroscience*, **14**, 351-355.

Bewick, G., Gardiner, J., Dhillo, W., Kent, A., White, N., Webster, Z., Ghatei, M. & Bloom, S. (2005a) Post-embryonic ablation of AgRP neurons in mice leads to a lean, hypophagic phenotype. *FASEB J*, **19**, 1680-1682.

Bewick, G.A., Gardiner, J.V., Dhillo, W.S., Kent, A.S., White, N.E., Webster, Z., Ghatei, M.A. & Bloom, S.R. (2005b) Post-embryonic ablation of AgRP neurons in mice leads to a lean, hypophagic phenotype. *The FASEB journal : official publication of the Federation of American Societies for Experimental Biology*, **19**, 1680-1682.

Brachmann, C., Sherman, J., Devine, S., Cameron, E., Pillus, L. & Boeke, J. (1995) The SIR2 gene family, conserved from bacteria to humans, functions in silencing, cell cycle progression, and chromosome stability. *Genes Dev*, **9**, 2888-2902.

Brand, M.D., Affourtit, C., Esteves, T.C., Green, K., Lambert, A.J., Miwa, S., Pakay, J.L. & Parker, N. (2004) Mitochondrial superoxide: production, biological effects, and activation of uncoupling proteins. *Free radical biology & medicine*, **37**, 755-767.

Brand, M.D. & Esteves, T.C. (2005) Physiological functions of the mitochondrial uncoupling proteins UCP2 and UCP3. *Cell Metabolism*, **2**, 85-93.

Brecher, G. & Waxler, S. (1949) Obesity in albino mice due to single injections of goldthioglucose. *P Soc Exp Biol Med*, **70**, 498-501.

Broadwell, R.D., Balin, B.J., Salcman, M. & Kaplan, R.S. (1983) Brain-blood barrier? Yes and no. *P Natl Acad Sci USA*, **80**, 7352-7356.

Broadwell, R.D. & Brightman, M.W. (1976) Entry of peroxidase into neurons of the central and peripheral nervous systems from extracerebral and cerebral blood. *The Journal of comparative neurology*, **166**, 257-283.

Brobeck, J. (1946) Mechanism of the development of obesity in animals with hypothalamic lesions. *Physiological reviews*, **26**, 541-559.

Broberger, C., Johansen, J., Johansson, C., Schalling, M. & Hokfelt, T. (1998) The neuropeptide Y agouti gene-related protein (AGRP) brain circuitry in normal, anorectic, and monosodium glutamate-treated mice. *P Natl Acad Sci USA*, **95**, 15043-15048.

Cannon, B., Hedin, A. & Nedergaard, J. (1982) Exclusive occurrence of thermogenin antigen in brown adipose tissue. *FEBS letters*, **150**, 129-132.

Carro, E., Nunez, A., Busiguina, S. & Torres-Aleman, I. (2000) Circulating insulin-like growth factor I mediates effects of exercise on the brain. *The Journal of neuroscience : the official journal of the Society for Neuroscience*, **20**, 2926-2933.

Carro, E., Trejo, J.L., Busiguina, S. & Torres-Aleman, I. (2001) Circulating insulin-like growth factor I mediates the protective effects of physical exercise against brain insults of different etiology and anatomy. *The Journal of neuroscience : the official journal of the Society for Neuroscience*, **21**, 5678-5684.

Chen, D., Bruno, J., Easlon, E., Lin, S., Cheng, H., Alt, F. & Guarente, L. (2008) Tissue-specific regulation of SIRT1 by calorie restriction. *Genes Dev*, **22**, 1753-1757.

Chen, D., Steele, A., Lindquist, S. & Guarente, L. (2005a) Increase in activity during calorie restriction requires Sirt1. *Science*, **310**, 1641.

Chen, D., Steele, A.D., Lindquist, S. & Guarente, L. (2005b) Increase in activity during calorie restriction requires Sirt1. *Science (New York, NY)*, **310**, 1641.

Chen, H., Charlat, O., Tartaglia, L.A., Woolf, E.A., Weng, X., Ellis, S.J., Lakey, N.D., Culpepper, J., Moore, K.J., Breitbart, R.E., Duyk, G.M., Tepper, R.I. & Morgenstern, J.P. (1996) Evidence that the diabetes gene encodes the leptin receptor: identification of a mutation in the leptin receptor gene in db/db mice. *Cell*, **84**, 491-495.

Chen, H.Y., Trumbauer, M.E., Chen, A.S., Weingarth, D.T., Adams, J.R., Frazier, E.G., Shen, Z., Marsh, D.J., Feighner, S.D., Guan, X.-M., Ye, Z., Nargund, R.P., Smith, R.G., Van der Ploeg, L.H.T., Howard, A.D., MacNeil, D.J. & Qian, S. (2004) Orexigenic action of peripheral ghrelin is mediated by neuropeptide Y and agouti-related protein. *Endocrinology*, **145**, 2607-2612.

Clark, J.T., Kalra, P.S., Crowley, W.R. & Kalra, S.P. (1984) Neuropeptide-Y and Human Pancreatic-Polypeptide Stimulate Feeding-Behavior in Rats. *Endocrinology*, **115**, 427-429.

Cohen, D., Supinski, A., Bonkowski, M., Donmez, G. & Guarente, L. (2009) Neuronal SIRT1 regulates endocrine and behavioral responses to calorie restriction. *Genes Dev*, **23**, 2812-2817.

Cohen, H., Miller, C., Bitterman, K., Wall, N., Hekking, B., Kessler, B., Howitz, K., Gorospe, M., de Cabo, R. & Sinclair, D. (2004) Calorie restriction promotes mammalian cell survival by inducing the SIRT1 deacetylase. *Science*, **305**, 390-392.

Coleman, D.L. (1973) Effects of parabiosis of obese with diabetes and normal mice. *Diabetologia*, **9**, 294-298.

Coleman, D.L. (1978) Obese and diabetes: two mutant genes causing diabetes-obesity syndromes in mice. *Diabetologia*, **14**, 141-148.

Coleman, D.L. (1982) Diabetes-obesity syndromes in mice. *Diabetes*, **31**, 1-6.

Coleman, D.L. & Hummel, K.P. (1969) Effects of parabiosis of normal with genetically diabetic mice. *The American journal of physiology*, **217**, 1298-1304.

Cone, R.D. (2005) Anatomy and regulation of the central melanocortin system. *Nature neuroscience*, **8**, 571-578.

Coppola, A., Liu, Z.-W., Andrews, Z.B., Paradis, E., Roy, M.-C., Friedman, J.M., Ricquier, D., Richard, D., Horvath, T.L., Gao, X.-B. & Diano, S. (2007) A central thermogenic-like mechanism in feeding regulation: an interplay between arcuate nucleus T3 and UCP2. *Cell Metabolism*, **5**, 21-33.

Cotman, C.W. & Berchtold, N.C. (2002) Exercise: a behavioral intervention to enhance brain health and plasticity. *Trends Neurosci*, **25**, 295-301.

Cotman, C.W. & Engesser-Cesar, C. (2002) Exercise enhances and protects brain function. *Exerc Sport Sci Rev*, **30**, 75-79.

Cowley, M.A., Smart, J.L., Rubinstein, M., Cerdán, M.G., Diano, S., Horvath, T.L., Cone, R.D. & Low, M.J. (2001) Leptin activates anorexigenic POMC neurons through a neural network in the arcuate nucleus. *Nature*, **411**, 480-484.

Cowley, M.A., Smith, R.G., Diano, S., Tschöp, M., Pronchuk, N., Grove, K.L., Strasburger, C.J., Bidlingmaier, M., Esterman, M., Heiman, M.L., Garcia-Segura, L.M., Nillni, E.A., Mendez, P., Low, M.J., Sotonyi, P., Friedman, J.M., Liu, H., Pinto, S., Colmers, W.F., Cone, R.D. & Horvath, T.L. (2003) The distribution and mechanism of action of ghrelin in the CNS demonstrates a novel hypothalamic circuit regulating energy homeostasis. *Neuron*, **37**, 649-661.

de Oliveira Dietrich, M.d.O., Souza, D.O. & Portela, L.V. (2004) Serum S100B protein: what does it mean during exercise? *Clinical journal of sport medicine : official journal of the Canadian Academy of Sport Medicine*, **14**, 368; author reply 368-369.

Dietrich, M., Antunes, C., Geliang, G., Liu, Z., Borok, E., Nie, Y., Xu, A., Souza, D., Gao, Q., Diano, S., Gao, X. & Horvath, T. (2010) Agrp neurons mediate Sirt1's action on the melanocortin system and energy balance: roles for Sirt1 in neuronal firing and synaptic plasticity. *J Neurosci*, **30**, 11815-11825.

Dietrich, M.O., Andrews, Z.B. & Horvath, T.L. (2008) Exercise-induced synaptogenesis in the hippocampus is dependent on UCP2-regulated mitochondrial adaptation. *Journal of Neuroscience*, **28**, 10766-10771.

Dietrich, M.O. & Horvath, T.L. (2009a) Feeding signals and brain circuitry. *The European journal of neuroscience*, **30**, 1688-1696.

Dietrich, M.O. & Horvath, T.L. (2009b) GABA keeps up an appetite for life. *Cell*, **137**, 1177-1179.

Dietrich, M.O. & Horvath, T.L. (2010) The role of mitochondrial uncoupling proteins in lifespan. *Pflügers Archiv : European journal of physiology*, **459**, 269-275.

Dietrich, M.O. & Horvath, T.L. (2011) Synaptic plasticity of feeding circuits: hormones and hysteresis. *Cell*, **146**, 863-865.

Dietrich, M.O., Mantese, C.E., Porciuncula, L.O., Ghisleni, G., Vinade, L., Souza, D.O. & Portela, L.V. (2005) Exercise affects glutamate receptors in postsynaptic densities from cortical mice brain. *Brain research*, **1065**, 20-25.

Dietrich, M.O., Muller, A., Bolos, M., Carro, E., Perry, M.L., Portela, L.V., Souza, D.O. & Torres-Aleman, I. (2007) Western style diet impairs entrance of blood-borne insulin-like growth factor-1 into the brain. *Neuromolecular medicine*, **9**, 324-330.

Dietrich, M.O., Tort, A.B., Schaf, D.V., Farina, M., Gonçalves, C.A., Souza, D.O. & Portela, L.V. (2003) Increase in serum S100B protein level after a swimming race. *Canadian journal of applied physiology = Revue canadienne de physiologie appliquée*, **28**, 710-716.

Echtay, K.S., Roussel, D., St-Pierre, J., Jekabsons, M.B., Cadenas, S., Stuart, J.A., Harper, J.A., Roebuck, S.J., Morrison, A., Pickering, S., Clapham, J.C. &

Brand, M.D. (2002) Superoxide activates mitochondrial uncoupling proteins. *Nature*, **415**, 96-99.

Giardina, T.M., Steer, J.H., Lo, S.Z. & Joyce, D.A. (2008) Uncoupling protein-2 accumulates rapidly in the inner mitochondrial membrane during mitochondrial reactive oxygen stress in macrophages. *Biochimica et biophysica acta*, **1777**, 118-129.

Gropp, E., Shanabrough, M., Borok, E., Xu, A.W., Janoschek, R., Buch, T., Plum, L., Balthasar, N., Hampel, B., Waisman, A., Barsh, G.S., Horvath, T.L. & Bruning, J.C. (2005) Agouti-related peptide-expressing neurons are mandatory for feeding. *Nature Neuroscience*, **8**, 1289-1291.

Hahn, T.M., Breininger, J.F., Baskin, D.G. & Schwartz, M.W. (1998) Coexpression of Agrp and NPY in fasting-activated hypothalamic neurons. *Nature Neuroscience*, **1**, 271-272.

Hetherington, A. (1944) Non-production of hypothalamic obesity in the rat by lesions rostral or dorsal to the ventro-medial hypothalamic nuclei. *The Journal of comparative neurology*, **80**, 33-45.

Hetherington, A.W. & Ranson, S.W. (1942) The relation of various hypothalamic lesions to adiposity in the rat. *Journal of Comparative Neurology*, **76**, 475-499.

Hetherington, A.W. & Ranson, S.W. (1983) Hypothalamic-Lesions and Adiposity in the Rat. *Nutrition Reviews*, **41**, 124-127.

Horvath, T., Naftolin, F., Kalra, S. & Leranth, C. (1992) Neuropeptide-Y innervation of beta-endorphin-containing cells in the rat mediobasal hypothalamus: a light and electron microscopic double immunostaining analysis. *Endocrinology*, **131**, 2461-2467.

Horvath, T.L., Bechmann, I., Naftolin, F., Kalra, S.P. & Leranth, C. (1997) Heterogeneity in the neuropeptide Y-containing neurons of the rat arcuate nucleus: GABAergic and non-GABAergic subpopulations. *Brain Research*, **756**, 283-286.

Horvath, T.L., Warden, C.H., Hajos, M., Lombardi, A., Goglia, F. & Diano, S. (1999) Brain uncoupling protein 2: uncoupled neuronal mitochondria predict thermal synapses in homeostatic centers. *Journal of Neuroscience*, **19**, 10417-10427.

Hummel, K.P., Dickie, M.M. & Coleman, D.L. (1966) Diabetes, a new mutation in the mouse. *Science*, **153**, 1127-1128.

Imai, S., Armstrong, C.M., Kaeberlein, M. & Guarente, L. (2000) Transcriptional silencing and longevity protein Sir2 is an NAD-dependent histone deacetylase. *Nature*, **403**, 795-800.

Ingalls, A., Dickie, M. & Snell, G. (1950) Obese, a new mutation in the house mouse. *Journal of Heredity*.

Kaeberlein, M., McVey, M. & Guarente, L. (1999) The SIR2/3/4 complex and SIR2 alone promote longevity in Saccharomyces cerevisiae by two different mechanisms. *Genes Dev*, **13**, 2570-2580.

Kim, M., Yoon, C., Park, K., Shin, C., Park, K., Kim, S., Cho, B. & Lee, H. (2003) Changes in ghrelin and ghrelin receptor expression according to feeding status. *Neuroreport*, **14**, 1317-1320.

Kojima, M., Hosoda, H., Date, Y., Nakazato, M., Matsuo, H. & Kangawa, K. (1999) Ghrelin is a growth-hormone-releasing acylated peptide from stomach. *Nature*, **402**, 656-660.

Krashes, M.J., Koda, S., Ye, C., Rogan, S.C., Adams, A.C., Cusher, D.S., Maratos-Flier, E., Roth, B.L. & Lowell, B.B. (2011) Rapid, reversible activation of AgRP neurons drives feeding behavior in mice. *The Journal of Clinical Investigation*, **121**, 1424-1428.

Lawlor, D.A. & Hopker, S.W. (2001) The effectiveness of exercise as an intervention in the management of depression: systematic review and meta-regression analysis of randomised controlled trials. *Bmj*, **322**, 763-767.

Lean, M.E., Branch, W.J., James, W.P., Jennings, G. & Ashwell, M. (1983) Measurement of rat brown-adipose-tissue mitochondrial uncoupling protein by radioimmunoassay: increased concentration after cold acclimation. *Biosci Rep*, **3**, 61-71.

Lin, S., Defossez, P. & Guarente, L. (2000) Requirement of NAD and SIR2 for life-span extension by calorie restriction in Saccharomyces cerevisiae. *Science*, **289**, 2126-2128.

Liu, Y., Dentin, R., Chen, D., Hedrick, S., Ravnskjaer, K., Schenk, S., Milne, J., Meyers, D., Cole, P., Yates, J.r., Olefsky, J., Guarente, L. & Montminy, M. (2008) A fasting inducible switch modulates gluconeogenesis via activator/coactivator exchange. *Nature*, **456**, 269-273.

Lopez-Lopez, C., LeRoith, D. & Torres-Aleman, I. (2004) Insulin-like growth factor I is required for vessel remodeling in the adult brain. *P Natl Acad Sci USA*, **101**, 9833-9838.

Luquet, S., Perez, F., Hnasko, T. & Palmiter, R. (2005) NPY/AgRP neurons are essential for feeding in adult mice but can be ablated in neonates. *Science*, **310**, 683-685.

Luquet, S., Phillips, C.T. & Palmiter, R.D. (2007) NPY/AgRP neurons are not essential for feeding responses to glucoprivation. *Peptides*, **28**, 214-225.

Mailloux, R.J. & Harper, M.E. (2011) Uncoupling proteins and the control of mitochondrial reactive oxygen species production. *Free Radic Biol Med*, **51**, 1106-1115.

Marshall, N.B., Barrnett, R.J. & Mayer, J. (1955) Hypothalamic lesions in goldthioglucose injected mice. *Proceedings of the Society for Experimental Biology and Medicine Society for Experimental Biology and Medicine (New York, NY)*, **90**, 240-244.

Müller, A.P., Cammarota, M., de Oliveira Dietrich, M.d.O., Rotta, L.N., Portela, L.V., Souza, D.O., Izquierdo, I., Bevilaqua, L.R.M. & Perry, M.L.S. (2008) Different effect of high fat diet and physical exercise in the hippocampal signaling. *Neurochemical research*, **33**, 880-885.

Neeper, S.A., Gomez-Pinilla, F., Choi, J. & Cotman, C. (1995) Exercise and brain neurotrophins. *Nature*, **373**, 109.

Nègre-Salvayre, A., Hirtz, C., Carrera, G., Cazenave, R., Troly, M., Salvayre, R., Pénicaud, L. & Casteilla, L. (1997) A role for uncoupling protein-2 as a regulator of mitochondrial hydrogen peroxide generation. *The FASEB journal : official publication of the Federation of American Societies for Experimental Biology*, **11**, 809-815.

Nemoto, S., Fergusson, M.M. & Finkel, T. (2004) Nutrient availability regulates SIRT1 through a forkhead-dependent pathway. *Science*, **306**, 2105-2108.

Nie, Y., Erion, D., Yuan, Z., Dietrich, M., Shulman, G., Horvath, T. & Gao, Q. (2009) STAT3 inhibition of gluconeogenesis is downregulated by SirT1. *Nat Cell Biol*, **11**, 492-500.

Norsted, E., Gömüç, B. & Meister, B. (2008) Protein components of the blood-brain barrier (BBB) in the mediobasal hypothalamus. *Journal of chemical neuroanatomy*, **36**, 107-121.

Olney, J. (1969) Brain lesions, obesity and other disturbances in mice treated with monosodium glutamate. *Science (New York, NY)*, **164**, 719-&.

Olney, J. (1971) Monosodium glutamate effects. *Science (New York, NY)*, **172**, 294-&.

Pinto, S., Roseberry, A.G., Liu, H., Diano, S., Shanabrough, M., Cai, X., Friedman, J.M. & Horvath, T.L. (2004) Rapid rewiring of arcuate nucleus feeding circuits by leptin. *Science*, **304**, 110-115.

Produit-Zengaffinen, N., Davis-Lameloise, N., Perreten, H., Becard, D., Gjinovci, A., Keller, P.A., Wollheim, C.B., Herrera, P., Muzzin, P. & Assimacopoulos-Jeannet, F. (2007) Increasing uncoupling protein-2 in pancreatic beta cells does not alter glucose-induced insulin secretion but decreases production of reactive oxygen species. *Diabetologia*, **50**, 84-93.

Ramadori, G., Lee, C., Bookout, A., Lee, S., Williams, K., Anderson, J., Elmquist, J. & Coppari, R. (2008) Brain SIRT1: anatomical distribution and regulation by energy availability. *J Neurosci*, **28**, 9989-9996.

Ranson, S., Fisher, C. & Ingram, W. (1938) Diposity and diabetes mellitus in a monkey with hypothalamic lesions. *Endocrinology*, **23**, 175-181.

Ravussin, E., Tschöp, M., Morales, S., Bouchard, C. & Heiman, M. (2001) Plasma ghrelin concentration and energy balance: overfeeding and negative energy balance studies in twins. *J Clin Endocrinol Metab*, **86**, 4547-4551.

Richard, D., Huang, Q., Sanchis, D. & Ricquier, D. (1999) Brain distribution of UCP2 mRNA: in situ hybridization histochemistry studies. *International journal of obesity and related metabolic disorders : journal of the International Association for the Study of Obesity*, **23 Suppl 6**, S53-55.

Richard, D., Rivest, R., Huang, Q., Bouillaud, F., Sanchis, D., Champigny, O. & Ricquier, D. (1998) Distribution of the uncoupling protein 2 mRNA in the mouse brain. *The Journal of comparative neurology*, **397**, 549-560.

Rodgers, J.T., Lerin, C., Haas, W., Gygi, S.P., Spiegelman, B.M. & Puigserver, P. (2005) Nutrient control of glucose homeostasis through a complex of PGC-1alpha and SIRT1. *Nature*, **434**, 113-118.

Rodgers, J.T. & Puigserver, P. (2007) Fasting-dependent glucose and lipid metabolic response through hepatic sirtuin 1. *P Natl Acad Sci USA*, **104**, 12861-12866.

Rogina, B. & Helfand, S. (2004) Sir2 mediates longevity in the fly through a pathway related to calorie restriction. *Proc Natl Acad Sci U S A*, **101**, 15998-16003.

Sanchis, D., Fleury, C., Chomiki, N., Goubern, M., Huang, Q., Neverova, M., Gregoire, F., Easlick, J., Raimbault, S., Levi-Meyrueis, C., Miroux, B., Collins, S., Seldin, M., Richard, D., Warden, C., Bouillaud, F. & Ricquier, D. (1998) BMCP1, a novel mitochondrial carrier with high expression in the central nervous system of humans and rodents, and respiration uncoupling activity in recombinant yeast. *The Journal of biological chemistry*, **273**, 34611-34615.

Satoh, A., Brace, C.S., Ben-Josef, G., West, T., Wozniak, D.F., Holtzman, D.M., Herzog, E.D. & Imai, S. (2010) SIRT1 promotes the central adaptive response to diet restriction through activation of the dorsomedial and lateral nuclei of the hypothalamus. *Journal of Neuroscience*, **30**, 10220-10232.

Stanley, B.G. & Leibowitz, S.F. (1984) Neuropeptide Y: stimulation of feeding and drinking by injection into the paraventricular nucleus. *Life sciences*, **35**, 2635-2642.

Strobel, A., Combettes-Souverain, M., Doare, L., Strosberg, A.D. & Issad, T. (1998) Rat uncoupling protein 2 (UCP2): expression in obese ventromedial hypothalamus (VMH)-lesioned animals. *International journal of obesity and*

related metabolic disorders : journal of the International Association for the Study of Obesity, **22**, 1121-1126.

Takahashi, K.A. & Cone, R.D. (2005) Fasting induces a large, leptin-dependent increase in the intrinsic action potential frequency of orexigenic arcuate nucleus neuropeptide Y/Agouti-related protein neurons. *Endocrinology*, **146**, 1043-1047.

Tatemoto, K., Carlquist, M. & Mutt, V. (1982) Neuropeptide Y--a novel brain peptide with structural similarities to peptide YY and pancreatic polypeptide. *Nature*, **296**, 659-660.

Teri, L., Gibbons, L.E., McCurry, S.M., Logsdon, R.G., Buchner, D.M., Barlow, W.E., Kukull, W.A., LaCroix, A.Z., McCormick, W. & Larson, E.B. (2003) Exercise plus behavioral management in patients with Alzheimer disease: a randomized controlled trial. *JAMA : the journal of the American Medical Association*, **290**, 2015-2022.

Tissenbaum, H. & Guarente, L. (2001) Increased dosage of a sir-2 gene extends lifespan in Caenorhabditis elegans. *Nature*, **410**, 227-230.

Tschöp, M., Wawarta, R., Riepl, R., Friedrich, S., Bidlingmaier, M., Landgraf, R. & Folwaczny, C. (2001) Post-prandial decrease of circulating human ghrelin levels. *J Endocrinol Invest*, **24**, RC19-21.

van Praag, H., Christie, B.R., Sejnowski, T.J. & Gage, F.H. (1999) Running enhances neurogenesis, learning, and long-term potentiation in mice. *P Natl Acad Sci USA*, **96**, 13427-13431.

Vaynman, S., Ying, Z. & Gomez-Pinilla, F. (2003) Interplay between brain-derived neurotrophic factor and signal transduction modulators in the regulation of the effects of exercise on synaptic-plasticity. *Neuroscience*, **122**, 647-657.

Vaynman, S., Ying, Z. & Gomez-Pinilla, F. (2004a) Exercise induces BDNF and synapsin I to specific hippocampal subfields. *Journal of neuroscience research*, **76**, 356-362.

Vaynman, S., Ying, Z. & Gomez-Pinilla, F. (2004b) Hippocampal BDNF mediates the efficacy of exercise on synaptic plasticity and cognition. *The European journal of neuroscience*, **20**, 2580-2590.

Wang, L., Saint-Pierre, D.H. & Taché, Y. (2002) Peripheral ghrelin selectively increases Fos expression in neuropeptide Y - synthesizing neurons in mouse hypothalamic arcuate nucleus. *Neuroscience letters*, **325**, 47-51.

Wu, Q., Boyle, M. & Palmiter, R. (2009) Loss of GABAergic signaling by AgRP neurons to the parabrachial nucleus leads to starvation. *Cell*, **137**, 1225-1234.

Wu, Q., Howell, M.P., Cowley, M.A. & Palmiter, R.D. (2008a) Starvation after AgRP neuron ablation is independent of melanocortin signaling. *P Natl Acad Sci USA*, **105**, 2687-2692.

Wu, Q., Howell, M.P. & Palmiter, R.D. (2008b) Ablation of neurons expressing agouti-related protein activates Fos and gliosis in postsynaptic target regions. *Journal of Neuroscience*, **28**, 9218-9226.

Wu, Q. & Palmiter, R.D. (2011) GABAergic signaling by AgRP neurons prevents anorexia via a melanocortin-independent mechanism. *European journal of pharmacology*, **660**, 21-27.

Yang, Y., Atasoy, D., Su, H.H. & Sternson, S.M. (2011) Hunger states switch a flip-flop memory circuit via a synaptic AMPK-dependent positive feedback loop. *Cell*, **146**, 992-1003.

Zhang, Y., Proenca, R., Maffei, M., Barone, M., Leopold, L. & Friedman, J.M. (1994) Positional cloning of the mouse obese gene and its human homologue. *Nature*, **372**, 425-432.

Zigman, J.M. & Elmquist, J.K. (2003) Minireview: From anorexia to obesity--the yin and yang of body weight control. *Endocrinology*, **144**, 3749-3756.